A STUDY OF THE ANTI-ATHEROSCLEROTIC AND ANTI-INFLAMMATORY EFFECTS OF SIROLIMUS

Thesis submitted for the degree of Doctor of Philosophy

To Faculty of Medicine

University of London

Kun Ling Ma

Centre for Nephrology

Royal Free & University College Medical School

Rowland Hill Street

London NW3 2PF

October, 2008

ProQuest LLC
789 East Eisenhower Parkway
P.O. Box 1346
Ann Arbor, MI 48106-1346

I, Kun Ling Ma, confirm that the work presented in this thesis is my own. Where information has been derived from other sources, I confirm that this has been indicated in the thesis.

ABSTRACT

Inflammation accelerates the progression of atherosclerosis. Sirolimus, a potent immunosuppressive agent, has been shown with pleiotropic antiatherosclerotic effects. This study was to explore potential anti-atherosclerotic mechanisms of Sirolimus using cell culture studies and apolipoprotein E knockout (apoE KO) mice under inflammatory stress.

Results showed that Sirolimus decreased cholesterol accumulation caused by inflammatory stress in human vascular smooth muscle cells (VSMCs), macrophages, and human hepatoblastoma cell line (HepG2). Sirolimus decreased formation of atherosclerotic plaques in the aortas of inflamed apoE KO mice. Sirolimus inhibited the mRNA expression of sterol regulatory element-binding protein (SREBP) cleavage activating protein (SCAP) and SREBP-2, and decreased translocation of SCAP/SREBP-2 complex from endoplasmic reticulum (ER) to Golgi in VSMCs and HepG2 cells in the presence of IL-1 β, thereby overriding IL-1β induced transcription of LDL receptor (LDLr) and 3-hydroxy-3-methyglutaryl coenzyme A reductase (HMGR). Insulin induced gene-1 (Insig-1) is a retention factor of SCAP in the ER and modulates HMGR degradation at posttranscriptional level. Interestingly, Sirolimus accelerated HMGR degradation by up-regulating Insig-1 expression in VSMCs. Sirolimus also reversed the reduction of cholesterol efflux induced by inflammatory stress through ATP-binding cassette transporter A1 (ABCA1) mediated pathway. This was mediated by increasing the gene and protein expression of ABCA1, peroxisome proliferator-activated receptor-α (PPARα), and liver X receptor-α (LXRα) both *in vitro and in vivo* studies. Sirolimus also directly inhibited the production of inflammatory cytokines shown in our experiments.

Taken together, both *in vivo* and *in vitro* findings demonstrated that Sirolimus ameliorated cholesterol homeostasis disrupted by inflammatory stress, which was through multiple pathways. Sirolimus down-regulated LDLr-mediated cholesterol influx, down-regulated HMGR-mediated cholesterol biosynthesis, and up-regulated ABCA1-mediated cholesterol efflux. Furthermore, Sirolimus inhibited the production of inflammatory cytokines. Our studies for the first time indicate that Sirolimus has very pronounced anti-inflammatory properties and highly beneficial anti-atherosclerosis effects expressed through rebalancing disrupted intracellular cholesterol homeostasis involving various molecular mechanisms.

ACKNOWLEDGEMENTS

This thesis is a conclusion of PhD project started from 2005 at Renal Laboratory, Centre for Nephrology, Royal Free & University College Medical School.

Firstly, I would like to express my deep and sincere gratitude to my supervisors, Dr. Xiong Zhong Ruan and Dr. Zac Varghese. Dr. Ruan's wide knowledge and research techniques have been of great value to me. His understanding, encouragement, and personal guidance have provided a solid basis for the fulfilment of thesis. Dr. Zac Varghese has been an endless source of advice and encouragement by sharing with me his knowledge in lipid and other research fields. Without his constant support, I could not have finished this work.

I am also very grateful to Professor John F. Moorhead, whose support and advice was very helpful for me to finish this work.

During this work, I have enjoyed the association with Professor Stephen H. Powis and collaborated with many colleagues for whom I have great regard, and I wish to extend my warmest thanks to all those who have helped me with my work in the Royal Free & University College Medical School. I am also grateful to all my Chinese friends working in Royal Free & University College Medical School for helping me get through the tough time of these years in U.K.

I owe my thanks to my loving wife and son. They have lost too much due to my research work in U.K. Without their understanding, encouragement, and constant support it would have been impossible for me to finish this work.

Finally I am indebted to Dr Zac Varghese for his financial support from Grant-115 through Royal Free hospital trustees. I also thank Wyeth Pharmaceuticals providing Sirolimus for this project.

Kun Ling Ma

October, 2008

PUBLICATIONS

1. **Ma KL**, Ruan XZ, Powis SH, Chen YX, Moorhead JF, and Varghese Z. Inflammatory stress exacerbates lipid accumulation in hepatic cells and fatty livers of apolipoprotein E knockout mice. Hepatology 2008; 48(3):770-781.

2. **Ma KL**, Ruan XZ, Powis SH, Chen Y, Moorhead JF, Varghese Z. Sirolimus modifies cholesterol homeostasis in hepatic cells: a potential molecular mechanism for Sirolimus-associated dyslipidemia. Transplantation 2007; 84(8):1029-36.

3. **Ma KL**, Ruan XZ, Powis SH, Moorhead JF, and Varghese Z. Anti-atherosclerotic effects of Sirolimus on human vascular smooth muscle cells. Am J Physiol Heart Circ Physiol. 2007; 292(6):H2721-8.

4. Ruan XZ, Moorhead JF, Tao JL, **Ma KL**, Wheeler DC, Powis SH, Varghese Z. Mechanisms of dysregulation of low-density lipoprotein receptor expression in vascular smooth muscle cells by inflammatory cytokines. Arterioscler Thromb Vasc Biol 2006; 26(5):1150-5.

5. **Ma KL**, Ruan XZ, Powis SH, Moorhead JF, and Varghese Z. Sirolimus modifies hepatic cell cholesterol homeostasis: A potential molecular mechanism for Sirolimus-associated dyslipidemia (oral presentation, FO022). (Presented at XLIV ERA-EDTA Congress 21-24th June, 2007, Barcelona, Spain).

6. **Ma KL**, Ruan XZ, Powis SH, Moorhead JF, and Varghese Z. Sirolimus affects liver cell cholesterol homeostasis: Potential molecular mechanisms for Sirolimus-associated dyslipidemia. (Poster, RA0148). (Presented at British Renal Association Conference 21-23rd May, 2007, Brighton, U.K).

7. **Ma KL**, Ruan XZ, Moorhead JF, Powis SH and Varghese Z. Sirolimus ameliorates the imbalance of intracellular cholesterol homeostasis in human vascular smooth muscle cells mediated by inflammatory cytokines (Poster, RA6354). (Presented at British Renal Association Conference, 3-5th May, 2006, Harrogate, U.K).

CONTENTS

LIST OF FIGURES

LIST OF TABLES

LIST OF ABBREVIATIONS

ABCA1	Adenosine triphosphate binding cassette transporter A1
ABCG1	Adenosine triphosphate binding cassette transporter G1
Ab	Antibody
ACAT	Acyl Co A: Cholesterol acyl transferase
AcLDL	Acetylated LDL
ACS	Acyl-CoA synthetase
ADH	Autosomal dominant hypercholesterolemia
AMP	Aenosine monophosphate
AMPK	AMP-activated protein kinase
Apo	Apolipoprotein
ApoA-I	Apolipoprotein A-I
ApoE	Apolipoprotein E
ApoE KO	Apolipoprotein E knockout
APS	Ammonium persulfate
AREs	AU-rich elements
A-SAA	Acute-phase serum amyloid A proteins
ATP	Adenosine triphosphate
bFGF	Basic fibroblast growth factor
bHLH-Zip	Basic-helix–loop–helix–leucine zipper
BHT	Butylated hydroxytoluene
BSA	Bovine serum albumin
CaMKK	Calmodulin-dependent protein kinase
CBP	CREBP binding protein
CCR2	C-C motif chemokine receptor–2
CDCA	Chenodeoxycholic acid

CD40L	CD40 ligand
CE	Cholesterol ester
CETP	Cholesterol ester transfer protein
CHO	Chinese hamster ovary
CMs	Chylomicrons
CoAS	Coenzyme A with the thiol proton dissociated
CREBP	CAMP response element-binding protein
CRP	C-reactive protein
DAB	Tetrahydrochloride
DCs	Dendritic cells
DEPC	Diethyl pyrocarbonate
DiI-acLDL	AcLDL labelled with 1, 1'-dioctadecy-3,3,3',3',-tetramethylindocarbocyanine
dH_2O	Distilled water
DMEM	Dulbecco's Modified Eagle's Medium
DMEM/F12	Dulbecco's Modified Eagle's Medium/Ham's Nutrient F-12
DTT	Dithiothreitol
EDTA	Ethylene diaminetetra-acetic acid
EGF	Epidermal growth factor
eNOS	Endothelial nitric oxide synthase
eIF-4E	Eukaryotic initiation factor 4E
ELISA	Enzyme Linked-Immunosorbent Assay
ER	Endoplasmic reticulum
ERK	Extracellular signal-regulated kinase
ET	Endothelin
FAs	Fatty acids
FAT	Fatty acid translocase

FBS	Fetal bovine serum
FC	Free cholesterol
FEEL-1	Fasciclin, EGF-like, laminin-type EGF-like and link domain-containing scavenger receptor-1
FF	Hypercholesterolemic fat-fed
FGF	Fibroblast growth factor
FH	Familial hypercholesterolaemia
FKBP12	FK506 binding protein
GAPDH	Glyceraldehyde-3-phosphate dehydrogenase
GM-CSF	Granulocyte monocyte colony stimulating factor
HB-EGF	Heparin-binding EGF-like growth factor
HDLs	High density lipoproteins
Hep	Heparin
HepG2 cells	Human hepatoblastoma cell line
H-FABP	Heart-type fatty acid-binding protein
HMGR	3-hydroxy-3-methylglutaryl coenzyme A reductase
HRP	Horseradish Peroxidase
HSP	Heat shock protein
HuB	Human apo B
ICAM-1	Intercellular adhesion molecule-1
IDL	Intermediate density lipoprotein
IGF	Insulin-like growth factor
IKK	IκB kinase
IL-1β	Interleukin-1β
IL-1Ra	IL-1 receptor antagonist
IL-6	Interleukin-6

IL-8	Interleukin-8
Insigs	Insulin induced genes
IP	Immunoprecipitation
IFN-γ	Interferon-γ
IGF-I	Insulin-like growth factor-I
Lamp	Lysosomal membrane glycoprotein
LPL	Lipoprotein lipase
LPS	Lipopolysaccharide
LCAD	Long chain acyl-CoA dehydrogenase
LCAT	Lecithin:cholesterol acyl transferase
LDH	Lactate dehydrogenase
LDLs	Low density lipoproteins
LDLr	Low density lipoprotein receptor
LIMP II	Lysosomal integral membrane protein II
LOX-1	Lectin-like oxidized LDL receptor-1
Lp(a)	Lipoprotein (a)
LPL	Lipoprotein lipase
LRP	LDL receptor-related protein
LXRα	Liver X receptor-α
MARCO	Macrophage receptor with collagenous structure
MCP-1	Monocyte chemoattractant prolein-1
MFI	Mean fluorescence intensity
M-CSF	Monocyte colony stimulating factor
MHCs	Major histocompatibility complexes
MIF	Macrophage migration inhibitory factor
MIP	Macrophage inflammatory protein

m-CSF	Monocyte colony stimulating factor
mTOR	Mammalian target of rapamycin
ndHDL	Nascent discoidal HDL
NAD	Nicotinamide adenine dinucleotide
NADPH	Nicotinamide adenine dinucleotide phosphate
NAFLD	Non-alcoholic fatty liver disease
NF- κB	Nuclear factor- κB
NKCs	Natural killer cells
nSREBP-1a	Nuclear sterol regulatory element binding protein-1a
oxLDL	Oxidized low-density lipoprotein
PAMPs	Pathogen-associated molecular patterns
PBS	Phosphate buffered saline
PBST	Phosphate buffered saline with 0.1% Tween
PCR	Polymerase chain reaction
PCNA	Proliferating cell nuclear antigen
PCSK-9	Proprotein convertase subtilisin/kexin-9
PDGF	Platelet derived growth factor
PGE2	Prostaglandin E2
PK	
PKA	Protein kinase A
PLs	
PLTP	Phospholipid transfer protein
PMA	Phorbol 12-myristate 13-acetate
PP2A	protein phosphatase 2A
PPAR	Peroxisome proliferator activated receptor
PPB	Potassium phosphate buffer

PTEN	Phosphatase and tensin homolog
RAG	Recombination activating genes
RANTES	Regulated upon Activation, Normal T-cell Expressed and Secreted
RCT	Reverse cholesterol transport
Rheb	Ras homolog enriched in brain
RNase	Ribonuclease
ROS	Reactive oxygen species
RT	Reverse transcription
RXR	Retinoid-X-receptor
SAA	Serum Amyloid A
SAP	Serum amyloid P component
SCAP	SREBP cleavage-activating protein
SD	Sprague-Dawley
SDS	Sodium dodecyl sulfate
SDS-PAGE	Sodium dodecyl sulphate-polyacrylamide gel electrophoresis
SRCL	Scavenger receptor with C-type lectin
SR-PSOX	Scavenger receptor binding phosphatidylserine and oxidized lipoprotein
Sir	Sirolimus
S6K	Ribosomal protein S6 kinases
LKB1	Serine/threonine kinase 11
SR-A	Scavenger receptor class A
SR-BI	Scavenger receptor class B type I
SRE	Sterol regulatory element
SREBP-2	Sterol response element binding protein-2
SSD	Sterol sensing domain
TBARS	Thiobarbituric acid reactive substances

TBS	Tris-buffered saline
TBST	Tris-buffered saline containing 0.1 % Tween 20
TC	Total cholesterol
TGs	Triglycerides
TEMED	N, N, N', N'-Tetramethylethylenediamine
Th1	T-Helper type1
THP-1 cells	Human acute monocytic leukaemia cell line
TIR	Toll/IL-1 resistance
TNFα	Tumour necrosis factor-α
TGFα	Transforming growth factor-α
TGFβ	Transforming growth factor-β
TLRs	Toll-like receptors
TMB	Tetramethyl benzidine
TNFR	Tumour necrosis factor receptor
TSC	Tuberous Sclerosis Complex
UTR	Untranslated region
UV	Ultraviolet
VCAM-1	Vascular cell adhesion molecule-1
VEGF	Vascular endothelial growth factor
VLDLs	Very low density lipoproteins
VLDLr	Very low density lipoprotein receptor
VSMCs	Vascular Smooth Muscle Cells
WHHL	Watanabe heritable hyperlipidaemic rabbit

CHAPTER 1. GENERAL INTRODUCTION

Cardiovascular disease due to atherosclerosis is the leading cause of death throughout Western world and the second most common cause worldwide (1). Atherosclerosis, a slow progressive disease characterised by the accumulation of lipids and fibrous connective tissue in the subendothelial space in the large arteries, constitutes the single most important contributor to this growing burden of cardiovascular disease.

Atherosclerosis has drawn the attention to investigators for over 2500 years. The ancient Greeks documented the typical symptoms of peripheral arterial disease approximately 300 B.C. The presence of calcified atherosclerotic lesions was suggested already in 1575. In 1914, Anitschkow first described the role of cholesterol accumulation in the vessel wall for the development of atherosclerosis, including the identification of foam cells (2). During this time, it was proposed that the lesions of atherosclerosis result from some forms of injury to the arterial wall. At the same time, it was suggested that the intimal thickening is due to the deposition of blood elements. Until the 1970s the link between lipids and atherosclerosis dominated our thinking. Association between hypercholesterolaemia and atheroma demonstrated by experimental and clinical studies strengthened this hypothesis (3). In the 1970s and 1980s, the clinical problems of restenosis following arterial intervention reinforced the interest in vascular growth regulation and thus the focus shifted towards growth factors and proliferation of vascular smooth muscle cells (VSMCs). A fusion of these views led to the concept of the atheroma as a graveyard of a cellular lipid debris covered by a capsule of proliferated VSMCs. More recently research has focused on the role of inflammation in atherosclerosis.

The current concept that inflammation and the immune response contributing to atherogenesis has gained increased interest (4, 5). In fact, this is not a new concept. Virchow discussed the importance of inflammation in cerebral arteries in his Archive of

1847. According to "response to injury" hypothesis of atherosclerosis developed by Ross and others (6), many stimulating factors, such as hyperlipidemia, diabetes, hypertension and smoking, can lead to endothelial injury, resulting in a cascade of immunologically mediated events. Firstly, there is an adhesion of monocytes and lymphocytes to the endothelial surface, migration of those cells beneath the endothelial surface, and subsequent subendothelial localization. Macrophages then take up lipid by scavenger receptor, forming foam cells. Activated macrophages release cytokines and growth factors, which lead to smooth muscle cell proliferation and fibrous plaque formation. Furthermore, increasing evidence showed that many chronic inflammatory diseases are increasingly recognized as risk factors for the development of premature atherosclerosis. Epidemiological studies showed that patients with rheumatoid arthritis have up to a 5-fold increase in cardiovascular morbidity and mortality. Patients with systemic lupus erythematosus exhibit an even higher increase in cardiovascular disease (7-9). There are significant chronic inflammatory processes in these diseases mediated by a variety of cells via innate and adaptive immune systems, suggesting that inflammation accelerates the progression of atherosclerosis.

1. 1 Atherosclerosis is an inflammatory disease

1.1.1 Immune mechanisms of inflammation in atherosclerosis

1.1.1.1 Evidence that the immune system is involved in atherosclerosis

The immune system is involved at all stages of the atherosclerotic disease process (10). Some evidence has been originated to link the immune system to the process of atherogenesis.

First, atherosclerotic lesions are characterised by the accumulation of lipid particles and cells of the immune system in subendothelial regions, leading to narrowing of the arterial lumen and following plaque rupture, to thrombosis. Autoimmune elements (e.g.

autoantibodies, autoantigens) as well as different inflammatory cells like monocytes, dendritic cells (DCs), macrophages (developing into foam cells), T cells, B cells, natural killer cells (NKCs) and mast cells are involved in these processes (6, 11-13).

Toll-like receptors (TLRs) expressed on endothelial cells can bind microbial or autologous heat shock protein (HSP, e.g. HSP60), providing the possibility for targeting adaptive or innate immunological effector mechanisms (14). Endothelial dysfunction is not only characterised by biosecretory dysfunction and a loss of anti-thrombogenic properties but also by an immune imbalance with a proinflammatory over an anti-inflammatory phenotype (6, 12, 15, 16). Hence, endothelial dysfunction results in enhanced adhesion and migration of peripheral circulating monocytes and DCs (17, 18). Retention of mononuclear (antigen-presenting) cells in the vessel wall is one of the crucial elements of atherogenesis (19, 20).

Cytokines are secreted by immune cells within the atherosclerotic plaque. These include interleukin (IL)-1, IL-2, IL-6, IL-8, IL-12, IL-10, tumour necrosis factor (TNF), interferon (IFN)-γ and platelet derived growth factor (PDGF) (21). The presence of both proinflammatory and anti-inflammatory cytokines suggests the coexistence of proatherogenic and antiatherogenic influences in lesions (21). The pattern of cell and cytokine involvement suggests a T-Helper type1 (Th1) lymphocyte dominance in atherosclerotic lesions progression (12, 13). Furthermore, the inflammatory process in the atherosclerotic artery may lead to increased blood levels of inflammatory cytokines and other acute phase reactants (12). Activation and differentiation of peripheral circulating immune cells have been linked with the progression of atherosclerosis (22, 23).

Second, more compelling evidence for the role of the immune system in atherogenesis derives from specific transgenic and knockout mice. Knockout of mediators of

monocyte chemotaxis, IFN-γ or its receptor, costimulatory molecules, CD40 ligand (CD40L), TLRs and recombination activating genes (RAG) , resulting in global immunodeficiency, all lead to a reduction in atherosclerosis in mouse models (11, 24). On the other hand, knockout of IL-10, a Th1 inhibitory cytokine, results in an increase in lesions (13).

Third, the direct transfer of immune mediators or immunization provides a basis for implicating the role of immune system in atherogenesis. IFN-γ, IL-12, or IL-18 injection all increase atherosclerosis (11, 24). The administration of antibodies to CD40L reduces lesion formation in LDL receptor knockout mice, whereas the use of antibodies to transforming growth factor-β (TGF-β) in the apoE KO mouse increases atherosclerosis, emphasizing the atheroprotective influence of this cytokine (11). When CD4+ cells from apoE KO mice in which the Th1 cell subtype is dominant are transferred to immunodeficient apoE KO mice, an increase in atherosclerosis is noted. On the other hand, the transfer of B-cells from apoE KO mice with or without T-cells reduces atherosclerosis (11, 13). Immunization with HSP increases atherosclerosis (25).

Fourth, atherosclerosis is aggravated in patients with dysregulation of the immune system in some autoimmune diseases (26). However, when these patients with autoimmune diseases were treated by anti-inflammatory therapies (including steroids), there is a beneficial net effect on cardiovascular morbidity and mortality (27, 28). In immunosuppressed patients after heart transplantation, cardiac allograft vasculopathy is the most important cause of death in the long term follow-up, which is characterised by endothelial dysfunction and early vascular inflammation (16).

1.1.1.2 Innate immunity in atherosclerosis

The innate immune system is critical to initial inflammatory responses. The innate immune system consists of epithelial/endothelial barriers, circulating cells, and some proteins. These proteins recognize microbes or substances produced in infections and initiate responses that eliminate the microbes (29). Crucial pattern recognition and signalling receptors are mannose receptors, scavenger receptors, and receptors for opsonins and TLRs (29).

The TLR family, including 12 identified mammalian TLRs so far, recognizes pathogen-associated molecular patterns (PAMPs) on bacterial and viral pathogens. Ligands include lipopolysaccharide (LPS) of Gram-negative bacteria (recognized by TLR4), various bacterial lipids, such as lipoteichoic acid of Gram-positive bacteria, peptidoglycan, and lipopeptides (recognized by TLR2 heterodimers with TLR1 or TLR6) (30), as well as viral nucleic acids, double-stranded RNA and DNA rich in CpG-motifs (recognized by intracellular TLR3, TLR7 and TLR 9). In addition to the classical bacterial and viral TLR ligands, several endogenous ligands (HSP; oxidized LDL, oxLDL), produced as a response to stress or tissue injury, have been proposed.

When any one of the several described TLR ligands binds to its TLR, one or several adapter molecules are recruited to propagate the signal via interaction of Toll/IL-1 resistance (TIR) domains presented on the TLR and its adapters (30). Activation of the adapter proteins (such as the myeloid differentiation protein-88, MyD88) and its downstream signals result in activation of the NF-κB and interferon pathway.

In particular, TLR1, TLR2 and TLR4 were found to be expressed in both human and mouse atherosclerotic lesions (31). Expression was mainly located to endothelial cells and macrophages within the lesion (32). Also, patients with acute coronary syndromes

or coronary arteriosclerosis disease showed increased TLR4 expression on circulating monocytes compared with control patients (31). The TLR-dependent atherosclerosis contribution may rely on endothelial TLR activation as well as on mononuclear cell TLR activation (23, 31, 32). Lack of TLR-4 or lack of the adapter protein MyD-88 reduced atherosclerosis (33, 34). Complete TLR2 deficiency in hyperlipidaemic mice resulted in an approximately 50% reduction in atherosclerotic lesion severity (35).

DCs play a key role in innate and adaptive immunity (36), expressing high levels of scavenger receptors and class II major histocompatibility complexes (MHCs), which present antigens to cells of the adaptive immune system. Dysfunctional endothelium has been shown to drive enhanced DC adhesion, migration and maturation, and activated vascular DCs have been demonstrated in early stages of atherosclerosis (18, 37). Some DCs cluster with T cells directly within atherosclerotic lesions, while others migrate to lymphoid organs to activate T cells (37). Dyslipidemia systemically alters DC function and recent findings suggest that DCs play a role in plaque destabilization (37). DCs seem to be concentrated in the rupture-prone areas of vulnerable human carotid artery plaques (38, 39). Plasmacytoid DCs in atherosclerotic plaque sense microbial motifs and amplify cytolytic T-cell functions, thus providing a link between host-infectious episodes and acute immune-mediated complications of atherosclerosis (40).

1.1.1.3 Adaptive immunity in atherosclerosis

Adaptive immunity is initiated by recognition of disease-related antigens, which include oxLDL, HSP and microbial macromolecules. In the artery wall, adaptive immune recognition mainly leads to Th1 effector responses, which are characterised by secretion of proinflammatory cytokines and by activation of macrophages and vascular cells. Therefore, both the innate and adaptive arms of the immune system lead to inflammation in the developing atherosclerotic lesion.

The adaptive immune system may influence atherosclerosis in several ways: (i) by cell–cell interaction between antigen-presenting cells (like DCs, macrophages, B-cells, NKCs) and T-cells (13); (ii) by the secretion of a variety of cytokines from activated T-cells, which in turn mediate further activation of plaque-invading inflammatory cells; or (iii) by the production of antibodies through B-cells in a T-cell-dependent or -independent manner. Some of these antibodies have the ability to block the import of modified lipoproteins via macrophage scavenger receptors.

1.1.2 Pathological phases for the role of inflammation in atherosclerosis

The role of inflammation in the atherosclerotic process can be divided into three phases: early development of atherosclerosis, progression of the atherosclerotic plaque, and acute plaque rupture. Monocyte-derived macrophages, and also T-lymphocytes, have been found in human fatty streaks of the earliest stage of the disease process (41, 42), suggesting that immune processes may play an initiating or early role in the development of the lesion. Cytokines, including several interleukins, interferons, TNFα, several growth factors, colony-stimulating factors and C-reactive Protein (CRP), have also been found within atheromatous lesions at all stages (43). Although the initial goal of the immune response, such as the scavenging activities of monocyte/macrophage through the accumulation of oxLDL and other cellular debris, is to contain the toxic exposure and prevent injury to the endothelium, activation of macrophages may propagate the inflammation by release of cytokines and growth factors (44).

As this process continues, there is an increase of inflammatory cells in the atheroma, which are recruited from blood but also proliferate itself within the lesion. Endothelial-derived leukointegrins cause adherence of monocytes and T cells, particularly at branch points of arteries, where turbulence is prominent (45, 46). Changes in shear stress at these sites lead to up-regulation of the genes responsible for the production of these

molecules (47, 48). Elevated levels of TNFα and IL-1β increase monocyte recruitment into developing atherosclerotic lesions in mice (49).

Plaque rupture, also involves inflammatory mechanisms. Rupture occurs at sites of the fibrous plaque where macrophages enter (50). Rupture may be stimulated by destabilisation and destruction of the fibrous cap through up-regulation and production of proteolytic enzymes, including metalloproteinases and collagenases derived from macrophages stimulated by activated T cells (51). The profile of inflammatory cytokines in more advanced lesions, such as those taken from endarterectomy specimens, shows predominantly a pro-inflammatory T cell response (52). Inflammatory profiles in certain plaque may correlate with acute plaque instability as well. Plaques from patients with unstable angina show greater expression of P-selectin (53) and other cytokines, and the systemic cytokine profile also differs between stable and unstable angina populations (54). These data correlated with the clinical scenario in cerebrovascular disease, as well as elevated levels of macrophages, T cells (55), intercellular adhesion molecule-1 (ICAM-1) and TNFα (56, 57), were found in endarterectomy specimens from the symptomatic compared with asymptomatic carotid stenosis patients. Although the precise mechanisms by which these cytokines cause atherosclerosis remain unclear, there is a consensus that inflammation plays an important role.

1.1.3 The main cellular constituents in atherosclerosis

The pathobiology of atherosclerosis may be characterised by the numerous cellular entities involved in atherosclerotic pathogenesis. These cells can be broadly organized into structural elements of the arterial wall (e.g., endothelial cell and the VSMCs), inflammatory cells that enter the arterial wall, and circulating elements (e.g., monocyte/ macrophages, platelets).

1.1.3.1 Endothelial cells

The endothelium is now recognized as a dynamic organ involved in metacrine, paracrine, and endocrine functions, and not simply a passive conduit (58, 59). As the interface between the circulation and the arterial wall, endothelial cells transduce responses to pathogenic stimuli such as hypertension, hyperglycemia, and smoking. One such critical endothelial response is the induction of adhesion molecules, a decisive step early in atherogenesis (60). Another important response is the change in the production of nitric oxide, a critical, short-lived molecule that helps maintain normal endothelial reactivity while limiting thrombosis and inflammation (61, 62). Nitric oxide production is an example of the critical role of the endothelium in the vasculature(63).

1.1.3.2 Monocyte-derived macrophages

All forms of atherosclerotic lesions contain specialized, chronic inflammation with large numbers of monocyte-derived macrophages, as well as varying numbers of T lymphocytes (64, 65). Normally, the macrophages are not only scavenger cells but can also be antigen-presenting cells. Macrophages are a rich source of growth regulatory molecules and cytokines, which may be the principal mediators of cell migration, proliferation, and inflammation within the lesions of atherosclerosis (66). Macrophages are also a principal source of foam cells in the lesions as they take up lipid and oxLDL through scavenger receptors or through bulk phase endocytosis or through a putative oxLDL receptor (67). Macrophages can oxidise LDL through various pathways, including the formation of lipoxygenase and nitric oxide. When they do so, fatty acids undergo peroxidation, become covalently cross-linked to the apoprotein B moiety of the LDL particle, and are taken up via the scavenger receptor to be localized in the macrophage, thus resulting in foam cell formation (68). The uptake of oxLDL and other substances within the lesions of atherosclerosis may serve as a stimulus to induce gene

expression for several growth regulatory molecules and cytokines, which can be chemotactic agents, growth agonists, or antagonists. Macrophages can make agents that induce monocyte proliferation (monocyte-colony stimulating factor (M-CSF), and granulocyte monocyte colony stimulating factor (GM-CSF)), smooth muscle proliferation (PDGF-AA, PDGF-BB, Heparin-binding EGF-like growth factor (HB-EGF), fibroblast growth factor (FGF), and TGF-β), and endothelial proliferation (vascular endothelial growth factor (VEGF), FGF, and TGFα) (69-71). Macrophages can also make growth inhibitors (IFNγ, IL-1, and TGFβ). Activated macrophages can also produce a series of chemotactic molecules for other monocytes (M-CSF, GM-CSF, MCP-1, oxLDL) for endothelial cells (VEGF, bFGF), and for VSMCs (TGFβ, PDGF, FGF) (66). Studies have shown that macrophages as well as VSMCs replicate within the atherosclerotic lesions (72, 73). Macrophage proliferation was demonstrated in hyperlipidaemic rabbits by incorporation of tritiated thymidine into immunocytochemically demonstrable macrophages (73) and by an antibody to proliferating cell nuclear antigen (PCNA), which is present in cells that are actively traversing the cell cycle (72). Thus replicating macrophages may be particularly important in progression of lesions. The relative numbers of macrophages, their localization within the lesions, and the genes that they express will have an impact on lesion progression. For example, if macrophages secrete growth-regulatory molecules and/or cytokines that stimulate other macrophages, VSMCs, or endothelium to migrate and replicate, the lesions will expand. At the same time, the macrophages, due to their capacity to oxLDL, can be an important source because oxLDL is thought to be the principal mode by which LDL induces atherogenesis. Macrophages are migratory cells. Once they arrive at the atherosclerotic lesions, the movement of these cells can be inhibited through macrophage migration inhibitory factor (MIF) and such molecules may be of importance in the progression of atherosclerosis. The presentation of antigen

by macrophages may play a role, particularly in immune-induced atherosclerosis, and possibly in common atherosclerosis. The role of immunity in this disease is poorly understood. Our knowledge of monocyte entrance into and macrophage exit from the lesions is rudimentary. Understanding macrophage turnover in the atherosclerotic lesion could lead to better control of their accumulation within the lesions. Because macrophages play a critical role in inflammatory responses, control of this component is essential in modifying the process of atherogenesis.

1.1.3.3 VSMCs

VSMCs located in the media constitute the bulk of the normal artery wall. By maintaining their attachments to neighbour cells and surrounding connective tissue matrix, VSMCs provide the tonus of the artery that normally dampens the differences between diastole and systole. In physiological conditions, the majority of VSMCs reside in the media, where they are quiescent and possess a "contractile" phenotype characterised by the abundance of actin and myosin-containing filaments (66, 74). In disease states, VSMCs re-enter the cell cycle, proliferate, and migrate from media to intima. After vessel injury, intimal VSMCs have a synthetic phenotype, characterised by hyperplasia or hypertrophy and matrix protein accumulation in the intima and/or media with or without lipid deposition, resulting in thickening and stiffness of the arterial wall. Various stimuli can induce VSMC migration and proliferation. These stimuli include Angiotensin II, homocysteine, chemotactic factors and mitogens, possibly released from neighbouring endothelium, from activated macrophages within the lesions, and from nearby VSMCs. VSMCs can be the source of a series of growth factors (e.g. PDGF, FGF, insulin-like growth factor-I (IGF-I), M-CSF, TGFβ, and HB-EGF) and cytokines (e.g. IL-1 and TNFα). When the genes of these molecules are induced by various agents, the cells can stimulate their neighbours in a paracrine fashion

or themselves in an autocrine fashion (75, 76). The susceptibility of the cells to activation partly depends on their phenotype. The changes in phenotypic state may also relate to cell-surface adhesive molecules such as specific integrins that form on the surface of the VSMCs (77). When VSMCs are in a contractile state, they can respond to agents such as endothelin (ET), catecholamines, Angiotensin II, prostaglandin E2 (PGE2), prostacyclin I2, neuropeptides, nitric oxide, and leukotrienes that induce vasoconstriction or vasodilatation. When the cells are in the synthetic state, they may express genes for the growth-regulatory molecules and cytokines and may be responsive to many of these factors as well.

Foam cells have been traditionally regarded as being derived from macrophages because they express macrophage markers. It's now known that VSMCs can also be converted into foam cells. The evidence includes: i) VSMCs in tissue culture can accumulate cholesterol (78); ii) Some lesional foam cells traditionally classified as macrophages are actually arterial VSMCs that have significantly altered their phenotype (79); iii) Significant numbers of foam cells are present in atherosclerotic lesions in mice deficient in genes responsible for monocyte recruitment (80), leucocyte adhesion (81), macrophage proliferation and differentiation (82); iv) in advanced lesions from both Watanabe heritable hyperlipidaemic (WHHL) and comparably hypercholesterolemic fat-fed (FF) rabbits (73) simultaneous thymidine autoradiography and immunostaining for cell type-specific markers revealed that approximately 30 % of the labelled cells were macrophages and 45 % were VSMCs.

1.1.4 Inflammatory markers in atherosclerosis

Considering the role of inflammation in initiating and exacerbating atherosclerosis, it seems logical to search for inflammatory molecules and mediators which are suitable for monitoring inflammation in general and furthermore to determine inflammatory

moieties which are actively involved in the atherosclerotic process. Many different markers have been selected for preclinical and clinical conditions to assess atherosclerotic risk.

1.1.4.1 CRP and SAA

1.1.4.1.1 CRP

CRP is an early acute phase protein. It increases in response to active infections or acute inflammatory processes. Minor elevations of CRP are also present in chronic inflammatory situations, such as atherosclerosis (83). CRP is closely related to traditional cardiovascular risk factors. Some studies have shown a significant correlation with markers of insulin sensitivity, triglycerides and HDL-cholesterol concentrations, whereas the relationship to total cholesterol and LDL-cholesterol remains equivocal (84-86). There is a general consensus that 'highly sensitive CRP assay' are very helpful in monitoring atherosclerosis.

CRP is synthesized by the liver and regulated by cytokines, predominately by IL-6 and TNFα (87). Although the principal source of CRP is the liver, recent data have shown that arterial tissue can also produce CRP (88). Two hypotheses have been proposed to explain the role of an elevated CRP in the pathogenesis of atherosclerosis. One mechanism may be the ongoing inflammation in the artery stimulated by oxLDL, which leads to the production of cytokines that may induce acute phase proteins such as CRP. Alternatively, chronic elevations of acute phase reactants could be due to smoking, chronic infections, ageing, obesity, hyperlipidemia or diabetes, all of which contribute to the development of atherosclerosis. However, these hypotheses are not mutually exclusive and both mechanisms might act together to account for the increase of CRP.

CRP is not only a serum biomarker of the atherosclerotic process but has also been involved in the pathogenesis of atherosclerosis by means of several mechanisms: a) CRP powerfully down-regulates endothelial nitric oxide synthase (eNOS) transcription in endothelial cells and destabilizes eNOS mRNA, which leads to a decrease in both basal and stimulated nitric oxide release (89); b) CRP causes the expression of adhesion molecules (ICAM-1 and vascular cell adhesion molecule-1 (VCAM-1)) by endothelial cells (90), induces MCP-1 (91) and enhances cholesterol uptake by macrophages (92); c) CRP can stimulate monocytes to produce tissue factors and proinflammatory cytokines through the up-regulation of nuclear factor-κB (NF-κB) (93); d) CRP stimulates VSMC migration, proliferation, neointimal formation and reactive oxygen species (ROS) production (94); e) CRP is an activator of the complement system, which has been shown to colocalize with the membrane attack complex in early atherosclerotic lesions (95).

1.1.4.1.2 SAA

Serum amyloid A (SAA), like CRP, is an acute phase protein synthesized by the liver. SAA is a homologous protein of a family that includes SAA1 and SAA2 which are major acute phase reactants (96), and SAA4 which is constitutively expressed in humans (97) but not in mice. In humans and mice, plasma SAA1 and SAA2 levels can increase by several hundred-fold in response to an acute inflammatory stimulus (96, 98). SAA can induce the expression of proteinases which are thought to degrade extracellular matrix, playing important role in tissue injury. Several recent clinical studies have demonstrated an association between elevated levels of SAA and increased risk of cardiovascular events (99-102). Epidemiologically, elevated SAA levels are associated with a number of atherosclerotic risk factors, including obesity and insulin resistance (100), which are features of the metabolic syndrome. A recent meta-analysis (103)

suggests that subjects with higher level of SAA have a significant increase in cardiovascular risk. These observations raise the possibility that SAA may serve as a marker for an increased risk of cardiovascular disease in humans. In mice, unlike in humans, CRP is found at very low concentration in the serum and has not yet been documented as an acute-phase reactant (104, 105). The documented acute-phase reactants in mice are SAA and serum amyloid P component (SAP) (105-107), therefore, SAA may be a good serum inflammatory marker in animal studies using mice models. However, it's unknown whether SAA is simply a marker for increased cardiovascular risk or actually participates in the pathogenesis of atherosclerosis.

1.1.4.2 IL-1β, IL-6 and TNFα

It has been demonstrated that serum levels of proinflammatory cytokines are elevated in hypercholesterolemic patients (108-111). The elevated plasma levels of these cytokines are closely associated with increased cardiovascular risk (101, 112). These main proinflammatory cytokines include IL-1, IL-6 and TNFα. IL-1 and IL-6 are pleiotropic cytokines with a broad range of humoral and cellular immune effects relating to inflammation, host defence and tissue injury. IL-6 is also a central mediator of the acute phase response and the primary determinant of CRP production.

IL-6 is expressed in human atherosclerotic lesions (113) as well as in genetically hyperlipidaemic rabbits (114). IL-6 is produced and secreted by endothelial cells, smooth muscle cells and macrophages and can contribute to the development of atherosclerotic lesion through several pathways (101, 115, 116). IL-6 levels predict cardiovascular mortality in healthy individuals and future cardiovascular events in healthy men, even after adjusting for traditional risk factors (117). In the Women's Health Study, IL-6 is also associated with the risk of cardiovascular events in more than 28,000 postmenopausal women followed-up prospectively, although it's not an

independent predictor after adjustment in a multivariate model including high-sensitive CRP (101). Moreover, elevated IL-6 levels are associated with poor outcomes in patients with unstable angina (118).

The IL-1 cytokine family comprises of different proinflammatory cytokines involved in atherogenesis. IL-1β is mainly produced by monocytes and macrophages, but also by many other cell types such as VSMCs, endothelial cells and activated platelets. IL-1β shares many effects with IL-6 and TNFα. IL-1β increases the expression of endothelial adhesion molecules thus facilitating the attachment of other inflammatory cells on the activated endothelium (119). Furthermore, IL-1β, together with TNFα, stimulates IL-6 production in VSMCs and increases the expression of CSF, PDGF, and FGF in macrophages, which are associated with the progression of the inflammatory process in atherosclerosis (120, 121). In addition, increased levels of IL-1β have been found in patients with coronary artery disease (122).

TNFα is another multifunctional cytokine with pleiotropic biological activities and plays a major role in the cytokine cascade as it stimulates the synthesis of the other cytokines. TNFα is secreted by activated macrophages, endothelial and VSMCs. Experimental data have shown that it is also expressed by adipocytes and skeletal muscle cells. Adipose tissue expression of TNFα has been implicated as a causal factor in the pathogenesis of obesity-linked insulin resistance (123). Furthermore, TNFα has also been shown to be an independent marker for recurrent myocardial infarction and coronary restenosis after atherectomy or percutaneous angioplasty (124, 125).

Cellular action of TNFα is mediated by the tumour necrosis factor receptor (TNFR) superfamily. Circulating level of TNFα is often undetectable or highly variable in healthy subjects. By contrast, soluble TNFRs are more stable proteins, remaining

elevated in the systemic circulation for longer periods and, therefore, being better markers for the activation of the TNFα system than TNFα itself (126).

1.1.4.3 Chemokines

Chemokines represent an expanding family of structurally related small molecular weight proteins that play a major role in leucocyte trafficking and activation (127). The involvement of chemokines in atherosclerosis is well documented. A considerable number of studies have been directed to determine their role in the initial stages of plaque formation. MCP-1 has been shown to be expressed mainly by macrophages in human lesions, but also by VSMCs as well as the luminal endothelium of early human atherosclerotic lesions (128-130). oxLDL can induce the expression of chemotactic molecules by endothelial cells, such as MCP-1 (131). The expression of the corresponding receptor for MCP-1 on monocytes, The C-C motif chemokine receptor–2 (CCR2), is up-regulated by hypercholesterolaemia, as demonstrated by a clinical study (132). Furthermore, MCP-1 or CCR2 knockout mice develop significantly less atherosclerotic lesions (80, 133, 134). IL-8 and its corresponding receptor CXCR2, which are both present in human atherosclerotic lesions, may also play a role in leucocyte trafficking (135, 136). In addition, MCP-4, macrophage inflammatory protein-(MIP)-1α, MIP-1β, and RANTES (regulated upon activation, normal T cell expressed and secreted) are also known to be expressed within atherosclerotic plaques (136).

1.2 The regulation of cholesterol homeostasis

The maintenance of lipid homeostasis is essential for keeping a stable range of lipid concentration in the plasma. Disturbances of lipid homeostasis are integral components of life-threatening diseases, such as the metabolic syndrome, atherosclerosis.

Over the last few decades, our understanding of the basic mechanisms involved in atherosclerosis has progressed significantly. Plasma cholesterol levels are an important factor in atherosclerosis. Regulation of cholesterol levels is a complicated process, involving cholesterol uptake, biosynthesis, efflux, transport, metabolism, and secretion, which significantly affect atherogenesis. For the most cells in mammals, intracellular cholesterol homeostasis is mainly governed by tight regulation of cholesterol biosynthesis, cholesterol influx and efflux pathways. The cellular requirements for cholesterol are mainly satisfied from the two resources: 1) Exogenously, such as cholesterol influx pathways involving cholesterol uptake mediated by various lipoprotein receptors; 2) Endogenously, such as cholesterol synthesis regulated by 3-hydroxy-3-methylglutaryl-coenzyme A reductase (HMGR) which is a rate-limiting enzyme (137). The cholesterol efflux pathways are mainly for the prevention of overloaded cholesterol accumulation in the cells, such as adenosine triphosphate (ATP) binding cassette transporter A1 (ABCA1) or ATP binding cassette transporter G1 (ABCG1) mediated cholesterol and phospholipid efflux pathways. In addition, reverse cholesterol transport (RCT), lipid metabolism and secretion by the liver may involve atherogenesis. These pathways in cholesterol homeostasis will be discussed further.

1.2.1 The regulation of lipid uptake by lipoprotein receptors

Lipids are essential for energy homeostasis, reproductive and organ physiology, and numerous aspects of cellular biology. To meet the different demands from a variety of tissues, the human body has evolved a sophisticated lipoprotein transport system to deliver cholesterol and fatty acid to the periphery. Mammals employ a multifaceted approach to control the activity of lipoprotein receptors in the metabolic pathways to maintain the concentration of lipid in the plasma at stable level. Thus, the role of some key lipoprotein receptors in charge of lipid uptake will be elucidated at the following.

1.2.1.1 LDLr pathway

The low density lipoprotein receptor (LDLr) is a key component in the feedback-regulated maintenance of cholesterol homeostasis in the body (138). As an active interface between extra- and intra-cellular cholesterol pools, it is itself subject to regulation at the cellular level. LDL-cholesterol (generated by hydrolysis of LDL-borne cholesteryl esters) and its intracellular generated oxidated derivatives mediate a complex series of feedback control mechanisms that protect the cell from overaccumulation of cholesterol. The key features of this pathway can be summarized as follows. First, (oxy) sterols suppress the activities of 3-hydroxy-3-methylglutaryl coenzyme A (HMG CoA) synthase and HMGR, two key enzymes in cellular cholesterol biosynthesis. Second, the cholesterol activates the cytoplasmic enzyme acyl-CoA: cholesterol acyltransferase (ACAT) which allows the cells to store excess cholesterol in re-esterified form. Third, the synthesis of new LDLr is suppressed, preventing further cellular entry of LDL and cholesterol overloading. The overall benefits and consequences of the LDLr-mediated regulatory system are coordination of the utilization of intra- and extra-cellular sources of cholesterol at the systemic level. Mammalian cells are able to subsist in the absence of exogenous cholesterol as they can synthesize cholesterol from acetyl-CoA. When LDL is available, most cells primarily use the LDLr to import LDL-cholesterol and keep their own synthetic activity suppressed. Thus, a constant level of cholesterol is maintained within the cell, while the external supply in the form of lipoproteins can undergo large fluctuation.

1.2.1.1.1 LDLr

LDLr is one of the important members in the LDL receptor family, which consists of more than 10 receptors. In addition to LDLr itself (139), LDLr-related protein (LRP) (140), megalin (GP330) (141), very low density lipoprotein receptor (VLDLr) (142),

apolipoprotein E receptor 2 (apoER2) (143), sorLA-1/LR11 (144), LRP3 (145), LRP4 (146), LRP5 (147), LRP6 (148), LRP1B/LRP-DIT (deleted in tumors) (149), and LRP9 (150) cDNA have been cloned. Among these receptors, VLDLr and apoER2 are most structurally similar to LDLr.

The human LDLr gene is located in the short arm of chromosome 19. It spans approximately 45 kb and consists of 18 exons, each coding for a different protein domain and 17 introns (151). The promoter is located on the 5′-flanking region, within which the majority of *cis*-acting DNA elements are found between base pairs (bp) –58 and –234, with the A of the initiator methionine codon as +1. The promoter region spans 177 bp, including three imperfect direct repeats with 16 bp of each, two TATA-like sequences, and several transcription initiation sites, all of which are essential for gene expression and regulation (Fig 1.1, (152)). Among the three direct repeats, repeats 1 and 3 contain sequences that can be recognized by the general transcription factor Sp1. Their role is to maintain the basic transcription level of the LDLr gene regardless of the presence or absence of sterols (152, 153). However, they are not sufficient for a high-level expression of the LDLr gene in the absence of sterols, in which the contribution from repeat 2 is needed. Repeat 2 contains a 10-bp DNA element termed sterol regulatory element (SRE) (Fig 1.1, (154)).

The human LDLr mRNA has a 5.3-kb sequence, which contains an 2.5-kb-long 3' untranslated region (UTR) (139). There are three AU-rich elements (AREs) in the 5' proximal region and three copies of *Alu*-like repeat in the 3' distal region of the 3' UTR. These structures play a key role in the stability of the LDLr mRNA and serve as *cis*-acting elements for the posttranscriptional regulation of the LDLr gene expression (139, 155).

Like other eukaryotic genes, the expression of the LDLr is under a complex regulation, either at the transcriptional or posttranscriptional level, mediated through intriguing signalling pathways. Cholesterol and derivatives, and nonsterol mediators, like cytokines, growth factors, and some hormones, are able to regulate LDLr expression (156, 157).

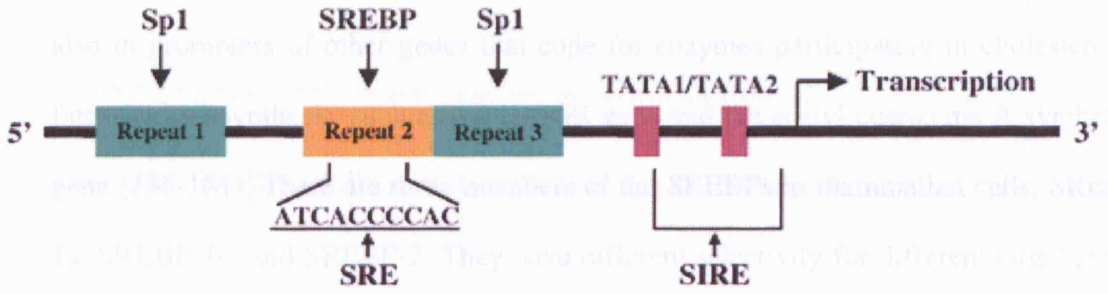

Fig 1.1 Promoter region of the LDLr gene (J Mol Med 2006; 84: 29–36.)

Three direct repeats (*Repeat 1–3*) and two TATA-like sequences are identified within the promoter region. The *cis*-acting element of sterols is located on repeat 2, whereas the regulatory element for cytokine OM (SIRE) overlaps the TATA-like sequences.

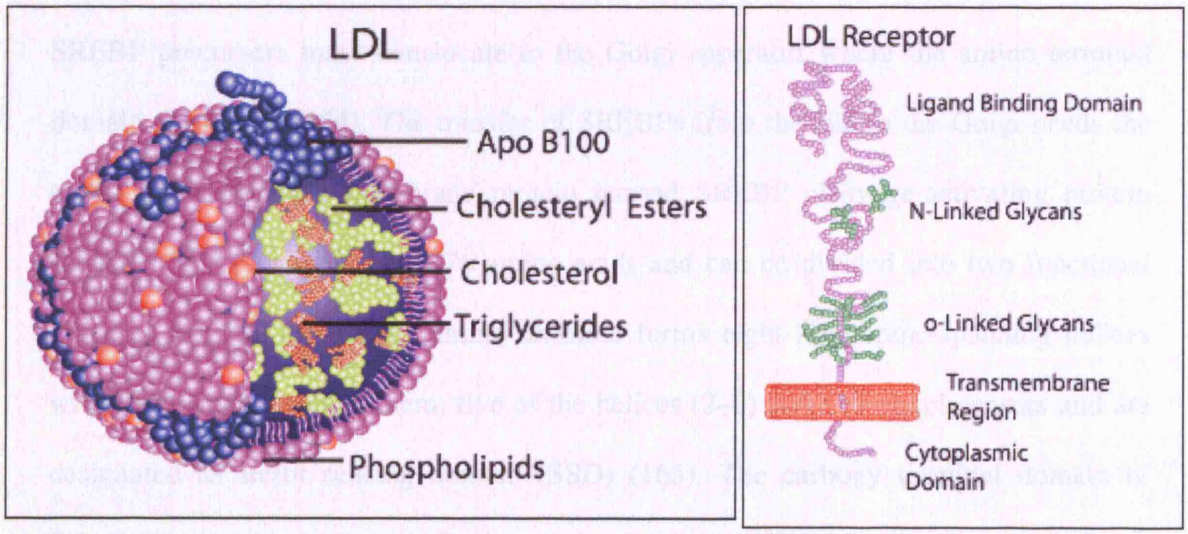

Fig 1.2 The structures of LDL and LDL receptor

(http://www.sigmaaldrich.com/Area_of_Interest/Biochemicals/Enzyme_Explorer/Key_Resources/Plasma__Blood_Protein/Lipoprotein_Function.html).

1.2.1.1.2 Transcriptional regulation of the LDLr

The sterol regulatory element-binding protein (SREBP) pathway is crucial in the transcriptional regulation of LDLr in response to cholesterol and its derivatives (158). The SREBPs are transcription factors belonging to the basic-helix–loop–helix–leucine zipper (bHLH-Zip) family (159). They were identified by Brown and Goldstein's laboratory to bind to SRE, which is not only present in the promoter of LDLr gene but also in promoters of other genes that code for enzymes participating in cholesterol or fatty acid biosynthesis, such as the HMGR gene and the acetyl coenzyme A synthetase gene (158-161). There are three members of the SREBPs in mammalian cells, SREBP-1a, SREBP-1c, and SREBP-2. They have different selectivity for different target genes. SREBP-2 is a major activator of the LDLr gene (162). The SREBPs are synthesized as inactive precursors embedded in the endoplasmic reticulum (ER) membrane with a molecular weight of about 125 kDa. They consist of approximately 1,150 amino acid residues and can be divided into three functional domains forming a hairpin structure, within which the amino terminal domain contains the bHLH-Zip transcription activator (Fig 1.2) (163). To enter the nucleus and activate the transcription of target genes, the SREBP precursors must translocate to the Golgi apparatus where the amino terminal domain is cleaved (164). The transfer of SREBPs from the ER to the Golgi needs the escort of another ER membrane protein termed SREBP cleavage-activating protein (SCAP). SCAP consists of 1,276 amino acids and can be divided into two functional domains (Fig1.3) (165). The amino terminal forms eight membrane-spanning helices with short loops between them; five of the helices (2–6) serve as sterol sensors and are designated as sterol sensing domain (SSD) (165). The carboxy terminal domain of SCAP mediates protein–protein interaction with the SREBP precursor and forms SREBP/SCAP complex (165, 166).

When cholesterol or its derivatives are abundant in cells, the SREBP pathway is suppressed, and the transcription of LDLr gene or other genes required for cholesterol synthesis are turned off. Cholesterol can bind directly to the SSD of SCAP, causing a conformational change of SCAP, which permits it to bind to a pair of ER membrane proteins named insulin-induced gene (Insig)-1 and -2 then forms SREBP/SCAP/Insig ternary complex (Fig 1.3) (167-171). The binding of Insig proteins traps SREBP/SCAP in ER membrane so that the SREBPs are not able to get to the Golgi apparatus for cleavage, and the expression levels of their target genes decrease accordingly. As a result, the uptake and synthesis of cholesterol are inhibited, and the cells establish cholesterol homeostasis (167-171).

On the contrary, when the cells are low of sterols, SCAP does not interact with the Insig proteins. The SREBP/SCAP complex is free to leave the ER (172). After getting into the Golgi apparatus, the transcriptional active domain of the SREBP precursor will be released by two sequential proteolytic cleavages catalyzed by two proteases residing in the Golgi membrane, while SCAP will return to the ER for recycling (Fig 1.3) (173, 174). The two proteases are site-1 protease (S1P) and site-2 protease (S2P), representing a serine protease and a zinc metalloprotease, respectively (175, 176). The cleavage of SREBP precursor results in the release of a fragment containing the bHLH-Zip domain; its molecular weight is about 68 kDa and termed as nuclear SREBP (nSREBP), or the mature form of SREBP. The nSREBP enters into the nucleus and activates the transcription of target genes (173-176). As a result, the cells uptake more cholesterol-containing lipoproteins and increase the cholesterol production to reach a new level of cholesterol homeostasis. The nSREBP is not stable and is polyubiquitinated and rapidly degraded by the proteasome with an estimated half-life of 3 hours (177).

In addition to cholesterol and derivatives, a number of nonsterol mediators such as hormones, cytokines, growth factors, and second messengers also regulate the transcription of the LDLr gene (156, 157, 178). Some of them are of physiological or pharmacological significance.

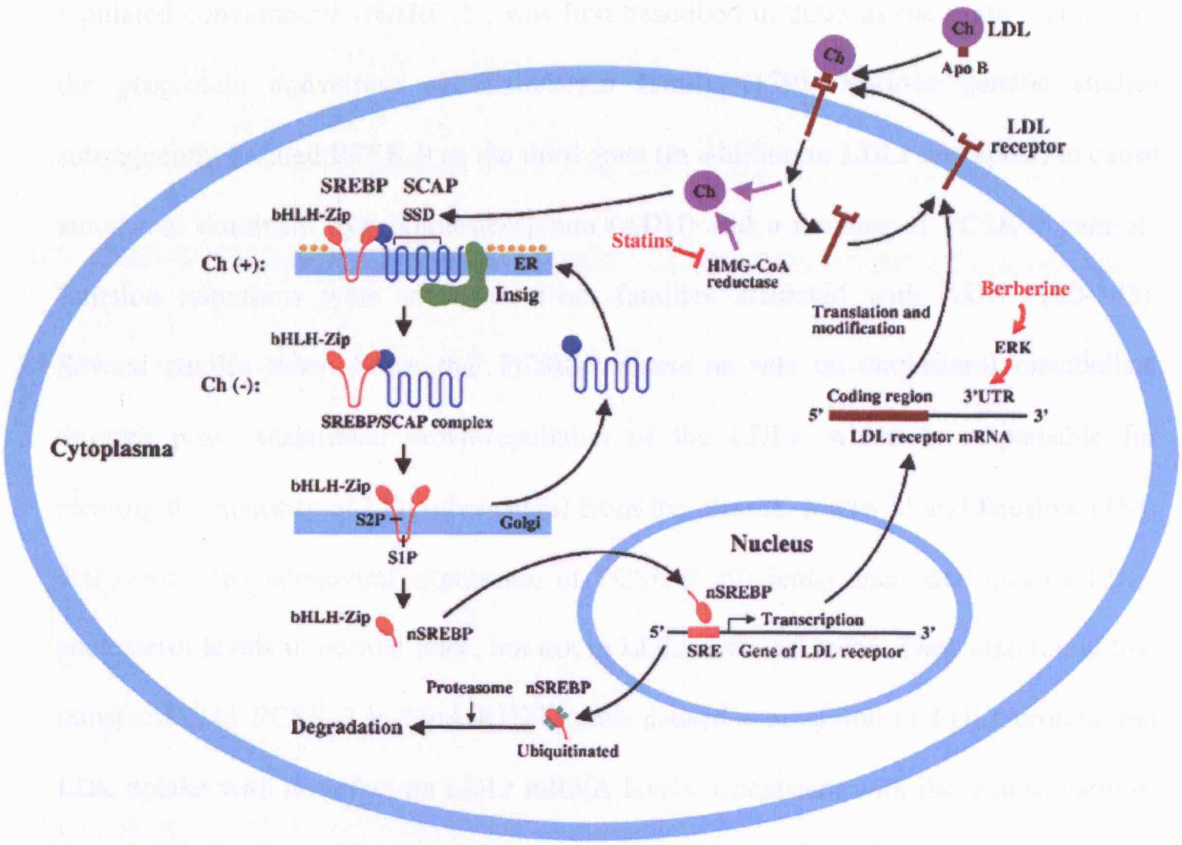

Fig 1.3 Intracellular regulation of LDLr gene expression (J Mol Med 2006; 84: 29–36.)

This figure illustrates how LDLr gene expression is regulated in the cells. As shown in this figure, the SREBP pathway plays an important role in the transcriptional regulation, while the 3' UTR of LDLr mRNA is a key factor for the posttranscriptional regulation. Targets and/or pathways for the clinical agents with cholesterol-lowering effect are demonstrated in the figure. bHLH-Zip, basic-helix–loop–helix–leucine zipper; Ch, cholesterol; ER, endoplasmic reticulum; ERK, extracellular signal-regulated kinase; HMG-CoA, 3-hydroxy-3-methylglutaryl coenzyme A; Insig, insulin-induced gene; LDL, low density lipoprotein; nSREBP, nuclear SREBP; S1P, site-1 protease; S2P, site-2 protease; SCAP, SREBP cleavage-activating protein; SRE, sterol regulatory element; SREBP, sterol regulatory element-binding protein; SSD, sterol sensing domain; UTR, untranslated region.

1.2.1.1.3 Post-transcriptional regulation of the LDLr

In addition to transcriptional regulation by sterols and various nonsterol mediators, the LDLr expression can be regulated at posttranscriptional levels as well.

Proprotein convertase subtilisin/kexin-9 (PCSK-9), also known as neural apoptosis-regulated convertase-1 (NARC-1), was first described in 2003 as the ninth member of the proprotein convertase subtilisin/kexin family (179). Various genetic studies subsequently defined PCSK-9 as the third gene (in addition to LDLr and apoB) to cause autosomal dominant hypercholesterolemia (ADH) and a number of PCSK-9 gain-of-function mutations were identified from families affiliated with ADH (180-183). Several studies have shown that PCSK-9 exerts its role on cholesterol metabolism through post-translational down-regulation of the LDLr, which is responsible for clearing the majority of LDL-cholesterol from the plasma. Maxwell and Breslow (184) discovered that adenoviral expression of PCSK-9 efficiently increased plasma LDL-cholesterol levels in normal mice, but not in LDLr-deficient mice. They also found that transfection of PCSK-9 in McA-RH777 cells caused a reduction in LDLr protein and LDL uptake with no effect on LDLr mRNA levels. Consistent with these observations, genetic deletion of PCSK-9 in mice resulted in increased LDLr protein levels, but not mRNA levels (185). PCSK-9 mediated reduction of LDLr protein has also been reported by Lagace *et al* (186) in a recent mouse parabiosis study where a loss of liver LDLr protein was observed in recipients of parabiosed PCSK-9 protein. The precise mechanism underlying PCSK-9 induced degradation of the LDL-R is unknown.

The mRNA stability is another mechanism for the posttranscriptional regulation of the LDLr gene expression (155). The LDLr mRNA has a constitutively short half-life of about 45 min in human hepatoblastoma cell line (HepG2) cells (187). The stability of a specific mRNA is largely determined by the structure of its 3' UTR. There are three

AREs being identified in the 5' proximal region of the LDLr 3' UTR (155). AREs have also been found in 3' UTRs of many other short-lived mRNA species, like the mRNAs for cytokines. These elements confer their destabilizing effects on mRNAs, including the LDLr mRNA (155, 188). Evidence has shown that after fusing the 5'-most ARE of the LDLr 3' UTR to the coding region of the beta-globin cDNA, the degradation rate of the fusion transcript increases threefold as compared to the wild-type beta-globin mRNA. Fusion of LDLr 3' UTR fragment containing all three AREs with the beta-globin gene increases the degradation rate of the fusion transcript by more than tenfold (155). The destabilizing effect of AREs has also been demonstrated in animals *in vivo*. Transgenic mice expressing human LDLr gene, with two AREs in the 3' UTR being truncated, can increase its mRNA stability up to threefold as compared to the native mice LDLr mRNA, resulting in a total of 2.5-fold increase in the LDLr expression in the mouse liver (189).

The stability of the LDLr mRNA can be regulated by several mediators, including phorbol ester PMA, chenodeoxycholic acid (CDCA), berberine, and a fibrate drug, gemfibrozil (155, 187, 190-192). PMA prolongs the half-life of the LDLr mRNA by more than twofold in HepG2 cells. The *cis*-acting element of PMA in the 3' UTR of LDLr mRNA has been located to the 3' distal region which contains three *Alu*-like repeats, and the stabilization effect of PMA also associates with the actin cytoskeleton in HepG2 cells (155, 187). Berberine is a natural compound isolated from herbs such as *Coptis chinensis*. It was shown to be capable of up-regulating LDLr expression through a posttranscriptional and sterol-independent mechanism in hepatocytes (Fig 1.3). The 5' proximal region of the LDLr 3' UTR containing three AREs is indispensable for berberine to stabilize the receptor mRNA. Berberine has also shown a promising LDL-cholesterol lowering effect and safety both in an animal model and in hypercholesterolemic patients (191). The *trans*-acting protein factors used by these

mediators to stabilize LDLr mRNA have not been identified yet and need extensive investigation. Interestingly, the stabilization of LDLr mRNA by berberine and CDCA also needs the activation of the extracellular signal-regulated kinase (ERK) signalling pathway in cells. Blocking this pathway abolishes their stabilization effects (191, 192). But how the ERK pathway, activated by these mediators, links to the LDLr 3' UTR to stabilize the receptor's mRNA remains to be clarified.

1.2.1.1.4 LDLr in atherosclerosis

Atherosclerotic lesions are characterised by the presence of lipid-loaded cells that are derived from monocyte/macrophages and smooth muscle cells. LDLr is highly expressed in atherosclerotic lesions and involved in cellular lipid uptake (193).

The LDLr pathway has two main functions: first, it supplies cells with cholesterol, thereby mediating the removal of cholesterol-rich lipoproteins from the bloodstream. Second, it protects cells from overaccumulation of cholesterol, because the cholesterol derived from lysosomal hydrolysis of LDL-cholesteryl esters governs a series of feedback mechanisms designed to maintain a constant level of cholesterol within the cell. Thus, high extracellular concentrations of LDL reduce cellular synthesis of cholesterol, stimulate its re-esterification, and decrease the number of LDL receptors, preventing further cellular entry of cholesterol.

The suppression of LDLr activity by high plasma levels of LDL is beneficial for most peripheral cells which plays very important role in the maintenance of cholesterol homeostasis to prevent atherogenesis. However, the consequences caused by reduction of LDLr activity in the liver can be devastating. This is of course best documented in Familial Hypercholesterolaemia (FH), which results from defects in the hepatic uptake and degradation of LDL via the LDLr pathway, commonly caused by a loss-of-function

mutation in the LDLr gene or by a mutation in the gene encoding apolipoprotein B. FH is characterised by raised serum LDL cholesterol levels, which result in excess deposition of cholesterol in tissues, leading to accelerated atherosclerosis and increased risk of premature coronary heart disease (194).

In summary, the LDLr mediated pathway in the liver or peripheral organs co-ordinately regulates to keep plasma cholesterol at constant level. At pathological conditions, disrupted feedback regulation of LDLr pathway may result in elevated cholesterol levels in the plasma or in the cell to accelerate foam cell formation and atherogenesis.

1.2.1.2 VLDLr pathway

1.2.1.2.1 VLDLr

In the LDL receptor family, VLDLr and apoER2 are most similar to the LDLr structurally (195). The human VLDLr gene contains 19 exons spanning approximately 40 kb. The exon-intron organization of the gene is almost the same as that of the LDLr gene except for an extra exon that encodes an additional repeat in the ligand-binding domain (LDLr contains a sevenfold repeat and VLDLr has an eightfold repeat). The VLDLr mRNAs produce two kinds of VLDLr proteins by alternative splicing type 1 VLDLr and type 2 VLDLr, which lack the O-linked sugar domain encoded by exon 16. Although the structure and organization of the VLDLr gene is highly similar to those of the LDLr gene, the two genes are located on different chromosomes: the LDLr gene is on chromosome 19 and the VLDLr gene on chromosome 9.

The VLDLr is expressed in heart, skeletal muscle, adipose tissue, uterus, and ovaries (142, 196). It binds apoE-containing VLDL and IDL but not apoB-100-containing LDL (142). With the difference from the negative feedback mechanism of LDLr pathway mediated by sterols, VLDLr expression can not be down-regulated by sterols as shown by Sadao *et al* in THP-1 cells (human acute monocytic leukaemia cell line) and rabbit resident alveolar macrophages (197, 198). 25-hydroxycholesterol can not not lead to sterol negative feedback on VLDLr expression (199). There is a sterol regulatory element (SRE)-1 in the human LDLr gene, however, in the VLDLr gene there are two sterol regulatory element (SRE)-1-like sequences (197). The SRE-1-like sequences in the VLDLr contain single nucleotide substitutions that disrupt the direct CAC repeats, which might be the reason why VLDLr expression is not regulated by intracellular

In addition, VLDLr expression is characterised with the tissue specificity in response to different conditions. For example, a fasting state induced high VLDLr expression in the heart and low expression in the fat tissue in mice, however, VLDLr expression in rats has not any change at fasting state (200, 201). Thyroid hormone was a positive regulator of the VLDLr in rat skeletal muscle but not in the fat or heart (200).

VLDLr expression in rabbits can be up-regulated by estrogen in the heart and down-regulated by GM-CSF in muscle (202, 203). In JEG-3 and BeWo choriocarcinoma cells, two trophoblast-derived cell lines, 8-bromo-cAMP suppresses VLDLr expression. Insulin and clofibrate up-regulate VLDLr expression. IFN-γ inhibits VLDLr expression in PMA-treated THP-1 cells, HL-60 cells and human monocyte-derived macrophages. However, this effect is not observed in normal THP-1 cells (204). In contrast with the non-sterol regulation of VLDLr expression *in vitro*, Tiebel *et al*

(205) examined dietary regulation of the VLDLr in C57BL/6, LDLr knockout, apoE KO and LDLr/ApoE double knockout mice. VLDLr mRNA expression is down-regulated threefold by administrating an atherogenic diet in the heart and skeletal muscle, in LDLr knockout mice. VLDLr mRNA is up-regulated by an atherogenic diet in the adipose tissue in all models except LDLr knockout mice and ApoE KO mice. These findings suggest that SRE-1-like sequences in the VLDLr gene may be functional in the heart and skeletal muscle when LDLr is absent, and that apoE is required for regulation of VLDLr expression.

Due to VLDLr expression in adipose tissue, striated muscle, and brain, but not in the liver (206-208) and its high affinity for apoE (142, 209), this receptor has been implicated in the extrahepatic metabolism of triglyceride-rich lipoproteins. The VLDLr is competent in binding and internalization of apoE-containing lipoproteins *in vitro* and *in vivo*. Close inspection of the expression sites in the relevant tissues (muscle, heart, and adipose tissue) reveals that the VLDLr resides on endothelial cells of capillaries and small arterioles rather than on parenchymal cells of these organs (196). The capillary endothelium in muscle and adipose tissue is continuous and therefore impermeable for particles with the size of lipoproteins. This is consistent with a scenario where TG-rich lipoproteins are taken up directly by endothelial cells and triglycerides or free fatty acids subsequently delivered to adipocytes or monocytes. Another possibility is that TG-rich particles are trapped on the surface of endothelial cells by the VLDLr and, subsequently, are lipolyzed by lipoprotein lipase (LPL) which also resides on endothelial cells. Furthermore, LPL might tether TG-rich articles to the cell surface by bridging them to proteoglycans (210, 211). Subsequently, triglycerides would become mobilized by the lipolytic action of LPL and the resulting remnants taken up by the VLDLr. However, as demonstrated by Argraves *et al* (212), the VLDLr is able to directly bind and catabolize LPL, suggesting that the VLDLr may serve as a regulator of

cell surface-bound LPL. In any case, all of these proposed functions would predict that the VLDLr plays a significant role in the metabolism of triglyceride-rich particles. Under a high-fat diet as well as after prolonged fasting, lack of the VLDLr results in a significant increase in serum triglyceride levels in VLDLr knockout mice, suggesting that the VLDLr is involved in peripheral triglyceride uptake. Furthermore, The most important finding of this study is that mice lacking a functional VLDLr are protected from obesity, obviously via a significant reduction in whole-body free fatty acid uptake (213). Taken together, the VLDLr seems to be part of machinery transporting triglycerides or free fatty acids to peripheral cells, but the molecular mechanism still remains to be elucidated.

1.2.1.2.3 VLDLr in Atherosclerosis

Familial hypercholesterolaemia patients lacking LDLr accumulate massive quantities of lipids in macrophages indicating that LDLr is not involved in macrophage foam cell formation. It has been proposed that there are two receptors that contribute to macrophage foam cell formation, scavenger receptors and β–VLDLr. It has been speculated that the VLDLr might be a so-called macrophage β–VLDLr by its ligand binding specificity (195). Sakai and Tacken *et al* reported that the VLDLr on THP-1 cells and rabbit alveolar macrophages was not down-regulated by incubation with β-VLDL (197, 214). Moreover, incubation of β-VLDL with LDL deficient CHO cells transfected with the rabbit VLDLr enabled these cells to accumulate cholesteryl ester, resulting in foam cell formation (214). Both apoE2/2 VLDL and apoE3/3 VLDL were recognized by the VLDLr identically (209). 1α, 25-dihydroxyvitamin D3 induces VLDLr mRNA expression in HL-60 cells in association with monocytic differentiation (215). Strickland and colleagues reported that the atherogenic lipoprotein Lp (a) was also recognized by the human VLDLr (216). VLDLr expression, primarily in

macrophages, has been confirmed in human and rabbit atherosclerotic lesions (216-219). Those findings suggest that the VLDLr might be crucial for macrophage foam cell formation especially in diabetes mellitus and type III hyperlipoproteinemia. Sadao *et al* looked for some agents that inhibited the expression of the VLDLr. They found that IFN-γ inhibited VLDLr expression in a dose-and time-dependent manner in macrophages (195). In THP-1 macrophages, VLDLr protein expression decreased at two days after PMA-treatment, but increased at 3 days and increased up to 5 days. ^{125} I-β-VLDL degradation study and Oil Red O staining showed that IFN-γ significantly inhibited foam cell formation following uptake of β-VLDL (remnant lipoprotein). LRP and LDLr expression that bound β-VLDL were not expressed in THP-1 macrophages. In PMA-treated HL-60 macrophages and human monocyte-derived macrophages, IFN-γ also inhibited VLDLr expression and foam cell formation by β-VLDL (204). Those data showed that the VLDLr might be a macrophage β-VLDLr. In addition, the controversial finding using mouse model *in vivo* was also reported. Yagyu *et al.* (220) showed that atherosclerosis was not different between HuB (human apo B) transgenic mice and VLDLr deficient HuB transgenic mice after 4 months of an atherogenic diet. They also detected that VLDLr deficient induced low LPL activity. As mentioned above, LPL activity is an important factor for the binding of TG-rich lipoproteins to the VLDLr. One explanation for the difference is that low LPL activity may reduce the uptake of TG-rich lipoproteins into macrophages in VLDLr deficient HuB transgenic mice. Second explanation is that there are some different factors between human and mouse atherosclerotic lesions. In fact, no enough amount of VLDLr expression was detected in mouse peritoneal macrophages and J774 mouse macrophage cells. Further experiments are needed to sort out this problem.

1.2.1.3 Scavenger receptor pathway

1.2.1.3.1 Scavenger receptor family

Scavenger receptors are integral membrane proteins that bind a wide variety of ligands including modified or oxidised LDL, apoptotic cells and pathogens. The scavenger receptor family has at least eight different subclasses (A–H) which bear little sequence homology to each other but recognize common ligands. The class A scavenger receptors comprise three related genes that encode at least five polypeptides, termed SR-AI, SR-AII, SR-AIII, macrophage receptor with collagenous structure (MARCO) and scavenger receptor with C-type lectin (SRCL) (221-226). The class B scavenger receptors contain CD36 and lysosomal integral membrane protein II (LIMPII)-related genes which include CD36, SR-B and LIMPII (227-229). The class C scavenger receptor gene (dSR-CI) is cloned from the fruit fly *Drosophila melanogaster* which at present lacks equivalent counterparts in other eukaryotes. The class D scavenger receptors comprise CD68 and lysosomal membrane glycoprotein (Lamp) gene products. The class E scavenger receptor currently has a single lectin-like gene product, lectin-like oxidized LDL receptor-1 (LOX-1). The class F scavenger receptors are mainly expressed on the endothelium in mammals and worms, which is called scavenger receptors expressed by endothelial cell (SRECs). The Class G scavenger receptor is termed the scavenger receptor binding phosphatidylserine and oxidized lipoprotein (SR-PSOX), which is also called Chemokine (C-X-C motif) ligand 16(CXCL16). The Class H scavenger receptors contain Fasciclin, EGF-like, laminin-type EGF-like and link domain-containing scavenger receptor-1 (FEEL-1) and the paralogous protein, FEEL-2, which share 39.8% sequence identity (230) (Fig 1.4).

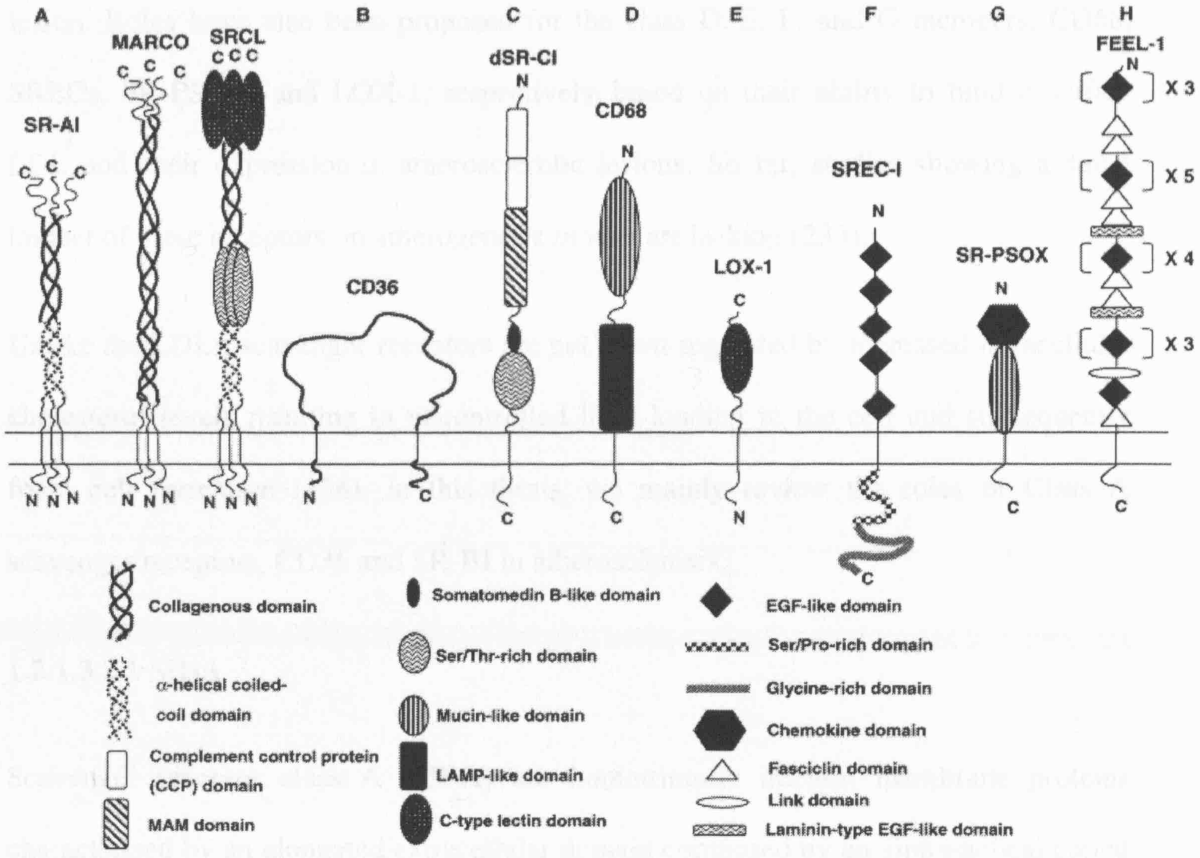

Fig 1.4 Schematic view of different classes of eukaryote scavenger receptors (Atherosclerosis 2005; 182(1):1-15.)

The eight different classes are denoted A–H and specific domains are highlighted by the codes indicated within the figure. The class C receptor (dSR-CI) is only found in the fruit fly at present. All the other receptor classes have mammalian orthologues.

1.2.1.3.2 Scavenger receptors in atherosclerosis

Scavenger receptors were originally implicated in the pathological deposition of cholesterol in the foam cells of atherosclerotic lesions through receptor-mediated uptake of modified LDL (231, 232). Multiple functions of scavenger receptors, including endocytosis, phagocytosis, adhesion and signal transduction triggered by the binding and uptake of modified LDL may also be involved in the development of atherogenesis. To date, there is genetic evidence that the A class SRs, SR-AI and SR-AII, and two members of the B class, CD36 and SR-BI, affect the development of atherosclerotic

lesion. Roles have also been proposed for the class D, E, F, and G members, CD68, SRECs, SR-PSOX, and LOX-1, respectively, based on their ability to bind modified LDL and their expression in atherosclerotic lesions. So far, studies showing a direct impact of these receptors on atherogenesis *in vivo* are lacking (233).

Unlike the LDLr, scavenger receptors are not down-regulated by increased intracellular cholesterol levels resulting in uncontrolled lipid loading in the cell and subsequently foam cell formation (234). In this thesis, we mainly review the roles of Class A scavenger receptors, CD36 and SR-BI in atherosclerosis.

1.2.1.3.2.1 SR-A

Scavenger receptor class A (SR-A) are homotrimeric integral membrane proteins characterised by an elongated extracellular domain composed by an alpha-helical coiled coil region and a collagenous domain (235-237). The SR-A gene generates two different forms of macrophage scavenger receptor proteins by alternative splicing; SR-A type I (SR-AI) has an additional carboxi-terminal cysteine-rich domain, which is not present in SR-A type II. The positively charged collagenous domain is critical for the ligand binding activity of SR-A. A structurally related macrophage scavenger receptor class A called MARCO (macrophage receptor with collagenous structure) shows a similar, but longer, collagenous domain without having the alpha-helical coiled coil region (221).

Several lines of evidence provided indirect support for the role of SR-A in atherogenesis. First, SR-A binds and internalizes oxLDL with high affinity (238, 239), which is a key modified lipoprotein receptor ligand for the pathogenesis of atherosclerosis (240). Second, the incubation of SR-A-transfected cultured cells with modified lipoproteins accelerates the formation of lipid-laden cells similar to the foam cells found in atherosclerotic plaques (241). Third, SR-A expression has been detected

in atherosclerotic lesions (242). Based on these findings, SR-A was proposed to play a critical role in modified lipoprotein metabolism and atherosclerosis.

The role of SR-A in atherosclerosis was initially evaluated by studying the effect of SR-A deficiency on an apoE KO mouse model, which spontaneously develops atherosclerotic plaques. Suzuki *et al* (243) demonstrated the absence of SR-A in apoE KO mice induced a 50% reduction in lesion size compared with the control apoE KO mice. This impressive reduction in atherosclerosis was found in spite of the fact that the plasma cholesterol levels were higher in the apoE KO and SR-A knockout mice compared with the control apoE KO mice. The basis for the higher plasma levels of cholesterol in the apoE KO and SR-A knockout mice was not clear. As macrophage-derived foam cells were present in the apoE KO and SR-A knockout mice, it suggests that other scavenger receptors must also participate in foam cell formation. Furthermore, the role of SR-A in atherogenesis was also studied in SR-A/LDLr double knockout mice after feeding an atherogenic diet (244). The atherosclerotic lesions were smaller in SR-A/LDLr knockout mice compared to LDLr single knockout mice. Foam cells were also observed in atherosclerotic lesions of both SR-A/apoE and SR-A/LDLr knockout mice. These foam cells were shown to express other macrophage scavenger receptors, such as MARCO, CD36, and macrosialin, suggesting that macrophage scavenger receptors other than SR-A also participate in atherogenesis. In contrast to the studies in apoE KO and LDLr knockout mice, de Winther *et al* (245) have reported that apoE·Leiden (E3L) transgenic mice null for SR-A showed a non-significant trend for an increase in lesion area, and the development of more complex lesions compared with the controls. The plasma lipid levels did not differ between female E3L mice null or wild-type for SR-AI/II. These data show that an elevated level of SR-A expression reduces atherosclerosis, potentially by modifying the response of macrophages to activated signals in the plaque. Taken together, these studies indicate that SR-A plays

important roles in atherogenesis, some of which are proatherogenic and some of which are anti-atherogenic depending on the predominant local pathogenic factor(s) involved in atherosclerotic plaque formation in different animal models of the disease.

1.2.1.3.2.2 CD36

CD36 is an 88 kDa membrane glycoprotein. This membrane glycoprotein is expressed by many cell-types including microvasculature endothelial (246) and smooth muscle cells (SMC) (247). Functional and structural characterisation showed CD36 to be a member of the scavenger receptor class B family with a capacity to bind oxLDL as well as various other ligands. CD36 and Scavenger Receptor class A (SRA I/II) are the principal receptors responsible for the binding and uptake of modified LDL in macrophages, which together account for 75% to 90% of the uptake and degradation of acetylated and oxidized LDL (248). Several lines of evidences, both *in vitro* and in animal models show the capacity of CD36 to bind and endocytose oxLDL and to be implicated in atherosclerotic lesions formation. The early observations are linked to the work of Endemann *et al*, who using a human epithelial kidney cell line (HEK293) transfected with CD36, showed the capacity of the scavenger receptor to bind specifically oxLDL (249). An absence of CD36 on monocytes, as observed in a small percentage of individuals in the Japanese population, results in 40% to 50% less oxLDL binding to monocytes-derived-macrophages compared to macrophages from normal subjects (250). This lowered level of binding and uptake of oxLDL is also observed when CD36 binding sites are blocked by a specific monoclonal antibody, such as OKM5, which reduced oxLDL binding to normal macrophages by 50% (250). The same type of results with OKM5 blocking CD36 functional sites are observed when using monocytic cell line (THP-1) treated with PMA (249). Investigation of monocytes/macrophages from CD36-deficient human subjects has not to be clearly

indicated if such individuals are less or more prone to atherosclerotic lesions and coronary diseases. However, work on a murine model with a combined ApoE and CD36 double knockout, has shown to be quite interesting in investigating the role of CD36 in atherosclerotic lesions under the different time of periods. One should note that apoE KO mice with a Balbc background, results in animals having very high circulating cholesterol levels and lesions developing at a very fast pace compared to the wild-type. Macrophages derived from 12-week old mice with a double CD36/apoE knockout displayed a very significant decrease (76.5%) of aortic tree lesion size when compared to single apoE KO mice. Moreover, macrophages of these double knockouts bound and internalized oxLDL less than 60% compared to single apoE KO mice (251). These results on double knockout mice suggest that CD36 deficiency in macrophages does affect the size of vascular lesions. Reintroduction of CD36 in the apoE/CD36 knockout mice by using stem cell transfer, as predicted, resulted in an increase in lesion area (252). The effects of CD36 deficiency in macrophages did not lapse with the age of the animals since work on 35-week old CD36/apoE double knockout mice also showed smaller atherosclerotic lesions compared to the control from single apoE KO mice (253). Strong evidence showed that CD36 deficiency reduced the size of atherosclerotic lesions in young and older apoE KO mice. Reducing the size of atherosclerotic lesions in apoE KO mice can also be apparently obtained by using a ligand (EP80317) derived from the growth hormone-releasing peptide family that also blocked the oxLDL binding site of CD36. Indeed, recent data by Marleau *et al* showed that injection of EP80317, in apoE KO mice fed with an atherogenic diet, induced a significant reduction (up to 51%) of the lesion areas compared to the animals without EP80317 treatment (254).

1.2.1.3.2.3 SR-BI

Scavenger receptor class B type I (SR-BI) was the first physiologically relevant HDL receptor to be identified (255). The SR-BI protein, which has 509 amino acids with short N- and C-terminal cytoplasmic and transmembrane domains and a large, heavily N-glycosylated extracellular loop, is most highly expressed in liver (hepatocytes) and steroidogenic tissues. SR-BII, a minor splice variant of SR-BI, differs from SR-BI only in that the 42 C-terminal residues in SR-BI's 47 residue C-terminal cytoplasmic domains are substituted in SR-BII by 39 amino acids encoded by an alternatively spliced exon of the SR-BI/II gene.

Functionally, SR-BI mediates the cellular selective uptake of cholesteryl esters and other lipids from HDL and has been proposed to play a key role in reverse cholesterol transport (256). In addition, SR-BI is able to mediate efflux of unesterified cholesterol from cells to lipoproteins and other extracellular acceptors (257).

Several lines of evidence indicate an antiatherogenic role for SR-BI in atherogenesis. Hepatic overexpression of SR-BI protects against the development of atherosclerosis (258-260). Interestingly, the expression level of SR-BI is critical for its effect on atherosclerosis susceptibility. If the SR-BI expression level is too high, HDL levels are too low to sustain net cholesterol movement through the reverse cholesterol transport pathway (260). Conversely, the atheroprotective effects of high HDL levels are lost if the turnover of HDL cholesterol is impaired as a result of a reduction of SR-BI expression. Genetic ablation of SR-BI/II in the mouse leads to elevated plasma cholesterol transported in abnormally large, unesterified cholesterol-rich HDL particles and reduced biliary cholesterol secretion (261-265), as well as accelerated atherosclerosis. LDLr knockout mice with an attenuated expression of SR-BI are more susceptible to atherosclerotic lesion development (266). Furthermore, disruption of SR-

BI in wild-type(267) as well as in LDLr knockout mice (268) results in a highly increased susceptibility to atherosclerotic lesion development. When cross-bred onto the apoE KO background, SR-BI deficiency leads to severe cardiac dysfunction and premature death (269, 270).

The proatherogenic effects of SR-BI deletion are largely attributed to its effects on the uptake of HDL cholesteryl esters by the liver. However, according to the current understanding that SR-BI removes apoB-containing lipoproteins, disruption of SR-BI can also increase the availability of these atherogenic lipoproteins in the arterial wall. Furthermore, SR-BI is expressed in lipid-laden macrophages in human and murine atherosclerotic lesions (271-273). SR-BI might thus also play an important role locally in the arterial wall. Bone marrow transplantation studies have shown that SR-BI on macrophages reduces the development of advanced atherosclerotic lesions in LDLr-/- (268, 274) and apoE KO mice (275). In contrast, the development of small fatty streak lesions in LDLr knockout mice is facilitated by macrophage SR-BI (274). Thus, it appears that, depending on the stage of lesion development, SR-BI in macrophages is either proatherogenic or antiatherogenic, indicating a unique dual role for SR-BI in the pathogenesis of atherosclerosis. The unique dual role is likely a direct effect of the multi-functional and multi-ligand qualities of SR-BI, which binds a wide array of native and modified lipoproteins and mediates the bi-directional flux of cholesterol between HDL and cells. Its function in the binding of atherogenic lipoproteins, like native βVLDL and oxLDL, is expected to induce foam cell formation, while efflux of intracellular cholesterol to HDL will prevent foam cell formation and thus atherosclerotic lesion development.

1.2.2 Regulation of cholesterol synthesis by HMGR

1.2.2.1 Regulation of HMGR

The ER–bound enzyme (276), HMGR, is generally regarded as catalyzing the rate-limiting step in the synthesis of cholesterol, a critical membrane lipid, precursor of bile acids and steroid hormones, and component of hedgehog protein, a signalling molecule involved in embryogenesis (277-279). Impairment in the synthesis of cholesterol, resulting in very low serum and tissue cholesterol levels, occurs in patients with the Smith-Lemli-Opitz syndrome (280). Craniofacial anomalies, syndactyly and polydactyly, delayed myelinization, holoprosencephaly, cleft palate, genital malformations, jaundice, and congenital heart disease characterise these patients (281). On the other hand, elevated serum cholesterol is a risk factor in the progresstion of atherosclerotic vascular disease (282). In healthy individuals, serum cholesterol levels are maintained within fairly narrow limits. HMGR is a 97 kDa integral membrane protein of the ER with eight transmembrane spans (283). This enzyme is highly regulated at the levels of transcriptional, translational, and post-translational control (137) that can result in changes of over 200-fold in intracellular levels of the enzyme.

The transcription factor SREBP-2 participates in the regulation of HMGR gene transcription in response to the levels of sterols (162); At the ER membrane or the nuclear envelope, SREBP-2 binds to SCAP to form a SCAP-SREBP complex that functions as a sterol sensor. Insig-1 or -2 bind to SCAP when cellular cholesterol levels are high and prevent movement of the SCAP-SREBP complex from the ER to the Golgi. In cells depleted of cholesterol, Insig-1 and Insig-2 allow activation of the SCAP-SREBP complex and its translocation to the Golgi, where SREBP is cleaved by site-1 proteinase and site-2 proteinase at two sites. Cleavage releases the amino-terminal basic helix-loop-helix (bHLH) domain, which enters the nucleus, where it functions as a

transcription factor that recognizes non-palindromic decanucleotide sequences of DNA called sterol-regulatory elements. Binding of the bHLH domain of SREBP to an SRE promotes transcription of the HMGR gene.

Degradation of HMGR involves its transmembrane regions: removal of two or more transmembrane regions abolishes the acceleration of HMGR degradation that occurs under certain conditions (137, 284): degradation is induced by a non-sterol, mevalonate-derived metabolite alone or by a sterol plus a mevalonate-derived non-sterol metabolite, possibly farnesyl pyrophosphate or farnesol. Four conserved phenylalanines in the sixth membrane span of the transmembrane region are essential for degradation of HMGR (285). Insig-1 also functions in the degradation of HMGR (286): when cholesterol levels are high, SCAP and HMGR compete for the binding to Insig-1. If SCAP binds Insig-1, the SCAP-Insig-1 complex is retained in the ER, whereas if HMGR binds Insig-1, HMGR is ubiquinated on lysine 248 and is rapidly degraded through a ubiquitin-proteasome mechanism (287).

The catalytic activity of the HMGRs of higher eukaryotes is attenuated by phosphorylation of a single serine, which in the case of HMGR is at position 872 (288). The location of this serine - six residues from the catalytic histidine, a spacing conserved in all higher eukaryote HMGRs, suggests that the phosphoserine may interfere with the ability of this histidine to protonate the inhibitory coenzyme A with the thiol proton dissociated (CoAS)-thioanion that is released in stage 2 of the reaction mechanism. Alternatively, it may interfere with closure of the flap domain, a carboxy-terminal region that is thought to close over the active site to facilitate catalysis, a step thought to be essential for formation of the active site (289). Subsequent dephosphorylation restores full catalytic activity. HMGR kinase, also called the adenosine monophosphate (AMP)-activated protein kinase (AMPK), phosphorylates

HMGR. The primary phosphatase *in vivo* is thought to be protein phosphatase 2A (PP2A). Both PP2A and PP2B can catalyze dephosphorylation of vertebrate HMGR *in vitro*(290). HMGR activity therefore responds to hormonal control through AMP levels and PP2A activity. Phosphorylation of serine 577 of *A. thaliana* HMGR isozyme 1 by a plant HMGR kinase that does not require 5'-AMP attenuates activity, and restoration of HMGR activity follows from dephosphorylation (291). As many plant genes encode a putative target serine surrounded by an apparent AMPK recognition motif, it is probable that most plant HMGRs are regulated by phosphorylation. Yeast HMGR activity is, however, unaffected by AMP kinase. The phosphorylation state of HMGR does not affect the rate at which the protein is degraded.

1.2.2.2 Significance of HMGR pathway in atherosclerosis

The process of atherosclerosis involves lipid accumulation in arterial walls narrowing the lumen of the artery and thus leading to compromised flow to target organs. For years the traditional risk factors, hypercholesterolaemia, was believed to be one of the major factors determining the pathogenesis of atherosclerosis. The significance of cholesterol biosynthesis to atherosclerosis is underscored by the effectiveness of HMGR inhibitors of this process in lowering serum cholesterol levels. Since their introduction in the late 1980s, HMGR inhibitors, also called statins, have revolutionized the treatment of hypercholesterolaemia and demonstrated their capacity to greatly reduce coronary morbidity and mortality in both primary and secondary intervention trials (292, 293). These lipid-lowering or non-lipid effects of statins are mainly achieved by the inhibition of HMGR activity in the liver, which shows the significance of cholesterol synthesis mediated by HMGR in atherogenesis. Furthermore, feedback mechanisms of HMGR for cholesterol biosynthesis in peripheral cells play key roles in the prevention of foam cell formation.

1.2.3 The regulation of cholesterol efflux

1.2.3.1 Pathways mediating cellular cholesterol efflux

When cholesterol is transported from the peripheral cells to the liver for its biological degradation, the first step of the pathway is efflux of cellular cholesterol to plasma lipoproteins. HDL is believed to play a primary role in this step by "accepting" the cellular cholesterol. Three distinct pathways of cellular cholesterol efflux involving HDL and its apolipoproteins have been described: 1) plasma HDL particles can promote cholesterol efflux by a process of passive aqueous diffusion (294). Free cholesterol molecules spontaneously desorb from the plasma membrane, diffuse through the aqueous phase, and incorporate into HDL particles by collision; 2) SR-BI, an HDL receptor that mediates the selective uptake of HDL cholesteryl esters into cells (255), also facilitates the efflux of cholesterol from cells to HDLs (273). Cholesterol efflux is blocked by antibodies that inhibit binding of HDLs to SR-BI (295), suggesting that the mechanism involves a direct interaction between HDL particles and the receptor and is therefore distinct from the aqueous diffusion mechanism. 3) ABCA1 mediates the active efflux of phospholipid and cholesterol from cells to lipid-poor apolipoproteins, such as apoA-I. ApoA-I binds and cross-links to ABCA1, suggesting a direct interaction that leads to cholesterol efflux (296).

Passive aqueous diffusion and SR-BI–facilitated efflux involve bidirectional exchange of cholesterol between cells and HDLs. In contrast, ABCA1/apolipoprotein–mediated cholesterol and phospholipid efflux is a unidirectional net transfer process (296). The specificity for cholesterol acceptors in the three pathways is different. Passive efflux is driven by the phospholipid content of lipoprotein acceptors (297). SR-BI can bind both apolipoproteins and HDL particles, but binding affinity is greatest for large, spherical HDL particles, suggesting that these may be the major substrate for SR-BI *in vivo* (298).

In contrast, ABCA1 binds and cross-links lipid-poor apoA-I, while showing minor interaction with smaller HDL_3 and no interaction with larger HDL_2 subspecies (299). Thus, ABCA1 shows limited interaction with the major HDL species isolated from plasma, emphasizing the importance of a small pool of lipid-poor apolipoproteins either secreted by cells or generated by lipid exchange and lipolysis of HDL particles in the bloodstream. ABCA1 probably mediates the rapid efflux of cellular cholesterol in response to pre-β HDL, a minor but metabolically significant fraction of plasma HDLs comprising free apoA-I and apoA-I associated with a small number of phospholipid and cholesterol molecules (300). Following addition of lipid to apoA-I by ABCA1, there is further growth of HDL particles as a result of phospholipid transfer by phospholipid transfer protein, cholesterol esterification by LCAT, and acquisition of apoE molecules. The large, apoE-rich HDLs are probably the optimal substrates for SR-BI. In summary, ABCA1 may play the major role in initiating cholesterol efflux from macrophages and other cells to lipid-poor apolipoproteins, while SR-BI principally clears cholesterol and cholesteryl ester from large HDLs in the liver and steroidogenic tissues.

1.2.3.2 ABCA1 mediated cholesterol efflux

The human ABCA1 gene has been mapped to chromosome 9q31 and is composed of 50 exons, which encode 2261-amino-acid residues (301). The ABCA1 protein is a full-size ABC transporter containing two transmembrane domains of six alpha-helices and two intracellular nucleotide binding domains. Its ATP-binding cassette consists of the Walker A and Walker B motifs, which are present in many proteins that utilise ATP. The topology of ABCA1 has been predicted based on hydropathy analysis and the study of glycosylation sites and epitopes. According to these models, ABCA1 has an amino-terminus orientated into the cytosol and two large extracellular loops that are highly glycosylated and linked by at least one cystein bond. Recently, mutations in ABCA1

were identified as the cause of Tangier disease, a severe HDL deficiency characterised by deposition of sterols in tissue macrophages (302).

To maintain cholesterol homeostasis, ABCA1 is tightly regulated both transcriptionally and posttranslationally. The transcription of ABCA1 is markedly induced by overloading cells with cholesterol. The large intracellular sterol concentration in foam cells plays a major role in ABCA1 regulation. Acetylated LDL up-regulates ABCA1 mRNA and protein which can be reversed by incubation of these macrophages in HDL (303). It was also reported that ABCA1 mRNA and protein were up-regulated in a time and dose dependent fashion by native LDL (304).

Nuclear receptors are ligand activated transcription factors that regulate the expression of their target genes. The tissue specific expression and ligand availability tightly control its activity (305). Liver X receptors (LXRs) and peroxisome proliferator-activated receptors (PPARs), belonging to a subgroup called adopted orphan nuclear receptor group, are the major players in ABCA1 regulation. LXRs act as cholesterol sensors that respond to elevated sterol concentrations and activate a cadre of genes that govern transport, catabolism and elimination of cholesterol (306). LXRα expressed in the macrophage is important in terms of plaque physiology as it seems to be capable of activating and suppressing the ABCA1 gene based on ligand availability (307). The ligands that activate these receptors in the macrophage are mainly oxysterols like 27-hydroxycholesterol (308). LXRα influences ABCA1 expression transcriptionally and post-transcriptionally. Studies have reported that the oxysterol induction of ABCA1 is partly through the LXR pathway (309, 310). PPARs have been implicated in the regulation of both inflammation and cholesterol homeostasis in the macrophage and polyunsaturated fatty acids serve as their ligands (305). PPARγ enhances cholesterol efflux by inducing the transcription of LXRα and thus ABCA1 (311, 312). The

observation that PPAR agonists and LXR ligands are ineffective in macrophages of Tangier disease patients (310, 312), indicates that functional ABCA1 is required for this pathway of cholesterol efflux. Taken together, LXRs and PPARs up-regulate expression of ABCA1, providing an amplification loop for ABCA1 expression (313). The PPARs–LXRs-ABCA1 cascade does represent a powerful means of cholesterol efflux from the macrophage and therefore could play a significant role in influencing the progression of atherosclerotic plaques.

Studies in mice have revealed a significant discordance between ABCA1 protein and mRNA levels, suggesting that post-transcriptional regulation plays a major role in ABCA1 protein expression (314). Unsaturated fatty acids have been found to promote ABCA1 protein degradation directly (315, 316) and indirectly (317, 318). This may be significant in disorders like Type 2 diabetes and insulin resistance, conditions with increased levels of fatty acids where accelerated atherosclerosis is observed. ABCA1 phosphorylation, which is reported to be influenced by apoA1 (319) and protein kinase C (320), may also have a major effect on protein stability. The PEST sequence (PEST sequence is a peptide sequence which is rich in proline (P), glutamic acid (E), serine (S), and threonine (T). This sequence is associated with proteins that have a short intracellular half-life; it is hypothesized that the PEST sequence acts as a signal peptide for protein degradation.) identified in ABCA1 by Wang *et al* (321) appears significant in protein degradation as deletion of this motif resulted in a 4–5-fold increase in ABCA1 protein, increased ABCA1 mediated efflux and enhanced apoA1 binding. *In vitro* experiments with peritoneal macrophages, transfected cells and mouse primary hepatocytes have shown that apoA1 binding increased ABCA1 protein without affecting mRNA levels (321). Interestingly this apoA1 mediated stabilization of ABCA1 protein is achieved by inhibition of PEST sequence mediated degradation by proteases (321, 322). There is also evidence that phospholipid transfer protein (PLTP)

interacts with ABCA1 for its function in cholesterol efflux and also stabilizes ABCA1 protein (323). It has been reported that, in human carotid atherosclerotic plaques, ABCA1 protein is significantly reduced despite increased mRNA (324). The observed up-regulation in this study of both LXRα and ABCA1 mRNA in atherosclerotic tissues could be attributed to the oxysterol-rich environment inside the plaque potentially amplified by low ABCA1 protein levels. It is possible that the degradation of ABCA1 protein in the plaque microenvironment might be the key factor influencing cholesterol homeostasis at the macrophage level. The resulting localized deficiency in ABCA1 function could lead to decreased cholesterol efflux, accumulation of oxysterols and acceleration of the atherosclerotic process.

1.2.3.3 ABCG1 mediated cholesterol efflux

The human ABCG1 gene has been mapped to chromosome 21q22.3. It is composed of 23 exons and has multiple transcripts. Two major transcripts were described to encode proteins with alternative amino-termini (325). ABCG1 is a half-transporter, which forms homodimers and is highly expressed in macrophages. Its inactivation by RNA interference results in reduced efflux of cholesterol and phospholipid to HDL. Conversely, its overexpression causes an increase in HDL-mediated cholesterol efflux and a reduction in cellular cholesterol mass (326-328). These results were confirmed in knockout and transgenic mice. The disruption of ABCG1 in mice on a high-fat and cholesterol-rich diet causes the accumulation of neutral lipids and phospholipids in hepatocytes and macrophages, although not affecting plasma lipids. In contrast, overexpression of ABCG1 is protective against lipid accumulation (329). ABCG1 mediates the transport of cholesterol from cells only to the major HDL fractions HDL_2 and HDL_3 but not to lipid-free apoA-I (326, 328). Interestingly, ABCG1 was also found to efflux cholesterol to LDL (328). It seems that ABCG1 redistributes cholesterol to cell

surface domains where it becomes accessible for removal by HDL but not lipid-free apoA-I (327). However, while the atheroprotective role of ABCA1 is well described by genetic studies in men and mice, so far it's only assumed that ABCG1 is atheroprotective.

Like ABCA1, ABCG1 mRNA levels are highly increased when macrophages are either incubated with LXR agonists or converted to cholesterol ester-loaded foam cells (326). Activation of PPARγ also induces the expression of ABCG1 but in a LXR-independent manner (330). Interestingly, cAMP has no effect on ABCG1 expression (331).

1.2.4 The role of liver in cholesterol homeostasis

The liver is a key organ in cholesterol trafficking and lipoprotein homeostasis (332). The liver plays very important role in maintaining plasma cholesterol balance by several major processes: 1) cholesterol synthesis and lipoprotein uptake; 2) formation of bile acids and biliary secretion of cholesterol; 3) secretion of very-low-density lipoproteins; 4) reversible conversion of cholesterol to cholesteryl esters; 5) reverse cholesterol transport (RCT).

1.2.4.1 Endogenous cholesterol transport by the liver

Cholesterol trafficking in the liver includes endogenous and exogenous cholesterol. Exogenous (dietary) cholesterol is delivered to the liver in chylomicron remnants (333, 334), which are derived from intestinal chylomicrons through the action of lipoprotein lipase. The remnants rapidly enter the liver by receptor-mediated endocytosis after binding to specific remnant receptors. Endogenous cholesterol transport begins when the liver releases endogenous triglyceride and cholesterol ester in VLDL. VLDL can be separated into two subclasses, VLDL1 and VLDL2, which differ in their triglyceride-content and size. Under conditions of increased hepatic triglyceride content, the rate of

production of triglyceride-rich VLDL1 release is increased. The same lipoprotein lipases quickly degrade endogenous triglyceride in VLDL, giving rise to intermediate density lipoproteins (IDL) that have had much of their triglyceride and surface apolipoproteins removed. IDL particles bind with high affinity to hepatic LDL receptors. Some of the particles are rapidly cleared from plasma by this route; other IDL particles are converted to LDL. Approximately 70% of LDL is removed by the liver via LDL receptors presented on the surface of hepatocytes and other cells which bind to apolipoprotein B100 (Fig 1.5). In addition, a small but significant amount of LDL appears to be removed from the circulation by non-receptor mediated pathways, including uptake by scavenger receptors on macrophages.

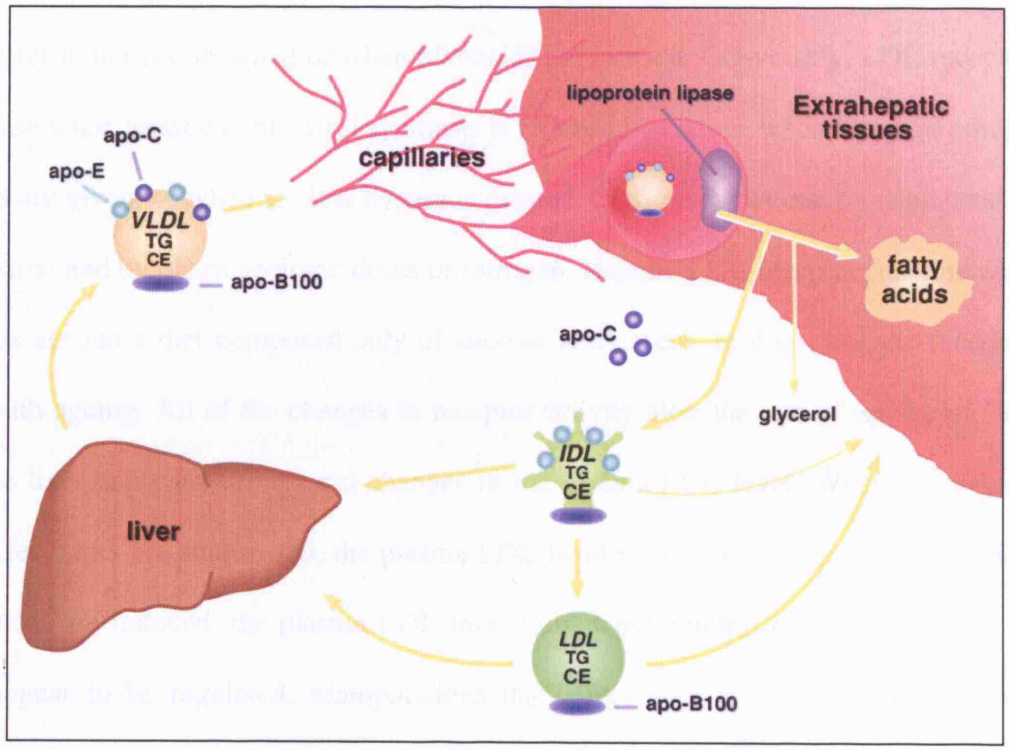

Fig 1.5 The VLDL, IDL, LDL pathway (Mol Biosyst 2007; 3(9):608-19.)

VLDL particles are assembled and secreted from the liver. Each particle carries one molecule of apoB as well as apoE and the C apolipoproteins, apoC1, C2, and C3. The particle carries amphipathic lipids (phospholipid and free cholesterol) on its surface and hydrophobic lipids (cholesterol ester and triglyceride) in its inner core. While in the circulation, the triglycerides are hydrolyzed by lipoprotein lipase, an enzyme residing on the luminal surface of the capillary endothelium in muscle and adipose

tissue. This leads to the loss of the C-proteins and the formation of intermediate density lipoprotein (IDL), also known as VLDL remnants. These particles have two competing fates. They can be rapidly cleared by the liver or they can continue to be processed to become LDL. The clearance of IDL from the circulation depends upon the interaction of apoE with the LDLr and other members of the LDL receptor family. LDL is a more stable particle than IDL. In humans, about two-thirds of cholesterol is carried on LDL particles. LDL clearance is mediated by the interaction of apoB100 with the LDLr, primarily in the liver, but also in virtually all other tissues.

1.2.4.2 The LDL/LDLr system in the liver

The LDL/LDLr system can be considered the primary transport mechanism for endogenous cholesterol. Most of the whole body LDLr activity is located in the liver (335, 336). Hepatic LDL receptors are suppressed whenever the demand for cholesterol in the liver increases or reduces. Thus, receptor suppression occurs when a high cholesterol diet is consumed or when bile acids are infused. Conversely, LDL receptors increase when hepatic cholesterol synthesis is blocked by statins, when bile acid binding resins are given, or when an ileal bypass is created. LDL receptors can be stimulated by thyroxine and by pharmacologic doses of estrogen. Hepatic LDL receptors decline when rabbits are fed a diet composed only of sucrose and casein. In dogs, hepatic receptors fall with ageing. All of the changes in receptor activity alter the rate of uptake of LDL by the liver and cause reciprocal changes in the plasma LDL level. Whenever hepatic LDL receptors are suppressed, the plasma LDL level rises; conversely, whenever these receptors are induced, the plasma LDL level falls. Chylomicron remnant receptors do not appear to be regulated. Manipulations that affect hepatic LDL receptors do not influence the hepatic uptake of chylomicron remnants, nor do they cause a significant change in the plasma levels of these lipoproteins (333, 337).

1.2.4.3 Cholesterol biosynthesis in the liver

The synthesis and utilization of cholesterol must be tightly regulated in order to prevent overaccumulation and abnormal deposition within the body. Slightly less than half of the cholesterol in the body derives from biosynthesis *de novo*. Biosynthesis in the liver accounts for approximately 10% of the amount produced each day. Cholesterol synthesis occurs in the cytoplasm and microsomes from the two-carbon acetate group of acetyl-CoA. The process has five major steps:1) Acetyl-CoA is converted to 3-hydroxy-3-methylglutaryl-CoA (HMG-CoA); 2) HMG-CoA is converted to mevalonate; 3) Mevalonate is converted to the isoprene based molecule, isopentenyl pyrophosphate (IPP), with the concomitant loss of CO_2; 4) IPP is converted to squalene; 5) Squalene is converted to cholesterol (Fig 1.6).

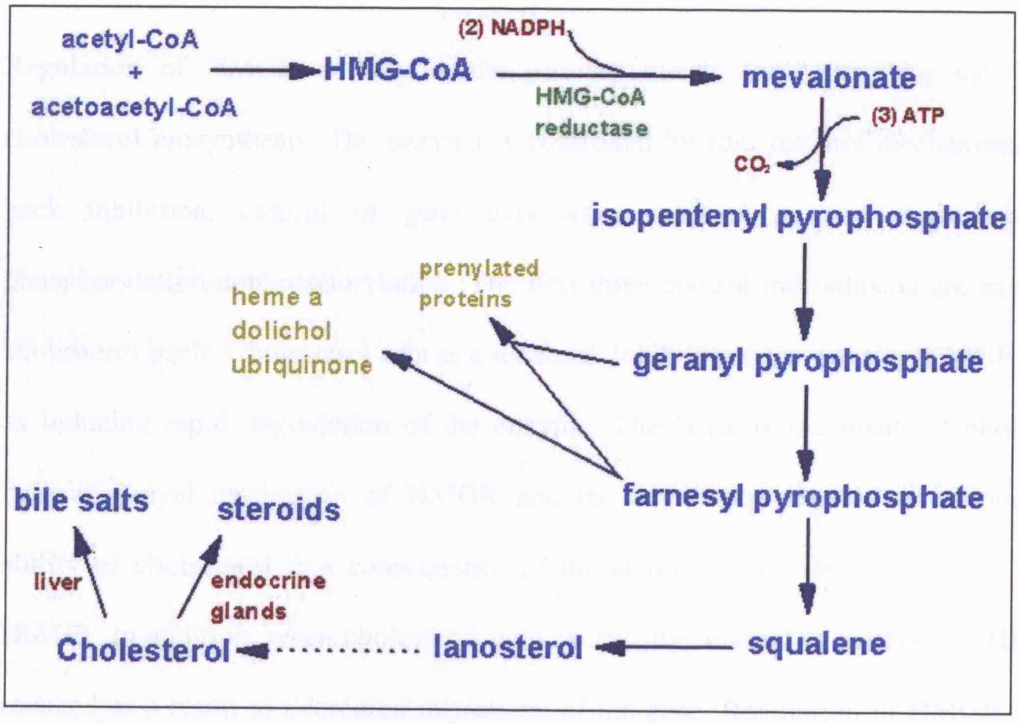

Fig 1.6 Pathway of cholesterol biosynthesis (http://themedicalbiochemistrypage.org/cholesterol.html.)

Synthesis begins with the transport of acetyl-CoA from the mitochondrion to the cytosol. The rate limiting step occurs at HMGR catalyzed step. The phosphorylation reactions are required to solubilize the

isoprenoid intermediates in the pathway. Intermediates in the pathway are used for the synthesis of prenylated proteins, dolichol, coenzyme Q and the side chain of heme *a*.

Normal healthy adults synthesize cholesterol at a rate of approximately 1g/day and consume approximately 0.3g/day. A relatively constant level of cholesterol in the body (3.88-5.17 mmol/l) is maintained primarily by controlling the level of *de novo* synthesis. The level of cholesterol synthesis is regulated in part by the dietary intake of cholesterol. Cholesterol from both diet and synthesis is utilized in the formation of membranes and in the synthesis of the steroid hormones and bile acids. The greatest proportion of cholesterol is used in bile acid synthesis. The cellular supply of cholesterol is maintained at a steady level by three distinct mechanisms: 1) Regulation of HMGR activity and levels; 2) Regulation of excess intracellular free cholesterol through the activity of ACAT; 3) Regulation of plasma cholesterol levels via LDLr-mediated uptake and HDL-mediated reverse transport.

Regulation of HMGR activity is the primary means for controlling the level of cholesterol biosynthesis. The enzyme is controlled by four distinct mechanisms: feed-back inhibition, control of gene expression, rate of enzyme degradation and phosphorylation-dephosphorylation. The first three control mechanisms are exerted by cholesterol itself. Cholesterol acts as a feedback inhibitor of pre-existing HMGR as well as inducing rapid degradation of the enzyme. The latter is the result of cholesterol-induced polyubiquitination of HMGR and its degradation in the proteosome. This ability of cholesterol is a consequence of the sterol sensing domain (SSD), SSD of HMGR. In addition, when cholesterol is in excess, the amount of mRNA for HMGR is reduced as a result of decreased expression of the gene. Regulation of HMGR through covalent modification occurs as a result of phosphorylation and dephosphorylation. The enzyme is most active in its unmodified form. Phosphorylation of the enzyme decreases its activity. HMGR is phosphorylated by AMPK. AMPK itself is activated via

phosphorylation. Phosphorylation of AMPK is catalyzed by at least two enzymes. The primary kinase sensitive to rising AMP levels is serine/threonine kinase 11 (LKB1). LKB1 was first identified as a gene in humans carrying an autosomal dominant mutation in Peutz-Jehgers syndrome. LKB1 is also found mutated in lung adenocarcinomas. The second AMPK phosphorylating enzyme is calmodulin-dependent protein kinase kinase (CaMKK). CaMKK induces phosphorylation of AMPK in response to increases in intracellular Ca^{2+} as a result of muscle contraction.

The activity of HMGR is additionally controlled by the cAMP signaling pathway. Increases in cAMP lead to activation of cAMP-dependent protein kinase A (PKA). In the context of HMGR regulation, PKA phosphorylates phosphoprotein phosphatase inhibitor-1 (PPI-1) leading to an increase in its activity. PPI-1 can inhibit the activity of numerous phosphatases including protein phosphatase 2C, HMGR and phosphatase which remove phosphates from AMPK and HMGR, respectively. This maintains AMPK in the phosphorylated and active state, and HMGR in the phosphorylated and inactive state. As the stimulus leading to increased cAMP production is removed, the level of phosphorylation decreases and that of dephosphorylation increases. The net result is a return to a higher level of HMGR activity. Since the intracellular level of cAMP is regulated by hormonal stimuli, regulation of cholesterol biosynthesis is hormonally controlled. Insulin leads to a decrease in cAMP, which in turn activates cholesterol synthesis. Alternatively, glucagon and epinephrine, which increase the level of cAMP, inhibit cholesterol synthesis.

The ability of both insulin in stimulating and glucagons in inhibiting HMGR activity are consistent with the effects of these hormones on other metabolic pathways. The basic function of these two hormones is to control the availability and delivery of energy to all cells of the body.

Long-term control of HMGR activity is exerted primarily through control over the synthesis and degradation of the enzyme. When levels of cholesterol are high, the level of expression of the HMGR gene is reduced. Conversely, reduced levels of cholesterol activate expression of the gene. Insulin also brings about long-term regulation of cholesterol metabolism by increasing the level of HMGR.

1.2.4.4 Cholesterol elimination by the liver

The end products of cholesterol utilization are the bile acids, synthesized in the liver. Synthesis of bile acids is one of the predominant mechanisms for the excretion of excess cholesterol. However, the excretion of cholesterol in the form of bile acids is insufficient to compensate for an excess dietary intake of cholesterol.

The most abundant bile acids in human bile are chenodeoxycholic acid (45%) and cholic acid (31%). These are referred to as the primary bile acids. Within the intestines the primary bile acids are acted upon by bacteria and converted to the secondary bile acids, identified as deoxycholate (from cholate) and lithocholate (from chenodeoxycholate). Both primary and secondary bile acids are reabsorbed by the intestines and delivered back to the liver via the portal circulation.

Within the liver the carboxyl group of primary and secondary bile acids is conjugated via an amide bond to either glycine or taurine before their being re-secreted into the bile canaliculi. These conjugation reactions yield glycoconjugates and tauroconjugates, respectively. The bile canaliculi join with the bile ductules, which then form the bile ducts. Bile acids are carried from the liver through these ducts to the gallbladder, where they are stored for future use. The ultimate fate of bile acids is secretion into the intestine, where they aid in the emulsification of dietary lipids. In the gut the glycine and taurine residues are removed and the bile acids are either excreted (only a small

percentage) or reabsorbed by the gut and returned to the liver. This process of secretion from the liver to the gallbladder, to the intestines and finally re-absorption is termed the enterohepatic circulation.

Bile acids perform four physiologically significant functions: 1) their synthesis and subsequent excretion in the feces represent the only significant mechanism for the elimination of excess cholesterol; 2) bile acids and phospholipids solubilize cholesterol in the bile, thereby preventing the precipitation of cholesterol in the gallbladder; 3) they facilitate the digestion of dietary triacylglycerols by acting as emulsifying agents that render fats accessible to pancreatic lipases; 4) they facilitate the intestinal absorption of fat-soluble vitamins.

1.2.4.5 Reverse cholesterol transport

The concept of "reverse cholesterol transport" was first introduced in 1968 by Glomset (338) to describe the process by which extrahepatic (peripheral) cholesterol is returned to the liver for excretion in the bile and ultimately the feces. The physiological need for this process is clear, as nonhepatic cells acquire cholesterol through uptake of lipoproteins and *de novo* synthesis and yet (with the exception of steroidogenic tissues that convert cholesterol to steroid hormones) are unable to catabolize it. Excess unesterified cholesterol is toxic to cells, and therefore, cells have developed several ways to protect themselves against cholesterol toxicity. A key pathway is the efflux of cholesterol to extracellular "acceptors." The return of this "peripheral" cholesterol to the liver is necessary to balance cholesterol intake and *de novo* synthesis and thus to maintain whole-body steady-state cholesterol metabolism.

The relationship of RCT to atherosclerosis was first suggested by Ross and Glomset (339), who hypothesized that atherosclerotic lesions develop when an imbalance occurs

between the deposition and removal of arterial cholesterol after endothelial injury. This concept was further developed by Miller *et al* (340), who suggested that on the basis of the inverse relation between HDL cholesterol and cardiovascular disease, emphasis should be placed on increasing HDL as a way to increase clearance of cholesterol from the arterial wall to prevent cardiovascular disease. Despite three decades of work, the relationship of RCT to atherosclerosis remains more of a hypothesis than an established fact.

Because the physiological process of RCT clearly occurs from all peripheral tissues, it has often been measured and discussed as a general peripheral process.

The sequence of events in RCT is described in Fig 1.7. ApoA-I is first produced mainly by the liver, and released into the plasma. Circulating apoA-I interacts with serum phospholipids and forms nascent discoidal HDL (ndHDL). Once ndHDL is generated, it triggers cholesterol efflux in the macrophages and fibroblasts in the subendothelial space. Externalized cholesterol is absorbed by ndHDL, and subsequently is esterified by LCAT. HDL particles are enriched with cholesteryl ester and become larger, resulting in HDL3 and HDL2. PLTP is involved in this process: for example, by fusing two HDL3 into one HDL2 molecule. If HDL molecules are enriched with triglyceride, they are processed by the enzyme hepatic lipase and become smaller and denser. Hepatic lipase can convert the phospholipid-rich HDL2 to HDL3. However, regulation of the balance of hepatic lipase and PLTP is not clear. Cholesterol ester transfer protein (CETP) facilitates the equimolar exchange of cholesteryl esters from HDL for triglycerides in apoB100-containing lipoproteins. These cholesteryl esters are then delivered back to the liver via LDL receptor, converted to bile salts, and eliminated through the gastrointestinal tract.

As acceptors such as apoA-I and HDL approach macrophages in subintimal space, intracellular cholesterol can be released outside the cells for excretion. This process is termed cholesterol efflux of macrophages. In this pathway, ABCA1 plays a major role in translocating cholesterol into the extracellular space. In addition to ABCA1, four other factors are known to be involved in the pathway. SR-BI can induce cholesterol efflux by enabling HDL to bind to cells and reorganize lipids within cholesterol-rich domains in the plasma membrane (341, 342). Caveolins are typically associated with caveolae, which are non-clatrin-coated plasma membrane microdomains rich in cholesterol and glycosphingolipids. Caveolins are small proteins (18–24 kDa) that have a hairpin loop conformation, with both the N and C termini exposed to the cytoplasm (343). These proteins have the capacity to bind cholesterol, and can transport cholesterol from the ER to the plasma membrane (344, 345). A report showed that over-expression of caveolins enhances cholesterol efflux in hepatic cells without affecting ABCA1 expression, indicating the presence of a caveolin-dependent pathway (345). Sterol 27-hydroxylase (CYP27A1) is also known as a contributor to cholesterol efflux (346). Chinese hamster ovary (CHO) cells transfected with CYP27A1 showed increased cholesterol efflux. Since ABCA1 expression was not altered, CYP27A1 could cause cholesterol efflux independent of other factors. In addition to these pathways, cholesterol efflux can also occur via passive diffusion, in which cholesterol is desorbed down to the concentration gradient onto acceptor molecules (347). Thus, RCT and cholesterol efflux constitute an efficient pathway by which excess cholesterol can be removed out of the body. Although extensive studies have recently been performed, RCT is a complicated process and its regulation mechanisms are largely unknown.

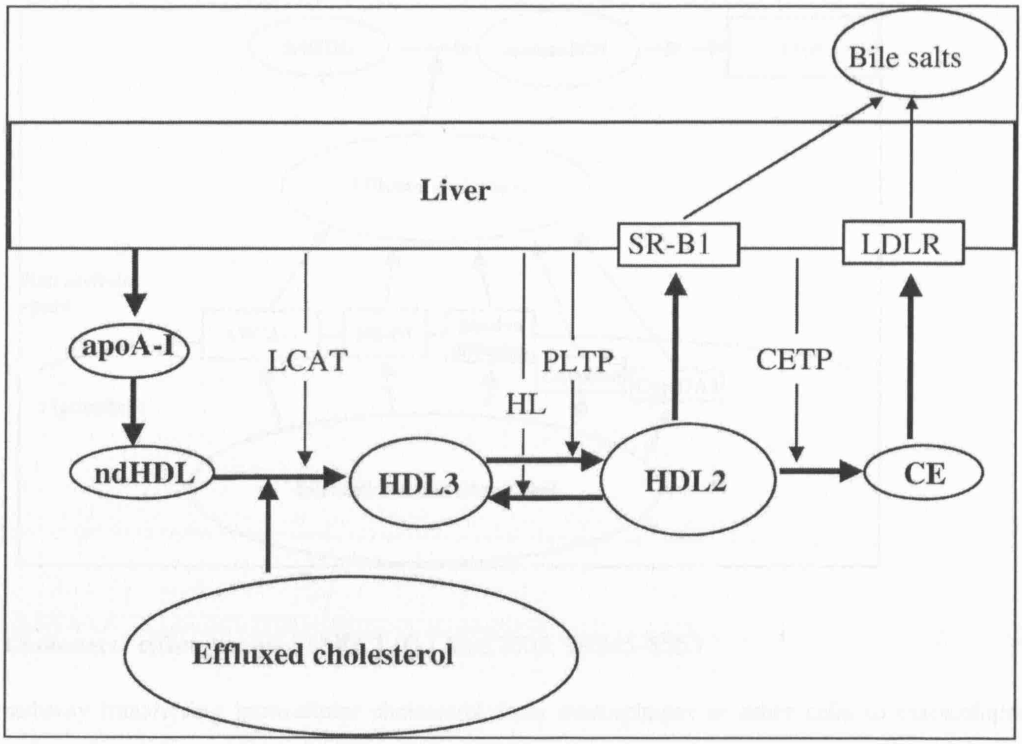

Fig 1.7 Reverse cholesterol transport (Q J Med 2005; 98:845–856.)

The reverse cholesterol transport (RCT) pathway delivers free cholesterol from macrophages or other cells to the liver or intestine for excretion. Major constituents of RCT include acceptors such as high-density lipoprotein (HDL) and apolipoprotein A-I (apoA-I), and enzymes such as lecithin: cholesterol acyltransferase (LCAT), phospholipid transfer protein (PLTP), hepatic lipase (HL) and cholesterol ester transfer protein (CETP), which regulate cholesterol transport. Eventually, cholesterols in the HDL are delivered to the liver via scavenger receptor B1 (SR-B1), converted to bile salts and eliminated through the gastrointestinal tract. Cholesteryl esters (CE) could also be delivered to the liver via the LDL receptor (LDLR). ndHDL, nascent discoidal HDL.

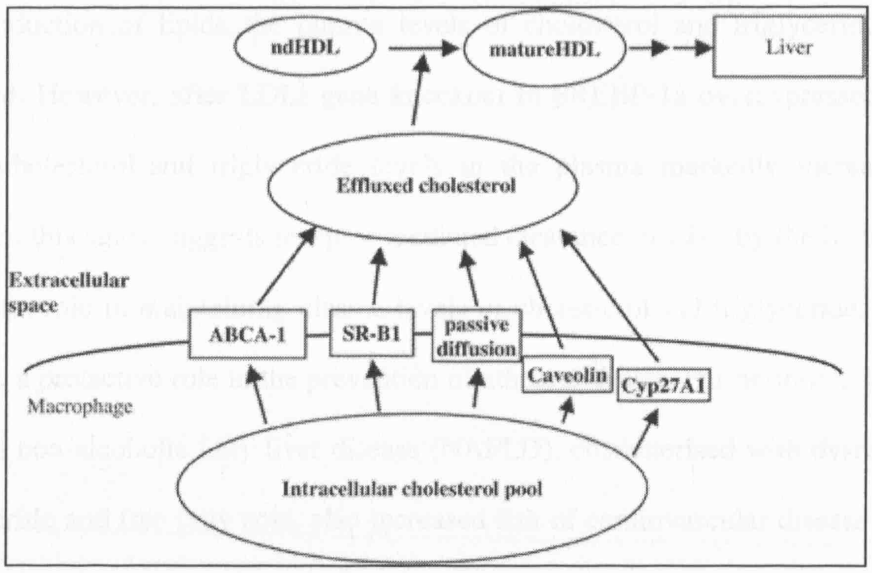

Fig 1.8 Cholesterol efflux is a part of RCT (Q J Med 2005; 98:845–856.)

It is a pathway transferring intracellular cholesterol from macrophages or other cells to extracellular acceptors such as apolipoprotein A-I (apoA-I) of high-density lipoprotein (HDL). It consists of five independent routes, including ATP-binding cassette transporter A1 (ABCA1), scavenger receptor B1 (SR-B1), caveolin, Cyp27A1 and passive diffusion.

1.2.4.6 The role of liver in atherosclerosis

The liver, as a central organ of lipid metabolism, has been paid more attention in the prevention of atherogenesis. A second area of future research that will generate much interest is the liver as a therapeutic target for atherosclerotic vascular disease, the leading cause of death in the industrialized world (348). Impaired cholesterol trafficking in the liver may cause dyslipidemia in the body, therefore accelerate progression of atherosclerosis.

Hypercholesterolaemia is one of the main risk factors in atherogenesis. Disrupted receptor-mediated clearance of LDL by the liver may result in hypercholesterolaemia. Horton *et al* (349) reported that overexpression of nuclear sterol regulatory element binding protein-1a (nSREBP-1a) in the liver of transgenic mice led to the accumulation of massive amounts of cholesterol and triglycerides in hepatocytes. Despite the hepatic

overproduction of lipids, the plasma levels of cholesterol and triglycerides were not elevated. However, after LDLr gene knockout in SREBP-1a overexpressed transgenic mice, cholesterol and triglyceride levels in the plasma markedly increased. Taken together, this study suggests receptor-mediated clearance of LDL by the liver plays very important role in maintaining plasma levels of cholesterol and triglyceride, which may provide a protective role in the prevention of atherosclerosis. Furthermore, some studies showed non-alcoholic fatty liver disease (NAFLD), characterised with dysregulation of triglyceride and free fatty acid, also increased risk of cardiovascular disease (350, 351). The severity of liver histology in NAFLD patients is closely associated with markers of early atherosclerosis such as greater carotid artery wall thickness and lower endothelial flow-mediated vasodilation independently of classical risk factors and components of the metabolic syndrome. Moreover, NAFLD is associated with greater overall mortality and independently predicts the risk of future events of cardiovascular diseases (350).

As nearly 50% of the body cholesterol is catabolized to bile acids, bile acid biosynthetic pathway is one of the pathways in maintaining cholesterol homeostasis. Increased hepatic bile acid synthesis decreases plasma LDL-cholesterol, thereby reducing atherosclerosis (352). On the contrary, suppression of bile Acid Synthesis deteriorates progression of atherosclerosis (353).

Recently, the connection of RCT with atherosclerosis has been paid more attention. It has been reported in patients with mutated ABCA1 genes, RCT and cholesterol efflux are impaired and atherosclerosis is increased (354). In studies with transgenic mice, disruption of ABCA1 genes can induce atherosclerosis. Levels of HDL are inversely correlated with incidences of cardiovascular disease. Supplementation with HDL or apoA-I can reverse atherosclerosis by accelerating RCT and cholesterol efflux. On the other hand, pro-inflammatory factors such as IFN-γ, endotoxin, TNFα and IL-1β, can be

atherogenic by impairing RCT and cholesterol efflux, according to *in vitro* studies. RCT and cholesterol efflux play a major role in anti-atherogenesis, and modification of these processes may provide new therapeutic approaches to cardiovascular disease.

In summary, the liver, as a central organ of lipid metabolism, plays a key role in the prevention of atherogenesis.

1.3 Inflammation may link dyslipidemia to atherogenesis

1.3.1 Lipids mediate inflammatory signals

Activation of vascular inflammation in response to lipid accumulation is generally believed to play a critical role in the initiation of atherosclerosis. The importance of hypercholesterolaemia in atherogenesis has been well documented in animal models, including LDLr knockout mice (355) or apoE KO mice (356). The chronic inflammatory influence of hypercholesterolaemia is thought to be mediated by induction of cytokines and chemokines (357), up-regulation of endothelial adhesion molecules (358), and immune reactions against oxidized moieties on lipoproteins (359, 360).

Lipoproteins might act as pro-inflammatory mediators. At certain concentrations cholesterol-rich lipoprotein (LDL) and triglyceride-rich lipoprotein (VLDL, IDL) enhanced the secretion of inflammatory cytokines, such as IL-6, TNFα, PDGF, and TGFβ by endothelial cells, VSMCs or macrophages. Ruan *et al* (361) also have shown that minimally modified LDL led to TNFα induction in rat mesangial cells. Some studies showed modified LDL induce VSMCs and/or endothelial cells to produce chemotactic and adhesive factors such as MCP-1 (362), monocyte M-CSF (44), IL-1β (363), and other adhesion molecules (364, 365). Modified LDL may also inhibit the motility of resident monocytes once they have differentiated into macrophages within the intima (366). Furthermore, Ding *et al* (367) demonstrated that macrophages obtained

from hypercholesterolaemia animals displayed higher expression of TGF-β mRNA by comparison with controls. Another study demonstrated that oxLDL inactivated endothelial cell nitric oxide (368). Rahman and Varghese *et al* also verified that hypercholesterolaemia diminished activity of nitric oxide in an isolated perfused rat kidney and oxLDL induced vasoconstriction mediated by decreased activity of nitric oxide which may result in systemic hypertension and endothelial injuries (369, 370). These results suggest that lipoprotein and its oxidative products may act as pro-inflammatory mediators. Lipoprotein-mediated cytokine production may cause recruitment of monocytes, lipid-mediated cell proliferation, and matrix production, thus contributing to atherosclerosis.

1.3.2 Inflammation accelerates lipid-mediated atherosclerosis by affecting cholesterol metabolism

A number of cytokines including TNFα and the interferons increase serum triglyceride levels due to an early increase in hepatic VLDL secretion, while the late increase may be due to a variety of factors including increased hepatic production of VLDL or delayed clearance secondary to a decrease in lipoprotein lipase activity and/or apoE levels on VLDL. Cytokines increase hepatic cholesterol synthesis by stimulating HMGR gene expression and decrease hepatic cholesterol catabolism by inhibiting cholesterol 7-α-hydroxylase, the key enzyme in the course of bile acid synthesis (371). Cytokines also decrease HDL cholesterol levels and induce alterations in its composition – apoA-I and the cholesterol ester content may decrease, while free cholesterol increases. Additionally, key proteins involved in HDL metabolism are altered by cytokines: LCAT activity, hepatic lipase activity, and CETP levels fall. Thus, cytokines induce marked changes in lipid metabolism that lead to hyperlipidemia (371).

Inflammatory mediators, including TNFα and IL-1β, may also induce oxygen radical production, which may then promote oxidation of lipoprotein (372, 373).

1.3.3 Inflammation accelerates lipid-mediated atherogenesis by affecting cholesterol homeostasis at the cellular level

Atherosclerosis is characterised by the presence of lipid-loaded cells derived from macrophages and VSMCs. Foam cell formation is a hallmark of the breakdown of intracellular cholesterol homeostasis, which is the balanced regulation between cholesterol influx and efflux. Inflammatory cytokines can affect lipid uptake, cholesterol efflux and modify cholesterol homeostasis in macrophages and VSMCs and transform them into foam cells. Several lipoprotein receptors may be involved in cellular lipid uptake, including LDLr, scavenger receptor, VLDLr, and LRP/α_2-macroglobulin receptor. Clearly no single receptor pathway is solely responsible for increased lipid uptake of cells involved in atherosclerotic lesion, but several redundant mechanisms may contribute to the uptake and degradation of lipoproteins in atherosclerotic lesions. For example, Ruan *et al* (374) demonstrated that inflammatory cytokines induced type A scavenger receptors in human mesangial cells. Ruan *et al* (375, 376) also have reported that inflammatory cytokines can modify cholesterol homeostasis through the dysregulation of the LDLr. In this study, using native LDL as a ligand they showed that inflammatory cytokines could overcome sterol-induced suppression of LDLr and make foam cells. This process is mediated through activation of SREBP by increasing SCAP expression which may result in atherosclerosis in arteries. The implication of these findings is that inflammatory cytokines are important risk factors for atherogenesis.

Since intracellular lipid content is governed by both influx and efflux mechanisms, the balance between lipid uptake by the lipoprotein receptor and cholesterol efflux mechanisms, becomes important in establishing cholesterol homeostasis. Ruan *et*

al(377) have observed that ABCA1 gene expression in human mesangial cells mediates cholesterol efflux and that inflammatory cytokine IL-1β inhibits both cholesterol efflux and ABCA1 gene expression. It appears that, in addition to increasing lipid uptake, inflammatory cytokines promote intracellular lipid accumulation by inhibiting cholesterol efflux through the ABCA1 pathway. These results suggest potential mechanisms whereby inflammation may exacerbate lipid-mediated cellular injury in the glomerulus and in other tissues.

1.4 The role of Sirolimus in atherosclerosis

The new understanding of the pivotal position of inflammation in the pathogenesis of atherosclerosis raises questions and opens opportunities in prevention and therapy of this disease. Recently, a new immunosuppressive agent, Sirolimus has been paid more and more attention by researchers in cardiovascular field as its obvious antiproliferative therapeutic effect in preventing re-stenosis following angioplasty, inhibiting intimal thickening in patients with coronary artery disease, and reducing the lesion size of atherosclerotic plaque.

Sirolimus (Rapamycin) is a natural fermentation product (macrolide antibiotic) produced by Streptomyces hygroscopicus, isolated from a soil sample collected from Easter Island (Rapanui). Sirolimus is a white to off-white powder and is insoluble in water, but freely soluble in benzyl alcohol, chloroform, acetone, and acetonitrile. The chemical formula for Sirolimus is C51H79NO13 (Fig 1.9) and its molecular weight is 914.2.

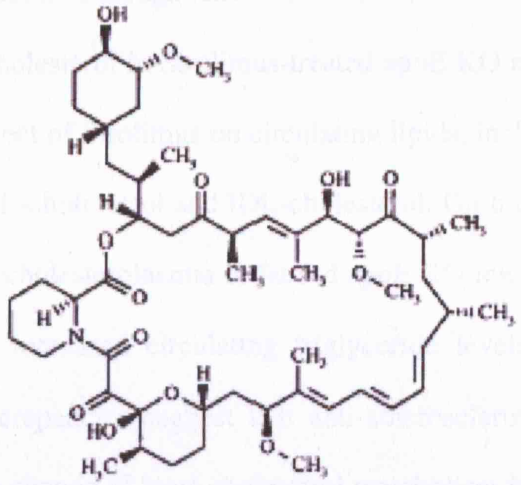

Fig 1.9 The structural formula of Sirolimus (http://www.rxlist.com/cgi/generic/sirolimus.htm)

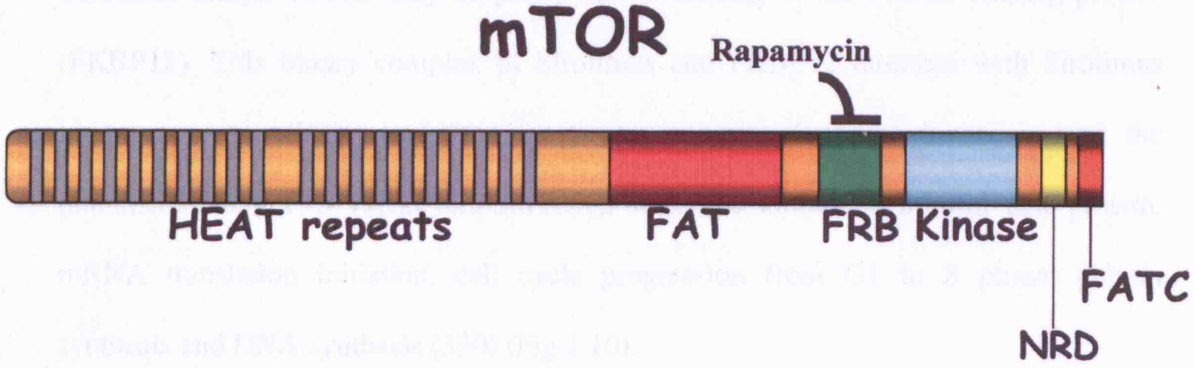

Fig 1.10 The primary structure of Mtor (Genes Dev 2004; 18(16):1926-45.)

Sirolimus is a potent immunosuppressive agent used for the prophylaxis of transplant rejection. Clinical trials have demonstrated the efficacy of Sirolimus therapy in reducing acute graft rejection in kidney (378), heart (379), liver (380) and lung (381) transplant recipients. Recent studies have demonstrated that Sirolimus also attenuates neointimal thickening and transplant atherosclerosis in animal models of angioplasty, and vessel and cardiac allograft (382, 383). Clinical trials have demonstrated a significant reduction in binary restenosis, late lumen loss and repeat revascularization rates in selected patient groups receiving Sirolimus-eluting stents compared with standard coronary stents (382, 384). Moreover, some studies showed that Sirolimus reduces atherosclerotic lesion size in apoE KO mice, both when administered intraperitoneally

(385, 386) or orally ((387). Although Elloso *et al* (386) have reported increased LDL-cholesterol and HDL-cholesterol in Sirolimus-treated apoE KO mice, Castro *et al* (385) found no significant effect of Sirolimus on circulating lipids, including LDL-cholesterol, HDL-cholesterol, VLDL-cholesterol and IDL-cholesterol. On the other hand, Sirolimus did not aggravate hypercholesterolaemia in fat-fed apoE KO mice (385, 386, 388, 389). In contrast, Sirolimus increased circulating triglyceride levels in the same animal model(389). These discrepancies suggest that anti-atherosclerotic effect of Sirolimus may be related with the change of local cholesterol metabolism in the tissues. However, the potential mechanisms are incompletely understood.

Sirolimus unique effects may be partly due to binding to the FK506 binding protein (FKBP12). This binary complex of Sirolimus and FKBP12 interacts with Sirolimus binding domain (FRB) and thus inactivates a serine-threonine kinase termed the mammalian target of rapamycin (mTOR), which is known to control cell growth, mRNA translation initiation, cell cycle progression from G1 to S phase, protein synthesis and DNA synthesis (390) (Fig 1.10).

mTOR is an integrator of multiple signals receiving input from insulin, growth factors, amino acids, and energy to signal to the downstream targets and adjust cell growth and proliferation as well as metabolic homeostasis (391, 392). mTOR signalling is negatively regulated by tumour suppressor gene products Tuberous Sclerosis Complex (TSC-1 and TSC-2), phosphatase and tensin homolog (PTEN), and LKB, and positively by proto-oncogene Ras homolog enriched in brain (Rheb), thus adding to the intricacy of mTOR regulation (393). Furthermore, mTOR phosphorylates two well-characterised downstream targets, namely, ribosomal protein S6 kinase 1 and 2 (S6K-1 and S6K-2) and the eukaryotic initiation factor 4E (eIF-4E) binding protein (4E-BP1) (Fig 1.11 and Fig 1.12). Therefore, Sirolimus, an mTOR inhibitor, leads to translational arrest by

regulating S6K-1 and 4E-BP1 and cell cycle arrest from G1 to S phase. At present some studies have reported that anti-atherosclerosis of Sirolimus through the property of anti-proliferation and anti-migration to VSMCs (394). However, the effect of Sirolimus/mTOR pathway on dyslipidemia in atherosclerosis is unknown.

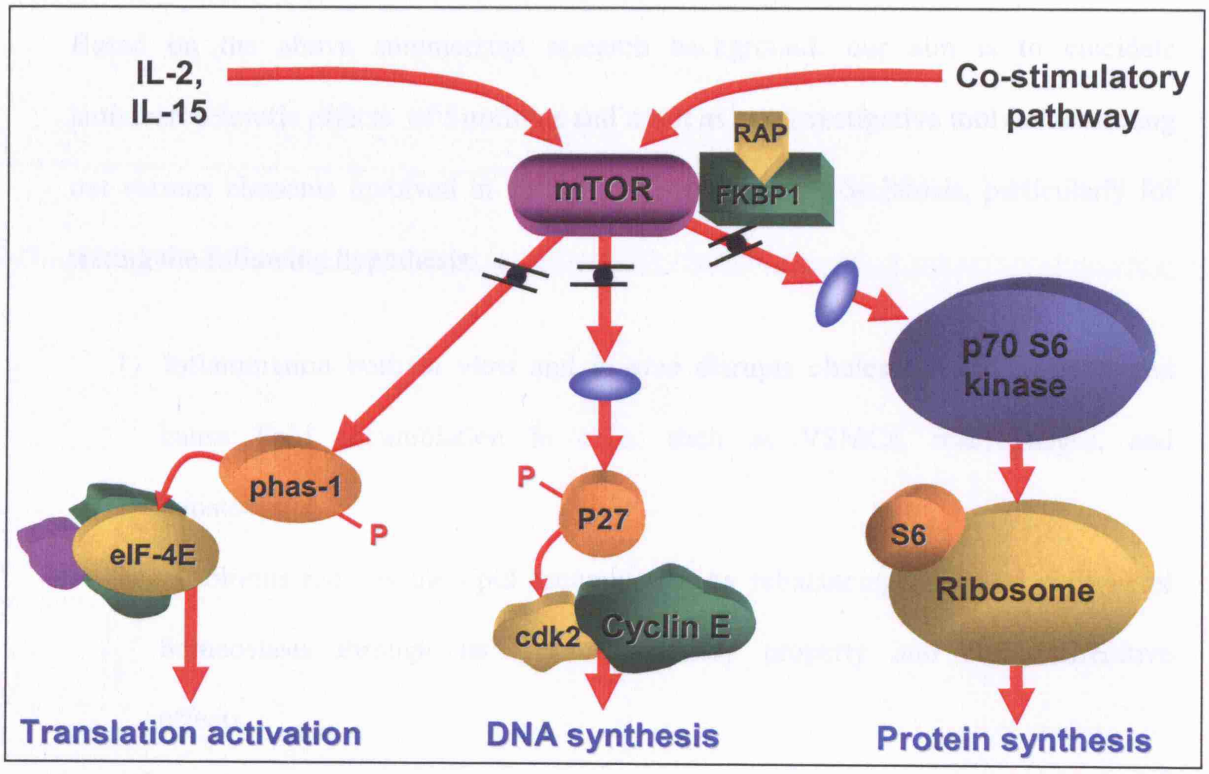

Fig 1.11 mTOR is a critical kinase (http://www.fda.gov/ohrms/dockets/ac/02/slides/3832s1_02_WA-Overview.ppt)

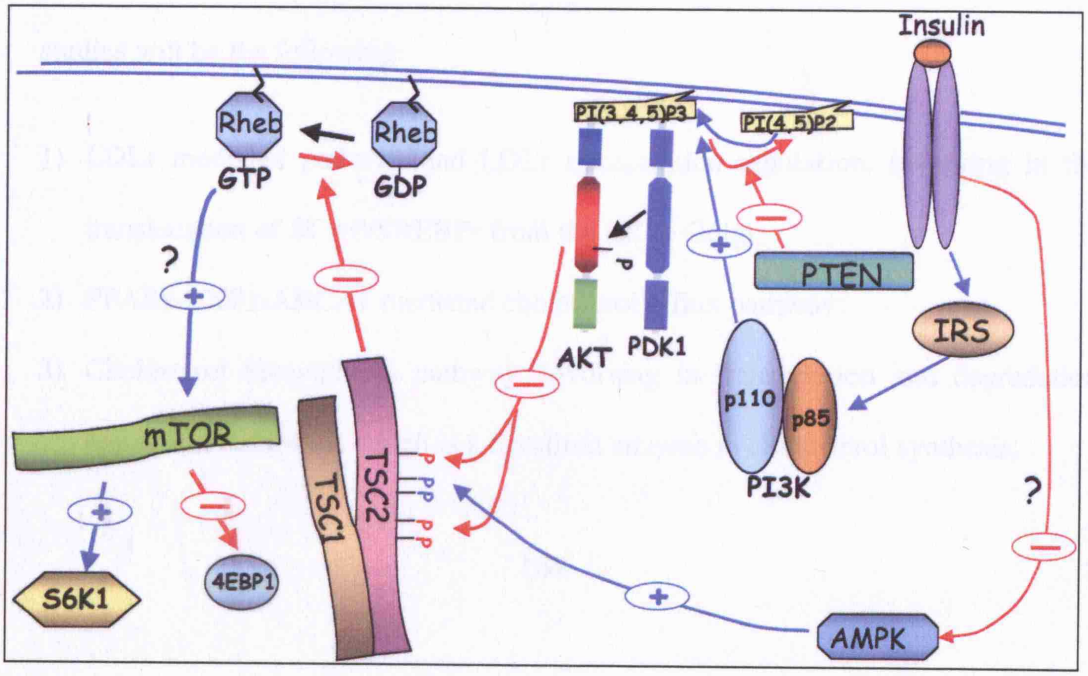

Fig 1.12 The regulation of mTOR activity by growth factors (Genes Dev 2004; 18 (16):1926-45.)

It is mediated by the PI3K/Akt signalling pathway leading to phosphorylation and inhibition of TSC2 by Akt and to the subsequent activation of Rheb, which activates mTOR by an as yet unknown mechanism. In addition, TSC2 is activated by AMPK. (+) activation; (–) inhibition

1.5 Aim of this thesis

Based on the above summarized research background, our aim is to elucidate antiatherosclerotic effects of Sirolimus and use it as an investigative tool for dissecting out various elements involved in the pathogenesis of atherosclerosis, particularly for testing the following hypothesis:

1) Inflammation both *in vitro* and *in vivo* disrupts cholesterol homeostasis and cause lipid accumulation in cells, such as VSMCs, macrophages, and hepatocytes.
2) Sirolimus reduces the lipid accumulation by rebalancing disrupted cholesterol homeostasis through its anti-inflammatory property and anti-proliferative effects.

We tested our hypothesis in both cell culture systems (human VSMCs, macrophages, and HepG2 cells) and apoE KO mice under inflammatory stress induced by IL-1β *in vitro* or 10% casein subcutaneously injection *in vivo*. The main studies will be the following:

1) LDLr mediated pathway and LDLr transcription regulation, involving in the translocation of SCAP/SREBPs from the ER to Golgi;
2) PPARs-LXRs-ABCA1 mediated cholesterol efflux pathway;
3) Cholesterol biosynthesis pathway, involving in transcription and degradation regulation of HMGR which is a rate-limit enzyme in cholesterol synthesis;

4) In addition, the effects of Sirolimus on inflammatory cytokine production *in vivo* and *in vitro* will be also investigated, which may be an additional mechanism of Sirolimus in anti-atherosclerosis.

We hope these studies will help us to elucidate the importance of these factors in the pathogenesis to define the requirement of an ideal antiatherosclerotic drug.

CHAPTER 2. GENERAL METHODS

This chapter mainly showed some shared research methods used in cell culture and animal studies. The unshared methods would be shown in each separated chapter.

2.1 Preparation of lipoprotein

2.1.1 Materials

1) Fresh AB plasma (Supplied by Blood Transfusion Department of Royal Free Hospital, London, UK)

2) Penicillin/ Streptomycin (Cat.NO.P4333, Sigma, Poole, Dorset, UK)

3) 100 mmol/l of disodium of ethylene diaminetetra-acetic acid (EDTA) (pH 7.4) (Cat.NO.E5134, Sigma, Poole, Dorset UK)

4) 20 mmol/l of Butylated hydroxytoluene (BHT) (Cat.NO.28067, BDH chemicals Ltd, Poole, UK)

5) Sodium bromide (Cat.NO.30116, Merck Ltd. Poole UK)

6) Quick-Seal centrifuge tubes (25×89mm) (Cat.NO.342414, Beckman, Buckinghamshire, UK)

7) PD-10 desalting columns (Cat.NO.17-0851-01, GE Healthcare, Buckinghamshire, UK)

8) L8-80M ultracentrifuge machine (Beckman, Buckinghamshire, UK)

9) 100 μg/ml stock solution of bovine serum albumin (BSA) standard (Cat.NO.A2153, Sigma, Poole, Dorset, UK)

10) Reagent A for LDL concentration assay: 2 % Na_2CO_3, 0.4 % NaOH, 0.16 % Sodium tartrate and 1 % SDS

11) Reagent B for LDL concentration assay: 4 % $CuSO_45H_2O$

12) Folin-Ciocalteu phenol solution (Cat.NO.F9252, Sigma, Poole, Dorset, UK): 1 mol/l of working solution: 2 mol/l of stock was diluted by dH_2O according to 1:1 (V: V).

13) Lipoprotein Electrophoresis System (Beckman, U.S.A)

2.1.2 Procedures

Fresh plasma was collected from healthy human volunteers. LDL was isolated by sequential density gradient ultracentrifugation (375). The study protocol was approved by the Institutional Review Board of Royal Free and Medical School, University College London and adhered to the tenets of the Declaration of Helsinki for experiments involving human samples. Anti-oxidants (100 μmol/l of EDTA and 20 μmol/l of BHT) and antibiotics (100 units/ml of penicillin and 100 μg/ml of streptomycin) were added into fresh plasma to prevent oxidation and contamination. The plasma was separated by centrifugation at 3000 rpm 4 °C for 15 minutes. The plasma was adjusted to a density of 1.019 g/ml using formula to calculate the amount of sodium bromide to be added ($X=V_i(d_f - d_i)/ (1-(V_x*d_f))$, X = sodium bromide (g) to be used for density adjustment; V_i = The initial volume of solution to be adjusted; d_i = Initial density of plasma (1.006); d_f = final density required; V_x= Partial specific volume of sodium bromide =0.235). Then plasma was centrifuged at 60,000 rpm for 22 hours at 4 °C using 70 Ti Rotor. After that, cut off ultracentrifuge tubes' caps and aspirate VLDL and IDL using a 10 ml syringe with a 19-gauge needle. The density was adjusted to 1.063 g/ml by adding sodium bromide using the formula given above and the plasma was centrifuged at 60,000 rpm for another 22 hours at 4 °C using 70 Ti rotors. After that, LDL fraction in the upper was aspirated and dialyzed by PD-10 desalting column. LDL concentration was measured by Lowry assay.

2.2 The acetylated modification of LDL

2.2.1 Materials

1) Acetic anhydride (Cat.NO.487813, Sigma, Poole, Dorset, UK)

2) Saturated sodium acetate solution (Cat.NO.S2889, Sigma, Poole, Dorset, UK)

2.2.2 Procedures

1) Ice cold LDL (2-5 mg/ml) was diluted 1:2 (V: V) with saturated sodium acetate solution and mix up.

2) The mixture was stirred continuously at 4 °C and 4 aliquots of acetic anhydride (1.5 µl per mg LDL) were added to the mixture in 60 minutes. Added one aliquot every 15 minutes.

3) Continued stirring 30 minutes without adding aliquot.

4) The acetylated LDL (acLDL) was then gone through column.

5) Before acLDL was gone through a column, cleaned the column with 25 ml of phosphate buffered saline (PBS).

6) After that, added acLDL into column until fully enter the column.

7) Then added 3 ml of PBS into the column.

8) Collected acLDL, disinfect with a 0.2 µm filter.

9) Checked the concentration of acLDL by Lowry assay.

2.3 Protein concentration assay

Four spectroscopic methods are routinely used to determine protein concentration (395). These include measurement of the protein's intrinsic ultraviolet (UV) absorbance and other three methods which generate a protein-dependent colour change, the Lowry assay (396), the Smith copper/bicinchoninic assay (397) and the Bradford dye assay (398). Next, we will show the basic procedures of Lowry protein assay and Bradford protein assay commonly used in our lab.

2.3.1 Modified Lowry protein assay

Lowry assay was firstly described in 1951 (396). Under alkaline conditions the divalent copper ion forms a complex with peptide bonds in which it is reduced to a monovalent ion. Monovalent copper ion and the radical groups of tyrosine, tryptophan, and cysteine react with Folin reagent to produce an unstable product that becomes reduced to molybdenum/tungsten blue.

The assay is relatively sensitive, but takes more time than other assays and is susceptible to many interfering compounds. The following substances are known to interfere with the Lowry assay: detergents, carbohydrates, glycerol, Tricine, EDTA, Tris, potassium compounds, sulfhydryl compounds, disulfide compounds, magnesium and calcium. Most of these interfering substances are commonly used in buffers for preparing proteins. This is one of the major limitations of Lowry assay.

The standard curve is linear in the 1 to 100 μg protein region. The absorbance can be read in the region of 500 to 750 nm. Most researchers use 660 nm, but other wavelengths also work and may reduce the effects of contamination (e.g. chlorophyll in plant samples interferes at 660 nm, but not at 750 nm).

2.3.1.1 Materials

1) 100 μg/ml stock solution of BSA (Cat.NO.A2153, Sigma, Poole, Dorset, UK)

2) Reagent A: 2 % Na_2CO_3, 0.4 % NaOH, 0.16 % Sodium tartrate and 1 % SDS

3) Reagent B: 4 % $CuSO_45H_2O$

4) 1 mol/l of Folin-Ciocalteu working solution: 2 mol/l of Folin-Ciocalteu (Cat.NO.F9252, Sigma, Poole, Dorset, UK) was diluted by dH_2O according to 1:1 (V: V).

5) Lambda 3B spectrophotometer (Perkin Elmer, U.S.A)

2.3.1.2 Procedures

Diluted the BSA stock with dH_2O to obtain a standard curve as follows: 0, 5, 10, 20, 40, 60, 80, 100 μg/ml.

Table 2.1 Preparation of standard curve in Lowry assay

BSA(μg/ml)	Volume dH_2O(μl)	Volume BSA stock(μl)
0	1000	0
5	950	50
10	900	100
20	800	200
40	600	400
60	400	600
80	200	800
100	0	1000

2) Added 3 ml of reagent C (Solution A: Solution B at 100:1) to 1 ml of sample containing 10-100 μg of protein and incubated for 10 minutes at room temperature.

3) Added 0.3 ml of Folin-Ciocalteu working solution and fully mixed up. Incubated for 45 minutes at room temperature.

4) Read absorbance at 660 nm and calculated protein concentration of samples using the BSA standard curve.

2.3.2 Bradford protein assay

Bradford assay is accurate and quick, measuring the same range of protein as Lowry assay. The Bradford is generally recommended for determining protein concentration of cell fractions and assessing protein concentrations for gel electrophoresis.

The Bradford protein assay is based on the observation that the absorbance maximum for an acidic solution of Coomassie Brilliant Blue G-250 shifts from 465 nm to 595 nm when binding to protein occurs (398, 399). Both hydrophobic and ionic interactions stabilize the anionic form of the dye, causing a visible colour change. Bradford (398) first demonstrated the usefulness of this principle in protein assay. Spector (400) found

that extinction coefficient of dye-albumin complex was constant over a 10-fold concentration range. Over a broader range of protein concentrations, the dye-binding method gives an accurate, but not entirely linear response.

2.3.2.1 Materials

1) Bio-Rad protein assay dye concentration (Cat.NO.500-0006, Bio-Rad, Hertfordshire, UK)
2) 25 μg/ml of BSA protein standard (Cat.NO.A2153, Sigma, Poole, Dorset, UK)
3) Model 3550 microplate reader (Bio-Rad, Hertfordshire, UK)

2.3.2.2 Procedures

1) Added 0.1 mol/l of NaOH 0.5 ml overnight, and made cells into debris.
2) Prepared samples and the dilutions of BSA Standard given at Table 2.2. Added 50 μl of dye working solution (diluted by dH_2O, 1:4 (V:V)) to standards and samples.
3) Mixed thoroughly on the shaker and incubated at room temperature for 5 minutes to 1 hour (Selected 20 minutes in our lab).
4) Measured OD_{595} by an Enzyme Linked-Immunosorbent Assay (ELISA) plate reader. Calculated the concentrations of samples by standard curve.

Table 2.2 Preparation of standard curve in Bradford protein assay

BSA(μg/ml)	Volume of BSA(μl)	Volume of H_2O((μl)
0.0	0	200
2.5	20	180
5.0	40	160
7.5	60	140
10.0	80	120
15.0	120	80
20.0	160	40
25.0	200	0

2.4 Lactate dehydrogenase for cytotoxicity assay

Traditionally, the toxic effects of unknown compounds have been measured *in vitro* by counting viable cells after staining with a vital dye. Alternative methods include the measurement of DNA synthesis by radioisotope incorporation, cell counting by automated counters, and other methods that rely on dyes and cellular activity. Lactate dehydrogenase (LDH) assay is a means of measuring either the number of cells via total cytoplasmic LDH or membrane integrity as a function of the amount of cytoplasmic LDH released into the medium. LDH method is simple and accurate, and yields reproducible results. The assay is based on the reduction of nicotinamide adenine dinucleotide (NAD) by the action of LDH. The resulting reduced NAD is utilized in the stoichiometric conversion of a tetrazolium dye. The resulting colored compound is measured spectrophotometrically. If the cells are lysed prior to assaying the medium, an increase or decrease in cell numbers results in a concomitant change in the amount of substrate converted. This indicates the degree of inhibition of cell growth (cytotoxicity) caused by the tested material. If cell-free aliquots of medium from cultures given different treatments are assayed, then the amount of LDH activity can be used as an indicator of relative cell viability as well as a function of membrane integrity. This technique has been utilized as an alternative to ^{51}Cr release for cell mediated cytotoxicity assays (401) as well as conventional cytotoxicity resulting from interaction of a tested material with the cell (402).

2.4.1 Materials

1) The LDH cytotoxicity assay kit (Cat. NO. TOX7, Sigma, Poole, Dorset, UK)

Table 2.3 Components in the LDH assay kit

Product NO.	Item	Quantity
L2402	LDH Assay Substrate Solution	25 ml
L2527	LDH Assay Cofactor preparation	25 ml
L2277	LDH Assay Dye Solution	25 ml
L2152	LDH Assay Lysis Solution	10 ml

2) Model 3550 Microplate Reader (Bio-Rad, Hertfordshire, UK)

2.4.2 Procedures

The LDH method of monitoring *in vitro* cytotoxicity is well suited to multiwell plates. For best results, cells in the log phase of growth should be employed and final cell number should not exceed 10^6 cells/ml. Each test should include a blank containing complete medium without cells. LDH activity can be assayed by either of the two methods described below. Step 1 provides a measure of total cell number. Step 2 assesses the membrane integrity of cells as a function of the amount of LDH leakage into the medium.

Step1: Total LDH

1) Removed cultures from incubator into laminar flow hood or other sterile work area.

2) Added 1/10 volume of LDH Assay Lysis Solution per well and returned plate to incubator for 45 minutes.

3) Centrifuged plate at 800 rpm for 4 minutes to pellet debris.

4) Transfered aliquot to clean flat-bottom plate and proceeded with enzymatic analysis.

Step2: LDH release

1) Removed cultures from incubator into laminar flow hood or other sterile work area.

2) Centrifuged plate at 800 rpm for 4 minutes to pellet cells.

3) Transfered aliquot to clean flat-bottom plate and proceeded with enzymatic analysis.

Step3: Enzymatic Assay

1) Prepared 25 ml of 1× LDH Assay Cofactor Preparation by adding 25 ml of tissue culture grade water to bottle of lyophilized cofactors. Stored reconstituted cofactor preparation at 0 °C (avoid frost-free freezers) in working aliquots to avoid repeated freeze/thaw procedures.

2) Prepared LDH Assay Mixture by mixing equal amounts of LDH Assay Substrate, Cofactor and Dye Solutions. Removed aliquot of medium for testing (approximately 1/2 of the volume of culture medium). Added assay mixture in an amount equal to 2× the volume of medium removed for testing to each sample. Prepared assay mixture at time of use, extended storage of the assay mixture was not recommended.

3) Covered the plate with an opaque material to protect from light (e.g. aluminum foil or a box) and incubated at room temperature for 20-30 minutes.

4) The reaction was terminated by adding 1/10 volume of 1mol/l HCl to each well.

5) Spectrophotometrically measured absorbance at a wavelength of 490 nm. Measured the background absorbance of multiwell plates at 690 nm and subtracted from the primary wavelength measurement.

6) Tests in multiwell plates could be read in a plate reader or the contents of individual wells could be transferred to appropriate size cuvets for spectrophotometric measurement.

2.5 Oil Red O staining

2.5.1 Materials

1) 5 % Formalin saline: 8.5 g NaCl, 50 ml formalin (40 % H.CHO, Cat.NO.F8775, Sigma, Poole, Dorset, UK), 950 ml dH_2O
2) Oil Red O (saturated solution): 0.2 g Oil Red O (Cat.NO.O0625, Sigma, Poole, Dorset, UK), dissolved in 100 ml isopropanol (Cat.NO.I9516, Sigma, Poole, UK)
3) Oil Red O working solution: Stock solution: distilled water (dH_2O) = 3:2 (V : V). Mixed up and kept shaking for 10 minutes, then filtered through Whatman No.1 filter paper for use within 1 hour.
4) Carazzi's haematoxylin (Cat.NO.MHS-16, Sigma, Poole, Dorset, UK): 500g Potassium or ammonium Alum, 1 g haematoxylin, 0.2 g potassium iodate, 800 ml

dH_2O, 200 ml glycerine. Dissolved the alumin in the water and then added the haematoxylin. When this has been completely dissolved, then added the potassium iodate to ripen. Finally added the glycerine when the solution has turned into purple.

5) 1, 2-Propanediol (Cat.NO.P1009, Sigma, Poole, Dorset, UK)

6) Chamber Slides (Cat.NO.354118, Becton Dickinson Labware, USA)

7) D-7082 Oberkochen Microscopy (Carl Zeiss, Germany)

2.5.2 Procedures

When experiments terminated, cells cultured in chamber were washed three times in PBS, fixed with 5 % formalin solution for 30 minutes and subjected to the following staining procedures:

1) Washed twice with dH_2O.

2) Incubated with 1, 2-Propanediol for 2 minutes.

3) Stained with Oil red O working solution for 30 minutes at room temperature.

4) Rinsed 3 times with dH_2O.

5) Stained by Carazzi's haematoxylin for 1-2 minutes.

6) Washed in tap water for 5 minutes.

7) Drained and mounted in glycerine jelly on glass slides.

Bright-field micrographs were taken by a Carl Zeiss microscope using a magnification of ×100 or ×200, captured by a digital camera connected with computer.

2.6 Quantitative assay of intracellular cholesterol

2.6.1 Materials

1) Cholesterol esterase (Cat.No.C5921, Sigma, Poole, Dorset, UK)

2) Cholesterol oxidase (Cat.No.C8649, Sigma, Poole, Dorset, UK)

3) Horseradish peroxidase (Cat.NO.P6140, Sigma, Poole, Dorset, UK)

4) 4-aminoantipyrine (Cat.NO.H4377, Sigma, Poole, Dorset, UK)

5) Phenol (Cat.NO.P5566, Sigma, Poole, Dorset, UK)

6) Cholesterol (Cat.NO.C3045, Sigma, Poole, Dorset, UK)

7) Potassium phosphate buffer (PPB) 0.1mol/l pH7.0

8) Sodium cholate Hydrate (Cat.NO.C1254, Sigma, Poole, Dorset, UK)

9) Triton X-100 (Cat.NO.T9284, Sigma, Poole, Dorset, UK)

10) MSE soniprep 150 (Sanyo Gallenkamp PLC, Leicester, UK)

11) SF60 vacuum machine (Genevac Ltd, Ipswich, UK)

4) 12) Model 3550 microplate reader (Bio-Rad, Hertfordshire, UK)

2.6.2 Solution preparation

2.6.2.1 Stock solution

1) PPB: 0.1mol/l pH 7.0

2) Cholesterol oxidase: 5 units/ml in PPB, store at -20 °C

3) Horseradish peroxidase: 50 units/ml in PPB, store at 4 °C

4) Sodium cholate Hydrate: 20 mmol/l

5) 1 % Triton X-100

6) 4-aminoantipyrine (FW 203.2): 5.5 mmol/l

7) Phenol (FW 94.11): 280 mmol/l

8) Cholesterol ester hydrolase: 25 units/ml in PPB, store at 4 °C

9) Cholesterol: 5 mg/ml

2.6.2.2 Assay solution

Stock solution should be kept at 4 °C in the dark, it should be stable for at least one month, and assay solution should be prepared on the day of use.

Table 2.4 Preparation of assay solution for intracellular cholesterol assay

Stock solution	FC assay (μl)	TC assay (μl)
PPB 0.1mol/l pH7.4	18 μl	16 μl
Cholesterol oxidase 5 units/ml in PPB	2 μl	2 μl
Horseradish peroxidase 50 units/ml in PPB	2 μl	2 μl
Sodium cholate Hydrate 20 mmol/l in PPB	5 μl	5 μl
1 % Triton X-100 in PPB	5 μl	5 μl
4-aminoantipyrine 5.5 mmol/l	13 μl	13 μl
Phenol 280mmol/l	5 μl	5 μl
Cholesterol ester hydrolase 25 units/ml in PPB	None	2 μl
Total Volume	50 μl	50 μl

2.6.3 Standard Curve Preparation

Firstly, prepared 0.5 μg/μl of cholesterol stock using 100 % ethanol.

Table 2.5 Preparation of standard curve in intracellular cholesterol assay

Cholesterol standard (μg/ml)	0.5 μg/μl cholesterol stock(μl)	Ethanol (μl)
0	0	50
40	4	46
80	8	42
120	12	38
160	16	34
200	20	30
240	24	26
280	28	22

2.6.4 Procedures

1) Collected cells in six-well plate into 1.5 ml universal microcentrifuge tubes and spun 10,000 rpm for 10 minutes.

2) Sucked the supernatant out, added 1ml of PBS to suspend the cell pellets, transfered it into 12 × 75 mm PP FACS tube.

3) Spun 2000 rpm for 10 minutes. Abandoned the supernatant, and added 1ml of chloroform/methanol mixture (V: V=2:1).

4) Sonicated each sample by MSE Soniprep 150 machine for 1 minute at power level 6.

5) Spun 3000 rpm for 10 minutes.

6) Carefully removed the liquid phase into 5 ml glass tube and dried the pellet in the tube at room temperature. Added 100 µl 1mol/l of NaOH to dissolve the pellet for at least 2 hours, and then checked the protein concentration by Lowry assay.

7) Dried the liquid phase in the glass tubes by Vacuum machine.

8) Dissolved in 1ml of 2-propanol containing 10 % Triton X-100 for assay. (The amount of 2-propanol added is depending on the amount of samples). Vortexed and took 50 µl of samples into a clean 96-well plate.

9) Added 50 µl of assay solution into each well and gently mixed up with sample.

10) Incubated the reaction for 60 minutes at 37 °C, protecting from light.

11) Measured in a microplate reader at OD_{500} nm by colorimetric assay.

12) Normalized the value of each sample by background control (The background reading must be minus from sample readings).

2.6.5 Calculation

Cholesterol concentrations of samples were calculated by the standard curve. Total cholesterol and free cholesterol concentration were normalized by total cell protein of each sample. Cholesterol ester = Total cholesterol – Free cholesterol

2.7 Intracellular cholesterol efflux assay

2.7.1 Materials

1) Cholesterol (Cat.NO.C3045, Sigma, Poole, Dorset, UK)

2) 25-hydroxycholesterol (Cat.NO.H1015, Sigma, Poole, Dorset, UK)

3) [1α, 2α(n)-^{3}H] cholesterol (Cat.NO.TRK330, GE Healthcare, Buckinghamshire, UK)

4) Recombinant IL-1β (Cat.NO.201-LB-005, IL-1β, R&D Systems, Abingdon, UK).

5) Sirolimus (Cat. NO. AY-22989-39, Wyeth, Berkshire, UK).

6) Methanol (Cat.NO.M3641, Sigma, Poole, Dorset, UK)

7) 24-well plate (Cat.NO.BC017, Appleton Woods Ltd, Birmingham, UK)

8) Microscint-20 (Cat.NO.MSB084, PerkinElmer, Bucks, UK)

9) Microplate Scintillation & Luminescence Counter (Cat. NO. C9904V1, PerkinElmer, Bucks, UK)

10) $ApoA_1$ (Cat.NO.178452, Calbiochem, Nottingham, UK)

2.7.2 Procedures

Cells were loaded with 30 μg/ml of cholesterol, 1 μg/ml of 25-hydroxy-cholesterol, and 1 μCi/well [1α, 2α(n)-^{3}H]-Cholesterol in serum-free DMEM/F12 medium for 48 hours. After that, fresh serum-free DMEM/F12 medium containing Sirolimus was added in the presence or absence of IL-1β for further 24 hours. After this incubation period, cells were washed three times in PBS and $ApoA_1$-mediated cholesterol efflux studies were immediately performed by adding fresh serum-free DMEM/F12 medium with or without 15 μg/ml of $ApoA_1$ for 6 hours. Supernatants were then collected and centrifuged at 13,000 rpm for 10 minutes to remove debris. Cells were lysed with 0.5 ml 0.1 mol/l of NaOH. The radioactivity in both the supernatants and cellular lipids was measured by scintillation counting. $ApoA_1$-induced [^{3}H]-cholesterol efflux was calculated as by subtracting the radioactivity in supernatants without $apoA_1$ from the counts in supernatants containing $apoA_1$. The data were normalized by total [^{3}H]-cholesterol radioactivity (including in the supernatants and cells) and were expressed as a percentage of the control.

2.8 Immunofluorescent staining for laser confocal microscopy observation

2.8.1 Materials

1) PBS pH 7.2

2) 10 % Formaldehyde in PBS (Cat.NO. F-1635, Sigma, Poole, Dorset, UK)

3) 0.25 % Triton X-100 in PBS (Cat.NO.T9284, Sigma, Poole, Dorset, UK)

4) PBS-Tween 20 (0.1 % Tween 20)

5) Block buffer (5 % skimmed milk in PBS with 0.1% Tween (PBST))

6) Cover-glasses (Cat. NO. L4095-2, Agar Scientific, UK)

7) Chamber slide (Cat.NO.354118, Becton Dickinson Labware, USA)

8) Rabbit anti-human SCAP antibody (Made by our lab)

9) Mouse anti-human Golgin-97 IgG_1, monoclonal CDF4 (Cat. NO. A21270, Invitrogen Ltd, Paisley, UK)

10) Alexa Fluor® 488 goat anti-rabbit IgG (H+L) (Cat. NO. A11034, Invitrogen Ltd, Paisley, UK)

11) Alexa Fluor 594 goat anti–mouse IgG (H+L) (Cat. NO. A11032, Invitrogen Ltd, Paisley, UK)

12) Citifluor^{TM} PBS solution (Cat. NO. R1322, Agar Scientific, UK)

13) LSM 410 laser scanning confocal microscope (Carl Zeiss, Germany)

14) Nail-polish (Maxfactor, UK)

15) Skimmed milk (Marvel, UK)

2.8.2 Procedures

1) Cells grown in chamber slides were incubated with different treatments for 24 hours.

2) Washed one time with PBS

3) Fixed with 10 % formaldehyde/PBS for 30 minutes

4) Washed 2 times with PBS

5) Permeabilized 15 minutes in 0.25 % Triton X-100/PBS

6) Washed one time with PBS

7) Blocked one hour using 5 % skimmed milk in PBST at room temperature

8) Washed three times with PBST for 5 minutes each time.

9) Added primary antibody 100 µl/well (A. Rabbit anti-human SCAP Ab (1:100); B. Mouse anti-human Golgi Ab (1:100); C. Overlap: A plus B) in Block Buffer with gentle movement on the orbital shaker for one hour at room temperature or 4 °C overnight.

10) Washed three times with PBST for 5 minutes each time.

11) Added second antibody 100 µl/well in block buffer (A. Goat anti-rabbit Fluor 488 (1:100, green); B. Goat anti-mouse Fluor 594 (1:100, red); C. Overlap: A plus B) for one hour at room temperature.

12) Washed three times with PBST for 5 minutes each time.

13) Dried samples in the air

14) If necessary, applied the appropriate mounting medium containing anti-fade agents (about 10-20 µl, depending on the volume of samples) to the central per well.

15) Wells were covered using cover-glasses and sealed the edge of the cover-glasses with nail-polish.

16) Slides were placed with cover-glasses in the dark at room temperature to allow mounting medium to harden.

17) Results were observed under confocal fluorescence microscopy.

2.9 Real-time RT–PCR

2.9.1 Materials

1) Ribonuclease (RNase)-Free water: dH_2O was treated by 0.1% diethyl pyrocarbonate (DEPC) (Cat.NO.P119C, Promega, Southampton, UK).
2) Isopropanol (Cat.NO.Z514A, Promega, Southampton, UK).
3) RNAgents denaturing solution (Cat.NO.Z5651, Promega, Southampton, UK).
4) Chloroform: Isoamyl alcohol (24:1) (Cat.NO.C0549, Sigma, Poole, Dorset, UK)
5) Phenol (Cat.NO.P4682, Sigma, Poole, Dorset, UK)
6) 2 mol/l of Sodium acetate (pH 4.0): 27.216g sodium acetate (Cat.NO.S2889, Sigma, Poole, Dorset, UK) was dissolved in DEPC treated dH_2O. Adjusted pH using glacial acetic acid. Filled up to 100 ml, and then was filtered.

7) 3 mol/l of Sodium acetate (pH 5.2): Dissolved 408.1 g of sodium acetate in DEPC treated dH_2O. Adjusted pH to 5.2 with glacial acetic acid and filled up to 1 liter. Dispensed into aliquots and sterilized by autoclaving.

8) Ice-cold ethanol, 75 %, RNase-free (Cat.NO.459836, Sigma, Poole, Dorset, UK)

9) Model 5415D Centrifuge (Eppendorf, Germany)

10) 10× PCR buffer II: 500 mmol/l of KCl, 100 mmol/l of Tris/HCl (Cat.NO.N808-0010, Applied Biosystems Ltd, Warrington, Cheshire, UK).

11) 25 mmol/l of $MgCl_2$ solution (Cat.NO.N808-0010, Applied Biosystems Ltd, Warrington, Cheshire, UK).

12) dNTPs: 10 mmol/l deoxyribonucleoside triphosphates (Cat.NO.N808-0007, Applied Biosystems Ltd, Warrington, Cheshire, UK).

13) Random Hexamers 50 μmol/l (Cat.NO.N808-0127, Applied Biosystems Ltd, Warrington, Cheshire, UK).

14) RNase inhibitor (20 units/μl) (Cat.NO.N808-0119, Applied Biosystems Ltd, Warrington, Cheshire, UK).

15) M-MLV reverse transcriptase (50 units/μl) (Cat.NO.N808-0018, Applied Biosystems Ltd, Warrington, Cheshire, UK).

16) Model 80-2103-98 RNA/DNA calculator (Pharmacia Biotech, Cambridge, UK)

17) GeneAmp PCR System 9700 (Applied Biosystems Ltd, Warrington, Cheshire, UK).

18) SYBR Green PCR Master Mix (Cat.NO.4309155, Applied Biosystems Ltd, Warrington, Cheshire, UK).

19) GP Centrifuge (Beckman, U.S.A)

20) The ABI PRISM® 7000 sequence detection system (Applied Biosystems Ltd, Warrington, Cheshire, UK).

21) Primer Express Software V2.0 (Applied Biosystems Ltd, Warrington, Cheshire, UK).

2.9.2. Procedures

2.9.2.1 Total RNA purification

Total RNA was isolated from cultured cells by the guanidinium method (403). In this method, Guanidine thiocyanate, in association with β-mercaptoethanol and N-lauroyl sarcosine powerfully inhibited RNase, also acted to disrupt nucleoprotein complex, allowing RNA to be released into solution. Intact RNA was purified away from contaminants by phenol: chloroform extraction. RNA selectively partitions into the aqueous phase, free from DNA and protein and was easily concentrated by precipitation with isopropanol (403, 404).

Cultured cells in 75-cm^2 flasks were collected, pelleted and washed once in ice-cold PBS. The cell pellet was lysed in ice-cold denature solution using 600 µl per flask (about 5×10^6 cells). Cell lysates were sheared 20 times through a 21-gauge needle. 60 µl of 2 mol/l sodium acetate (pH 4.0) was added to the lysate and mixed thoroughly by inverting the tube 4-5 times. 0.6 ml of phenol: chloroform: isoamylalcohol was added. The mixture was vortexed for at least 10 seconds. The emulsion was incubated on ice for 15 minutes and then centrifuged at 12,000 rpm for 20 minutes at 4 °C. The aqueous phase was carefully transferred to a fresh RNase free tube, added an equal volume of isopropanol, mixed, and precipitated at -20 °C for at least 2 hours. The crude RNA pellet was recovered by centrifugation at 12,000 rpm for 20 minutes at 4 °C and washed by resuspending in 0.8 ml of 75 % ice-cold ethanol. The RNA was recovered by centrifugation at 12,000 rpm for 10 minutes at 4 °C. The pellet was dried in air and resuspended in 150 µl RNase free water. 10 µl of 3 mol/l sodium acetate (pH 5.2) was added, mix thoroughly by inverting the tube 4-5 times. 150 µl of phenol: chloroform: isoamylalcohol was added. The mixture was

vortexed for at least 10 seconds, then centrifuged at 12,000 rpm for 10 minutes at 4 °C. The aqueous phase was carefully transferred to a fresh RNase free tube, added an equal volume of 2 volume of ethanol (100 %), mixed, and precipitated at -20 °C at least 2 hours. The concentration of RNA was determined by measuring the absorbance at 260 nm.

2.9.2.2 Reverse transcription

The thermostable polymerases used in the basic PCR process require a DNA template. In order to apply PCR methodology to the study of RNA, the RNA sample firstly must be reversely transcribed to cDNA to provide the necessary DNA template for thermostable polymerase. This process is called reverse transcription (RT).

Total RNA (500 ng) was used for RT. The RT reaction was set up in a 40 µl mixture containing 50 mmol/l KCl, 10 mmol/l Tris/HCl, 5 mmol/l $MgCl_2$, 1 mmol/l of each dNTPs, 2.5 µmol/l random hexamers, 20 U of RNase inhibitor, and 50 U of M-MLV reverse transcriptase. Incubations were performed in a DNA Thermal Cycler (PerkinElmer 9600) for 10 minutes at room temperature, followed by 30 minutes at 42 °C and 5 minutes at 99 °C. After cDNA synthesis by RT, Stored it at 4 °C for real-time PCR.

2.9.2.3 Real-time PCR

The real-time PCR system is based on the detection and quantitation of a fluorescent reporter. This signal increases in direct proportion to the amount of PCR product in a reaction. By recording the amount of fluorescence emission at each cycle, it is possible to monitor the PCR reaction during exponential phase where the first significant increase in the amount of PCR product correlates to the initial amount of target template. The higher the starting copy number of the nucleic acid target, the sooner a significant increase in fluorescence is observed. A significant increase in fluorescence above the baseline value measured during the 3-15 cycles indicates the detection of accumulated PCR product.

After cDNA synthesis by RT, cDNA was split for the separate amplification for target genes using specific primers designed by Taqman Primer Express Software V2.0 as shown in Table 2.1 and Table 2.2. Real-time PCR was performed in an ABI 7000 using SYBR Green PCR kit according to the manufacturer's protocol. After the PCR, a dissociation curve (melting curve) was constructed in the range of 60 °C to 95 °C. Relative amount of PCR Products was calculated using the comparative CT method (ΔΔCt method). The amplification efficiencies of the target and reference were shown to be approximately equal with a slope of log input amount to Ct < 0.1. Controls consisting of H_2O or samples that were not reversely transcribed were negative for target and reference.

Table 2.6 Mouse TaqMan primers for real-time PCR

Genes	Mouse TaqMan primers
LDLr	5'-CTGTGGGCTCCATAGGCTATCT -3'-sense
	5'-GCGGTCCAGGGTCATCTTC -3'-antisense
SCAP	5'-ACTGGACTGAAGGCAGGTCAA -3'-sense
	5'-GCCTCTAGTCTAGGTCCAAAGAGTTG -3'-antisense
SREBP-2	5'-CGATGCCCTTCAGGAGCTT-3'-sense
	5'-GCGCCAGGAGAACATGGT -3'-antisense
Insig-1	5'-TCACAGTGACTGAGCTTCAGCA -3'-sense
	5'-TCATCTTCATCACACCCAGGAC -3' anti-sense
HMGR	5'-TCTGGCAGTCAGTGGGAACTATT -3'-sense
	5'-CCTCGTCCTTCGATCCAATTT -3' anti-sense
$ABCA_1$	5'-CTCCTGTGGTGTTTCTGGATGA -3'-sense
	5'-ACTTAGGGCACAATTCCACAAGA -3'-antisense
ABCG1	5'-TCTCTCGAAGTGAATGAAATTTATCG -3'-sense
	5'-AGGTCTCAGCCTTCTAAAGTTCCTC -3'-antisense
LXRα	5'-TCAAGCGGATCTGTTCTTCTGA -3'-sense
	5'-GGAGTGTCGACTTCGCAAATG -3'-antisense
PPARα	5'-TCAGGGTACCACTACGGAGTTCA -3'-sense
	5'-CCGAATAGTTCGCCGAAAGA-3'-antisense
PPARγ	5'-GCAGCTACTGCATGTGATCAAGA-3'-sense
	5'-GTCAGCGGGTGGGACTTTC -3'-antisense
TNFα	5'-ACAAGGCTGCCCCGACTAC -3'-sense
	5'-TTTCTCCTGGTATGAGATAGCAAATC -3'-antisense
MCP-1	5'- TCTCACTGAAGCCAGCTCTCTCTCT-3'-sense
	5'- GCAGGCCCAGAAGCATGA -3'-antisense
β-actin	5'-ACGGCCAGGTCATCACTATTG -3'-sense
	5'-CACAGGATTCCATACCCAAGAAG -3'-antisense

Table 2.7 Human TaqMan primers for real-time PCR

Genes	Human TaqMan primers
VLDLr	5'-TGAAGCAGTCTATGGTGCCAAT-3'-sense
	5'-CTTGGGCATCATTCAGGTTGT-3'-antisense
LDLr	5'-GTGTCACAGCGGCGAATG-3'-sense
	5'-CGCACTCTTTGATGGGTTCA-3'-antisense
SCAP	5'-GGGAACTTCTGGCAGAATGACT-3'-sense
	5'-CTGGTGGATGGTCCCAATG-3'-antisense
SREBP-2	5'-CCGCCTGTTCCGATGTACAC-3'-sense
	5'-TGCACATTCAGCCAGGTTCA-3'-antisense
Insig-1	5'-TGCAGATCCAGAGGAATGTCAC-3'-sense
	5'-CCAGGCGGAGGAAAAGATG-3' anti-sense
SR-A	5'-GCGTTGGACAGGTCGTCTGT-3'-sense
	5'-CTTGTGCACGGCTTGAACAC-3'-antisense
CD36	5'-TCTTTCCTGCAGCCCAATG-3'-sense
	5'-AGCCTCTGTTCCAACTGATAGTGA-3'-antisense
HMGR	5'-GGCCCAGTTGTGCGTCTT-3'-sense
	5'-TTTCGAGCCAGGCTTTCACT-3' anti-sense
$ABCA_1$	5'-GCAGCAGAGCGAGTACTTCGTT-3'-sense
	5'-CAAGACTATGCAGCAATGTTTTTGT-3'-antisense
ABCG1	5'-GCGAGTACGGTGATCAGAACAG-3'-sense
	5'-GGTCTGAGTCACACATGCCCT-3'-antisense
LXRα	5'-AGAAGAACAGATCCGCCTGAAG-3'-sense
	5'-GGCAAGGATGTGGCATGAG-3'-antisense
PPARα	5'-CGTGCTTCCTGCTTCATAGATAAG-3'-sense
	5'-GTGGTAGCGCTGGTCTAC-3'-antisense
PPARγ	5'-GCTTCATGACAAGGGAGTTTCTAAA-3'-sense
	5'-TTGAGTTTGAACCCGAGGTATTTC-3'-antisense
IL-6	5'-AGCCGCCCCACACAGA-3'-sense
	5'-CCGTCGAGGATGTACCGAAT-3'-antisense
TNFα	5'-CTCGAACCCCGAGTGACAA-3'-sense
	5'-GCTGCCCCTCAGCTTGAG-3'-antisense
IL-8	5'-AAGGAACCATCTCACTGTGTGTAAAC-3'-sense
	5'-ATCAGGAAGGCTGCCAAGAG-3'-antisense
MCP-1	5'-CCATTGTGGCCAAGGAGATC-3'-sense
	5'-TGTCCAGGTGGTCCATGGA-3'-antisense
β-actin	5'-CCTGGCACCCAGCACAAT-3'-sense
	5'-GCCGATCCACACGGAGTACT-3'-antisense

2.10 Western Blot

Sodium dodecyl sulfate polyacrylamide gel electrophoresis (SDS-PAGE) has become one of the most important methods for the analysis of protein. In this technique, the sample to be fractionated was denatured and coated with detergent by heating in the presence of SDS and a reducing agent. The SDS coating gave the protein a high net

negative charge that was proportional to the length of the polypeptide chain. The sample was loaded on a polyacrylamide gel with high voltage, causing the protein components to migrate toward the positive electrode. The protein was then transferred to a nitrocellulose membrane, and detected using antisera or specific antibodies. The method of electrophoretic transfer of proteins from SDS gels to nitrocellulose and radiographic detection with antibody was defined as Western Blot.

2.10.1. Materials

1) Nuclear extract kit (Cat.NO.40010, Active Motif, Belgium)
2) GS-6 Centrifuge (Beckman, U.S.A)
3) Autoclave machine (Boxer Laboratory Equipment Ltd, Ware, Hertfordshire, UK)
4) Model VX-100 vortex mixer (Jencons PLS Ltd, UK)
5) Model 5415D Centrifuge (Eppendorf, Germany)
6) Disposable cell scraper (Cat. NO. 08-773-2, Fisher Scientific, UK)
7) Model SHT 2D test tube heater (Stuart Scientific, UK)
8) 10 % SDS solution (Cat.NO.161-0416, Bio-Rad, Hertfordshire, UK)
9) Laemmli sample buffer (Cat.NO.161-0737, Bio-Rad, Hertfordshire, UK): 62.5 mmol/l Tris-HCl, pH 6.8, 2 % SDS, 25 % glycerol, 0.01 % bromophenol blue (Bio-Rad, Hertfordshire, UK)
10) 30 % Acrylamide/Bis (29:1) solution (Cato.NO.161-0156, Bio-Rad, Hertfordshire, UK)
11) 10 % Ammonium persulfate (APS, Cat.NO.A3678, Sigma, Poole, Dorset, UK): dissolve 0.1 g APS in 1ml dH_2O.
12) N,N,N',N'-tetramethylethylenediamine (TEMED) (Cat.NO.161-0800, Bio-Rad, Hertfordshire, UK)
13) β-mercaptoethanol (Cat.NO.M7522, Sigma, Poole, Dorset, UK)

14) Precision plus protein^{TM} all blue standards (Cat.NO.161-0373, Bio-Rad, Hertfordshire, UK)

15) 10×Running buffer: 250 mmol/l Tris, pH 8.3, 1.92 M glycine, 1 % SDS. (Cat.NO.161-0734, Bio-Rad, Hertfordshire, UK)

16) 10× Blot transfer buffer: 10×Running buffer containing 20 % methanol (Cat. NO. 161-0734, Bio-Rad, Hertfordshire, UK)

17) Coomassie brilliant blue G-250 staining solution (Cat.NO.B8647, Sigma, Poole, Dorset, UK)

18) Ponceau S solution: 0.1 % Ponceau S (w/v) in 5 % acetic acid (v/v) (Cat.NO.P7170, Sigma, Poole, Dorset, UK)

19) 10×PBS: 10 mmol/l sodium phosphate, 150 mmol/l NaCl pH 7.4 (Cat.NO.161-0780, Bio-Rad, Hertfordshire, UK)

20) 1×TBST (Tris-Buffered Saline/0.1 % Tween 20): 0.1 % Tween 20 in Tris-Buffered Saline(containing 1ml Tween-20, 8.8 g NaCl and 20 ml 0.5 mol/l pH 8.0 Tris-HCl per liter).

21) Stripping buffer (Containing 100 mmol/l β-mercaptoethanol, 2% SDS (w/v), 62.5 mmol/l of Tris-HCl pH 6.7).

22) Model size1 hot box oven (Gallenkamp, UK)

23) Model 820 UP Lancer Washer (Lancer, UK)

24) AF-10 automatic ice machine (Scotsman, U.S.A)

25) Model R100 rotatest shaker (Luckham, UK)

26) Model SS-660 magnetic stirrer (Gallenkamp, UK)

27) Model PW9421 pH meter (Philips, UK)

28) Model HM-120 analytical balance (A&D, Japan)

29) Antibody dilution buffer: 2 % Blocker (From Kit, Cat.NO.RPN2135, GE Healthcare, Buckinghamshire, UK) in TBST

30) Chicken anti-human LDLr polyclonal antibody (Cat.NO.ab14056, Abcam, Cambridge, UK)

31) Rabbit anti-human VLDLr polyclonal antibody (Cat.NO.sc-20745, Santa Cruz Biotechnology, Inc. Wembley, UK)

32) Mouse anti-human ABCA1 monoclonal antibody (Cat.NO.ab18180, Abcam, Cambridge, UK)

33) Rabbit anti-human LXRα polyclonal antibody (Cat.NO.ab3585, Abcam, Cambridge, UK)

34) Rabbit anti-human PPARα polyclonal antibody (Cat.NO.ab24509, Abcam, Cambridge, UK)

35) Mouse anti-human PPARγ monoclonal antibody (Cat.NO.sc-7273, Santa Cruz Biotechnology, Inc. Wembley, UK)

36) Mouse anti-human SREBP-2 monoclonal antibody (purified from Hybridoma, Cat.NO.CRL-2545^{TM}, LGC Promochem, Teddington, Middlesex, UK)

37) Rabbit anti-human HMGR polyclonal antibody (Cat.NO. 07-572, Upstate, Hampshire, UK)

38) Rabbit anti-human SCAP polyclonal antibody (Made by our lab)

39) Rabbit anti-human Insig-1 polyclonal antibody (Cat. NO.ab54040, Abcam, Cambridge, UK)

40) Rabbit anti-human actin polyclonal antibody (Cat.NO.A2066, Sigma, Poole, Dorset, UK)

41) Rabbit anti-human TNFα polyclonal antibody (Cat.NO.ab6671, Abcam, Cambridge, UK)

42) Armenian hamster anti-human MCP-1 monoclonal antibody (Cat.NO.ab21396, Abcam, Cambridge, UK)

43) Horseradish peroxidase (HRP)-linked rabbit anti-Hamster (Armenian) polyclonal IgG (Cat.NO.ab5745, Abcam, Cambridge, UK)

44) HRP-linked goat anti chicken polyclonal IgY (Cat.NO.ab6877, Abcam, Cambridge, UK)

45) HRP-linked goat anti-rabbit polyclonal IgG (Cat.NO.7074, New England Biolabs, UK)

46) HRP-linked rabbit anti-mouse polyclonal IgG (Cat.NO.ab6728, Abcam, Cambridge, UK)

47) HRP-linked rabbit anti-goat polyclonal IgG (Cat.NO.ab6741, Abcam, Cambridge, UK)

48) Bio-Rad mini protein II apparatus (Cat.NO.165-2940, Bio-Rad, Hertfordshire, UK)

49) PowerPac 3000 power supply, 200/240 V (Cat.NO.165-5057, Bio-Rad, Hertfordshire, UK)

50) Inner glass plates (Cat.NO.165-2907, Bio-Rad, Hertfordshire, UK)

51) Outer glass plates (Cat.NO.165-2908, Bio-Rad, Hertfordshire, UK)

52) Hybond^{TM}-ECL^{TM} nitrocellulose membrane (Cat.NO.RPN203D, GE Healthcare, Buckinghamshire, UK)

53) Hyperfilm^{TM} ECL (Cat.NO.RPN3103K, GE Healthcare, Buckinghamshire, UK)

54) ECL^{TM} Western Blot analysis system (Cat.NO.RPN2109, GE Healthcare, Buckinghamshire, UK)

55) ECL advance^{TM} Western Blot detection kit (Cat.NO.RPN2135, GE Healthcare, Buckinghamshire, UK)

56) Model Compact X4 film processor. (Xograph Imaging Systems, Gloucestershire, UK)

57) Model Gel Doc 2000 gel documentation system (Bio-Rad, Hertfordshire, UK)

2.10.2. Procedures

2.10.2.1 The extraction of protein

2.10.2.1.1 Method 1 (by kit):

Preparation of Whole-Cell Extract

Table 2.8 Preparation of buffer for the whole-cell extraction

Reagents to Prepare	Components	60 mm plate or 3.2×10^6 cells	100 mm plate or 8.8×10^6 cells	150 mm plate or 2×10^7 cells
PBS/Phosphatase Inhibitors	10X PBS	0.4 ml	0.8 ml	1.6 ml
	Distilled water	3.4 ml	6.8 ml	13.6 ml
	Phosphatase Inhibitors	0.2 ml	0.4 ml	0.8 ml
	TOTAL REQUIRED	4.0 ml	8.0 ml	16.0 ml
Complete Lysis Buffer	10 mM DTT	10.0 µl	30.0 µl	90.0 µl
	Lysis Buffer	89.0 µl	267.0 µl	801.0 µl
	Protease Inhibitor Cocktail	1.0 µl	3.0 µl	9.0 µl
	TOTAL REQUIRED	100.0 µl	300.0 µl	900.0 µl

The following protocol was based on samples of approximately 8.8×10^6 cells, which corresponded to HeLa cells grown to confluence in a 100 mm tissue culture plate. Each sample was one reaction. Prepared PBS/Phosphatase Inhibitors and Complete Lysis Buffer as described above in the section of Buffer Preparation. Adjusted the volumes accordingly using the chart above if using plates of different sizes. Placed buffers and any tubes needed on ice before starting assay.

Step 1: Cell collection

1) Aspirated media out of dish. Washed with 5 ml ice-cold PBS/phosphatase inhibitor. Aspirated solution out, and added 5 ml ice-cold PBS/Phosphatase inhibitor.

2) Removed cells from dish by gently scraping with cell lifter. Transferred cells to a pre-chilled 15 ml conical tube.

3) Centrifuged cell suspension for 5 minutes at 1000 rpm at 4 °C.

4) Discarded supernatant. Kept cell pellet on ice.

Step 2: Cell lysis

1) Resuspended cell pellet in 300 µl Complete Lysis Buffer by pipetting up and down. Vortexed for 10 seconds at the highest setting.

2) Passed lysate through 21-gauge needle 20 times to shear the DNA.

3) Incubated suspension for 30-60 minutes on ice on a rocking platform set at 150 rpm.

4) Vortexed for 30 seconds at highest setting. Centrifuged for 20 minutes at 14,000 rpm at 4 °C. Transferred supernatant (whole-cell extract) into a pre-chilled microcentrifuge tube.

5) Measured protein concentration in supernatant.

6) Aliquoted and stored at –80 °C. Avoided freeze/thaw cycles.

The presence of certain detergents is known to interfere with protein determination assays such as the Bradford or BCA assay. If these protein assays were performed, the Complete Lysis Buffer was recommended as the blank, performing a 1:50 or 1:250 dilutions of samples.

Table 2.9 Preparation of buffer for the nuclear-cell extract

Reagents to Prepare	Components	60 mm plate or 3.2×10^6 cells	100 mm plate or 8.8×10^6 cells	150 mm plate or 2×10^7 cells
PBS/Phosphatase Inhibitors	10X PBS	0.4 ml	0.8 ml	1.6 ml
	Distilled water	3.4 ml	6.8 ml	13.6 ml
	Phosphatase Inhibitors	0.2 ml	0.4 ml	0.8 ml
	TOTAL REQUIRED	4.0 ml	8.0 ml	16.0 ml
1X Hypotonic Buffer	10X Hypotonic Buffer	25.0 µl	50.0 µl	100.0 µl
	Distilled water	225.0 µl	450.0 µl	0.9 ml
	TOTAL REQUIRED	250.0 µl	500.0 µl	1.0 ml
Complete Lysis Buffer	10 mM DTT	2.5 µl	5 µl	10.0 µl
	Lysis Buffer AM1	22.25 µl	44.5 µl	89.0 µl
	Protease Inhibitor Cocktail	0.25 µl	0.5 µl	1.0 µl
	TOTAL REQUIRED	25.0 µl	50.0 µl	100.0 µl

Step 1: Cell collection (based on or $8.8*10^6$ cells)

1) Aspirated media out of dish. Washed with 5 ml ice-cold PBS/phosphatase inhibitor. Aspirated solution out and added 3 ml ice-cold PBS/phosphatase inhibitor.

2) Removed cells from dish by gently scraping with cell lifter. Transferred cells to a pre-chilled 15 ml conical tube.

3) Centrifuged cell suspension for 5 minutes at 500 rpm at 4 °C.

4) Discarded supernatant. Kept cell pellet on ice.

Step 2: Cytoplasmic fraction collection

1) Gently resuspended cells in 500 µl 1× Hypotonic Buffer by pipetting up and down several times. Transferred to a pre-chilled microcentrifuge tube. Incubated for 15 minutes on ice.

2) Added 25 µl Detergent and vortexed for 10 seconds at highest setting.

3) Centrifuged suspension for 30 seconds at 14,000 rpm at 4 °C.

4) Transferred supernatant (cytoplasmic fraction) into a pre-chilled microcentrifuge tube. (If you began working from tissue, combined this supernatant with that obtained in Step 1, No. 3 of the Nuclear Extract protocol for tissue.) Stored the supernatant at –80 °C until ready to use. Used the pellet for nuclear fraction collection.

Step 3: Nuclear fraction collection

1) Resuspended nuclear pellet in 50 µl of Complete Lysis Buffer by pipetting up and down. Vortexed for 10 seconds at highest setting.

2) Incubated suspension for 30 minutes on ice on a rocking platform set at 150 rpm.

3) Vortexed 30 seconds at highest setting. Centrifuged for 10 minutes at 14,000 rpm at 4 °C. Transferred supernatant (nuclear fraction) into a pre-chilled microcentrifuge tube.

4) Aliquoted and stored at –80 °C. Avoided freeze/thaw cycles.

The presence of certain detergents may interfere with the Bradford or BCA assay, thus use the Complete Lysis Buffer as the blank and perform a 1:50 or 1:250 dilutions of samples.

2.10.2.1.2 Method 2. (Set up by our lab according to the literatures) (405, 406)**:**

Cytoplasmic and nuclear protein extraction

Solutions

1) Buffer A

10 mmol/l HEPES-KOH at pH 7.9, 1.5 mmol/l $MgCl_2$, 10 mmol/l KCl, 0.5 mmol/l dithiothreitol (DTT), 1mmol/l sodium EDTA, 1mmol/l sodium EGTA supplemented with proteinase inhibitors (0.1 mmol/l Pefabloc, 5 μg/ml pepstatin A, 10 μg/ml leupeptin, 2 μg/ml aprotinin)

2) Buffer B

20 mmol/l HEPES-KOH at pH 7.9, 25 % [v/v] glycerol, 0.5 mol/l NaCl, 1.5 mmol/l $MgCl_2$, 1mmol/l sodium EDTA, 1mmol/l sodium EGTA supplemented with proteinase inhibitors (0.1 mmol/l Pefabloc, 5 μg/ml pepstatin A, 10 μg/ml leupeptin, 2 μg/ml aprotinin)

DTT and proteinase inhibitors were added fresh to the buffers just before use.

Cell fractionation

The standard method for fractionation of cells and purification of nuclei was based on the method of Dignam *et al* (405). All operations were carried out at 4 °C.

Nuclear extraction procedures

1) Cells were centrifuged at 1200 rpm for 10 minutes.

2) Estimated the packed cell volume (PCV), e.g. 200 µl.

3) The pellets were resuspended in 5× PCV of buffer A, avoided foam formation.

4) Incubated the packed cells in lysis buffer on ice for 15 minutes, allowing cells to swell.

5) The pellets were disrupted by passing through a 21-gauge needle for 20 times and centrifuged for 10 minutes at 14000 rpm in a microcentrifuge tube.

6) Transferred the supernatant to a fresh tube. This fraction was the cytoplasmic fraction.

7) The resulting crude nuclear pellet was extracted with an equal volume of Buffer B. The pellets were disrupted either by passing through a 21-gauge needle for 20 times and shaken gently for 30 minutes.

8) Centrifuged at 14,000 rpm for 30 min in a microcentrifuge tube. The supernatant was designated as nuclear extract.

9) Snap-froze the supernatant in aliquots with liquid nitrogen or stored at –70 °C.

Soluble fraction (S-100) fraction and the membrane fraction (P-100) procedure

10) The supernatant from the initial centrifuge (above) was further spun at 100,000 rpm for 1 hour to obtain an S-100 fraction (supernatant) and a membrane fraction (pellet). The membrane fraction was washed using Buffer B, then centrifuge at 100,000 rpm for another 1 hour. The pellet was resuspended in Buffer B.

2.10.2.2 Electrophoresis

The concentration of protein from each sample was measured. The same amount of total protein from cell lysates per sample was denatured with 2 volume of sample buffer at 95 °C for 10 minutes, then subjected electrophoresis on a 5 % stacking and 8 % separating

SDS polyacrylamide gel. Electrophoresis was performed in a Bio-Rad mini protein II apparatus in 1×running buffer at 200 Volts for 1 hour.

Preparation of 8 % separating SDS polyacrylamide gel (20 ml): Mixed 9.2 ml of dH_2O, 5.0 ml of 1.5 mol/l Tris-HCl (pH 8.8), 0.2 ml of 10 % SDS, 5.4 ml of 30 % acrylamide/Bis, 0.2 ml of 10 % APS and 0.012 ml of TEMED.

Preparation of 5 % stacking SDS polyacrylamide gel (10 ml): Mixed 6.8 ml of dH_2O, 1.26 ml of 1.0mol/l Tris-HCl (pH6.8), 0.1 ml of 10 % SDS, 1.66 ml of 30 % acrylamide/Bis, and 0.1 ml of 10 % APS and 0.01 ml of TEMED.

2.10.2.3 Coomassie stain of protein gel

If necessary, protein gel staining procedures will be done to show protein bands after electrophoresis.

Solutions:

Protein gel stain

Added to a 500 ml bottle: 1.2 g of Comassie Brilliant Blue G-250, 300 ml of methanol, 60 ml of acetic acid, and 240 ml of H_2O

Shook well and stored at room temperature. It could be reused numerous times until staining became noticeably weaker.

Protein gel destain

Added to a 500 ml bottle: 50 ml of methanol, 50 ml of acetic acid, and 400 ml of H_2O. Fully mixed together for use.

Procedures

1) After electrophoresis of protein gel, transferred gel to round staining tray. Added ~200 ml protein gel stain.

2) Microwaved for ~45 seconds until the solution just started to boil. Incubated at room temperature with gentle shaking for 10-15 minutes. Heating allowed the gel to stain faster (Alternatively, soaked gel in stain for 1 hour at room temperature).

3) Poured stain back into bottle for later re-use. Rinsed gel with water. Added ~200 ml protein gel destain. Microwaved ~45 seconds until the solution just started to boil. Incubated with gentle shaking at room temperature for ~15 minutes (Alternatively, soaked gel with gentle shaking at room temperature ~45 minutes).

4) Discarded destain and added remainder of stain. Microwaved as before and incubated with shaking at room temperature until gel was destained the desired amount. (Alternatively, the microwave step could be omitted and the gel destained an additional hour or overnight).

2.10.2.4 Electrophoresis transfer

The samples were transferred to nitrocellulose membrane at 100 Volts, 350 mA for 1.5 hours in 1× Blot transfer buffer in a Bio-Rad mini Trans-Blot Transfer Cell.

2.10.2.5 Identification of transferring:

If necessary, the membrane was stained with Ponceau S solution for 10 minutes. The protein bands would be shown as red after washing off excess Ponceau S solution from membrane. The staining was reverse.

2.10.2.6 Blotting

In general, antigens immobilised on membranes were detected with antibodies in a three-step process. First, the primary antibody, an IgG directed against the antigen, was added to bind potential antigenic sites. In the second step, a secondary antibody-enzyme conjugate which recognises general features of all IgGs (anti-IgG), was added to find locations where the primary antibody bound. The HRP conjugated to the secondary antibody catalysed an emission of light reaction in the third step. When ECL detection

reagents were added, the light produced by a chemiluminescent reaction to deposition of HRP conjugated to the secondary antibody on the membrane at the reaction site. The maximum light emission was at a wavelength of 428 nm which could be detected by a short expose to blue-light sensitive autoradiography film.

The membrane was washed twice in TBST, and then blocked with 2 % blocker for 1 hour at room temperature followed by two five-minute washes in TBST. The membrane was incubated with specific primary antibodies for 1 hour at room temperature followed by 4 five-minute washes in TBST. The HRP-linked secondary antibodies were incubated with the membranes for another 1 hour at room temperature followed by 4 five-minute washes in TBST. Actin as an internal reference was also examined using a rabbit anti-actin antibody and a HRP-linked goat anti-rabbit IgG. Finally, the signals were detected using ECL advanced system. The bands of target proteins were captured by Gel Documentation System and the density of bands were analysed by Bio-Rad Quantity-One software.

2.10.2.7 Stripping and reprobing membrane

The complete removal of primary and second antibodies from the membranes was possible. The membranes might be stripped of bound antibodies and reprobed several times. Membranes should be stored wet wrapped in Stripping buffer in a refrigerator (2-8 °C) after each immunodetection.

Procedures

1) Submerged the membrane in stripping buffer (100 mmol/l β-mercaptoethanol, 2 % (w/v) SDS, 62.5 mmol/l Tris-HCl pH 6.7) and incubated at 50 °C for 30 minutes with occasional agitation.

2) Washed the membranes for 2 × 10 minutes in TBST at room temperature using large volumes of wash buffer.

3) Blocked the membranes in blocking solution for 1 hour at room temperature.

4) Repeated the immunodetection protocols as shown before.

2.11 The isolation and purification of mouse anti-human SREBP-2 monoclonal antibody

2.11.1 Materials

1) Hybridoma for mouse anti-human SREBP-2 monoclonal antibody (Cat.NO.CRL-2545^{TM}, LGC Promochem, Teddington, Middlesex, UK)

2) DMEM (Cat. NO. 30-2002, LGC Promochem, Teddington, Middlesex, UK)

3) Fetal Bovine Serum (FBS) (Cat. NO. S1820, Biosera, UK)

4) Centricon plus-70 (Cat. NO. UFC710008, Millipore Ltd, Hertfordshire, UK)

2.11.2 Procedures

1) Cell culture for CRL-2545 hybridoma cells: Thawed the vial by gentle agitation in a 37 °C water bath. Transferred the vial contents to a 75-cm^2 tissue culture flask and diluted with the recommended complete culture medium. Incubated the cells at 37 °C in a humidified 95 % air, 5 % CO_2 incubator at 37 °C and the medium was changed every 48 hours. Counted cells and viability, then adjusted the cell density of the suspension to 2~5×10^5/ml. Maintained the cell density of the culture at $1 \times 10^5 \sim 1 \times 10^6$ viable cells/ml.

2) SREBP-2 Antibody Collection released in the supernatants by hybridoma: Collected cells suspension into 15 ml tube, centrifuged at 800 rpm for 10minutes. Collected supernatants, placed in -70 °C

3) Concentrated the supernatants by Centricon plus-70 to get mouse anti-human SREBP-2 monoclonal antibody.

2.12 Data analysis

In all experiments, groups of data were evaluated for statistical significance by one-way analysis of variance. Data were considered significant if the P value< 0.05.

CHAPTER 3. THE ANTI-ATHEROSCLEROTIC EFFECTS OF SIROLIMUS ON HUMAN CORONARY ARTERY SMOOTH MUSCLE CELLS (PART 1.)

3.1 Introduction

Atherosclerosis is a multi-factorial disease to which disordered lipid metabolism and chronic inflammation are important contributory factors (4, 6). VSMCs, one of the main cell components of atherosclerotic lesions, play a key role in the pathogenesis of vascular lesion. In normal vessels the majority of VSMCs reside in the media, where they are quiescent and possess a "contractile" phenotype characterised by their abundant actin and myosin-containing filaments (66, 74). In disease states VSMCs re-enter the cell cycle, proliferate, and migrate from media to intima (66). After vessel injury, intimal VSMCs have a synthetic phenotype characterised by hyperplasia or hypertrophy and matrix protein accumulation in the intima and/or media with or without lipid deposition, resulting in thickening and stiffness of the arterial wall. Foam cells traditionally have been regarded as being derived from macrophages because they express macrophage markers. However it is now known that VSMCs can also be converted into foam cells. Evidence for this includes: (i) VSMCs in tissue culture can accumulate cholesterol (78); (ii) some lesional foam cells traditionally classified as macrophages are actually arterial VSMCs that have significantly altered their phenotype (79); (iii) significant numbers of foam cells are present in atherosclerotic lesions in mice deficient in genes responsible for monocyte recruitment (80), leucocyte and macrophage proliferation and differentiation (81, 82); (iv) in advanced lesions from both WHHL and FF rabbits (73) simultaneous tritium labelled methyl-thymidine autoradiography and immunostaining for cell type-specific markers revealed that approximately 30% of the labelled cells were macrophages and 45% were smooth muscle cells. Xu *et al* (407) also reported that VSMCs are amongst the first cells participating in the development of atherosclerosis. As the atherosclerotic lesion progresses, VSMCs increase from 5% to 30%.

In the general introduction section of Chapter 1, we have reviewed the anti-atherosclerotic effects of Sirolimus including some discrepancies caused by Sirolimus-associated dyslipidemia in animal and clinical studies. These findings suggest that the antiproliferative and anti-inflammatory effects of Sirolimus may be related to its anti-atherosclerosis properties via changes in local cholesterol metabolism in the tissues, which may result in dose-related dyslipidemia. The studies described in the next two chapters particularly address the question of how the anti-inflammatory effects of Sirolimus modify lipid-mediated vascular injury through effects on intracellular cholesterol homeostasis.

The intracellular lipid content of most cells is governed by tight regulation of cholesterol influx and efflux pathways. The intracellular level of cholesterol is controlled by the uptake and synthesis of cholesterol through feedback regulation. Recent studies strongly indicated that atherogenesis is initiated by the interplay between cholesterol and cellular secretion of cytokines (especially IL-6) and apoE within the arterial wall (408). Ruan *et al* also reported that inflammatory cytokines can cause lipid accumulation by increasing native LDL uptake via LDLr or reducing efflux of intracellular lipid via ABCA1 in human mesangial cells (374, 376, 377). Therefore, the present study was undertaken to evaluate whether Sirolimus ameliorates the imbalance of intracellular cholesterol homeostasis in human VSMCs mediated by inflammatory cytokines.

3.2. Materials and methods

3.2.1 Cell culture

3.2.1.1 Materials

1) Primary human coronary artery smooth muscle cell (Cat. NO. ZHC-3211, Batch No. 26723T, TCS CellWorks Ltd, Buckinghamshire, UK).

2) Smooth muscle cell basal medium (Cat. NO. ZHM-3933, TCS CellWorks Ltd, Buckinghamshire, UK).

3) Smooth muscle cell growth supplements (Cat. NO. ZHS-8951, TCS CellWorks Ltd, Buckinghamshire, UK).

4) Dulbecco's Modified Eagle's Medium/Ham's Nutrient mixture F-12 (DMEM/F12, Cat. NO. D6421, Sigma, Poole, Dorset UK)

5) L-glutamine solution (Cat. NO. G7513, Sigma, Poole, Dorset UK)

6) Penicillin/ streptomycin (Cat.NO.P4333, Sigma, Poole, Dorset, UK)

7) BSA, fatty acid free (Cat. NO. A8806, Sigma, Poole, Dorset UK)

8) Trypsin-EDTA solution (Cat.NO.T3924, Sigma, Poole, Dorset UK)

9) 75-cm^2 culture flask (Cat. NO. BC301, Appleton Woods, Birmingham, UK)

10) 6-well plate, 12-well plate, 24-well plate, 96-well plate (Cat. NO. BC010, BC011, BC012, BC015, Appleton Woods, Birmingham, UK)

11) 5 ml, 10 ml, 25 ml of Pipettes (Cat. NO. SS208, SS214, SS216, Appleton Woods, Birmingham, UK)

12) 0.2 μm syringe filter (Cat. NO. FC121, Appleton Woods, Birmingham, UK)

13) Rechargeable pipetting aid (Cat. NO. GNX701, Appleton Woods, Birmingham, UK)

14) 5 ml, 12.5 ml dispenser tips (Cat. NO. DT114, DT115, Appleton Woods, Birmingham, UK)

15) 0.2-2 μl, 2-20 μl, 50-200 μl, 200-1000 μl Gilson Pipetman (Cat. NO. F144801, F123600, F123601, F123602, Anachem, France)

16) 1-10 μl, 20-200 μl Multi-channel Gilson Pipetman (Cat. NO. F21022, F21025, Anachem, France)

17) 0.1-10 µl, 1-200 µl, 101-1000 µl Pipette tips (Cat. NO. TA609, TA659, TA668, Appleton Woods, Birmingham, UK)

18) 0.1-10 µl, 1-200 µl, 101-1000 µl, RNase, DNase, pyrogen free pipette tips (Cat. NO. TA601, TA621, TA661, Appleton Woods, Birmingham, UK)

19) 1 ml, 20 ml, 50 ml, syringes (Cat. NO. GS572, GS577, GS586, Appleton Woods, Birmingham, UK)

20) 21-gauge, 25-gauge needles (Cat. NO. GS358, GS354, Appleton Woods, Birmingham, UK)

21) Chamber slides (Cat.NO.354118, Becton Dickinson Labware, USA)

22) Model M20229 Microflow® Peroxide Class II Advanced Biological Safety Cabinet (BioQuell Ltd, Hants, UK)

23) Model CK2 inverted phase contrast microscopy (Olympus, Japan)

24) Research CO_2 incubator (Cat. NO. 388-020, LEEC Ltd, UK)

3.2.1.2 Background data for VSMCs

Certificate of Analysis

Product code	ZHC-3211
Product Description	Human Coronary Artery Smooth Muscle Cells HCASMCp supplied as proliferating cells in T flasks
Batch number	26723T

Donor information

Age	19yr
Sex	Male

Cell Characterisation

Cells per ampoule	0.54×10^6
Viability	85.0%

Immunohistochemistry

Factor VIII-related antigen	Negative
α-actin	Positive

Safety Data

Potential Adventitious Agents		Test	Result
Bacteria		Long term culture	negative
Fungi		Long term culture	negative
Mycoplasma		Hoescht stain and culture	negative
Viruses	HIV-1	RT-PCR	negative
	Hepatitis B	RT-PCR	negative
	Hepatitis C	RT-PCR	negative

The cells in this lot were obtained from accredited institutions. Informed consent was obtained by these institutions from the donor or from the donors next of kin, for use of the tissue and derivatives for research purposes

Warning
Although cells test negative for HIV-1, hepatitis B, hepatitis C, mycoplasma, bacteria and fungi, no known test procedure can guarantee the absence of all known and unknown infectious agents. Consequently, products of human origin should be considered potentially biohazardous and appropriate precautions taken.

For research use only, not for diagnostic or therapeutic use.

TCS CellWorks Ltd Botolph Claydon Buckingham MK18 2LR UK
Tel +44 (0) 1296 713120 **Fax** +44 (0) 1296 713122 **email**
office@tcscellworks.co.uk
Registered Office 'b Castle Street Liverpool L2 4XE

TCS CellWorks
Discovery in Bioscience

3.2.1.3 Procedures

The primary human VSMCs from coronary artery were cultured in a basal medium supplemented with 5 % FBS, insulin, human epidermal growth factor, human fibroblast growth factor, 2 mmol /l L-glutamine, 0.5 ml 25 mg/ml gentamicin, and 50 μg/ml amphotericin B. Cell cultures were maintained in a humidified 95 % air, 5 % CO_2 incubator at 37 °C and the medium was changed every 48 hours. Cells were sub-cultured with 0.25 % trypsin /0.01% EDTA when cells were grown to sub-confluence. The cells and all reagents for cell culture were obtained from TCS CellWorks Ltd. All experiments were carried out in serum-free DMEM/F12 (1:1) medium containing 0.2 % of fatty acid-free BSA.

3.2.2 Lipoprotein preparation

The native LDL was isolated by sequential density gradient ultracentrifugation as previously described in Chapter 2 (Fig 3.1).

3.2.3 Morphological examination

The lipid accumulation in VSMCs was checked by Oil Red O staining as previously described in Chapter 2.

3.2.4. Cell Proliferation Assay

3.2.4.1 Materials

1) [methyl-^{3}H]-thymidine ([^{3}H]-TdR, Cat. NO. TRK686, GE Healthcare, Buckinghamshire, UK)

2) Unifilter-96 Harvester (Cat. NO. C961961, PerkinElmer, Bucks, UK)

3) MicroScint™-O (Cat. NO. 6013611, PerkinElmer, Bucks, UK)

4) Microplate Scintillation & Luminescence Counter (Cat. NO. C9904V1, PerkinElmer, Bucks, UK)

3.2.4.2 Procedures

1) VSMCs were planted in a 96-well plate at a density of 1.5×10^4 cells /well in the growth medium and cultured until nearly confluent.

2) The cells were synchronised to the quiescent state by incubation in serum-free medium for 24 hours, then each well was washed in PBS.

3) The cells were incubated in DMEM/F12 medium containing 2 % of FBS in the presence of different concentrations of Sirolimus (0, 0.01, 0.1, 1, 10, 50, 100 ng/ml) for (24, 48, 72 hours).

4) Washed one time with PBS, then added [^{3}H]-TdR 1μl/well and incubated for 18 hours before terminating experiments.

5) Washed one time with PBS, the cells were digested by 0.25 % trypsin /0.01 % EDTA and harvested to a filter plate by Unifilter-96 Harvester.

6) After the final wash by Unifilter-96 Harvester, the filter plate was placed in an oven (not exceeding 60 °C) until the filter material was completely dry.

7) Added 70 μl/well of MicroScint™-0 and covered the plate by plate cover. Radioactivity associated with DNA of proliferating cells was measured by Microplate Scintillation Luminescence Counter.

8) Calculated inhibitive percentage of proliferation. The formula was as following:

Inhibitive percentage of proliferation [%] = [cpm (untreated) - cpm (treated)] / cpm (untreated).

3.2.5 Lactate dehydrogenase release for cytotoxicity assay

The procedures were already previously described in Chapter 2.

3.2.6 Quantitative assay of intracellular cholesterol

The procedures were already previously described in Chapter 2.

3.2.7 Intracellular cholesterol efflux assay

The procedures were already previously described in Chapter 2.

3.2.8 Real-time RT–PCR

The procedures and the Taqman primers for real-time RT-PCR were already previously shown in Chapter 2.

3.2.9 Western Blot

The procedures were already previously described in Chapter 2.

3.2.10 Determination of IL-6, TNFα, IL-8 and MCP-1 release

3.2.10.1 Materials

1) IL-6 DuoSet ELISA Development System (Cat. NO. DY206, R&D Systems, UK)

2) IL-8 DuoSet ELISA Development System (Cat. NO. DY208, R&D Systems, UK)

3) TNFα DuoSet ELISA Development System (Cat. NO. DY210, R&D Systems, UK)

4) MCP-1 DuoSet ELISA Development System (Cat. NO. DY279, R&D Systems, UK)

5) NOVAPATH^{TM} Washer (Bio-Rad, Hertfordshire, UK)

6) Model 3550 Microplate Reader (Bio-Rad, Hertfordshire, UK)

3.2.10.2 Preparation of solutions

1) PBS: NaCl 40g, KCl 1.0g, Na_2HPO_4 5.75g, and KH_2PO_4 1.0 g were dissolved in 5 litres of dH_2O, fully mixing up.

2) Wash buffer: 0.05 % Tween 20 in PBS, pH 7.2-7.4.

3) Block buffer: 1 % BSA (5g/500mL), 5 % (25g/500ml) Sucrose in PBS with 0.05 % (0.25g/500ml) NaN3.

4) Reagent diluent: 0.1 % BSA, 0.05 % Tween 20 in Tris-buffered saline (20 mmol/l Trizma base, 150mmol/l NaCl) pH 7.3, 0.2 μm filtered.(500mL: 0.5 g BSA, 0.25 ml Tween 20, 1.211 g Tris, 4.383 g NaCl).

5) Substrate solution: 1:1 mixture of Colour Reagent A (H_2O_2) and Colour Reagent B (Tetramethylbenzidine).

6) Stop solution: 2 N H_2SO_4.

7) Reagent diluent of MCP-1: 1% BSA in PBS, pH 7.2-7.4, 0.2 μm filtered.

Note: For IL-6, TNFα, IL-8 and MCP-1, Reagent diluent was the same except that Reagent diluent of MCP-1 was different.

3.2.10.3 Preparation of antibodies and streptavidin-horseradish Peroxidase

Table 3.1 Preparation of capture antibody for ELISA

Name	Capture antibody	PBS Buffer	Stock	Working concentration
IL-6	360 μg	1.8 ml	200 μg/ml	2 μg/ml
TNFα	720 μg	1.8 ml	400 μg/ml	4 μg/ml
IL-8	720 μg	1.8 ml	400 μg/ml	0.5 μg/ml
MCP-1	180 μg	1.8 ml	100 μg/ml	1 μg/ml

Dilution: 100 μL Stock + 9.9ml PBS, then mixed up.

Table 3.2 Preparation of detection antibody for ELISA

Name	Detection antibody	Reagent diluent	Stock	Working concentration
IL-6	36 μg	1.8 ml	20 μg/ml	200 ng/ml
TNFα	54 μg	1.8 ml	30 μg/ml	300 ng/ml
IL-8	3.6 μg	1.8 ml	2 μg/ml	20 ng/ml
MCP-1	18 μg	1.8 ml	10 μg/ml	100 ng/ml

Dilution: 100 μL Stock + 9.9ml Reagent diluent, then mixed up.

Table 3.3 Preparation of standard for ELISA

Name	Standard	dH_2O	Stock	Working concentration
IL-6	15 ng	500 µl	30 ng/ml	600 pg/ml
TNFα	35 ng	700 µl	50 ng/ml	1000 pg/ml
IL-8	45 ng	225 µl	200 ng/ml	2000 pg/ml
MCP-1	35 ng	350 µl	100 ng/ml	1000 pg/ml

Dilution1 (for IL-6 and TNFα): 10 µl Stock + 490 µl Reagent diluent, then mixed up.

Dilution2 (for IL-8): 10 µl Stock + 990 µl Reagent diluent then mixed up.

Dilution3 (for MCP-1): 10 µl Stock + 990 µl Reagent diluent, then mixed up.

4) Preparation of streptavidin-HRP: According to the ratio of 1:200, then diluted to working solution with Reagent diluent buffer.

3.2.10.4 Procedures

1) VSMCs in 6-well plates were grown to confluence, and then cultured in serum-free medium containing 0.2% fatty acid-free BSA for 24 hours before the experiment.

2) After addition of the stimuli, cells were incubated for 24 hours, and then the supernatants of conditioned medium was collected and frozen at -70°C.

3) Assays for IL-6, TNFα, IL8 and MCP-1 were performed with an ELISA Kit according to the manufacturer's instructions.

4) Diluted the capture antibody to the working concentration in PBS without carrier protein. Took 100 µl of capture antibody and added to 9.9 ml of PBS.

5) Immediately coated a 96-well microplate with 100 µl per well of the diluted capture antibody. Sealed the plate and incubated overnight at room temperature.

6) Next day washed the plate three times with wash buffer by plate washer.

7) Blocked plates by adding 300 µl of Block Buffer to each well. Incubated at room temperature for a minimum of 1 hour.

8) Washed the plates three times with wash buffer by plate washer. The plates were dried by aspiration.

9) Added 100 μl of samples and standards per well, covered with an adhesive strip and incubated 2 hours at room temperature.

* Preparation of Standards:

• IL-6 standard concentration (pg/ml): 600, 300, 150, 75, 37.5, 18.75, 9.375, 0. At the NO.1 tube, added 10 μl IL-6 stock and 490 μl Reagent Diluent, then mixed by inversion. Dispensed 250 μl Reagent Diluent into labelled micro-centrifuge tubes, aspirated 250 μl from NO.1 tube into the second tube, and then made one by one dilution.

• TNFα standard concentration (pg/ml): 1000, 500, 250, 125, 62.5, 31.25, 15.625, 0. At the NO.1 tube, added 10 μl TNFα stock and 490 μl Reagent Diluent, then full mixed. Dispensed 250 μl Reagents Diluent into labelled micro-centrifuge tubes, aspirated 250 μl from NO.1 tube into the second tube, and then made one by one dilution.

• IL-8 standard concentration (pg/ml): 2000, 1000, 500, 250, 125, 62.5, 31.25, 0. At the NO.1 tube, added 10 μl IL-8 stock and 990 μl Reagent Diluent, then fully mixed up. Dispensed 250 μl Reagents Diluent into labelled micro-centrifuge tubes, aspirated 250 μl from NO.1 tube into the second tube, and then made one by one dilution.

• MCP-1 standard concentration (pg/ml): 1000, 500, 250, 125, 62.5, 31.25, 15.625, 0. At the NO.1 tube, added 50 μl MCP-1 stock and 450 μl Reagent Diluent, then fully mixed up. Dispensed 250 μl Reagent Diluent into labelled micro-centrifuge tubes, aspirated 250 μl from NO.1 tube into the second tube, and then made one by one dilution.

* Preparation of Samples:

VSMCs samples were diluted 100 times for checking IL-6 and MCP-1, 200 times for checking for IL-8. As TNFα concentration was almost undetective in the supernatants in VSMCs, no dilution was needed for checking TNFα.

10) Washed the plates three times with wash buffer by plate washer.

11) Added 100 μl of the detection antibody which was diluted in Reagent Diluent to each well. Covered with a new adhesive strip and incubated 2 hours at room temperature.

12) Washed the plates three times with wash buffer by plate washer.

13) Added 100 μl of the working Dilution of streptavidin-HRP to each well. Covered the plate and incubated for 20 minutes at room temperature. Avoided placing the plate in direct light.

14) Washed the plates three times with wash buffer by plate washer.

15) Added 100 μl of substrate solution to each well. Incubated for 20 minutes at room temperature. Avoided placing the plate in direct light.

16) Added 50 μl of Stop solution to each well. Gently tapped the plate to ensure thorough mixing.

17) Determined the optical density of each well immediately, using a microplate reader set to dual wavelength (Measurement wavelength was 450 nm; Reference wavelength was 540 nm.).

3.3 Results

3.3.1 The effect of Sirolimus on the proliferation of VSMCs

Firstly we examined the effects of Sirolimus on VSMC proliferation by using tritium labelled thymidine incorporation assay. As shown in Fig 3.2a, Sirolimus inhibited VSMC proliferation in a dose dependent manner. Sirolimus also exerted a constant

inhibitive effect as the incubation time was extended (Fig 3.2b). Furthermore, Sirolimus significantly inhibited VSMC proliferation stimulated by IL-1β (Fig 3.2c). These results suggest that anti-proliferation is one of the main anti-atherosclerotic effects mediated by Sirolimus, which is in accordance with previous studies (394).

3.3.2 The observation of cytotoxic effect in Sirolimus treated VSMCs

In order to exclude cytotoxicity, we measured the release of LDH into the supernatants of cultured VSMCs treated with different doses of Sirolimus. As shown in Fig 3.3, there was no difference between Sirolimus treated groups and controls, suggesting that inhibition of VSMC proliferation mediated by Sirolimus is not due to cytotoxicity and it's safe to investigate the anti-atherosclerotic effect of Sirolimus on VSMCs in the dose range 0-100 ng/ml.

3.3.3 The effect of Sirolimus on lipid accumulation in VSMCs induced by inflammatory cytokines

Using Oil Red O staining, we checked the effect of Sirolimus on cholesterol accumulation in VSMCs loaded with native LDL in the presence or absence of IL-1β. We found that IL-1β significantly increased lipid droplet accumulation in VSMCs (Fig 3.4a, B). However, Sirolimus reduced IL-1β associated lipid droplet accumulation in VSMCs (Fig 3.4a, D). Furthermore, quantitative assay of intracellular cholesterol demonstrated that Sirolimus reduced cholesterol ester accumulation induced by IL-1β in VSMCs (Fig 3.4b), suggesting that Sirolimus provides a protective role in decreasing cholesterol accumulation induced by inflammatory stress.

3.3.4 The effect of Sirolimus on the expression of lipoprotein receptors in VSMCs

Next, we investigated effects of Sirolimus on the gene and protein expression of lipoprotein receptors that mediate cholesterol uptake. Sirolimus significantly decreased the gene and protein expression of VLDLr and LDLr in VSMCs in the presence or

absence of IL-1β (Fig 3.5a, Fig 3.5b & 3.5c). We also checked the mRNA expression of SR-A and CD36 but found no difference between Sirolimus treated groups and controls.

3.3.5 Sirolimus overrides reduction of cholesterol efflux induced by IL-1β in VSMCs by up-regulating the expression of PPARs, LXRα, ABCA1 and ABCG1

We also examined the effects of Sirolimus on cholesterol efflux under inflammatory stress. Results showed that IL-1β significantly reduced $ApoA_1$-mediated cholesterol efflux from cholesterol-loaded VSMCs. However, Sirolimus overrode the reduction of cholesterol efflux induced by IL-1β (Fig 3.6). The ABCA1 mediated cholesterol efflux is a common cellular cholesterol efflux pathway that plays an important role in maintaining cholesterol homeostasis. Therefore, we further evaluated the effect of Sirolimus on the gene expression of PPARα, LXRα, and ABCA1 in VSMCs. IL-1β exerted an inhibitory effect on the ABCA1 mediated cholesterol efflux pathway. However, Sirolimus significantly increased the gene and protein expression of PPARα, LXRα, and $ABCA_1$ in cholesterol-loaded VSMCs even in the presence of IL-1β (Fig 3.7, Fig 3.8a & 3.8b). These results suggest that Sirolimus overrides the suppression of ABCA1 pathway induced by IL-1β. Since ABCG1 also plays a pivotal role in mediating cellular efflux of phospholipids and cholesterol to apoA-I containing lipoproteins, we also investigated the effect of Sirolimus on the gene expression of ABCG1 in VSMCs. The results showed that Sirolimus also overrode the suppression of ABCG1 gene expression induced by IL-1β (Fig 3.9).

3.3.6 Sirolimus inhibits the expression of inflammatory cytokines

Interestingly, Sirolimus inhibited mRNA (Fig 3.10a & 3.10b) and protein (Fig 3.11a, 3.11b & 3.11c) expression of inflammatory cytokines in VSMCs in the presence or absence of cholesterol loading, suggesting that Sirolimus may decrease cholesterol accumulation by indirectly inhibiting the production of inflammatory cytokines.

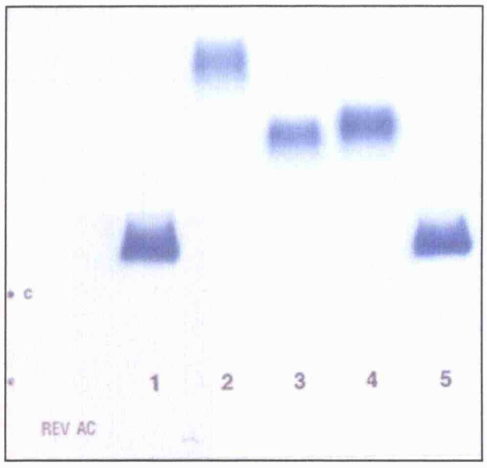

Fig 3.1 Agarose gel electrophoretic mobility of native LDL, acLDL, and oxLDL. Lipoproteins (2 μl/well) were loaded in Beckman paragon Lipo Gel for electrophoresis. Lane 1&5: freshly isolated native LDL, Lane 2: acLDL, Lane 3&4: oxLDL.

Fig 3.2a

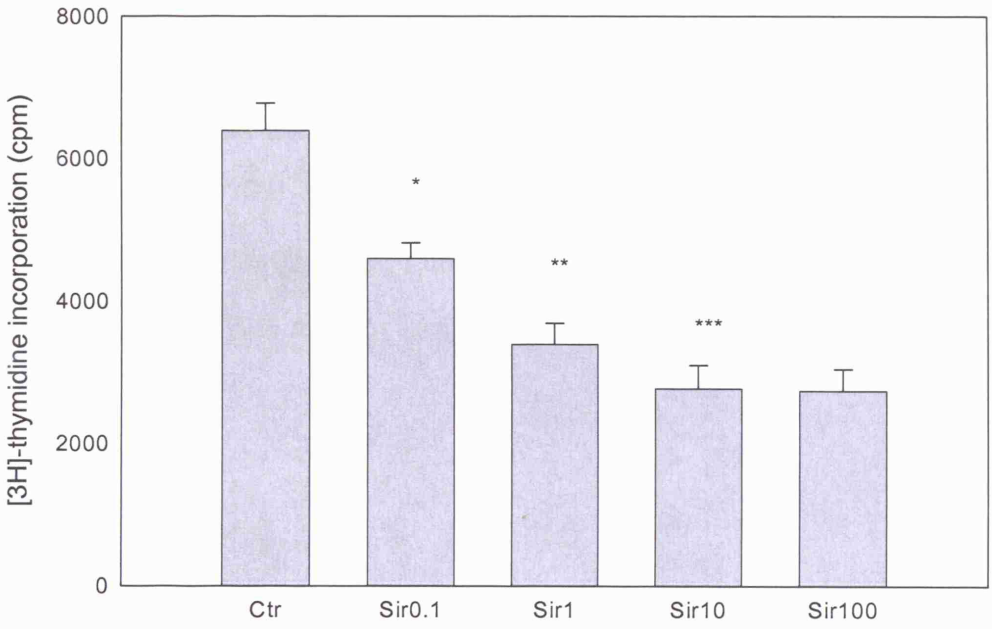

Fig 3.2a Sirolimus inhibited VSMC proliferation in dose dependent manner. VSMCs were incubated in serum-free medium with different concentrations of Sirolimus (Sir, 0-100 ng/ml) for 24 hours. The radioactivity of [^{3}H]-thymidine incorporation was checked by Microplate Scintillation & Luminescence Counter. Results were expressed as Mean ± SD (n=8 wells). * P<0.001 *vs* control, ** P<0.001 *vs* Sir0.1, *** P<0.005 *vs* Sir1.

Fig 3.2b

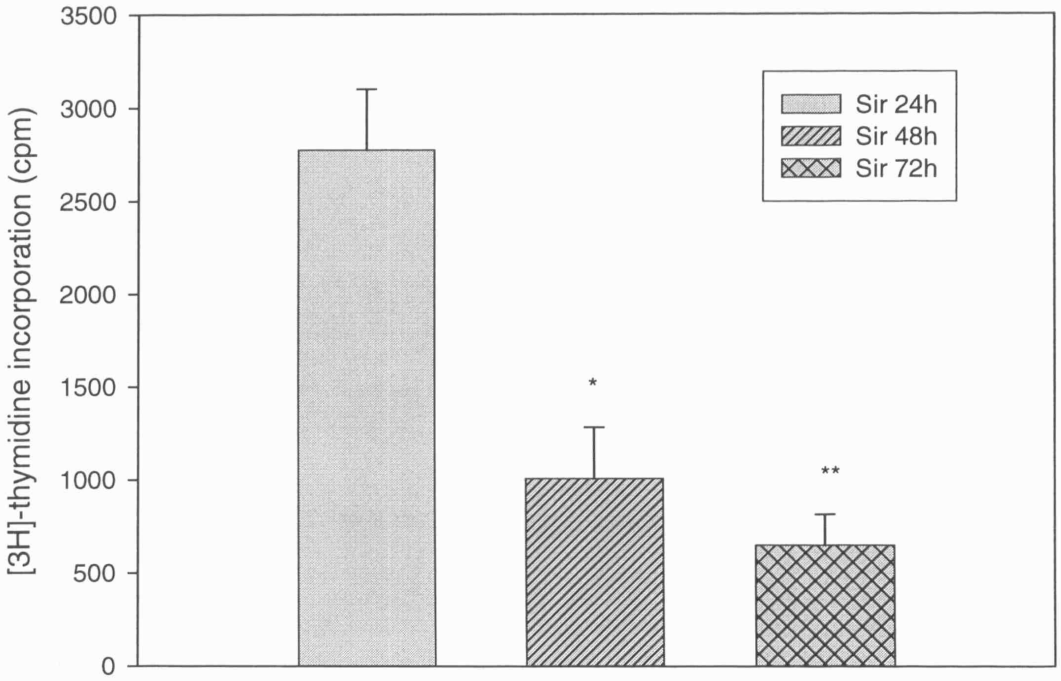

Fig 3.2b Time-course effect of Sirolimus on VSMC proliferation. VSMCs were incubated in serum-free medium with 10 ng/ml of Sirolimus for 24, 48, 72 hours respectively. The radioactivity of [^{3}H]-thymidine incorporation was checked by Microplate Scintillation & Luminescence Counter. Results were expressed as Mean ± SD (n=8 wells). * $P<0.001$ *vs* Sir 24h, ** $P<0.01$ *vs* Sir 48h.

Fig 3.2c

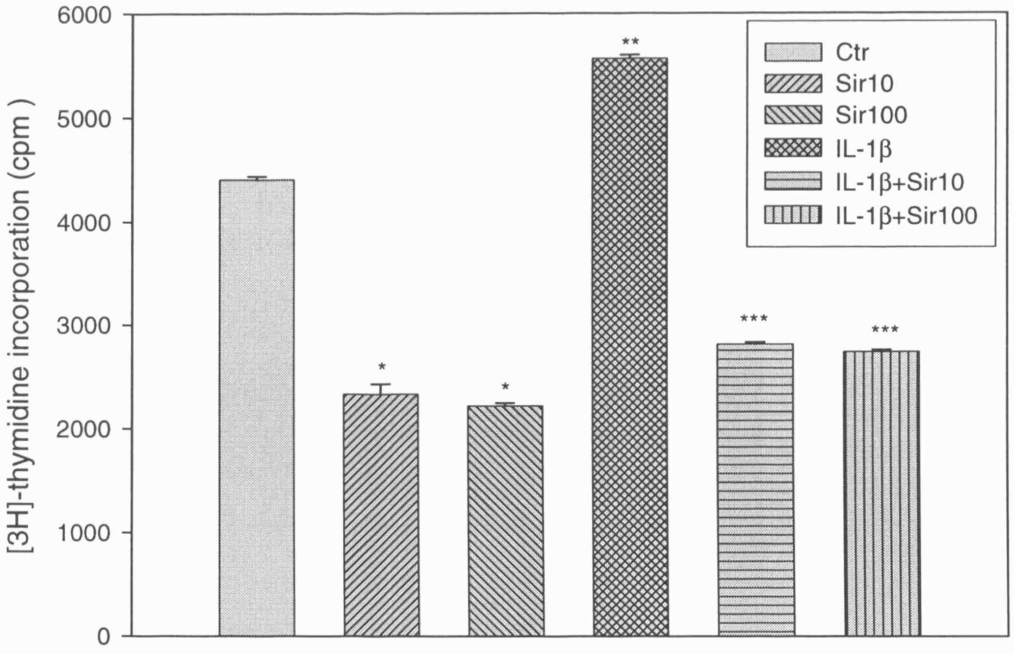

Fig 3.2c The effects of Sirolimus on VSMC proliferation stimulated by IL-1β. VSMCs were incubated in serum-free medium (control, Ctr), 10 ng/ml of Sirolimus (Sir10), 100 ng/ml of Sirolimus (Sir100), 5 ng/ml of IL-1β (IL-1β), 5 ng/ml of IL-1β plus 10 ng/ml of Sirolimus (IL-1β+Sir10), and 5 ng/ml of IL-1β plus 100 ng/ml of Sirolimus (IL-1β+Sir100) for 24 hours respectively. The radioactivity of [^{3}H]-thymidine incorporation was checked by Microplate Scintillation & Luminescence Counter. Results were expressed as Mean ± SD (n=8 wells). * P<0.001 *vs* control, ** P<0.001 *vs* control, *** P<0.001 *vs* IL-1β.

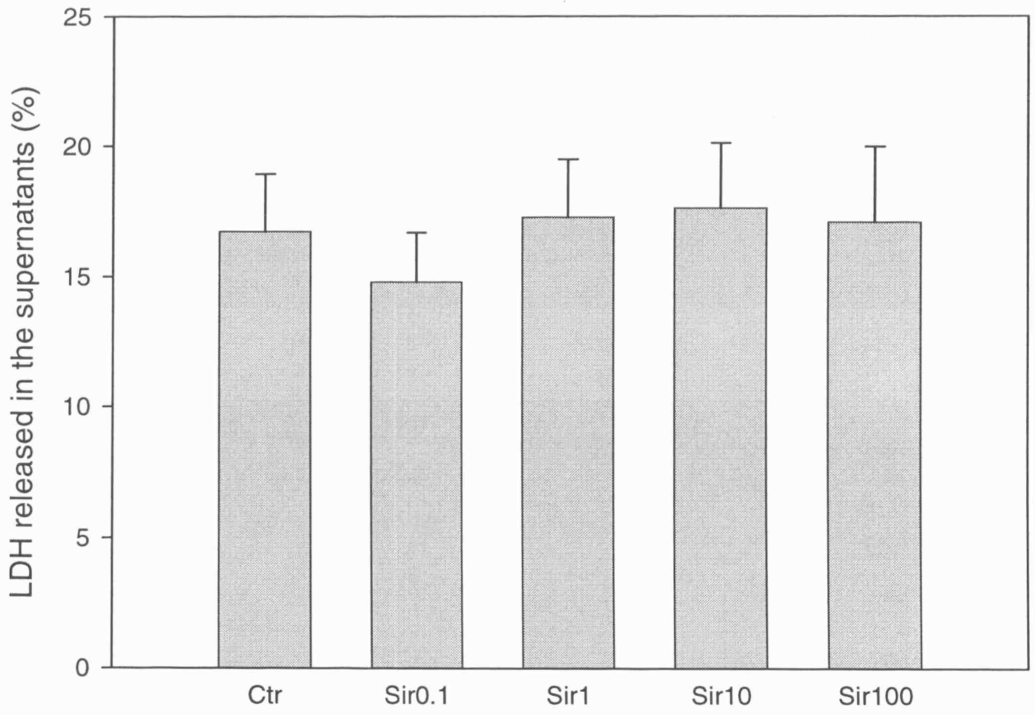

Fig 3.3 The observation of cytotoxic effect in VSMCs treated by Sirolimus. VSMCs were incubated in serum-free medium without (Ctr) or with different concentrations of Sirolimus (0.1, 1, 10, 100 ng/ml) for 24 hours. Supernatants were collected and cells were lysed for LDH assay. The percentage of LDH in the supernatants was expressed as Mean ± SD (n=8 wells). There was no significance among the Sirolimus treated groups compared to controls.

Fig 3.4a

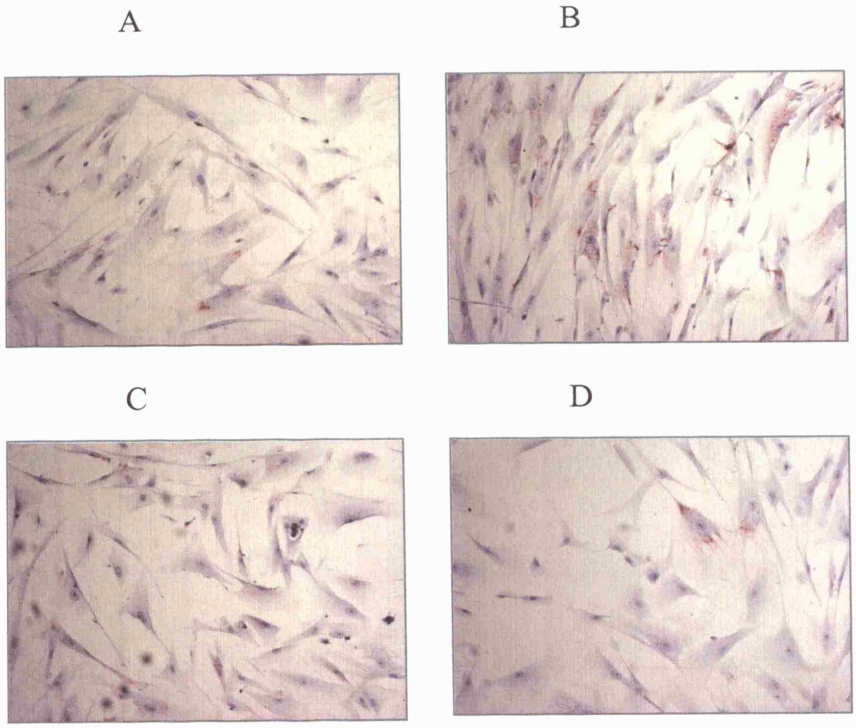

Fig 3.4a Visualisation of LDL uptake and lipid droplets in VSMCs after Sirolimus treatment. VSMCs were incubated for 24 hours in serum-free medium containing 200 μg/ml of native LDL in the absence (A) or presence of 5 ng/ml of IL-1β (B) or 10 ng/ml of Sirolimus (C) or 5 ng/ml of IL-1β plus 10 ng/ml Sirolimus (D). The cells were examined for lipid inclusions by Oil Red O staining. The results were typical of those observed in four separate experiments (100x).

Fig 3.4b

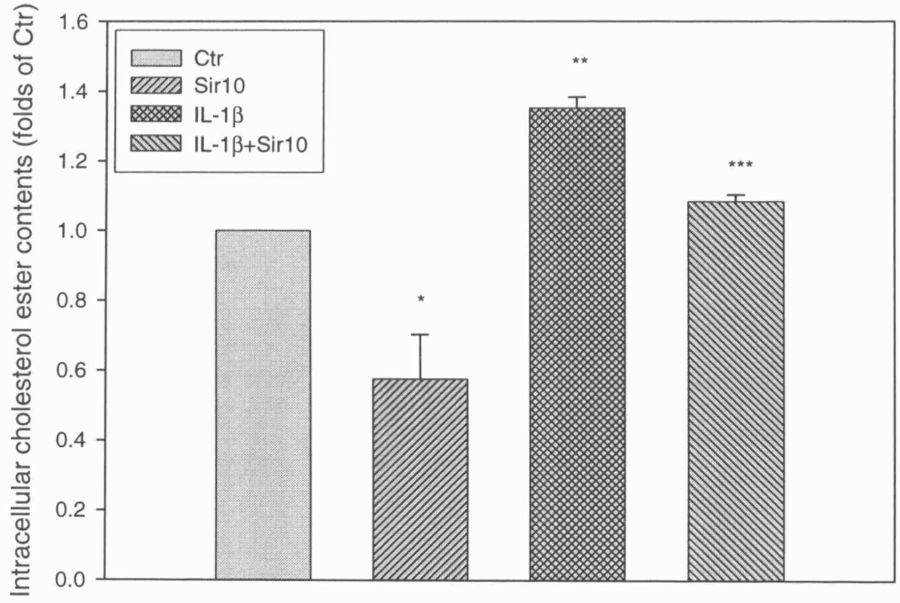

Fig 3.4b The effect of Sirolimus on intracellular cholesterol ester contents in LDL-loaded VSMCs. VSMCs were cultured in serum-free medium containing 200 μg/ml of native LDL in the absence (control, Ctr) or presence of 5 ng/ml of IL-1β (IL-1β) or 5 ng/ml of IL-1β plus 10 ng/ml of Sirolimus (IL-1β+Sir10) for 24 hours. Intracellular cholesterol ester contents were measured as described in MATERIALS AND METHODS. Values were expressed Mean ± SD of duplicate wells from four experiments. *$P < 0.05$ *vs* control. **$P < 0.01$ *vs* control. ***$P < 0.01$ *vs* IL-1β.

Fig 3.5a

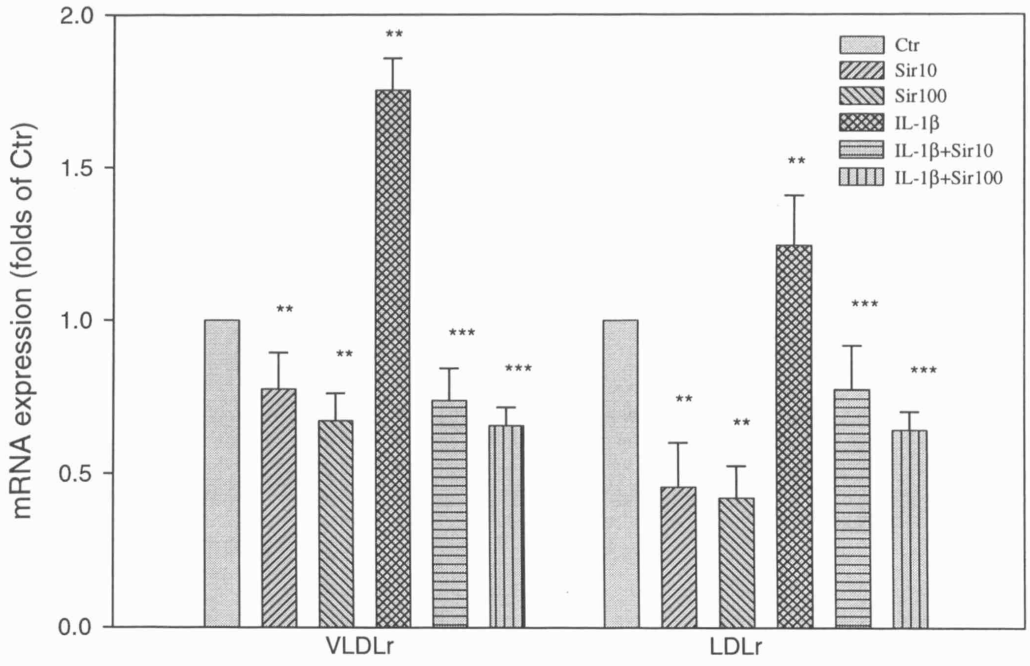

Fig 3.5a The effect of Sirolimus on the mRNA expression of lipoprotein receptors in VSMCs. VSMCs were incubated in serum-free medium (control, Ctr) or serum-free medium with 10-100 ng/ml of Sirolimus (Sir10, Sir 100) or 5 ng/ml of IL-1β (IL-1β) or 5 ng/ml of IL-1β plus 10-100 ng/ml of Sirolimus (IL-1β+Sir10, IL-1β+Sir100) for 24 hours. The mRNA expression of VLDLr and LDLr were determined following the ΔΔCt protocol for real-time RT-PCR as described in the section of Methods. β-actin served as the housekeeping gene. Results represented the Mean ± SD from four experiments. ** p <0.01 *vs* control, *** p <0.01 *vs* IL-1β group.

Fig 3.5b

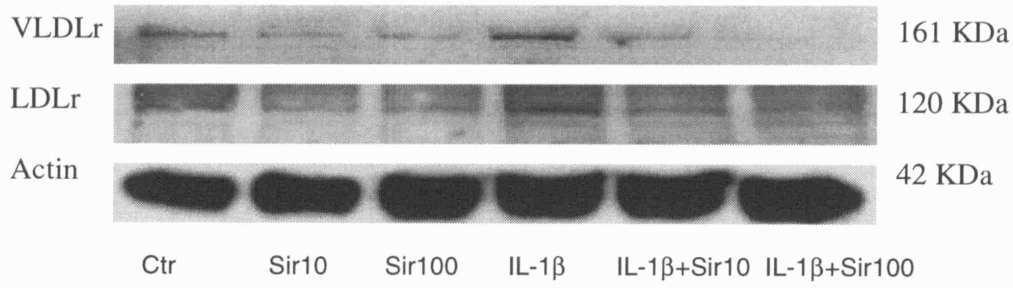

Fig 3.5c

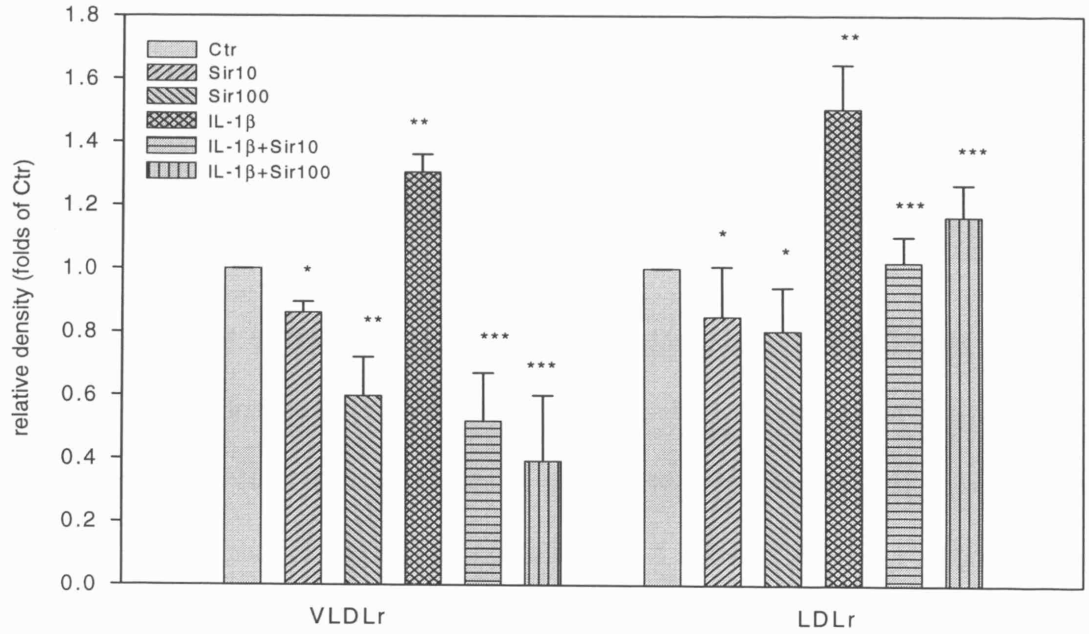

Fig 3.5b & 3.5c The effect of Sirolimus on the protein expression of lipoprotein receptors in VSMCs. VSMCs were incubated in serum-free medium (control, Ctr) or serum-free medium with 10-100 ng/ml of Sirolimus (Sir10, Sir 100) or 5 ng/ml of IL-1β (IL-1β) or 5 ng/ml of IL-1β plus 10-100 ng/ml of Sirolimus (IL-1β+Sir10, IL-1β+Sir100) for 24 hours. The protein levels of VLDLr and LDLr were examined by Western Blot. The histogram represented Mean ± SD of the densitometric scans of the VLDLr and LDLr protein bands from four experiments, normalised by comparison with actin, and expressed as a percentage of the control. * p <0.05 *vs* control, ** p <0.01 *vs* control, *** p <0.01 *vs* IL-1β group.

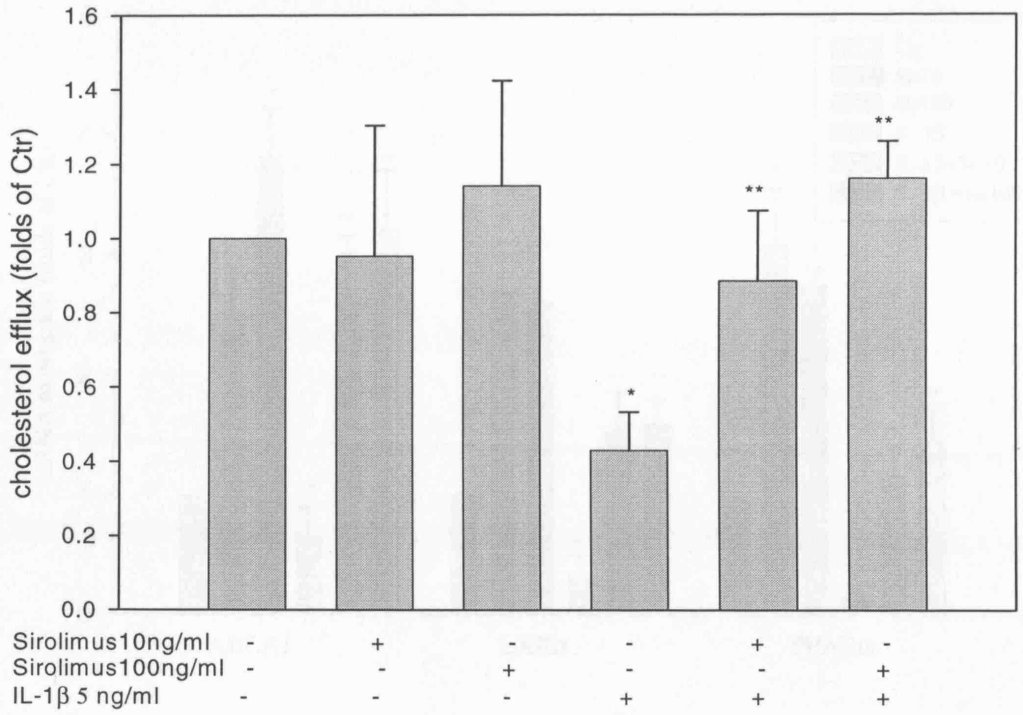

Fig 3.6 The effect of Sirolimus on the intracellular cholesterol efflux of VSMCs. VSMCs were pre-loaded with cholesterol as described in the section of Methods. The cholesterol loaded cells were incubated in serum-free medium (control) or serum-free medium with 10 ng/ml or 100 ng/ml of Sirolimus or 5 ng/ml of IL-1β, or 5 ng/ml of IL-1β plus 10 ng/ml of Sirolimus or 5 ng/ml of IL-1β plus 100 ng/ml of Sirolimus for 24 hours. The cholesterol efflux was measured by radioactive counts. Data represented the Mean ± SD of four independent experiments. * p <0.01 *vs* control, ** p <0.01 *vs* IL-1β group.

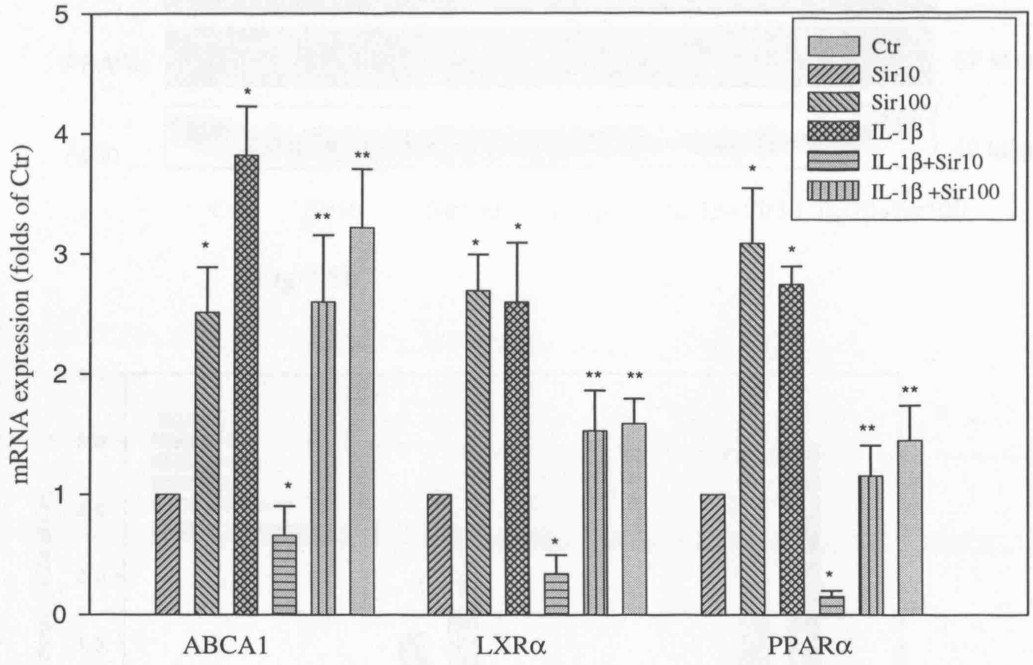

Fig 3.7 The effect of Sirolimus on the mRNA expression of LXRα, PPARα and ABCA1 in cholesterol-loaded VSMCs. VSMCs were loaded with 30 μ g/ml cholesterol, 1 μg/ml 25-hydroxy-cholesterol in serum-free medium for 48 hours. After that, VSMCs were incubated in serum-free medium (control, Ctr) or serum-free medium with 10-100 ng/ml of Sirolimus (Sir10, Sir 100) or 5 ng/ml of IL-1β (IL-1β) or 5 ng/ml of IL-1β plus 10-100 ng/ml of Sirolimus (IL-1β+Sir10, IL-1β+Sir100) for 24 hours. The mRNA expression of PPARα, LXRα and ABCA1 were determined following the ΔΔCt protocol for real-time RT-PCR as described in the section of Methods. β-actin served as the housekeeping gene. Results represented the Mean ± SD from four experiments. * p <0.001 *vs* control, ** p <0.001 *vs* IL-1β group.

Fig 3.8a

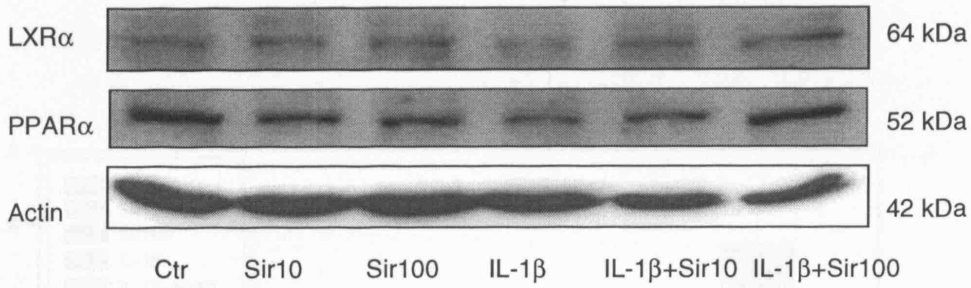

Fig 3.8b

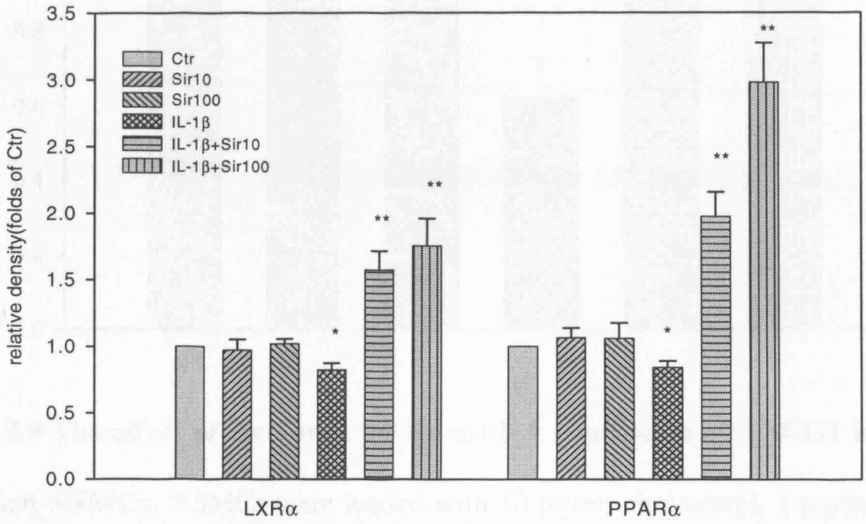

Fig 3.8a & 3.8b The effect of Sirolimus on the protein expression of LXRα and PPARα in cholesterol-loaded VSMCs. VSMCs were loaded with 30 μ g/ml cholesterol, 1 μg/ml 25-hydroxy-cholesterol in serum-free medium for 48 hours. After that, VSMCs were incubated in serum-free medium (control, Ctr) or serum-free medium with 10-100 ng/ml of Sirolimus (Sir10, Sir 100) or 5 ng/ml of IL-1β (IL-1β) or 5 ng/ml of IL-1β plus 10-100 ng/ml of Sirolimus (IL-1β+Sir10, IL-1β+Sir100) for 24 hours. The protein levels of PPARα, LXRα were examined by Western Blot. The histogram represented Mean ± SD of the densitometric scans of the PPARα and LXRα protein bands from four experiments, normalised by comparison with actin, and expressed as a percentage of the control. * p <0.05 *vs* control, ** p <0.01 *vs* IL-1β group.

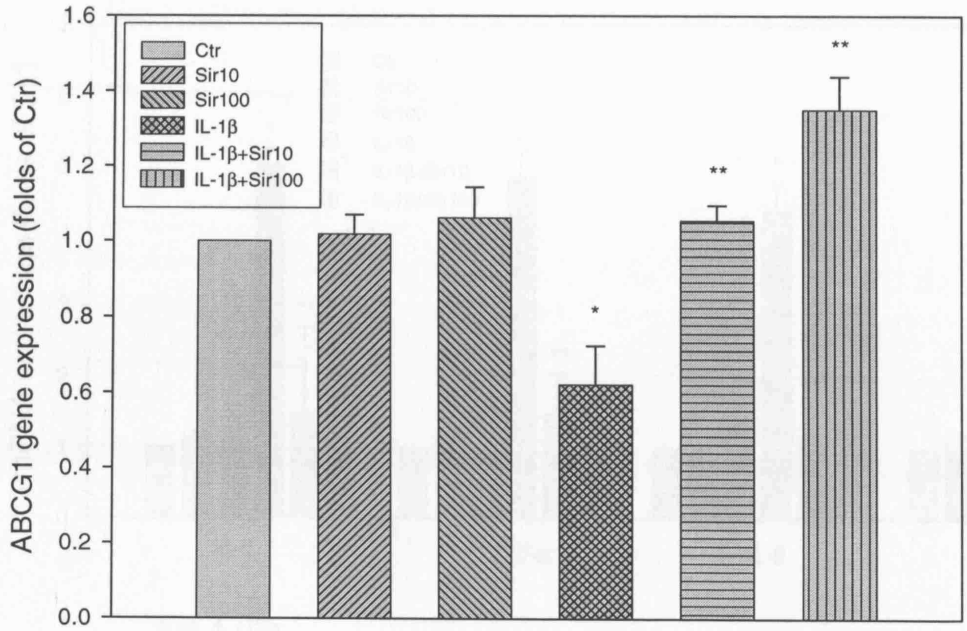

Fig 3.9 The effect of Sirolimus on the mRNA expression of ABCG1 in cholesterol-loaded VSMCs. VSMCs were loaded with 30 μg/ml cholesterol, 1 μg/ml 25-hydroxy-cholesterol in serum-free medium for 48 hours. After that, VSMCs were incubated in serum-free medium (control, Ctr) or serum-free medium with 10-100 ng/ml of Sirolimus (Sir10, Sir 100) or 5 ng/ml of IL-1β (IL-1β) or 5 ng/ml of IL-1β plus 10-100 ng/ml of Sirolimus (IL-1β+Sir10, IL-1β+Sir100) for 24 hours. The mRNA expression of ABCG1 was determined following the ΔΔCt protocol for real-time RT-PCR as described in the section of Methods. β-actin served as the housekeeping gene. Results represented the Mean ± SD from four experiments. * p <0.001 *vs* control, ** p <0.001 *vs* IL-1β group.

Fig 3.10a

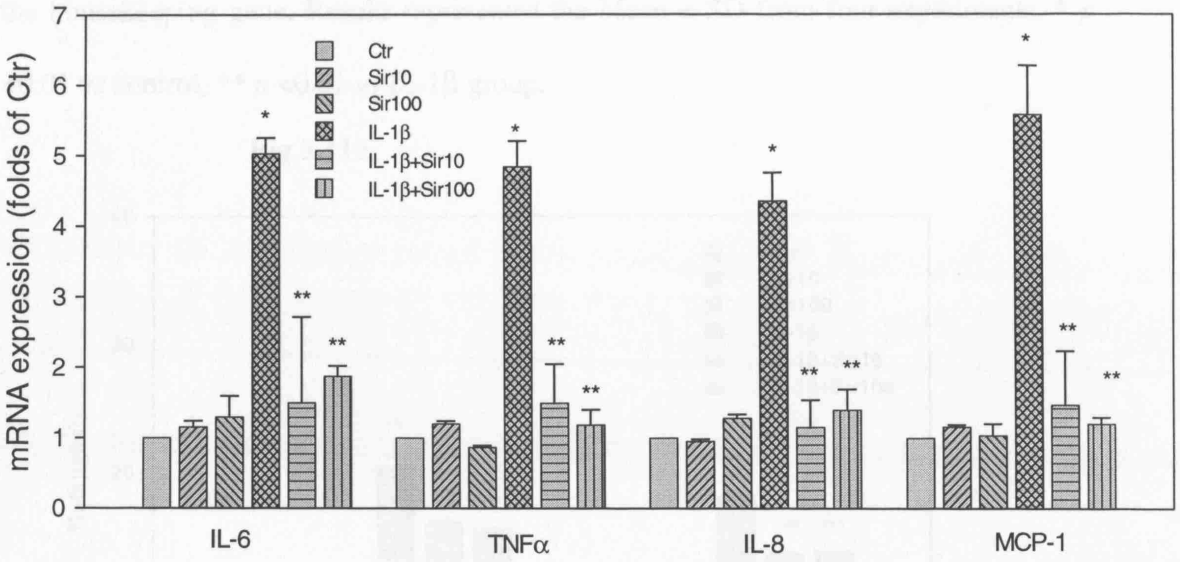

Fig 3.10b

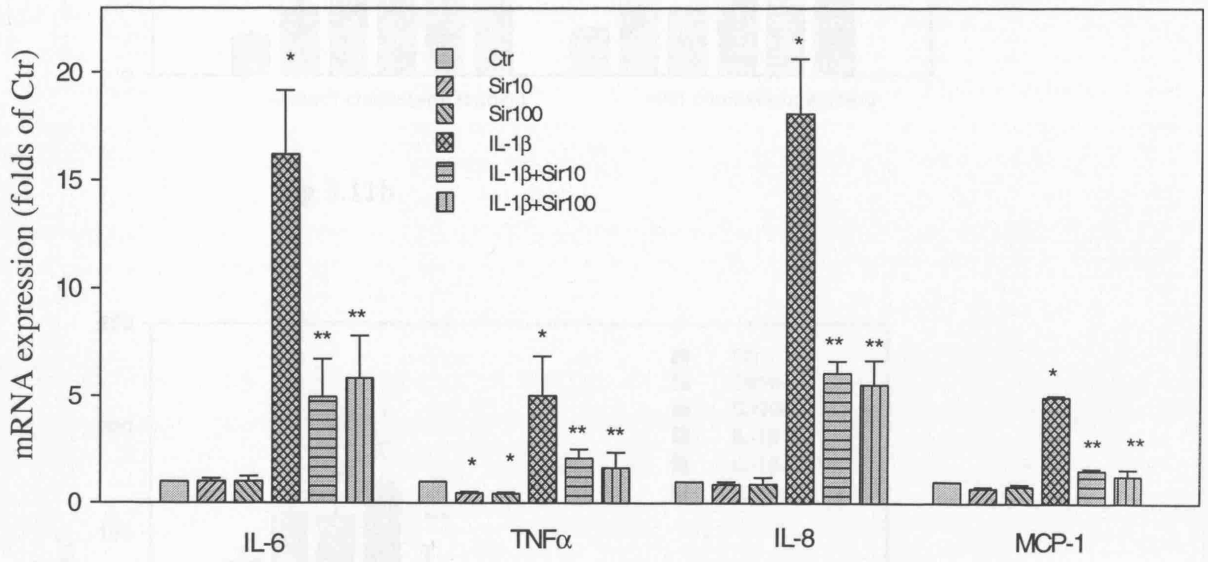

Fig 3.10a & 3.10b The effect of Sirolimus on the gene expression of inflammatory cytokines in VSMCs without or with cholesterol loading. VSMCs were pre-loaded with 30 μg/ml cholesterol, 1 μg/ml 25-hydroxy-cholesterol in serum-free medium for 48 hours. Both normal and cholesterol loaded VSMCs were incubated in serum-free medium (control, Ctr) or serum-free medium with different concentrations (10-100 ng/ml) of Sirolimus (Sir10 and Sir100) or 5 ng/ml of IL-1β (IL-1β) or 5 ng/ml of IL-1β plus different concentrations of Sirolimus (IL-1β+Sir10, IL-1β+Sir100) for 24 hours.

The mRNA of IL-6, TNFα, IL-8 and MCP-1 were determined following the ΔΔCt protocol for real-time RT-PCR as described in the section of Methods. β-actin served as the housekeeping gene. Results represented the Mean ± SD from four experiments. * p <0.01 *vs* control, ** p <0.01 *vs* IL-1β group.

Fig 3.11a

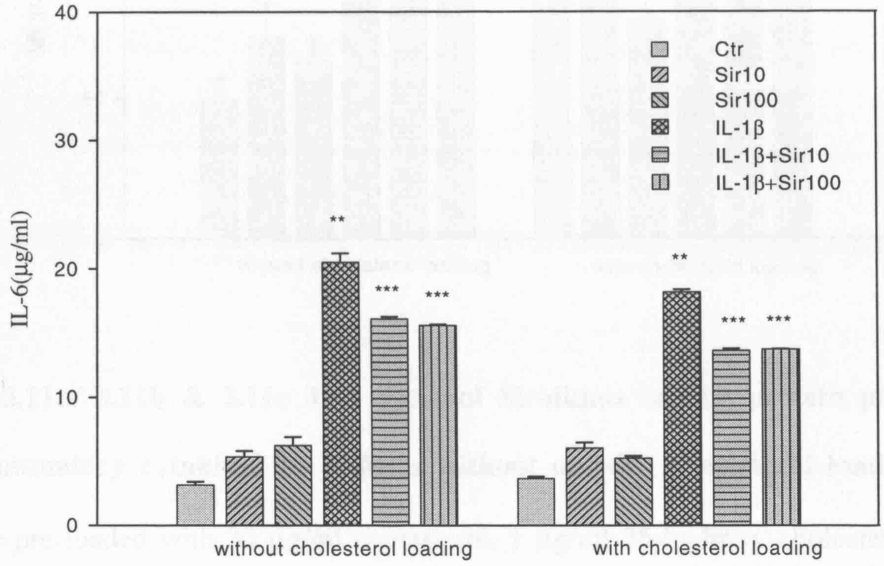

Fig 3.11b

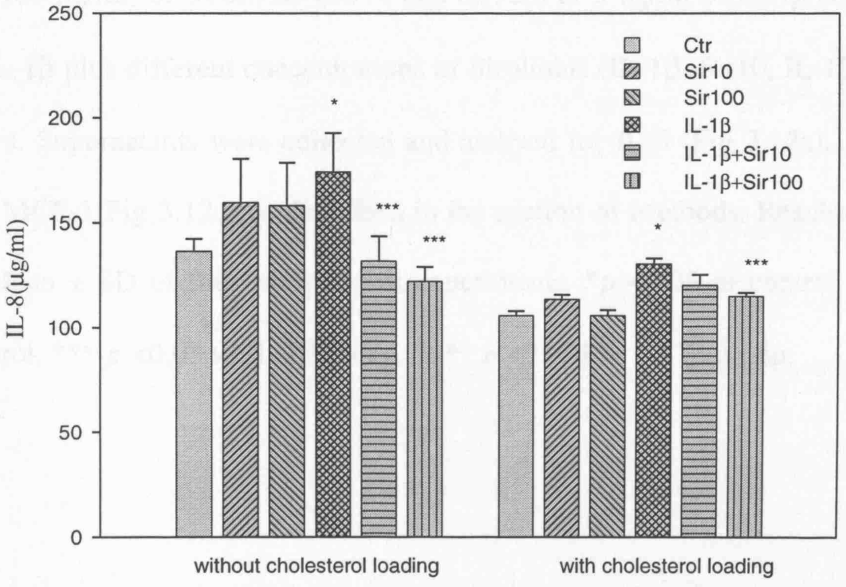

Fig 3.11c

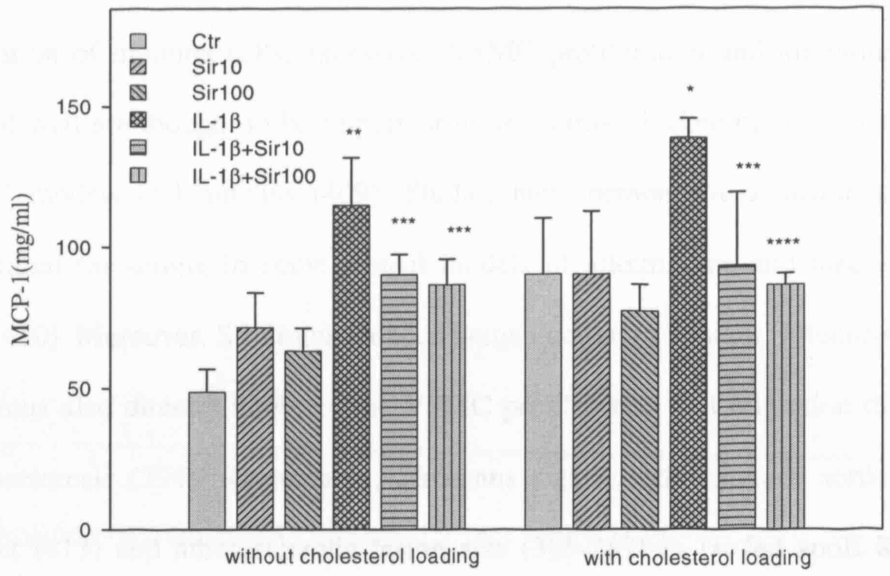

Fig 3.11a, 3.11b & 3.11c The effect of Sirolimus on the protein production of inflammatory cytokines in VSMCs without or with cholesterol loading. VSMCs were pre-loaded with 30 μg/ml cholesterol, 1 μg/ml 25-hydroxy-cholesterol in serum-free medium for 48 hours. Both normal and cholesterol loaded VSMCs were incubated in serum-free medium (control, Ctr) or serum-free medium with different concentrations (10-100 ng/ml) of Sirolimus (Sir10 and Sir100) or 5 ng/ml of IL-1β (IL-1β) or 5 ng/ml of IL-1β plus different concentrations of Sirolimus (IL-1β+Sir10, IL-1β+Sir100) for 24 hours. Supernatants were collected and assayed for IL-6 (Fig 3.12a), IL-8 (Fig 3.12b) and MCP-1(Fig 3.12c) as described in the section of Methods. Results were expressed as Mean ± SD of four independent experiments. *p <0.05 *vs* control, ** p <0.001 *vs* control, *** p <0.05 *vs* IL-1β group, **** p <0.001 *vs* IL-1β group.

3.4. Discussion

Activation of immune cells, excessive VSMC proliferation and migration within the arterial wall are thought to be important in neointimal thickening in both experimental animal models and humans (409). Studies have demonstrated Sirolimus attenuated neointimal thickening in some animal models of alloimmune and mechanical injury (385, 410). Moreover, Sirolimus reduced human coronary in-stent restenosis (411, 412). Sirolimus also directly inhibited the VSMC proliferation and migration that promoted atherosclerosis (394). Remarkably, Sirolimus significantly reduced aortic cholesterol content (413) and atherosclerotic lesion size (385-387) in fat-fed apoE KO mice. In spite of the demonstrated atheroprotective effect of Sirolimus in apoE KO mice, caution must be used with respect to its possible clinical use in patients experiencing atherosclerosis since several studies have shown that Sirolimus exacerbated pre-existing hypercholesterolaemia and hypertriglyceridemia in human (414-416). In this study, we examined the effect of Sirolimus on intracellular cholesterol homeostasis and determined if this compound reduced intracellular lipid accumulation and foam cell formation in the human coronary artery smooth muscle cells in the presence of inflammatory cytokine.

IL-1β is a prototypic pro-inflammatory cytokine which plays an important role in the vascular inflammation and pathogenesis of atherosclerosis. IL-1β can be synthesized by macrophages, endothelial cells and VSMCs, and the levels of IL-1β in the vessel walls are elevated in atherosclerosis (417-419). It is well-known that IL-1β induces the production of cytokines and chemokines and increases the expression of adhesion molecules on endothelial cells, thus leading to the recruitment of inflammatory cells. In addition, IL-1β promotes the development of tissue damage by stimulating cell proliferation and the release of matrix metalloproteases (420), leading to destabilization

and eventual rupture of vulnerable atherosclerotic plaques. At a clinical level, circulating cytokines have a prognostic role and are useful in predicting future coronary events in patients with advanced atherosclerosis and in patients after acute coronary syndromes (421).

Our results showed that Sirolimus reduced lipid droplet accumulation and cholesterol ester content in VSMCs caused by IL-1β. We have demonstrated previously that IL-1β induced cholesterol esterification by increasing ACAT activity in VSMCs (422). Taken together, these findings may suggest that Sirolimus inhibits IL-1β-induced cholesterol esterification.

We demonstrated that IL-1β increased the mRNA and protein expression of VLDLr and LDLr in VSMCs, suggesting that IL-1β disrupts cholesterol homeostasis by increasing receptor mediated cholesterol uptake. Sirolimus decreased intracellular lipid accumulation of VSMCs by reducing mRNA and protein expression of VLDLr and LDLr even in the presence of IL-1β. Our results also demonstrated that Sirolimus overrode the suppression of cholesterol efflux induced by IL-1β in VSMCs by mediating the up-regulation of LXRα, PPARα, ABCA1 and ABCG1 gene expression. Thus, Sirolimus may ameliorate disruption of intracellular cholesterol homeostasis in VSMCs caused by inflammatory cytokines, in agreement with the anti-atherosclerotic effect of Sirolimus in some animal models and clinical studies of human cardiovascular diseases.

Our results may also partly explain some dose-dependent adverse effects of Sirolimus, especially hyperlipidemia with a high plasma concentration of VLDL and LDL in transplant patients after Sirolimus treatment (414, 416, 423). Sirolimus reduced lipids influx to peripheral cells such as VSMCs by inhibiting receptor-mediated uptake of LDL and VLDL, the carriers of cholesterol and triglyceride, respectively. In addition,

some studies reported that Sirolimus altered the insulin signalling pathway by increasing adipose tissue lipase activity and/or decreasing lipoprotein lipase activity, resulting in increased hepatic synthesis of triglyceride, increased secretion of VLDL, and hypertriglyceridemia (423). However, Sirolimus also significantly increased cholesterol efflux from cells through the ABCA1 and ABCG1 pathway as demonstrated here, which may reduce intracellular cholesterol level and increase HDL formation, thereby protecting from atherosclerosis. Our findings demonstrated that Sirolimus reduced intracellular cholesterol concentration of VSMCs in spite of its hyperlipidaemic potential.

Inflammation is a risk factor for atherosclerosis (6). We assumed that Sirolimus directly inhibited inflammatory processes. Therefore, we examined the effect of Sirolimus on the inflammatory cytokine excretion of VSMCs using IL-1β as stimulator. Our results showed that Sirolimus directly inhibited mRNA expression of inflammatory cytokines, IL-6, TNFα, IL-8, and MCP-1. The reduction of IL-6, IL-8, and MCP-1 protein levels was confirmed by ELISA assay (TNFα level was too low to be measured in the supernatants of VSMC cultures). Some previous studies have also demonstrated effects of Sirolimus on the expression and excretion of inflammatory cytokines and chemokines in mesangial cells and in a macrophage cell line (424), as well as in transplant models(425, 426).

It's clear that VSMCs in mature, normal blood vessels exhibit a differentiated, quiescent, contractile morphology, but injury induces a phenotypic modulation toward a proliferative, dedifferentiated, migratory phenotype with up-regulated extracellular matrix protein synthesis (synthetic phenotype), which contributes to intimal hyperplasia. Our results demonstrated that Sirolimus inhibited the proliferation of VSMCs in a dose-dependent manner and were in accordance with previous studies (394). Martin *et al* have demonstrated that Sirolimus treatment induced differentiation

in cultured VSMCs with synthetic phenotype from multiple species. VSMCs treated with Sirolimus assumed a contractile morphology, quantitatively reflected by a 67% decrease in cell area. Sirolimus inhibited the total protein and collagen synthesis and induced expression of VSMC differentiation markers-smooth muscle alpha-actin, calponin, and smooth muscle myosin heavy chain. The interaction among mTOR pathway, cell phenotype, and cholesterol homeostasis needs to be investigated.

In summary, our results suggest that inflammatory cytokines caused lipid accumulation by disrupting cholesterol homeostasis in VSMCs. Sirolimus prevented this lipid accumulation by (i) inhibiting gene and protein expression of VLDLr and LDLr; (ii) up-regulating the gene expression of $ABCA_1$ and ABCG1 pathways thereby overriding the reduction of cholesterol efflux induced by IL-1β; (iii) reducing inflammatory cytokine production. These may be one of the main mechanisms for its antiatherosclerotic effects.

CHAPTER 4. THE ANTI-ATHEROSCLEROTIC EFFECTS OF SIROLIMUS ON HUMAN CORONARY ARTERY SMOOTH MUSCLE CELLS (PART 2.)

4.1 Introduction

VSMCs are active in foam cell formation in the early stages of atherosclerosis (427). Cholesterol accumulation in cells is caused by an imbalance of between cholesterol influx and efflux pathways. Our previous studies demonstrated that inflammatory stress increased LDLr mediated cholesterol uptake and inhibited ABCA1 mediated cholesterol efflux, thereby increasing cholesterol accumulation in VSMCs (422, 428). However, the effect of inflammatory stress on endogenous cholesterol biosynthesis remains unclear.

HMGR is a key rate-limiting enzyme in cholesterol biosynthesis (137). The feedback regulation of HMGR at transcriptional level has been fully described in Chapter 1. At its core is the interaction of Insigs with the complex of SCAP/SREBPs in response to different sterol conditions in which the SCAP/SREBPs complex is either retained in the ER or released into the Golgi for gene transcription. At the posttranscriptional level, HMGR is regulated by the protein degradation pathway, which is mainly achieved through the interaction of Insig protein with HMGR (286). Under cholesterol-replete conditions, accumulation of cholesterol in the ER membranes triggers binding of the membrane domain of HMGR to a subset of Insigs that carry a membrane-anchored ubiquitin ligase called gp78, which initiates ubiquitination of HMGR (429). Ubiquitination marks HMGR for proteasomal degradation, reducing the half-life of the protein from 12 hours in cholesterol-depleted cells to less than 1 hour.

Therefore, Insig-1 could be a key regulator for the gene transcription and protein degradation of HMGR by changing complex levels of Insig-1/SCAP or Insig-1/HMGR.

In Chapter 3, we have shown that Sirolimus can re-establish cholesterol homeostasis in VSMCs through its anti-inflammatory effects to decrease cholesterol influx and increase cholesterol efflux (428). To explore whether Sirolimus also plays an important

role in cholesterol biosynthesis, the study was designed to investigate the effect of Sirolimus on HMGR pathways in both gene transcription and protein degradation levels in VSMCs under inflammatory stress.

4.2 Materials and methods

4.2.1 Cell culture

The procedures were already previously described in Chapter 3.

4.2.2 Measurement of cellular cholesterol biosynthesis (430)

4.2.2.1 Materials

1) 0.1 mol/l of Sodium hydroxide (Cat.NO.S0899, Sigma, Poole, Dorset, UK)

2) 90 % Potassium hydroxide (Cat.NO.P5958, Sigma, Poole, Dorset, UK): dissolved 90 g KOH in 100 ml of dH_2O.

3) [1-^{14}C] Acetic acid, sodium salt (Cat.NO.CFA13-250UCI, GE Healthcare, Buckinghamshire, UK)

4) 0.1 mol/l of Sodium acetate (Cat.NO.S2889, Sigma, Poole, Dorset, UK)

5) Hexane (Cat.NO.RH1002, Rathburn Chemicals Ltd, Borders, UK)

6) Absolute alcohol 100 (Hayman Limited, Essex, UK)

7) PBS containing 2 mg/ml of BSA: dissolved 1g BSA in 500 ml PBS, and then filtered through 0.2 μm of filter membrane for use.

8) Microplate Scintillation & Luminescence Counter (Cat. NO. C9904V1, PerkinElmer, bucks, UK)

4.2.2.2 Procedures

1) VSMCs were grown in 24-well plates with 0.2 % BSA serum-free DMEM/F12 medium for 24 hours. After that, VSMCs were treated by different reagents using

DMEM/F12 medium containing 5 % lipid-depletion FBS for 6 hours, and then [^{14}C]-acetic acid sodium (1 μCi/ml) was added for another 18 hours.

2) The cells were washed twice with PBS/BSA and three times with PBS.

3) The cells were dissolved in 0.6 ml of 0.1 mol/l of NaOH and 0.1 ml was removed for total protein estimation. 0.5 ml was added to a Teflon-lined, screw-capped tube containing 0.5 ml of ethanol and 0.1 ml of 90 % KOH.

4) The mixture was saponified by heating for 3 hours at 80 °C, and then nonsaponifiable lipids were extracted into 1.0 ml of hexane.

5) The hexane layer was taken for radioactivity measurement. The result of the incorporating [^{14}C] radioactivity into nonsaponifiable lipids normalized by total cell proteins was shown as sterol synthesis.

4.2.3 Real-time RT–PCR

The procedures and the Taqman primers for real-time RT-PCR were already previously shown in Chapter 2.

4.2.4 Western Blot

The procedures were already previously described in Chapter 2.

4.2.5 Pulse-chase analysis of HMGR degradation (286, 431)

Pulse-chase experiments allow studying the degradation of proteins after synthesis. To radiolabel newly synthesized proteins, the cells are incubated with radiolabelled amino acid for short periods (pulse labelling). Then the pulse is followed by a chase in which cells are further incubated with the excess amount of unlabeled counterpart of the precursor used for labelling. The radiolabelled protein of interest is analyzed by electrophoresis after isolation from other cellular proteins by immunoprecipitation. Labelling of cellular proteins is metabolically achieved by placing cells in a medium containing all components necessary for growth of cells in culture, except for one (or

two) amino acid(s) that are substituted by its radiolabelled form. The radiolabelled amino acids are transported across the plasma membrane and incorporated into newly synthesized proteins. The common means of labelling amino acids is substituting radioisotopes, such as ^{35}S, ^{3}H, or ^{14}C in place of their nonradioactive counterparts. Methionine and cysteine are conveniently labelled with ^{35}S and most often used in pulse-chase experiments.

4.2.5.1 Materials

1) Methionine / cysteine free DMEM (Cat. NO. 21013-024, Invitrogen, Paisley, UK)

2) BSA, fatty acid-free (Cat. NO. A8806, Sigma, Poole, Dorset, UK)

3) Compactin (mevastain) (Cat. NO. M2537, Sigma, Poole, Dorset, UK)

4) Mevalonate (Cat. NO. M4667, Sigma, Poole, Dorset, UK)

5) [^{35}S] Methionine (Cat. NO. AG1094, GE Healthcare, Buckinghamshire, UK)

6) L-methionine (Cat. NO. M5308, Sigma, Poole, Dorset, UK)

7) L-cysteine (Cat. NO. C7352, Sigma, Poole, Dorset, UK)

8) Rabbit anti-human HMGR polyclonal antibody (Cat. NO. 07-572, Upstate, Hampshire, UK)

9) Immunoprecipitation Starter Pack (Cat. NO. 17-6002-35, GE Healthcare, Buckinghamshire, UK)

10) RIPA buffer (Cell lysis buffer) (Cat. NO. RO278, Sigma, Poole, Dorset, UK)

11) Protease inhibition cocktail (Cat. NOP8340, Sigma, Poole, Dorset, UK)

12) GelAir dryer (Cat. NO. 165-1778, Bio-Rad, Bio-Rad, Hertfordshire, UK)

13) Model Compact X4 film processor. (Xograph Imaging Systems, Gloucestershire, UK)

4.2.5.2 Solutions

1) Medium A (serum-free medium): DMEM containing 0.2 % BSA, 100 units/ml of penicillin, and 100 μg/ml of streptomycin sulfate.

2) Medium B (starvation medium): methionine/cysteine-free DMEM containing 100 units/ml of penicillin, 100 μg/ml of streptomycin sulfate, 0.2 % BSA, 50 μmol/l of compactin and 50 μmol/l of mevalonate.

3) Medium C (chase medium): medium B containing 2 mmol/l of methionine; 2 mmol/l of cysteine).

4.2.5.3 Procedures

1) The cells in 6-well-plate were grown for 24 hours in 2 ml of medium A.

2) The cells were washed 3 times with PBS and starved for 1 hour in 1ml of medium B.

3) The cells were radio-labelled for 1 hour in 1ml of the starvation medium B containing 25 μCi/ml [^{35}S]-methionine.

4) The labelling medium was removed; the cells were washed 4 times with PBS and chased by different treatments for 0, 2, 4, 8 hours in 2 ml of medium C.

5) Following the chase, the medium was removed; the cells were washed three times with cold PBS, lysed by 1ml of lysis buffer (containing Protease Inhibition Cocktail) in the 6-well plates. Incubated for 20 minutes on ice with rocking. Transferred the supernatant (whole-cell extract) into a pre-chilled microcentrifuge tube. Further disrupted cell by vortexing for 30 seconds at highest setting and cleared by centrifuging at 14,000 rpm for 10 minutes at 4 ° C. Transferred the supernatant to a fresh tube on ice.

6) Measured protein concentration of supernatant by Bradford assay for normalisation.

7) Protein G Sepharose was washed three times with lysis buffer. Centrifuged at 12000 rpm for 20 seconds between the washes and discarding the supernatants. Prepared 50 %

slurry by mixing equal volumes of media and lysis buffer. Stored at 4 ° C and fully mixed before use.

8) Added 5-10 µl of HMGR antibody to the eppendorf tube containing the cold precleared lysate. Then incubated at 4°C for 1 hour.

9) Added 50 µl of washed Protein G slurry and incubated for 1 hour at 4°C on a rocking platform or a rotator.

10) Spun the eppendorf tube at 10,000 rpm for 30 seconds at 4 °C.

11) Carefully removed supernatant completely and washed the beads 3-5 times with 500 µl of Lysis Buffer. To minimize background, care should be given to remove the supernatant completely in these washes.

12) After the last wash, aspirated supernatant and added 50 µl of 1× Laemmli sample buffer to the bead pellet. Vortexed and heated at 90-100°C for 10 minutes.

13) Spun at 10,000 rpm for 5 minutes, collected supernatants and loaded onto the gel for SDS-PAGE.

14) Dried the gel in GelAir dryer.

15) Then the gel was exposed to X-ray film and detected by autophotograph machine.

4.2.6 Confocal microscopy observation

The procedures were already previously described in Chapter 2.

4.2.7 Co-immunoprecipitation analysis

4.2.7.1 Materials

1) Rabbit anti-human HMGR polyclonal antibody (Cat.NO. 07-572, Upstate, Hampshire, UK)

2) Rabbit anti-human SCAP polyclonal antibody (Made by our lab)

3) Rabbit anti-human Insig-1 polyclonal antibody (Cat. NO.ab54040, Abcam, Cambridge, UK)

4) Immunoprecipitation Starter Pack (Cat. NO. 17-6002-35, GE Healthcare, Buckinghamshire, UK)

5) RIPA buffer (Cat. NO. RO278, Sigma, Poole, Dorset, UK)

6) Cell lysis buffer A: 10 mmol/l HEPES-KOH at pH 7.9, 1.5 mmol/l $MgC1_2$, 10 mmol/l KCl, 0.5 mmol/l dithiothreitol (DTT), 1mmol/l sodium EDTA, 1mmol/l sodium EGTA supplemented with proteinase inhibitors (0.1 mmol/l Pefabloc, 5 μg/ml pepstatin A, 10 μg/ml leupeptin, 2 μg/ml aprotinin)

7) Cell lysis buffer B: 20 mmol/l HEPES-KOH at pH 7.9, 25 %glycerol, 0.5 mol/l NaCl, 1.5 mmol/l $MgCl_2$, 1mmol/l sodium EDTA, 1mmol/l sodium EGTA supplemented with proteinase inhibitors (0.1 mmol/l Pefabloc, 5 μg/ml pepstatin A, 10 μg/ml leupeptin, 2 μg/ml aprotinin)

DTT and proteinase inhibitors were added fresh to the buffers just before use.

8) Protease Inhibition Cocktail (Cat. NOP8340, Sigma, Poole, Dorset, UK)

9) Model Compact X4 film processor. (Xograph Imaging Systems, Gloucestershire, UK)

4.2.7.2 Procedure

Table 4.1 Binding characteristics of some immunoglobulins of primary antibodies

Species	Protein A	Protein G
Human IgG_1	++	++
Human IgG_2	++	++
Human IgG_3	–	++
Human IgG_4	++	++
Rabbit IgG	++	++
Cow IgG	+	++
Horse IgG	–	++
Goat IgG	+	++
Guinea pig IgG	++	+
Sheep IgG	–	++
Dog IgG	++	+
Pig IgG	++	++
Rat IgG*	–/+	–/+*
Mouse IgG**	+	+
Chicken IgG	–	–

Step I preparing the media

Protein A Sepharose and Protein G Sepharose were supplied preswollen in 20 % ethanol. Washed the media three times with lysis buffer. Centrifuged at 14000 rpm for 20 seconds and discarded supernatant. Mixed equal volumes of media and lysis buffer to prepare 50 % slurry. Stored at 4° C and fully mixed before use.

Step II Cell lysis (See methods in Chapter 2.)

Step III: Cell Lysate Pre-clearing (optional)

1) Transferred 50 µl of the protein G beads slurry (commercially available from several vendors) to an eppendorf tube and added 450 µl cold lysis buffer. Spun at 14000 rpm for 30 seconds and removed the lysis buffer. Washed one more time with 500 µl of cold lysis buffer. Resuspended the beads in 50 µl of cold lysis buffer.

2) Added this 50 µl of prepared protein G slurry and 500 µl of cell lysate to an eppendorf tube and incubated on ice for 30-60 minutes with gentle rotation.

3) Spun at 14000 rpm for 10 minutes at 4°C and transferred the supernatant to a fresh eppendorf. If any bead had been transferred, spun again and carefully transferred the supernatant to another fresh eppendorf tube.

Step IV: Co-immunoprecipitation

1) Added 5-10 µg of rabbit anti-human SCAP antibody or rabbit anti-human HMGR antibody to the eppendorf tube containing the cold precleared lysate.
2) Incubated at 4°C for 1 hour.
3) Added 50 µl of washed protein G slurry in prechilled lysis buffer (prepared as instructed in Preclearing Step 1 above).
4) Incubated for 1 hour at 4°C on a rocking platform or a rotator.
5) Spun the eppendorf tube at 14000 rpm for 30 seconds at 4°C.
6) Carefully removed supernatant completely and washed the beads 3-5 times with 500 µl of RIPA Buffer. To minimize background, care should be given to remove the supernatant completely in these washes.
7) After the last wash, aspirated supernatant and added 50 µl of 1× Laemmli sample buffer to bead pellet. Vortexed and heated to 90-100°C for 10 minutes.
8) Spun at 14000 rpm for 5 minutes, collected supernatant and loaded onto the gel.
9) Followed manufacturer's instructions for SDS-PAGE.
10) Followed staining procedures of Western Blot in Chapter 2. Precipitated proteins by anti-SCAP and anti-HMGR antibody were checked by rabbit anti-human Insig-1 antibody. The bands were detected by ECL advanced system and relative densities of protein bands were analysed by Bio-Rad Quantity One software.

4.3 Results

4.3.1 The effect of Sirolimus on cholesterol synthesis in VSMCs

To further explore potential mechanisms of Sirolimus in anti-atherosclerosis, we investigated the effect of Sirolimus on cholesterol biosynthesis in VSMCs with or without IL-1β. As shown in Fig 4.1, IL-1β increased cholesterol biosynthesis in VSMCs. However, Sirolimus inhibited cholesterol biosynthesis induced by IL-1β. This suggests that Sirolimus decreases intracellular cholesterol level induced by inflammatory cytokine through the cholesterol biosynthesis pathway.

4.3.2 The effect of Sirolimus on the expression of HMGR and SCAP translocation from the ER to the Golgi in VSMCs

Next, we checked the effect of Sirolimus on HMGR expression in VSMCs. Our results showed that Sirolimus inhibited the gene and protein expression of HMGR in VSMCs in the absence or presence of IL-1β (Fig 4.2, Fig 4.3a and Fig 4.3b). Using confocal immunofluorescent staining, we further investigated SCAP translocation escorting SREBP-2 from the ER to the Golgi in VSMCs. SCAP translocation was increased by cholesterol depletion and decreased by LDL loading in VSMCs. Interestingly, IL-1β increased SCAP accumulation even in the present of LDL loading in the Golgi. However, Sirolimus attenuated SCAP accumulation in the Golgi induced by IL-1β (Fig 4.4). Further analysis showed that IL-1β increased the mRNA expression of SCAP and SREBP-2 and decreased the mRNA expression of Insig-1 in VSMCs. Sirolimus significantly inhibited the mRNA expression of SCAP and SREBP-2 and increased the mRNA expression of Insig-1 in VSMCs (Fig 4.5).

4.3.3 The effect of Sirolimus on the degradation of HMGR in VSMCs.

The regulation of HMGR activity at post-transcriptional level is via protein degradation, which is modulated by Insig-1. Therefore, we further checked the effect of Sirolimus on

the degradation of HMGR in VSMCs by pulse-chase analysis. Results showed that Sirolimus accelerated the degradation of HMGR compared to the control (Fig 4.6a and Fig 4.6b).

4.3.4 The effects of Sirolimus on the protein interaction of Insig-1 with SCAP and HMGR inVSMCs

By co-immunoprecipitation we further observed protein interaction by measuring the protein levels of Insig-1/SCAP or Insig-1/ HMGR complexes. As shown in Fig 4.7a and Fig 4.7b, Sirolimus increased levels of Insig-1/SCAP and Insig-1/ HMGR in these complexes, suggesting that Sirolimus potentiates the binding of Insig-1 to SCAP and HMGR in VSMCs under inflammatory stress.

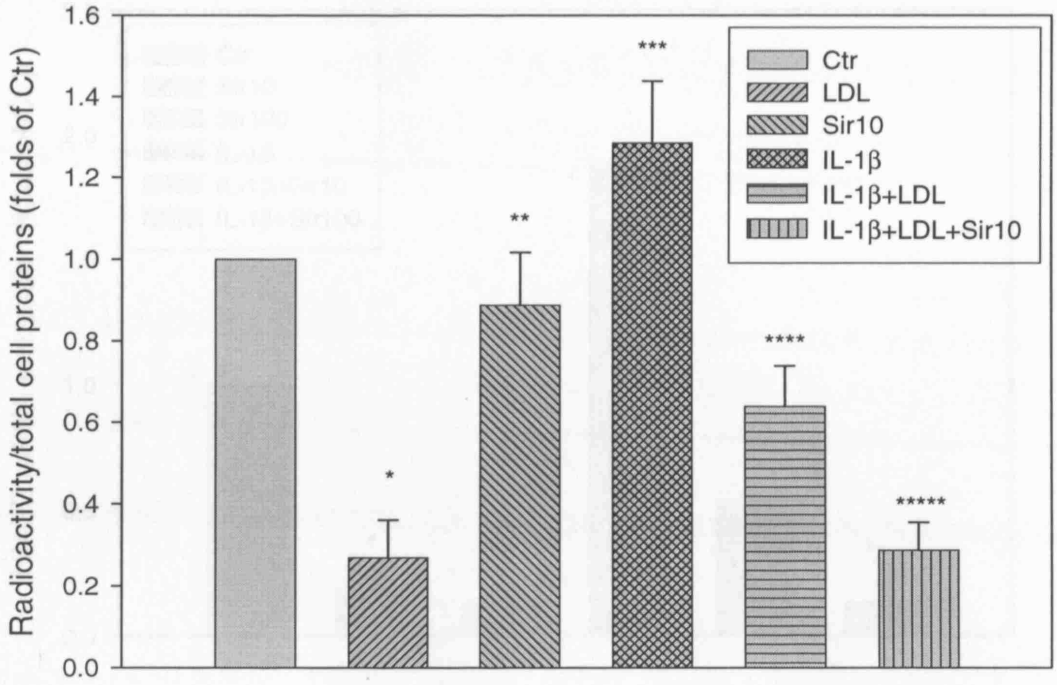

Fig 4.1 The effect of Sirolimus on cholesterol biosynthesis in VSMCs. VSMCs were incubated in DMEM/F12 medium containing 5% lipid-depletion FBS in the absence (control, Ctr) or presence of native LDL 200 μg/ml (LDL) or Sirolimus 10 ng/ml (Sir10) or 5 ng/ml of IL-1β (IL-1β) or 5 ng/ml of IL-1β plus native LDL 200 μg/ml (IL-1β+LDL) or 5 ng/ml of IL-1β plus native LDL 200 μg/ml and 10 ng/ml of Sirolimus (IL-1β+LDL+Sir10) for 24 hours. Cholesterol biosynthesis was determined by incorporated [^{14}C] radioactivity as described in the section of Methods. The radioactivity of every group was normalized by the amount of total cell protein. The concentration of total cell protein was examined by Lowry assay. Results represented the Mean ± SD from six wells, expressed as folds of the control. * p <0.001 *vs* control, ** p <0.05 *vs* control, *** p <0.01 *vs* control, **** p<0.01 *vs* LDL, ***** p<0.01 *vs* IL-1β+LDL.

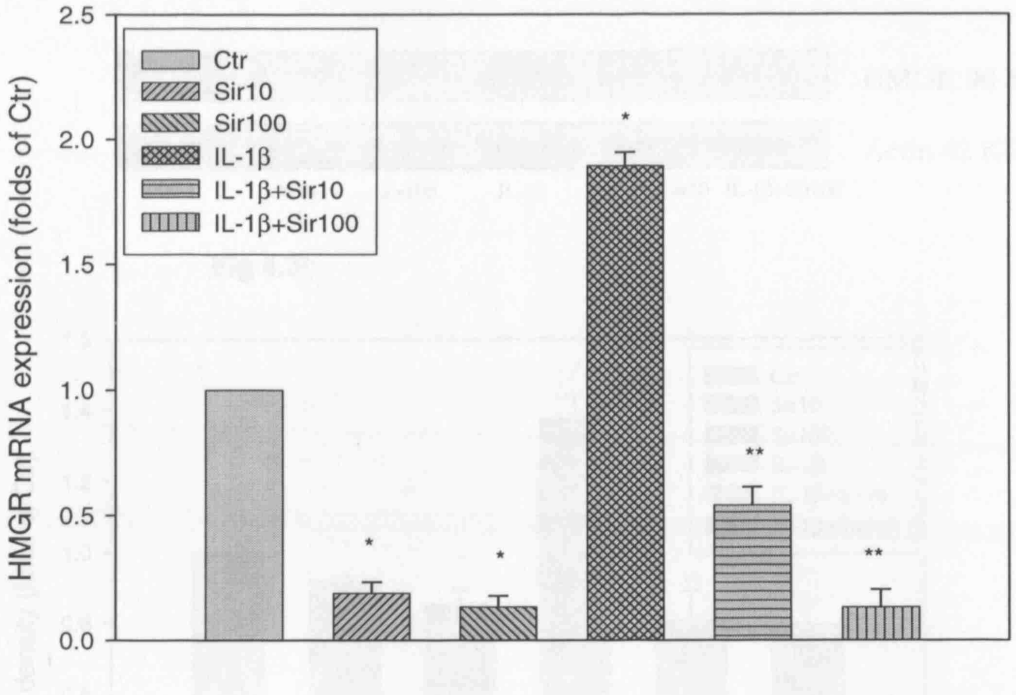

Fig 4.2 The effect of Sirolimus on the mRNA expression of HMGR in VSMCs. VSMCs were incubated in serum-free medium (control, Ctr) or serum-free medium with 10-100 ng/ml of Sirolimus (Sir10, Sir 100) or 5 ng/ml of IL-1β (IL-1β) or 5 ng/ml of IL-1β plus 10-100 ng/ml of Sirolimus (IL-1β+Sir10, IL-1β+Sir100) for 24 hours. The mRNA expression of HMGR was determined following the ΔΔCt protocol for real-time RT-PCR as described in the section of Methods. β-actin served as the housekeeping gene. Results represented the Mean ± SD from four experiments. * p <0.001 *vs* control, ** p <0.001 *vs* IL-1β group.

Fig 4.3a

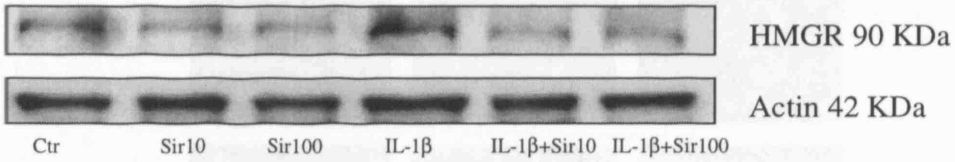

Fig 4.3b

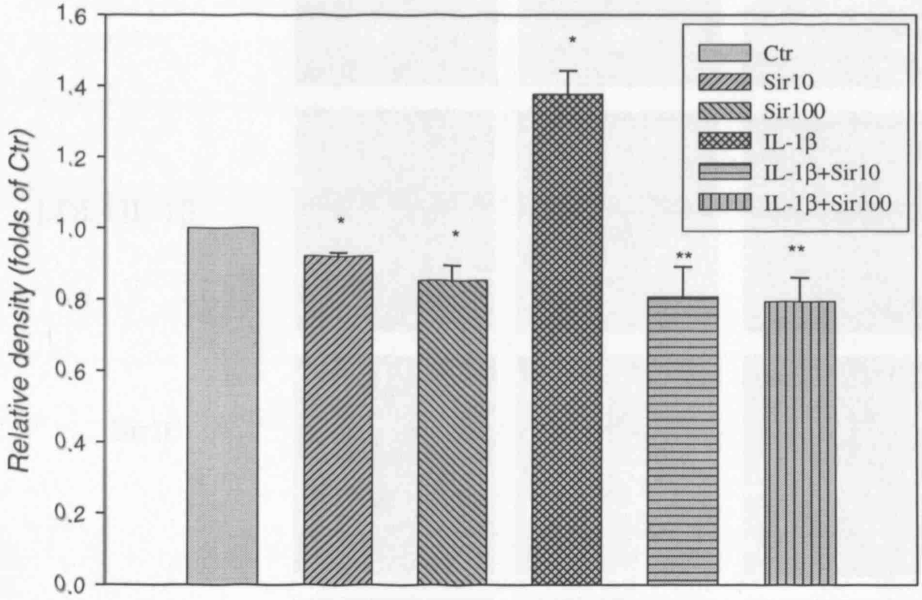

Fig 4.3a & 4.3b The effect of Sirolimus on the protein expression of HMGR in VSMCs. VSMCs were incubated in serum-free medium (control, Ctr) or serum-free medium with 10-100 ng/ml of Sirolimus (Sir10, Sir 100) or 5 ng/ml of IL-1β (IL-1β) or 5 ng/ml of IL-1β plus 10-100 ng/ml of Sirolimus (IL-1β+Sir10, IL-1β+Sir100) for 24 hours. The protein levels of HMGR were examined by Western Blot. The histograms represented Mean ± SD of the densitometric scans of HMGR protein bands from four experiments, normalised by comparison with actin, and expressed as a percentage of the control. * p <0.001 *vs* control, ** p <0.001 *vs* IL-1β group.

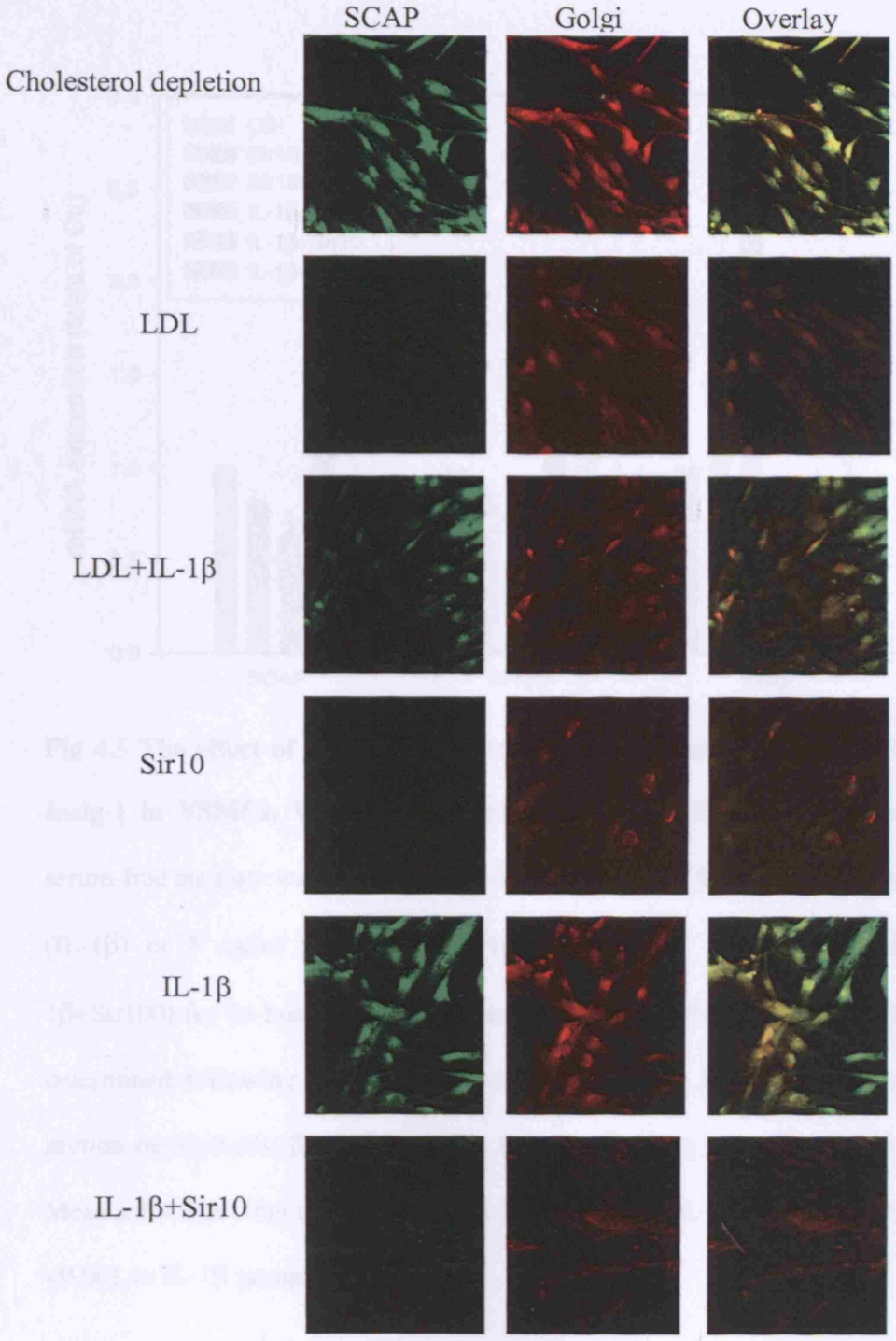

Fig 4.4 The effect of Sirolimus on the translocation of SCAP between ER and Golgi in VSMCs. VSMCs cultured in chamber slides were washed, fixed, and permeabilized. The cells were then incubated with rabbit anti-human SCAP antibody (1:200 dilution) and an anti-human Golgi antibody (mouse anti-human Golgi-97, 1:200 dilution), followed by a secondary fluorescent antibodies (goat anti-rabbit Fluor 488 for SCAP and goat anti-mouse Fluor 594 for Golgi). After washing, the cells were examined by confocal microscopy.

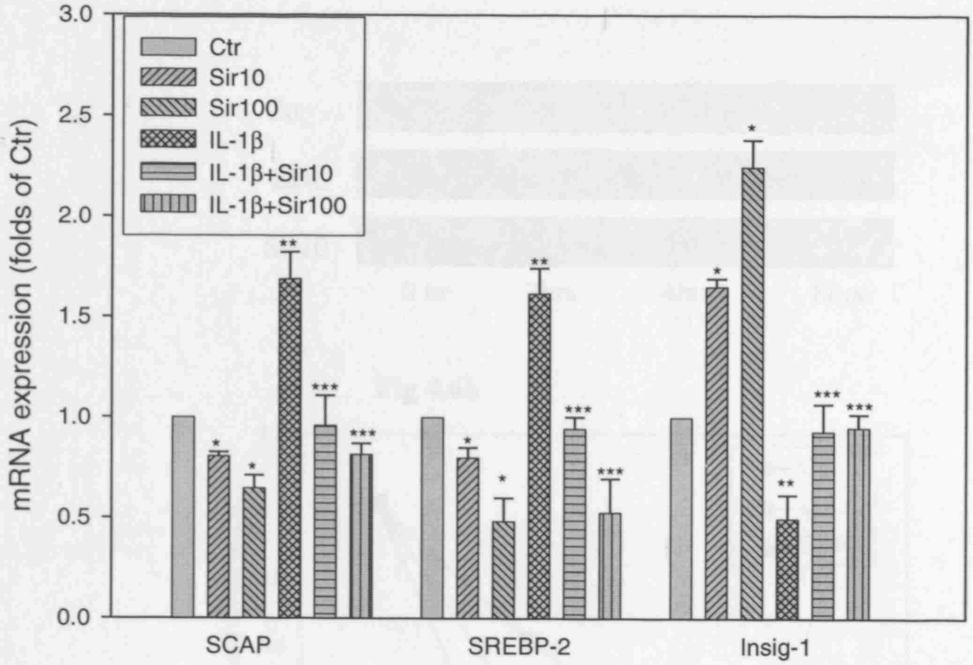

Fig 4.5 The effect of Sirolimus on the mRNA expression of SCAP, SREBP-2 and Insig-1 in VSMCs. VSMCs were incubated in serum-free medium (control, Ctr) or serum-free medium with 10-100 ng/ml of Sirolimus (Sir10, Sir 100) or 5 ng/ml of IL-1β (IL-1β) or 5 ng/ml of IL-1β plus 10-100 ng/ml of Sirolimus (IL-1β+Sir10, IL-1β+Sir100) for 24 hours. The mRNA expression of SCAP, SREBP-2, and Insig-1 was determined following the ΔΔCt protocol for real-time RT-PCR as described in the section of Methods. β-actin served as the housekeeping gene. Results represented the Mean ± SD from four experiments. * p <0.001 *vs* control, ** p <0.001 *vs* control, *** p <0.001 *vs* IL-1β group.

Fig 4.6a

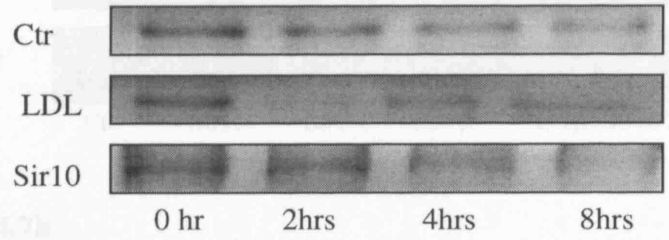

Fig 4.6b

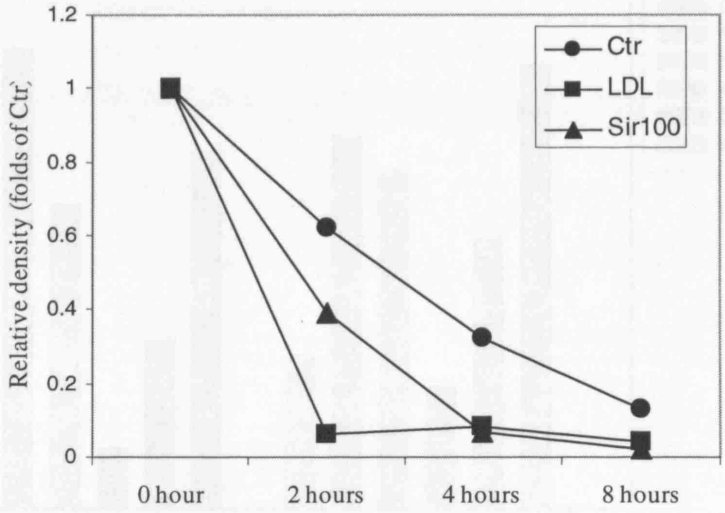

Fig 4.6a & 4.6b The effect of Sirolimus on the degradation of HMGR in VSMCs. VSMCs were starved for 1 hour in 1ml of Medium B. Then the cells were radio-labelled for 1 hour in 1ml of Medium B containing 25 μCi/ml [^{35}S]-methionine. Cells were then chased in medium C in the absence or presence of 200 μg/ml of native LDL or 10 ng/ml of Sirolimus for 0, 2, 4, 8 hours. After the indicated chase period, cells were harvested, lysed, and subjected to immunoprecipitation with polyclonal anti-HMGR antibody. Identical amounts of immunoprecipitates were subjected to SDS-PAGE. Gels were then dried and exposed to the films for one week. The bands of target proteins were scanned by Gel Documentation System and the relative density of bands were analysed by Bio-Rad Quantity-One software.

Fig 4.7a

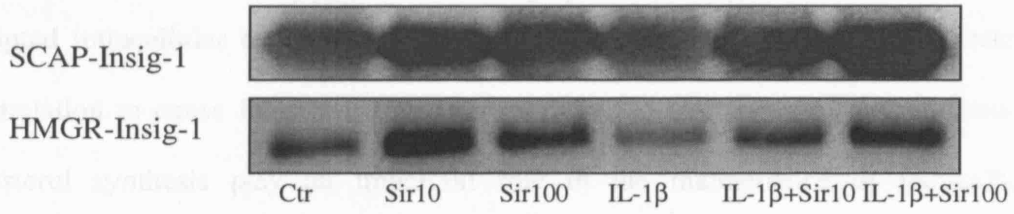

Fig 4.7b

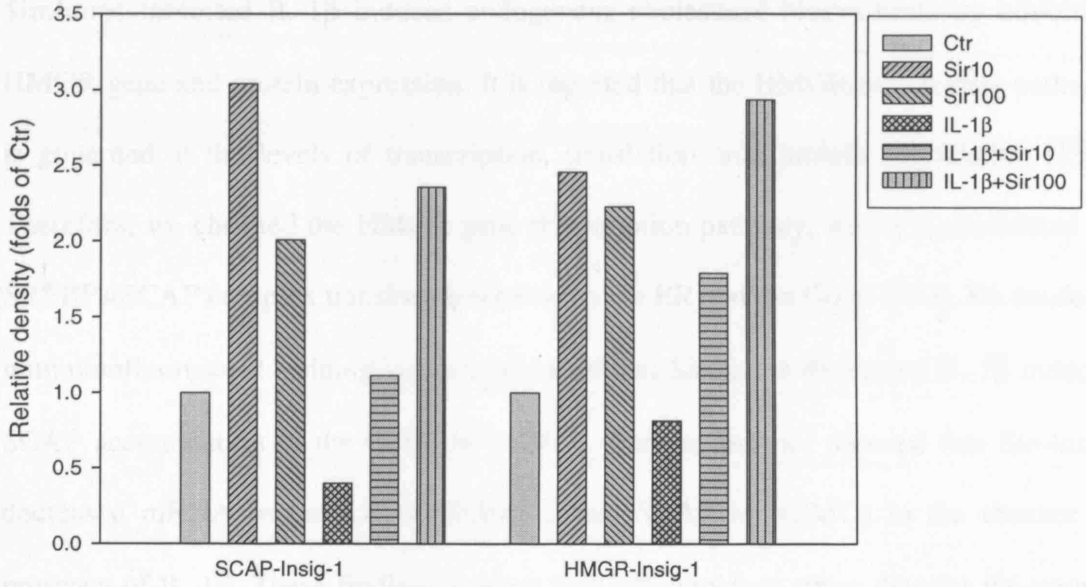

Fig 4.7a & 4.7b The effects of Sirolimus on the protein interaction of Insig-1 with SCAP and HMGR in VSMCs. VSMCs were incubated in serum-free medium (control, Ctr) or serum-free medium with 10, 100 ng/ml of Sirolimus (Sir10, Sir 100) or 5 ng/ml of IL-1β (IL-1β) or 5 ng/ml of IL-1β plus 10, 100 ng/ml of Sirolimus (IL-1β+Sir10, IL-1β+Sir100) for 24 hours. The protein interactions of Insig-1 with SCAP and Insig-1 with HMGR were then checked by co-immunoprecipitation analysis. The relative densities of protein bands were analysed by Bio-Rad Quantity One Software.

4.4 Discussion

Disrupted intracellular cholesterol homeostasis permits unlimited cellular cholesterol accumulation to cause foam cell formation (376, 422). The feedback mechanisms of cholesterol synthesis play an important role in the maintenance of intracellular cholesterol homeostasis (137, 432). Our results demonstrated that IL-1β significantly increased cholesterol biosynthesis even in the presence of LDL loading. However Sirolimus inhibited IL-1β induced endogenous cholesterol biosynthesis by inhibiting HMGR gene and protein expression. It is reported that the HMGR/mevalonate pathway is governed at the levels of transcription, translation, and protein degradation (137). Therefore, we checked the HMGR gene transcription pathway, which is modulated by SREBPs/SCAP complex translocation between the ER and the Golgi (433). By confocal inmmunofluorescent staining we demonstrated that Sirolimus decreased IL-1β induced SCAP accumulation in the Golgi in VSMCs. Further analysis showed that Sirolimus decreased mRNA expression of SREBP-2 and SCAP in VSMCs in the absence or presence of IL-1β. These findings suggest that inflammatory stress disrupts the normal feedback regulation of HMGR to induce endogenous cholesterol accumulation in cells. However, Sirolimus ameliorates the dysregulation of HMGR induced by inflammatory cytokines.

Insigs are key regulators for the activation of HMGR gene transcription binding with SCAP to regulate the translocation of SREBPs/SCAP complex between the ER and the Golgi (434). Our results showed that IL-1β decreased Insig-1 mRNA expression in VSMCs. However, Sirolimus overrode this effect to increase Insig-1 mRNA expression, resulting in decreased the ratio of HMGR/ Insig-1 mRNA expression. Furthermore co-immunoprecipitation analysis demonstrated that Sirolimus potentiated the protein binding of Insig-1 to SCAP in VSMCs inhibited by IL-1β. These suggest that Insig-1

plays a central role in the down-regulation of HMGR gene transcription mediated by Sirolimus.

It has been demonstrated that HMGR protein is rapidly degraded in response to sterols and further enhanced by specific non-sterol intermediates of the mevalonate pathway. This process requires Insigs (434). Insigs regulate HMGR protein degradation by binding or unbinding to HMGR in response to sterol overload or scarcity (286, 287). Our results showed that Sirolimus accelerated HMGR degradation in VSMCs compared to controls, which was mainly through increasing the binding of Insig-1 to HMGR.

Taken together, our results suggest that inflammatory stress increases intracellular cholesterol synthesis and foam cell formation by disrupting the normal feedback regulation of HMGR. However, Sirolimus ameliorates dysregulation of HMGR induced by inflammatory stress in VSMCs through: i) inhibiting gene and protein expression of HMGR; ii) accelerating HMGR degradation. These findings may provide an explanation for the potentially anti-atherosclerotic mechanisms of Sirolimus.

CHAPTER 5. THE ANTI-ATHEROSCLEROTIC EFFECTS OF SIROLIMUS ON HUMAN MACROPHAGES

5.1 Introduction

Atherosclerosis is the final result of a cascade of events involving cells in the vascular wall, circulating cells, and various bioactive molecules within and outside the vasculature. Monocyte adhesion, transendothelial migration, transformation into activated macrophages, cholesterol accumulation and foam cell formation are critical processes in atherogenesis. Macrophages play key roles both in the initiation and progression of atherosclerosis. Macrophages are able to produce ROS in respiratory bursts through nicotinamide adenine dinucleotide phosphate (NADPH)-oxidase; ROS has been implicated in inflammatory responses in macrophages via its effects on the production of inflammatory cytokines. Macrophages also contribute to the formation of necrotic core which may affect the stability of atherosclerotic lesion.

A pathological hallmark of atherosclerosis is excessive accumulation of cholesterol by macrophages leading to their transformation into foam cells (6). Cholesterol homeostasis in macrophages is of primary importance at an early stage in the initiation of atherosclerosis, as dysregulation of the balance of cholesterol influx and cholesterol efflux will lead to excessive accumulation of cholesterol in macrophages and their transformation into foam cells.

Maintenance of cholesterol homeostasis is a challenge for all peripheral cells, and is particularly important in macrophages. Cholesterol may enter macrophages via several different pathways involving rapid receptor-mediated coated-pit endocytosis. Macrophages express high levels of scavenger receptors, which bind and internalize oxLDLs. Furthermore, macrophages also contain several other types of binding sites that are involved in the accumulation of unmodified lipoproteins and lipoprotein remnants, including the LDLr, LRP, VLDLr, and proteoglycans. Kruth *et al* (435) demonstrated a very significant non-receptor mediated fluid phase endocytosis for LDL accumulation in macrophages. As macrophages are incapable of limiting the uptake of

lipids via their wide variety of uptake mechanisms, they depend mainly on cholesterol efflux pathways to maintain cellular lipid homeostasis. A key transporter involved in the efflux of cholesterol and phospholipids from macrophages is ABCA1 (436). ABCA1 is a member of the ABC transporter superfamily that utilizes ATP as a source of energy to transport various molecules across membranes (437). The ABCA1 gene consists of 50 exons spanning 149 kb and encodes a protein that contains 2261 amino acids (301). It is a full transporter, consisting of two 6-helix transmembrane domains that serve as a pathway for the translocation of substrates across membranes and two nucleotide-binding domains that bind ATP and provide the energy for transport. ABCA1 mediates the transport of cholesterol and phospholipids to lipid-free apolipoproteins such as apoA-I (438). LXRs and PPARs are important transcription factors, which up-regulate expression of ABCA1, providing an amplification mechanism for ABCA1 expression (313). The PPARs-LXRs-ABCA1 pathway represents a powerful means of cholesterol efflux from macrophages and therefore could play a significant role in influencing the progression of atherosclerotic plaques (439).

In addition to ABCA1, macrophages also express ABCG1, which is induced during cholesterol uptake in macrophages (440, 441) and is activated via LXR (310, 442). ABCG1 is a half transporter with a single 6-helix transmembrane domain and a single nucleotide domain that needs to form either homodimer or heterodimer with another ABC-transporter to be functional. In contrast to ABCA1, ABCG1 facilitates cellular cholesterol and phospholipid efflux from macrophages to mature HDL, but not to lipid-free apolipoproteins (328, 329, 443). ABCA1-mediated cholesterol efflux, however, transforms lipid-free apoA-I into an efficient substrate for ABCG1-dependent efflux, suggesting that ABCA1 and ABCG1 may synergize to mediate cholesterol efflux to apoA-I. Thus, ABCG1 in macrophages may also play an important role in the development of atherosclerotic lesion.

Our previous studies in human VSMCs demonstrated that Sirolimus inhibits foam cell formation by ameliorating intracellular cholesterol homeostasis (428). However the anti-atherosclerotic effect of Sirolimus on macrophages is unknown. Therefore, the present study was undertaken to investigate the effect of Sirolimus on cholesterol homeostasis in human monocyte-derived macrophages under inflammatory stress.

5.2 Materials and methods

5.2.1 Isolation and culture of human monocyte-derived macrophages

5.2.1.1 Materials

1) Human buffy coats (National Blood Services, Colindale, North London, UK)

2) RosetteSep™ Human Monocyte Enrichment Cocktail (Cat NO. 15068, StemCell Technologies Inc, London, UK)

3) Lympholyte-H 500 ml (CL5020, Cedarlane Laboratories Ltd, Tyne & Wear, UK)

Other materials used for human macrophages have been fully listed in Chapter 3.

4) Human serum, from human male AB plasma, sterile-filtered (For cell culture, Cat. NO. H4522, Sigma, Poole, Dorset, UK)

5) Fluorescein (FITC) conjugated mouse anti-human CD14 monoclonal antibody (Cat. NO. ab16174, Abcam, Cambridge, UK)

5.2.1.2 Procedures

1) Human buffy coats were kindly provided from National Blood Services in Colindale of North London.

2) Added RosetteSep™ Human Monocyte Enrichment Cocktail at 50 µl/ml of buffy coats (e.g. for 2 ml of buffy coats, add 100 µl of cocktail).

3) Incubated 20 minutes at room temperature.

4) Diluted samples with an equal volume of PBS containing 2 % FBS.

5) Added 15 ml Lympholyte-H into sufficient 50 ml Falcon tubes.

6) Gently layered 30 ml of the diluted buffy coats onto the lympholyte-H by trickling the blood slowly down the side of the tube; divided it equally between the tubes (Be careful, don't mix sample and Lympholyte-H together).

7) Centrifuged for 25 minutes at 2500 rpm 20 ^{o} C, braked off.

8) Using a Pasteur or serological pipette removed the white cell layers from the interface of the cushion from each tube and pooled into several 50ml tubes.

9) Added at least 2-3 volumes of PBS and then centrifuge.

10) Aspirated off the supernatants with a serological pipette and re-suspended the cells in a final volume of 10 ml of PBS or appropriated medium in each tube ready for counting the cells.

10) The mononuclear fraction was resuspended in DMEM/F12 containing 10 % human AB serum, 2 mmol/l L-glutamine, 100 units/ml of penicillin and 100 μg/ml of streptomycin. Monocytes were seeded at a density of $1.5\text{-}2\times10^{6}$ cells/ml and were allowed to adhere for 3 hours at 37 °C in 75-cm^2 flasks. Then flasks were gently swirled to resuspend non-adherent cells, medium was removed and replaced by fresh medium.

5.2.2 Lipoprotein preparation

Fresh plasma was collected from healthy human volunteers. LDL was isolated by sequential density gradient ultracentrifugation as previously described in Chapter 2.

5.2.3 Morphological examination

Human monocyte-derived macrophages were seeded and cultured in chamber slides (Becton Dickinson Labware, USA) for 10 days. After that, the medium was replaced by serum-free DMEM/F12 medium for 24 hours. The cells were then treated by serum-free DMEM/F12 medium with acetylated LDL (acLDL) in the absence or presence of 10 ng/ml of Sirolimus, or 5 ng/ml of IL-1β, or 5 ng/ml of IL-1β plus 10 ng/ml of Sirolimus for 24 hours. The lipid accumulation was checked by Oil Red O staining as previously described in Chapter 2.

5.2.4 Lactate dehydrogenase release for cytotoxicity assay

The procedures were already previously described in Chapter 2.

5.2.5 Quantitative assay of intracellular cholesterol

The procedures were already previously described in Chapter 2.

5.2.6 Intracellular cholesterol efflux

The procedures were already previously described in Chapter 2.

5.2.7 Immunohistochemistry analysis

ABC peroxidase system is particularly important in the localization of antigens presented in low amounts or in cases where the cost of primary antibodies is significant. The increased sensitivity also provides an option to substantially reduce staining times. Avidin is a 68,000 molecular weight glycoprotein with an extraordinarily high affinity for the small molecular weight vitamin, biotin. Because this affinity is over one million times higher than that of antibody for most antigens, the binding of avidin to biotin

(unlike antibody-antigen interactions) is essentially irreversible. In addition to this high affinity, the Biotin/Avidin System can be effectively exploited because avidin has four binding sites for biotin and most proteins (including antibodies and enzymes) can be conjugated with several molecules of biotin. These aspects provide the potential for macromolecular complexes to be formed between avidin and biotinylated enzymes. An immunoperoxidase procedure based on these properties was devised for localizing a variety of histologically significant antigens and other markers. This technique employs unlabeled primary antibody, followed by biotinylated secondary antibody and then a preformed avidin and biotinylated horseradish peroxidase macromolecular complex. This has been termed the ABC technique.

5.2.7.1 Materials

1) Primary antibody: Mouse anti-human CD68 monoclonal antibody (Cat.NO.ab955, Abcam, Cambridge, UK); Rabbit anti-human LXRα polyclonal antibody (Cat.NO.ab3585, Abcam, Cambridge, UK); Rabbit anti-human PPARα polyclonal antibody (Cat.NO.ab24509, Abcam, Cambridge, UK); Mouse anti-human PPARγ monoclonal antibody (Cat.NO.sc-7273, Santa Cruz Biotechnology, Inc, UK);

2) Biotinylated secondary antibody: Anti-rabbit IgG (Cat. No. BA-1000, Vector Laboratories, Bath, UK); Anti-mouse IgG (Cat.NO. BA-2000, Vector Laboratories, Bath, UK)

3) Blocking serum: Normal goat serum (Cat. No. S-1000, Vector Laboratories, Bath, UK)

4) Reagent A and B (Cat. No. PK-6102, Vector Laboratories, Bath, UK).

5) Endogenous avidin + Biotin blocking system: Avidin blocking and Biotin blocking (Cat. No. ab3387, Abcam, Cambridge, UK)

6) Peroxidase substrate kit tetrahydrochloride (DAB) (Cat. No. SK-4100, Vector Laboratories, Bath, UK).

5.2.7.2 Working solution preparation

A number of different buffers were used in the VECTASTAIN® ABC system. The VECTASTAIN® working solutions were prepared as follows:

1) Blocking serum (Normal Serum): added three drops (150 µl) of stock (yellow label) to 10 ml of buffer in mixing bottle (yellow label). The preferred serum for blocking was prepared from the same species in which the biotinylated secondary antibody was made.

2) Biotinylated Antibody: added three drops (150 µl) of normal blocking serum stock (yellow label) to 10 ml buffer in mixing bottle and then added one drop (50 µl) of biotinylated antibody stock (blue label).

3) VECTASTAIN® ABC Reagent: added exactly two drops of Reagent A (grey label) to 5 ml of buffer in the ABC Reagent large mixing bottle. Then added exactly two drops of REAGENT B (grey label) to the same mixing bottle, mixed immediately, and allowed VECTASTAIN® ABC Reagent to stand for about 30 minutes before use.

5.2.7.3 Preparation of DAB immunohistochemical Staining

Immediately before use, prepared the substrate solution as follows:

1) To 5.0 ml of dH_2O, added 2 drops of Buffer Stock Solution and mixed well.

2) Added 4 drops of DAB Stock Solution and mixed well.

3) Added 2 drops of the Hydrogen Peroxide Solution and mixed well.

4) If a grey-black stain was desired, added 2 drops of the Nickel Solution and mixed well. Incubated tissue sections with the substrate at room temperature until suitable staining develops. Developing time should be determined by the investigator, generally

2-10 minutes providing good staining intensity. Washed the sections for 5 minutes in water. Counterstained and mounted.

5.2.7.4 Standard ABC (Avidin Biotin Complex) procedures

The macrophages cultured in chamber slides were processed for immunohistochemical staining.

1) Fixed 30 minutes using 4 % paraformaldehyde/PBS.

2) Washed 2 times with PBS.

3) Incubated samples with Peroxidase Blocking Reagent (Peroxidase Blocking Reagent: 0.3 % H_2O_2 in either methanol or water) for 10 minutes (If quenching of endogenous peroxidase activity was required, otherwise, omitted).

4) Rinsed with PBS (or TBS buffer) for 5 minutes. Washed sample gently since hydrogen peroxide might loosen tissues from the slide.

5) Incubated samples with Serum Blocking Reagents (for anti-mouse second antibody using normal horse serum; for anti-rabbit second antibody using normal goat serum) for 15 minutes. Drained slides and carefully wiped off excess Blocking Reagent before going to the next step.

6) Incubated sample with avidin Solution for 15 minutes at room temperature.

7) Rinsed with PBS (or TBS buffer) for 5 minutes.

8) Incubated samples with the biotin Solution for 15 minutes.

9) Rinsed with PBS (or TBS buffer) for 5 minutes.

10) Incubated samples for 30 minutes with primary antiserum diluted in buffer.

11) Rinsed with PBS (or TBS buffer) for 5 minutes.

12) Incubated sections for 30 minutes with diluted biotinylated secondary antibody solution.

13) Rinsed with PBS (or TBS buffer) for 5 minutes.

14) Incubated sections for 30 minutes with VECTASTAIN® ABC Reagent.

15) Rinsed with PBS (or TBS buffer) for 5 minutes.

16) Incubated sections in peroxidase substrate solution until desired stain intensity developed.

17) Rinsed samples in tap water.

18) Counterstained with Mayer's Haematoxylin Solution for 30 seconds if desired.

5.2.8 Real-time RT–PCR

The procedures and the Taqman primers for real-time RT-PCR were already previously shown in Chapter 2.

5.3 Results

5.3.1 Morphological observation for isolation, identification and induction of monocytes

Isolated monocytes were induced into macrophages after incubating for 10-12 days, (Fig 5.1a & 5.1b). CD14 and CD68 are specific cell markers of human monocytes and were checked by immunofluorescent staining and immunochemical staining respectively. Monocytes showed positive expression of CD14 and CD68 (Fig 5.2a and Fig 5.2b).

5.3.2 The observation of cytotoxic effect in Sirolimus treated macrophages

In order to exclude a cytotoxic effect of Sirolimus, the release of LDH in the supernatants in macrophages was checked by LDH assay. As shown in Fig 5.3, there was no difference between Sirolimus treated groups and controls. It was considered safe

to investigate the anti-atherosclerotic effect of Sirolimus on macrophages at a dose of 0-100 ng/ml.

5.3.3 The effect of Sirolimus on lipid accumulation in macrophages induced by inflammatory cytokines

Using Oil Red O staining, we checked the effect of Sirolimus on cholesterol accumulation in macrophages loaded with acLDL in the presence or absence of IL-1β. We found that IL-1β significantly increased lipid droplet accumulation in macrophages (Fig 5.4a, C). However, Sirolimus reduced lipid droplet accumulation in macrophages caused by IL-1β (Fig 5.4a, D). Quantitative assay of intracellular cholesterol confirmed that Sirolimus reduced cholesterol ester accumulation induced by IL-1β in macrophages. It suggests that Sirolimus provides a protective effect for cholesterol accumulation in macrophages under inflammatory stress (Fig 5.4b).

5.3.4 Sirolimus increases cholesterol efflux in macrophages by up-regulating ABCA1 and ABCG1 mediated pathways

To explore potential mechanisms of the inhibition of lipid accumulation by Sirolimus, we firstly checked gene expression of some molecules involving lipoprotein receptor mediated pathways (VLDLr, LDLr, Scavenger receptor A-I, CD36, SREBP2, and SCAP). However, there was no difference between Sirolimus-treated groups and controls. Therefore, we further examined the effects of Sirolimus on cholesterol efflux under inflammatory stress. Results showed that IL-1β reduced apoA-I mediated cholesterol efflux from cholesterol loaded macrophages. Interestingly, Sirolimus overrode the suppression of cholesterol efflux induced by IL-1β (Fig 5.5). We further examined the effect of Sirolimus on ABCA1 mediated pathway in cholesterol loaded macrophages. Sirolimus significantly increased the gene expression of ABCA1, LXRα, PPARα, and PPARγ in cholesterol-loaded macrophages even in the presence of IL-1β

(Fig 5.6a & Fig 5.6b). Sirolimus also significantly increased ABCG1 gene expression in cholesterol loaded macrophages in the absence or presence of IL-1β (Fig 5.6c). Furthermore, immunochemical staining showed that Sirolimus increased LXRα, PPARα and PPARγ protein expression in macrophages in the presence of IL-β (Fig 5.7a, Fig 5.7b, and Fig 5.7c) in accordance with the results at the mRNA level. These results suggest that Sirolimus up-regulates cholesterol efflux pathways in macrophages under inflammatory stress.

Fig 5.1a Cell culture of monocytes (The first day)

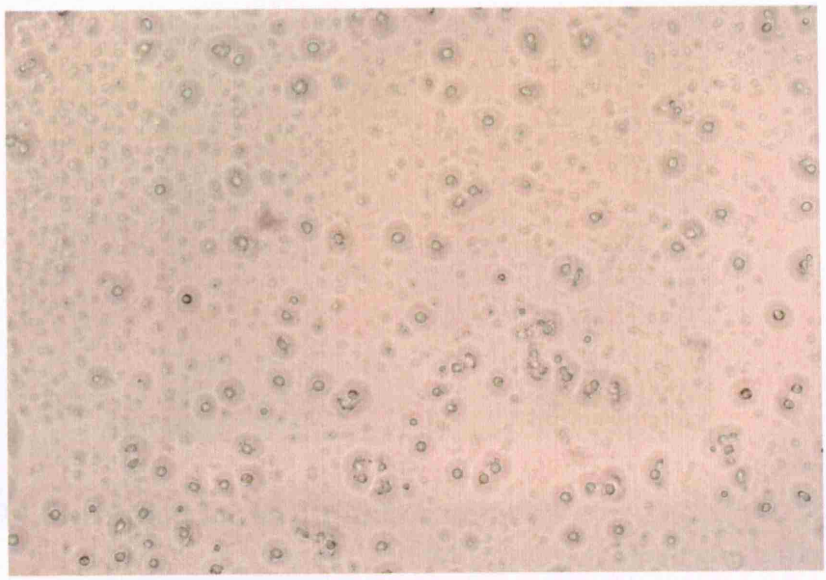

Fig 5.1b Cell culture of monocytes (The 10th day)

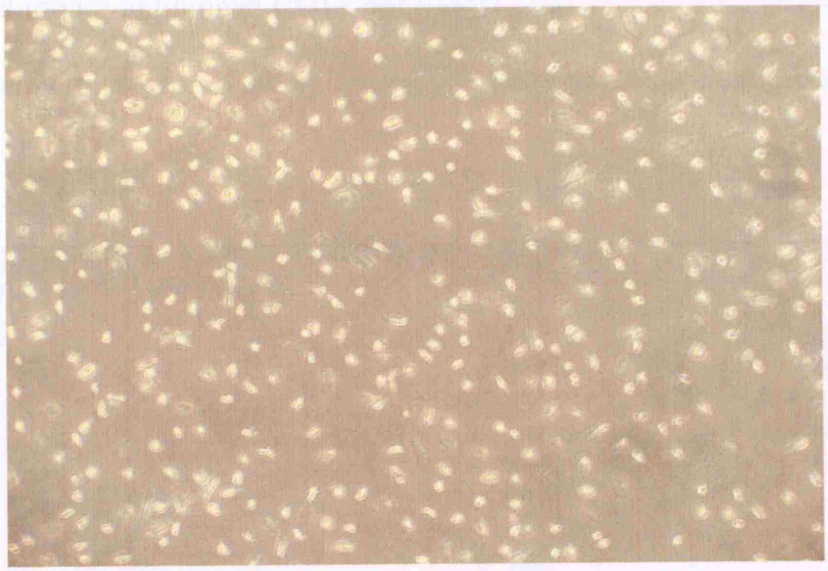

Fig 5.1a & 5.1b Morphological observation for isolation and induction of monocytes. Human peripheral blood monocytes were suspended in DMEM/F12 containing 10 % human AB serum. After the incubation of 10-12 days, Monocytes were induced to macrophages. Fig 5.1a & 5.1b showed the morphological change of human monocytes suspended in the medium.

Fig 5.2a

Fig 5.2a CD14 expression for identification of monocytes

Human monocyte marker CD14 was checked by immunofluorescent staining using FITC labelled mouse antihuman CD14 polyclonal antibody. The signals were captured by laser scanning microscopy (200×). Monocytes showed positive expression of CD14.

Fig 5.2b

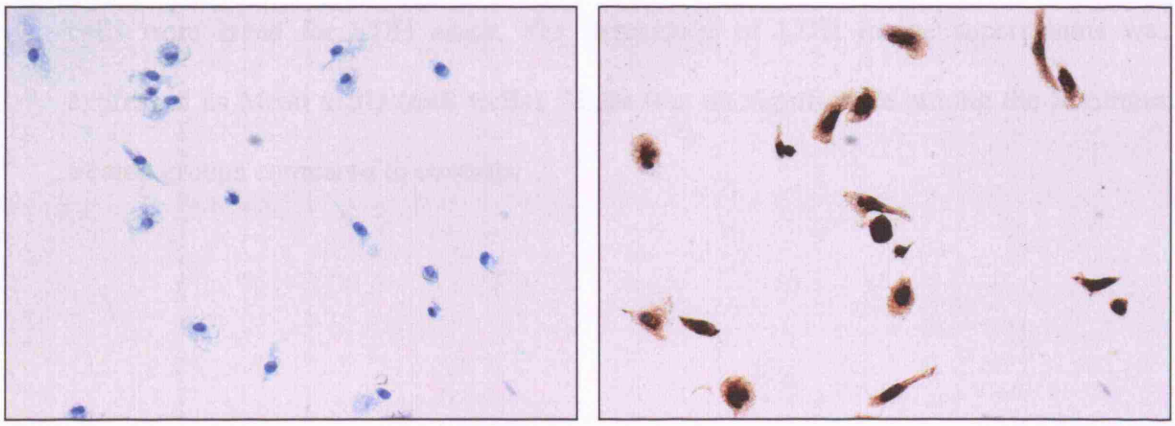

Negative Control CD68 expression

Fig 5.2b CD68 expression for the identification of monocytes. CD68 expression in human monocytes was checked by immunochemical staining using mouse antihuman CD68 monoclonal antibody. The results showed positive expression of CD68 in monocytes with brown colour stained by DAB (200x).

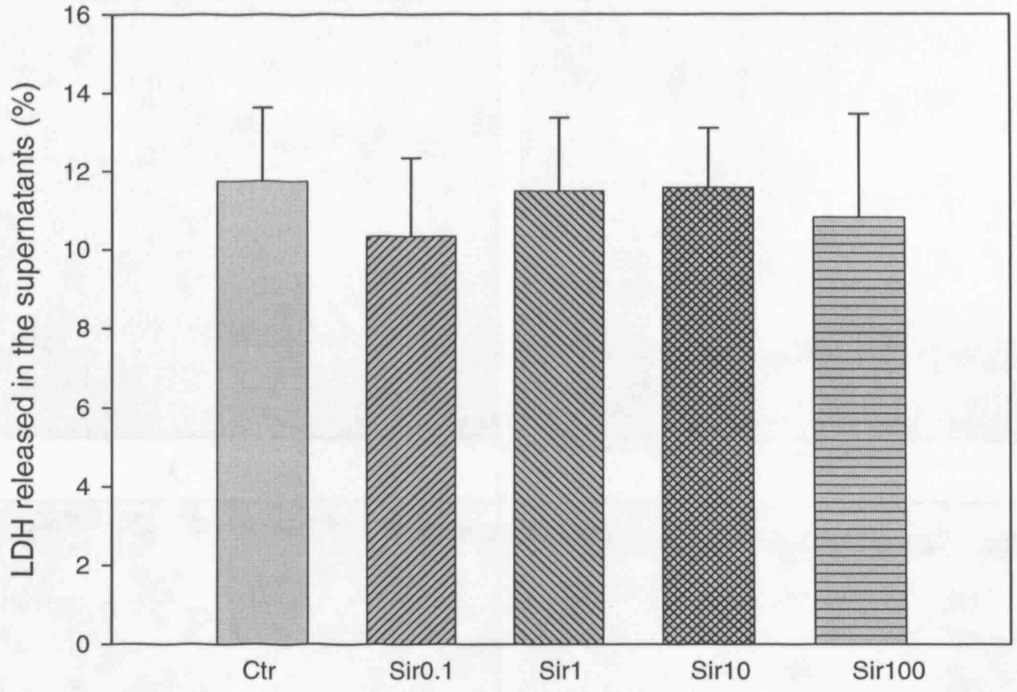

Fig 5.3 The observation of cytotoxic effect in macrophages treated by Sirolimus. Macrophages were incubated in serum-free medium with different concentrations of Sirolimus (Sir 0, 0.1, 1, 10, 100 ng/ml) for 24 hours. Supernatants were collected and cells were lysed for LDH assay. The percentage of LDH in the supernatants was expressed as Mean ± SD (n=8 wells). There was no significance among the Sirolimus treated groups compared to controls.

Fig 5.4a

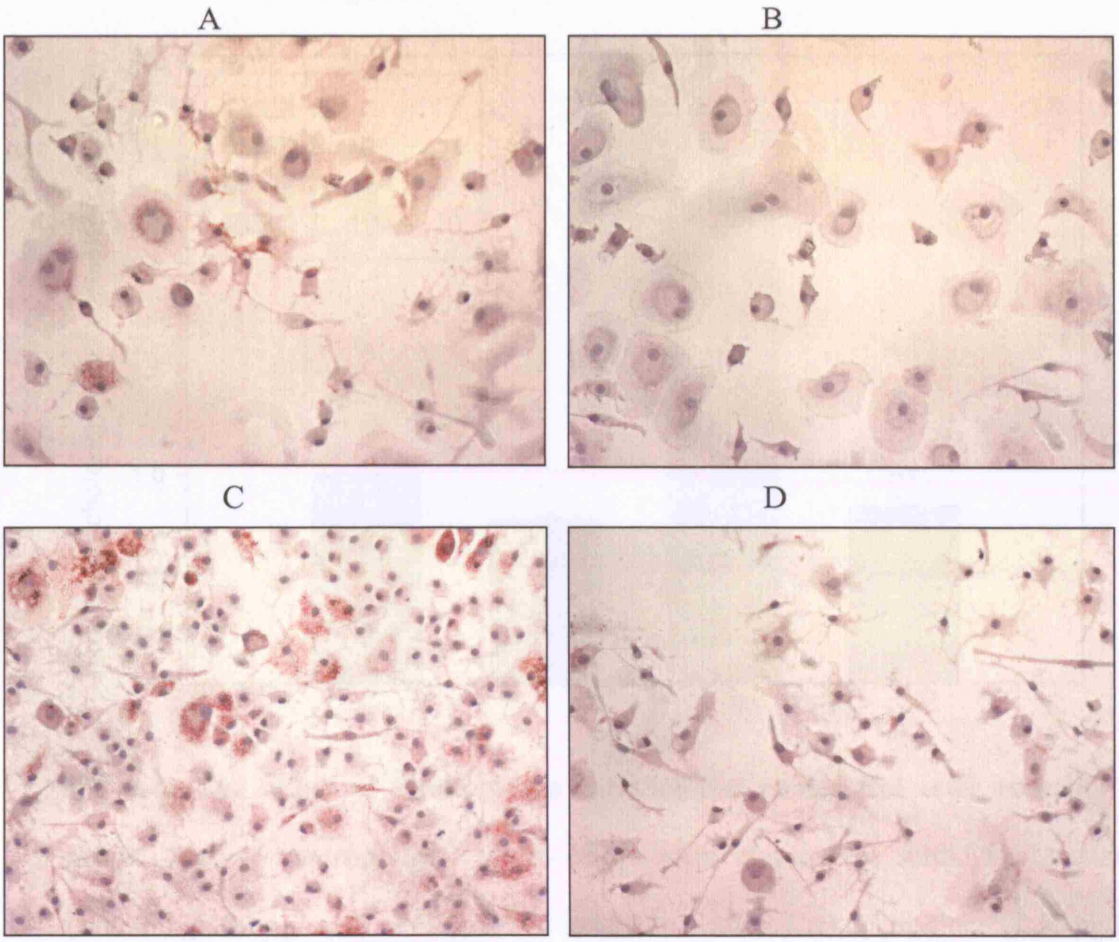

Fig 5.4a Visualisation of acLDL uptake and lipid droplets in macrophages treated with Sirolimus. Macrophages were incubated for 24 hours in serum-free medium containing 100 μg/ml of acLDL in the absence (A) or presence of 10 ng/ml of Sirolimus (B) or 5 ng/ml of IL-1β (C) or 5 ng/ml of IL-1β plus 10 ng/ml Sirolimus (D). The cells were examined for lipid inclusions by Oil Red O staining. The results were typical of those observed in four separate experiments (200x).

Fig 5.4b

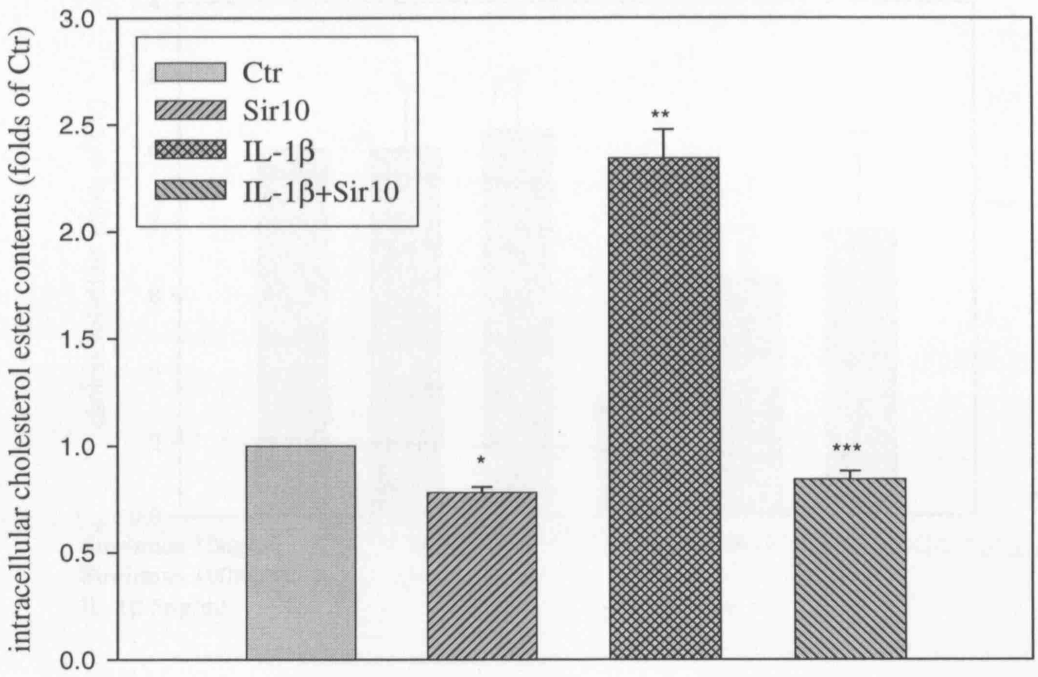

Fig 5.4b The effect of Sirolimus on intracellular cholesterol ester contents in acLDL-loaded macrophages. Macrophages were cultured in serum-free medium containing 100 μg/ml of acLDL in the absence (control, Ctr) or presence of 10 ng/ml of Sirolimus or 5 ng/ml of IL-1β or 5 ng/ml of IL-1β plus 10 ng/ml of Sirolimus for 24 hours. Intracellular cholesterol ester contents were measured as described in MATERIALS AND METHODS. Values were expressed Mean ± SD of duplicate wells from four experiments. *$P < 0.01$ *vs* control. **$P < 0.01$ *vs* control. ***$P < 0.01$ *vs* IL-1β.

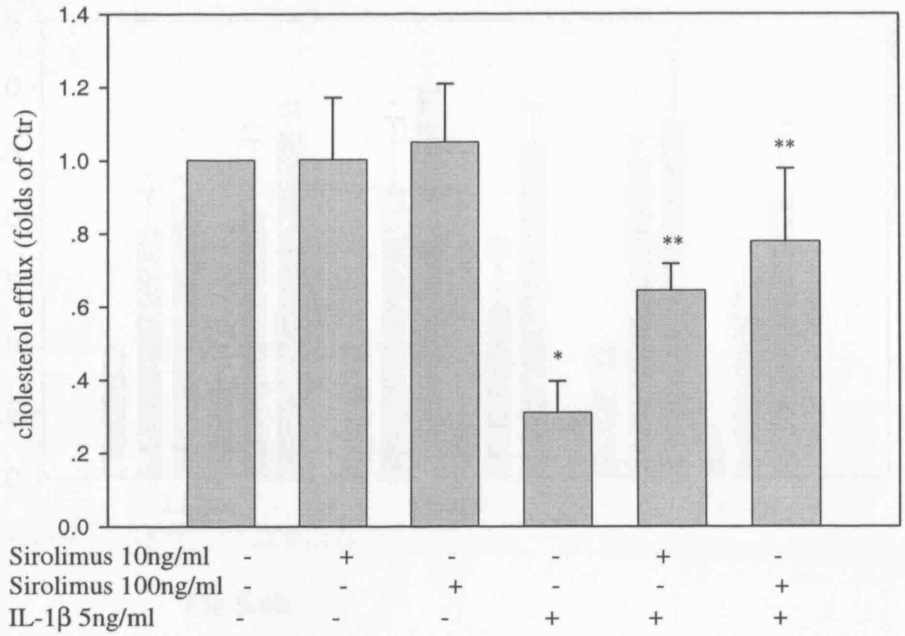

Fig 5.5 The effect of Sirolimus on the intracellular cholesterol efflux of macrophages loaded with cholesterol. Macrophages were preloaded with 30 μg/ml cholesterol, 1 μg/ml 25-hydroxy-cholesterol, and 1 μCi/well [1α, 2α(n)-^{3}H]-Cholesterol in serum-free DMEM/F12 medium for 48 hours. The cells were then incubated in serum-free medium (control, Ctr) or serum-free medium with 10 ng/ml or 100 ng/ml of Sirolimus (Sir10, Sir100) or 5 ng/ml of IL-1β (IL-1β), or 5 ng/ml of IL-1β plus 10 ng/ml of Sirolimus (IL-1β+Sir10) or 5 ng/ml of IL-1β plus 100 ng/ml of Sirolimus (IL-1β+Sir100) for 24 hours. After this incubation period, $ApoA_1$-mediated cholesterol efflux studies were immediately performed by adding fresh serum-free DMEM/F12 medium with or without 15 μg/ml $ApoA_1$ for 6 hours. The cholesterol efflux was then measured by radioactive counts. Data were expressed as Mean ± SD (n=6). * p <0.001 *vs* control, ** p <0.001 *vs* IL-1β group.

Fig 5.6a

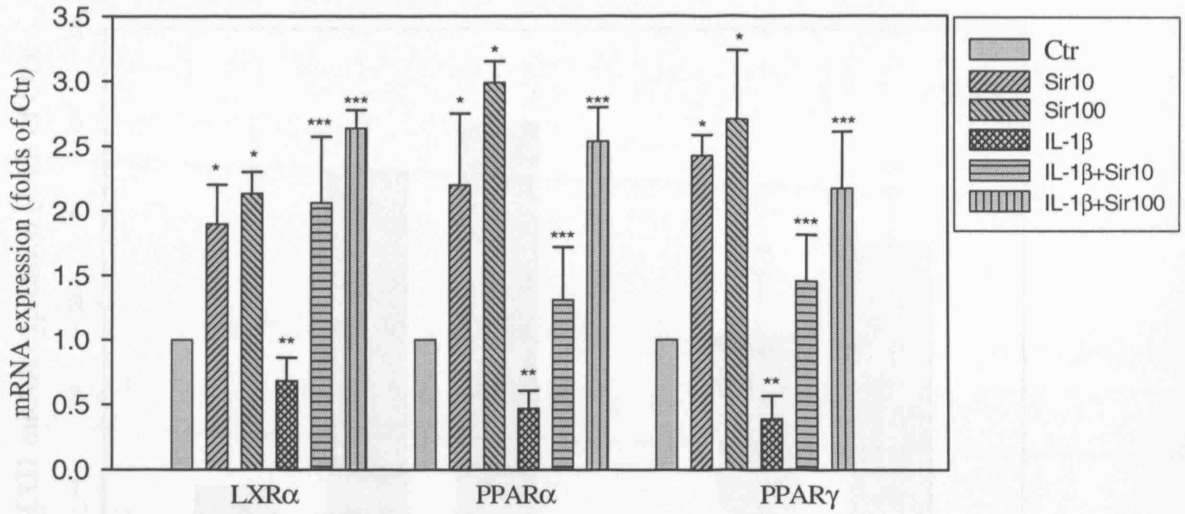

Fig 5.6b

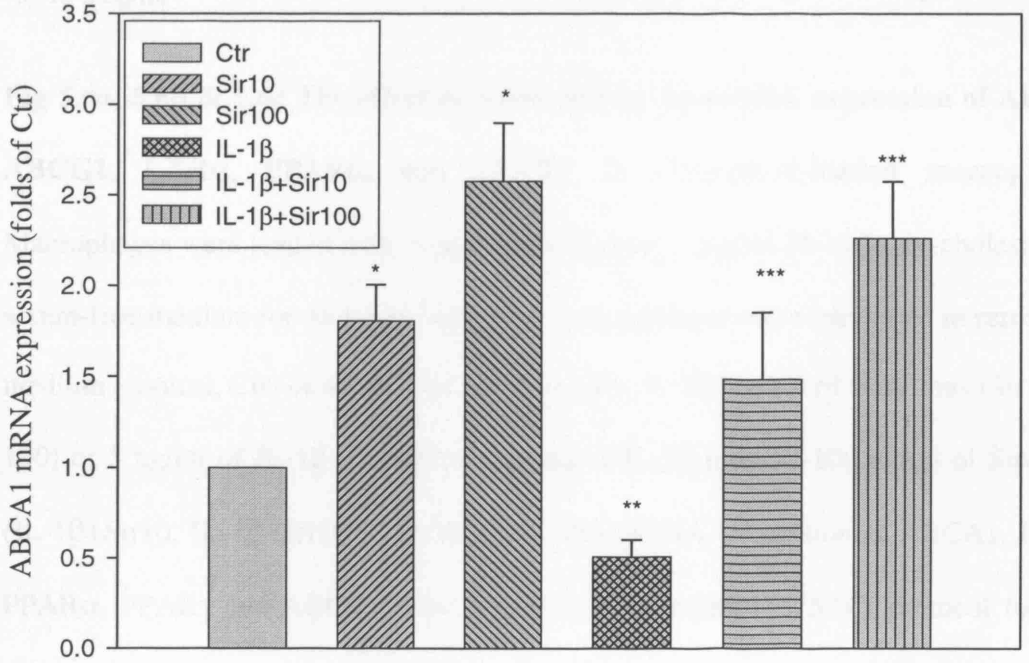

Fig 5.6c

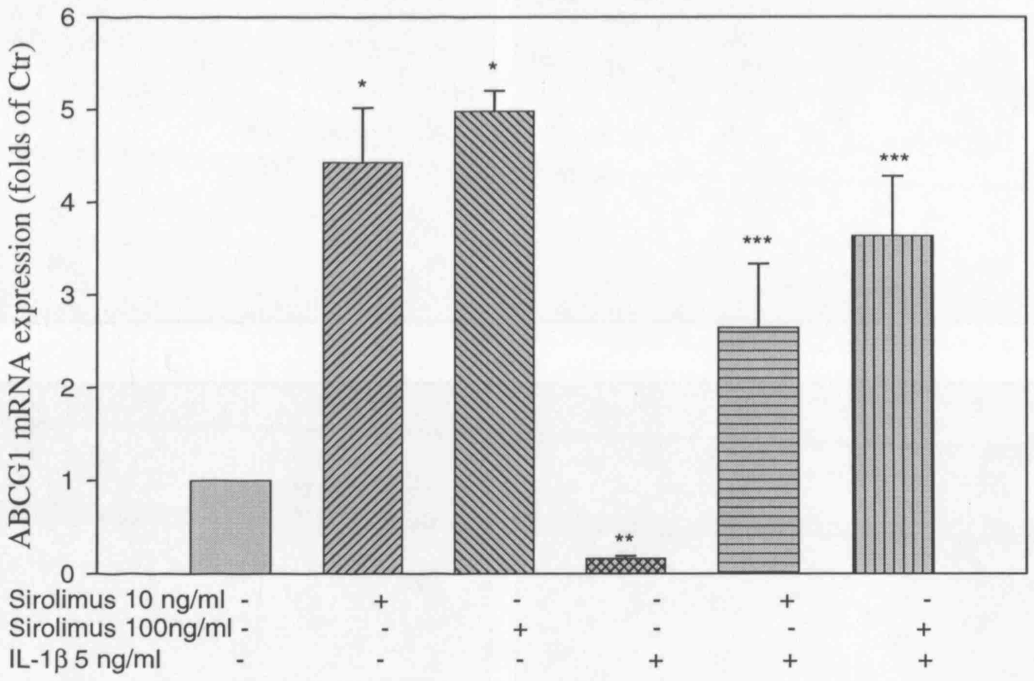

Fig 5.6a, 5.6b & 5.6c The effect of Sirolimus on the mRNA expression of ABCA1, ABCG1, LXRα, PPARα, and PPARγ, in cholesterol-loaded macrophages. Macrophages were loaded with 30 μg/ml cholesterol, 1 μg/ml 25-hydroxy-cholesterol in serum-free medium for 48 hours. After that, macrophages were incubated in serum-free medium (control, Ctr) or serum-free medium with 10-100 ng/ml of Sirolimus (Sir10, Sir 100) or 5 ng/ml of IL-1β (IL-1β) or 5 ng/ml of IL-1β plus 10-100 ng/ml of Sirolimus (IL-1β+Sir10, IL-1β+Sir100) for 24 hours. The mRNA expression of ABCA1, LXRα, PPARα, PPARγ and ABCG1 were determined following the ΔΔCt protocol for real-time RT-PCR as described in the section of Methods. β-actin served as the housekeeping gene. Results represented the Mean ± SD from four experiments. * p <0.01 *vs* control, ** p <0.01 *vs* control, *** p <0.01 *vs* IL-1β group.

Fig 5.7a: LXRα

A

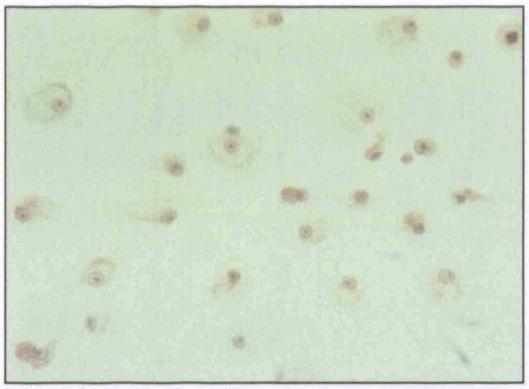

B

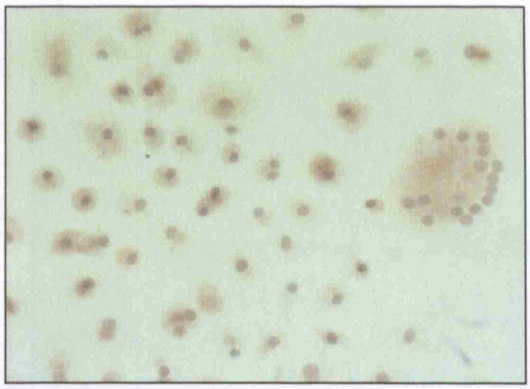

C

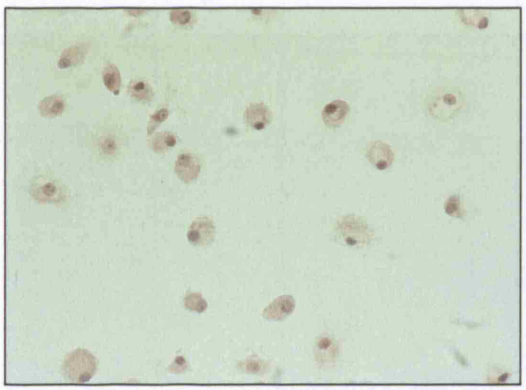

D

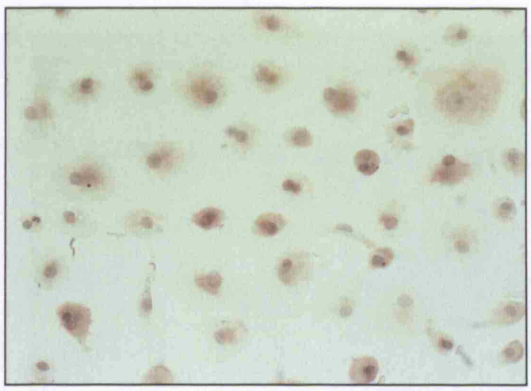

Fig 5.7b: PPARα

A

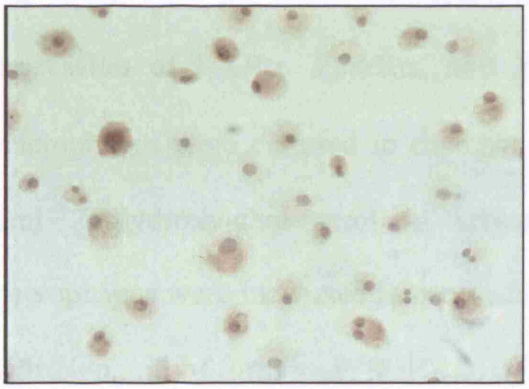

B

C

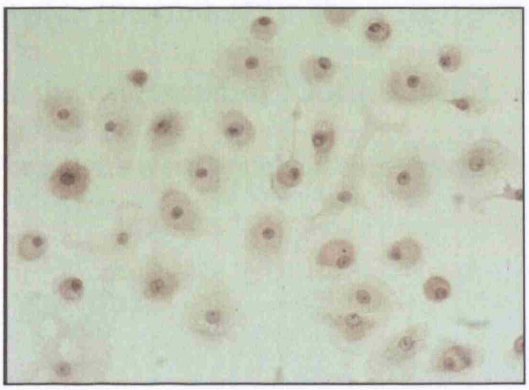

D

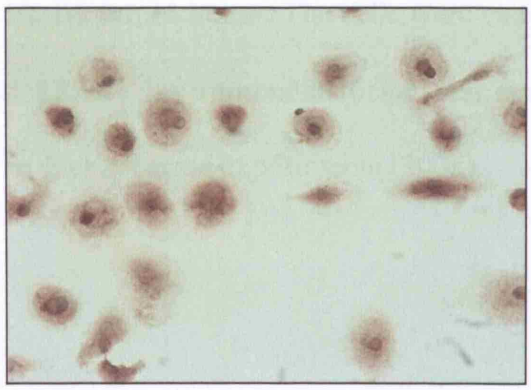

Fig 5.7c: PPARγ

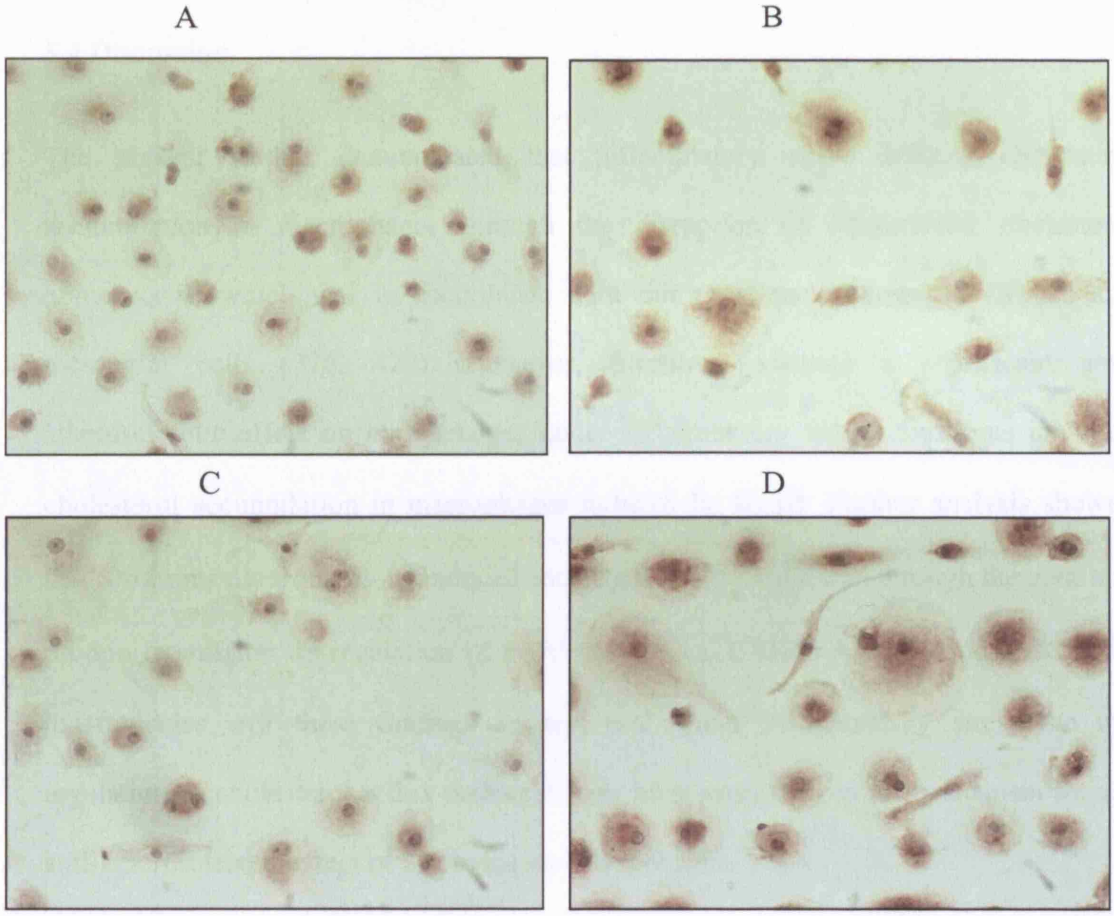

Fig 5.7a, 5.7b & 5.7c The immunohistochemistry analysis for the protein expression of LXRα, PPARα, and PPARγ in cholesterol-loaded macrophages. Macrophages were cultured in chamber slides loaded with 30 μg/ml cholesterol, 1 μg/ml 25-hydroxy-cholesterol in serum-free medium for 48 hours. After that, macrophages were incubated in serum-free medium (control, A) or serum-free medium with 10 ng/ml of Sirolimus (Sir10, B) or 5 ng/ml of IL-1β (IL-1β, C) or 5 ng/ml of IL-1β plus 10 ng/ml of Sirolimus (IL-1β+Sir10, D) for 24 hours. The cells were examined for the expression of LXRα, PPARα, and PPARγ by immunohistochemical staining. The results were typical of those observed in four separate experiments (200x).

5.4 Discussion

The present studies demonstrated that inflammatory stress induced cholesterol accumulation in macrophages through the disruption of intracellular cholesterol homeostasis, which was in accordance with our previous findings in VSMCs and mesangial cells (376, 422). However, Sirolimus showed a significant anti-atherosclerotic effect on macrophages under inflammatory stress. Sirolimus inhibited cholesterol accumulation in macrophages induced by IL-1β. Further analysis showed that Sirolimus overrode IL-1β induced cholesterol efflux reduction through the gene and protein expression up-regulation of PPARα, PPARγ, LXRα, ABCA1 and ABCG1 in macrophages. All these findings suggest that under inflammatory stress the up-regulation of cholesterol efflux pathways may be a main molecular mechanism for the anti-atherosclerotic effect of Sirolimus on macrophages.

It is well known that macrophages use two mechanisms to reduce high levels of intracellular cholesterol. Firstly, excess free cholesterol may undergo re-esterification by ACAT to form cholesterol esters. Secondly, cholesterol efflux pathways are activated to transport free cholesterol out of the cell. Two common efflux pathways are present in macrophages. One is an active transport pathway mediated by ABCA1 and ABCG1, which might synergize to mediate cholesterol efflux to apolipoprotein A-I. The other is a passive transport pathway facilitated by apoE that transfers cholesterols to HDL, which then transports cholesterol into the liver, a process termed reverse cholesterol transport. These two pathways collaborate to reduce the content of intracellular cholesterol (444). As macrophages are incapable of limiting the uptake of lipids via their numerous uptake mechanisms, cholesterol efflux pathways play very important role in maintaining cellular lipid homeostasis in these cells. Our results suggest that Sirolimus ameliorates the dysregulation of cholesterol efflux pathways in

macrophages induced by inflammatory stress. Furthermore, increased expression of nuclear transcription factors (LXRα, PPARs) by Sirolimus provides an amplification effect for cholesterol efflux.

We also investigated the effect of Sirolimus on lipoprotein receptor mediated lipid uptake (VLDLr, LDLr, scavenger receptor A-I, and CD36). However, we did not find a significant difference between Sirolimus treated groups and controls.

Taken together, our findings demonstrated that, under inflammatory stress, Sirolimus inhibits cholesterol accumulation in macrophages mainly through up-regulating ABCA1 and ABCG1 mediated cholesterol pathways, thereby preventing macrophage-derived foam cell formation.

CHAPTER 6. SIROLIMUS MODIFIES CHOLESTEROL HOMEOSTASIS IN HEPATIC CELLS: A POTENTIAL MOLECULAR MECHANISM FOR SIROLIMUS-ASSOCIATED DYSLIPIDEMIA

6.1 Introduction

Although Sirolimus has shown remarkable therapeutic efficacy in anti-atherosclerosis, Sirolimus-associated dyslipidemia was also reported in some clinical patients. 45 % of liver transplant patients (445) and about 40 % of renal transplant patients (446) experience this effect. In addition, phase II clinical trials also described the occurrence of hypertriglyceridemia or hypercholesterolaemia with administration of a Sirolimus analogue (CCI-779) in the treatment of metastatic melanoma and glioblastoma multiforme (447). These observations indicate that hyperlipidemia is a significant side effect of Sirolimus administration in both organ transplantation and anti-tumour treatment and may compromise patients' health. However, Massy *et al* (448) demonstrated that there was no significant difference in the lipoprotein lipase and hepatic lipase activities between renal transplant recipients whether treated with Sirolimus or Cyclosporine A. Interestingly, recent studies demonstrated that Sirolimus diminished atherosclerotic lesion size in the apoE KO mice and did not aggravate hypercholesterolaemia in fat-fed apoE KO mice (386). Furthermore, Chueh *et al* (449) reported that there was no significant difference in the incidence of cardiovascular events within four years after transplantation among patients treated with Sirolimus compared to the control. The dyslipidemia associated with Sirolimus therapy does not seem to represent a major risk factor for the early emergence of cardiovascular complications. In addition a randomized study (450) showed that coronary heart disease risks associated with these cholesterol elevations were lower compared with the baseline risks of the transplant population. These data suggest that the anti-inflammatory effects of Sirolimus prevent drug induced dyslipidemia from being atherogenic. However, the mechanisms and effects of Sirolimus-associated dyslipidemia in humans have not been fully explored.

The liver is the central organ in the clearance of LDL and HDL cholesterol by both endocytosis of whole lipoprotein particles and lipid selective uptake. The feedback mechanisms of LDLr in the liver are of primary importance in binding and internalization of plasma-derived LDL-cholesterol and in regulating plasma LDL concentration. The liver also participates in the final step of reverse cholesterol transport by selective uptake of cholesterol from HDL via a receptor-mediated pathway that clears excess peripheral cholesterol. PPAR-LXR-ABCA1 mediated cholesterol efflux is an important source of circulating HDL as demonstrated by showing that the inactivation of ABCA1 in the liver of mice causes a profound lowering of plasma HDL (451). Furthermore, PPAR-LXR-ABCA1 interactions are integral to the regulation of cholesterol homeostasis (439). All these studies conclude that liver cholesterol homeostasis is tightly regulated to maintain free cholesterol at low physiological levels.

The HepG2 cells are commonly used for lipid metabolism studies and retain many liver-specific functions. We have investigated potential molecular mechanisms for Sirolimus anti-atherosclerotic effects in human VSMCs and macrophages. In the present study we further investigated the effects of Sirolimus on LDLr mediated cholesterol uptake and ABCA1 mediated cholesterol efflux in HepG2 cells under inflammatory stress. This may provide an explanation at the cellular and molecular levels for Sirolimus-associated dyslipidemia in clinical patients.

6.2 Materials and methods

6.2.1 HepG2 Cell culture

6.2.1.1 Materials

1) HepG2 cells (European Collection of Cell Cultures, UK)

2) Other materials for cell culture were already previously listed in Chapter 3.

6.2.1.2 Background

HepG2 cells were established from liver tumour biopsies obtained during extended lobectomies of a 15-year-old Caucasian male from Argentina in 1975 (452). Tumour minces were cultured on irradiated mouse cell layers. The cell line was established after these biopsies had been cultured for several months, which was designated HepG2. Since HepG2 cell line was set up, more than 250 studies using this resource have been published. The morphological characteristics and epithelial cell shape of HepG2 cells are compatible with normal liver parenchymal cells. HepG2 cells retain many liver-specific functions, such as protein synthesis and secretion of many important enzymes. Furthermore, HepG2 cells have been found to express a wide variety of liver-specific metabolic functions. Some of those functions are closely related to cholesterol and triglyceride metabolism. Confluent HepG2 monolayer expresses normal LDL receptors and continues to internalize and metabolize chylomicrons, VLDL, LDL, and HDL. In lipoprotein-free medium, apolipoprotein A-I, A-II, B, C, and E accumulate in the medium together with cholesterol, cholesteryl ester, triglyceride, primary bile acids and other components of cholesterol and triglyceride metabolism (453). Thus, HepG2 cell line is a useful model for lipid metabolism and other liver research field.

6.2.1.3 Procedures

HepG2 cells were cultured in DMEM/F12 containing 100 units/ml of penicillin, 100 μg/ml of streptomycin, 2 mmol/l of L-glutamine and 10 % FBS. The cell medium was changed once every 48 hours. The cells were subcultured one time with 0.25 % trypsin/0.01 % EDTA when cells were grown to subconfluence. All experiments were performed in serum-free DMEM/F12 medium containing 0.2 % fatty acid-free BSA. For native LDL treated experiments, the medium were supplemented with 100 μmol/l of EDTA and 20 μmol/l of BHT for antioxidation.

6.2.2 Lipoprotein preparation

Fresh plasma was collected from healthy human volunteers. LDL was isolated by sequential density gradient ultracentrifugation as previously described in Chapter 2.

6.2.3 Morphological examination

The lipid accumulation in HepG2 cells was checked by Oil Red O staining as previously described in Chapter 2.

6.2.4 Lactate dehydrogenase release for cytotoxicity assay

The procedures were already previously described in Chapter 2.

6.2.5 Quantitative assay of intracellular cholesterol

The procedures were already previously described in Chapter 2.

6.2.6 Intracellular cholesterol efflux

The procedures were already previously described in Chapter 2.

6.2.7 Real-time RT–PCR

The procedures and the Taqman primers for real-time RT-PCR were already previously shown in Chapter 2.

6.2.8 Western Blot

The procedures were already previously described in Chapter 2.

6.2.9 Confocal microscopy observation

The procedures were already previously described in Chapter 2.

6.3 Results

6.3.1 The observation of cytotoxic effect in Sirolimus treated HepG2 cells

In order to exclude the cytotoxic effect of Sirolimus, the release of LDH in the supernatants in HepG2 cells treated by Sirolimus was checked by LDH assay. As shown

in Fig 6.1, there was no difference between Sirolimus treated groups and controls. Therefore the dose range 0-100 ng/ml was considered safe for investigating the role of Sirolimus in cholesterol trafficking in HepG2 cells.

6.3.2 The effect of Sirolimus on lipid accumulation in HepG2 cells induced by inflammatory cytokines

Using Oil Red O staining, we checked the effect of Sirolimus on cholesterol accumulation in HepG2 cells loaded with native LDL in the presence or absence of IL-1β. We found that IL-1β significantly increased lipid droplet accumulation in HepG2 cells (Fig 6.2a, B). However, Sirolimus reduced lipid droplet accumulation of HepG2 cells caused by IL-1β (Fig 6.2a, D). Furthermore, quantitative intracellular cholesterol analysis confirmed that Sirolimus reduced IL-1β induced cholesterol ester accumulation in HepG2 cells, suggesting that Sirolimus may inhibit inflammatory stress induced cholesterol accumulation in these cells (Fig 6.2b).

6.3.3 The effect of Sirolimus on the expression of lipoprotein receptors in HepG2 cells

To investigate the potential mechanisms of these phenomena, we investigated effects of Sirolimus on gene expression of LDLr which mediates cholesterol uptake. Sirolimus significantly reduced LDLr gene expression in HepG2 cells induced by cholesterol depletion (serum free) and IL-1β (Fig 6.3a). Sirolimus also reduced LDLr protein expression, especially when induced by IL-1β as demonstrated by Western Blot, which is consistent with the results at mRNA level (Fig 6.3b & 6.3c).

6.3.4 The effect of Sirolimus on the SCAP and SREBP-2 mRNA expression and SCAP/SREBP-2 complex translocation from the ER to the Golgi in HepG2 cells.

Furthermore, we investigated the effect of Sirolimus on the gene expression of SCAP and SREBP-2 in HepG2 cells. IL-1β increased SCAP and SREBP-2 mRNA expression. Sirolimus dose-dependently inhibited both SCAP and SREBP2-mRNA expression in the absence or presence of IL-1β (Fig 6.4a & 6.4b).

Using immunofluorescent staining, we further investigated the translocation of SCAP/SREBP-2 complex from the ER to the Golgi in HepG2 cells in cholesterol depletion/loading and inflammatory stress conditions in the absence or presence of Sirolimus. By dual staining with anti-human SCAP and anti-human Golgi antibodies, we demonstrated that cholesterol depletion of cells increased SCAP accumulation in Golgi. Interestingly, Sirolimus attenuated SCAP accumulation in Golgi induced by cholesterol depletion and IL-1β (20 ng/ml) (Fig 6.4c), suggesting that Sirolimus interferes with the SCAP translocation between the ER and Golgi at the normal and inflammatory conditions.

6.3.5 The effect of Sirolimus on the LXRs-PPARs-ABCA1 pathway mediated cholesterol efflux in cholesterol-loaded HepG2 cells

Intracellular cholesterol homeostasis is controlled by influx and efflux pathways. We further investigated the effect of Sirolimus on ABCA1 mediated intracellular cholesterol efflux in HepG2 cells. We demonstrated that IL-1β inhibited cholesterol efflux from cholesterol loaded HepG2 cells. However, Sirolimus overrode the reduction of cholesterol efflux induced by IL-1β (Fig 6.5). Further analysis showed that Sirolimus increased the gene and protein expression of ABCA1, LXRα and PPARα in cholesterol-loaded HepG2 cells in the absence or presence of IL-1β (Fig 6.6, Fig 6.7,

Fig 6.8a & Fig 6.8b). These results suggest that Sirolimus ameliorates cholesterol efflux from HepG2 cells disrupted by inflammatory stress, which may correlate with the up-regulation of the LXRα-PPARα-ABCA1 mediated pathway.

6.3.6 The effect of Sirolimus on the expression of TNFα and MCP-1 in HepG2 cells

We also observed the effect of Sirolimus on inflammatory cytokine synthesis in HepG2 cells under inflammatory stress. As predicted, Sirolimus inhibited gene and protein expression of TNFα and MCP-1 in HepG2 cells (Fig 6.9, Fig 6.10a and Fig 6.10b).

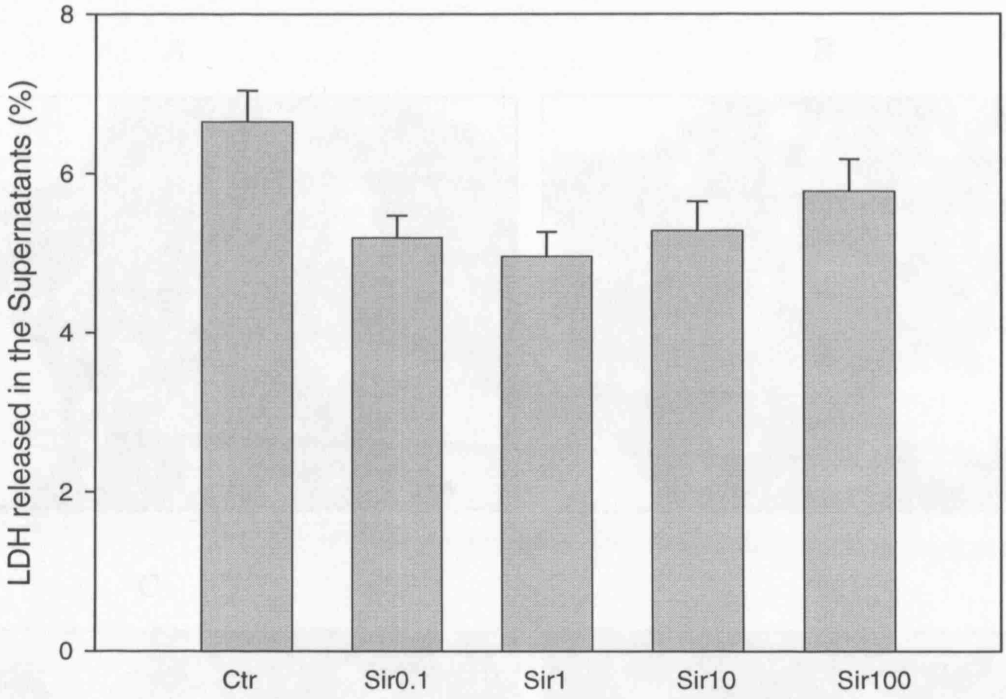

Fig 6.1 The observation of cytotoxic effect in HepG2 cells treated by Sirolimus. HepG2 cells were incubated in serum-free medium with different concentrations of Sirolimus (Sir 0, 0.1, 1, 10, 100 ng/ml) for 24 hours. Supernatants were collected and cells were lysed for LDH assay. The percentage of LDH in the supernatants was expressed as Mean ± SD (n=8 wells). There was no significance among the Sirolimus treated groups compared to controls.

Fig 6.2a

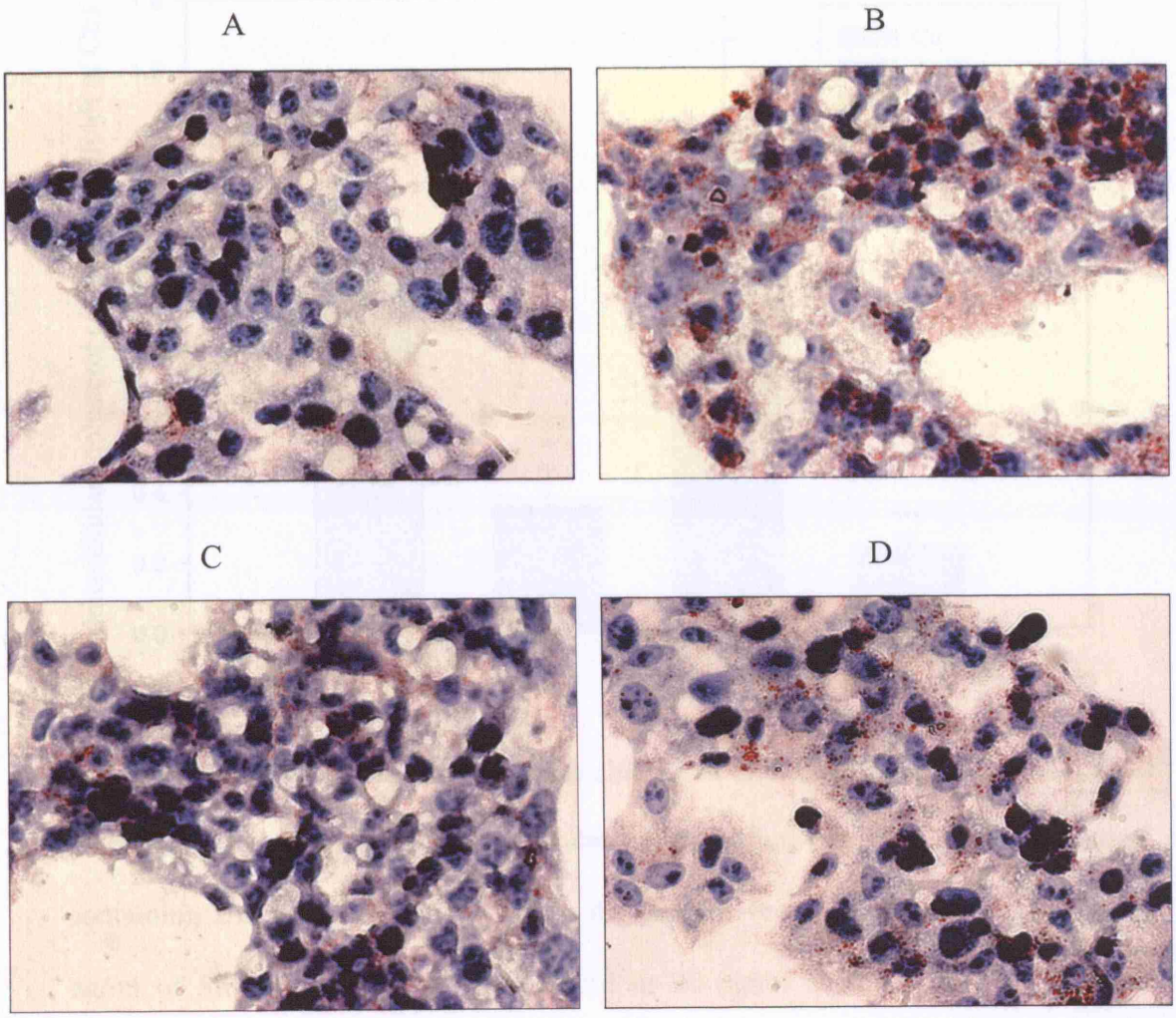

Fig 6.2a Visualisation of LDL uptake and lipid droplets in HepG2 cells treated with Sirolimus. HepG2 cells were incubated for 24 hours in serum-free medium containing 200 μg/ml of native LDL in the absence (A) or presence of 20 ng/ml of IL-1β (B) or 10 ng/ml of Sirolimus (C) or 20 ng/ml of IL-1β plus 10 ng/ml of Sirolimus (D). The cells were examined for lipid inclusions by Oil Red O staining. The results were typical of those observed in four separate experiments (400x).

Fig 6.2b

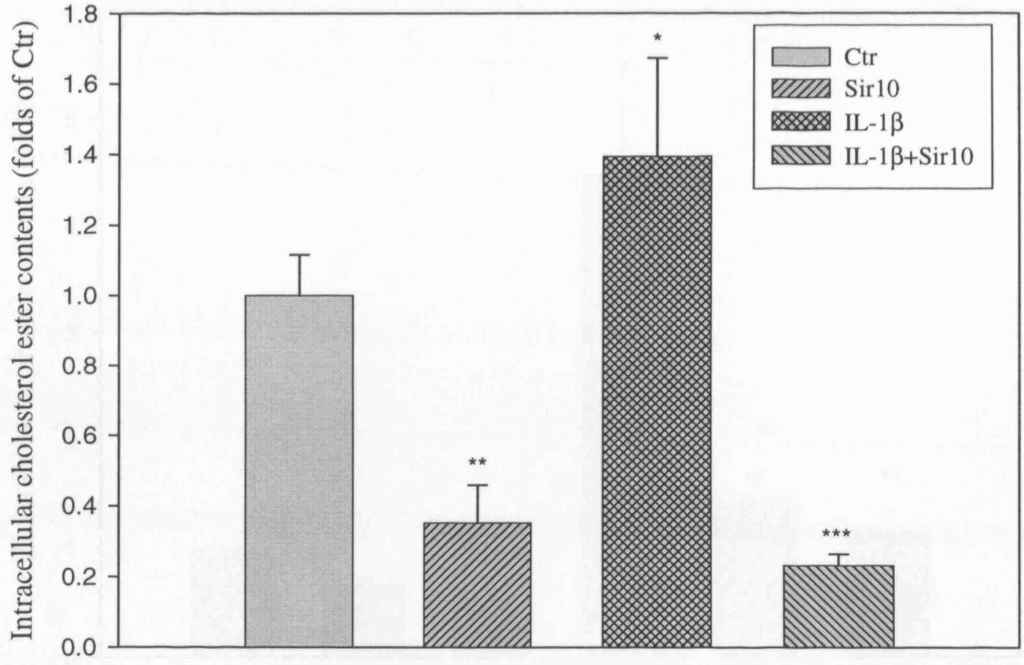

Fig 6.2b The effect of Sirolimus on the change of cholesterol ester in LDL-loaded HepG2 cells. HepG2 cells were cultured in serum-free DMEM/F12 medium containing 200 μg/ml of native LDL in the absence (control, Ctr) or presence of 10 ng/ml of Sirolimus or 20 ng/ml of IL-1β or 20 ng/ml of IL-1β plus 10 ng/ml of Sirolimus for 24 hours. Intracellular cholesterol ester was assayed as described in MATERIALS AND METHODS. Values were Mean ± SD of duplicate wells from four experiments. $*P < 0.05$ *vs* control. $**P < 0.001$*vs* control. $***P < 0.001$ *vs* IL-1β.

Fig 6.3a

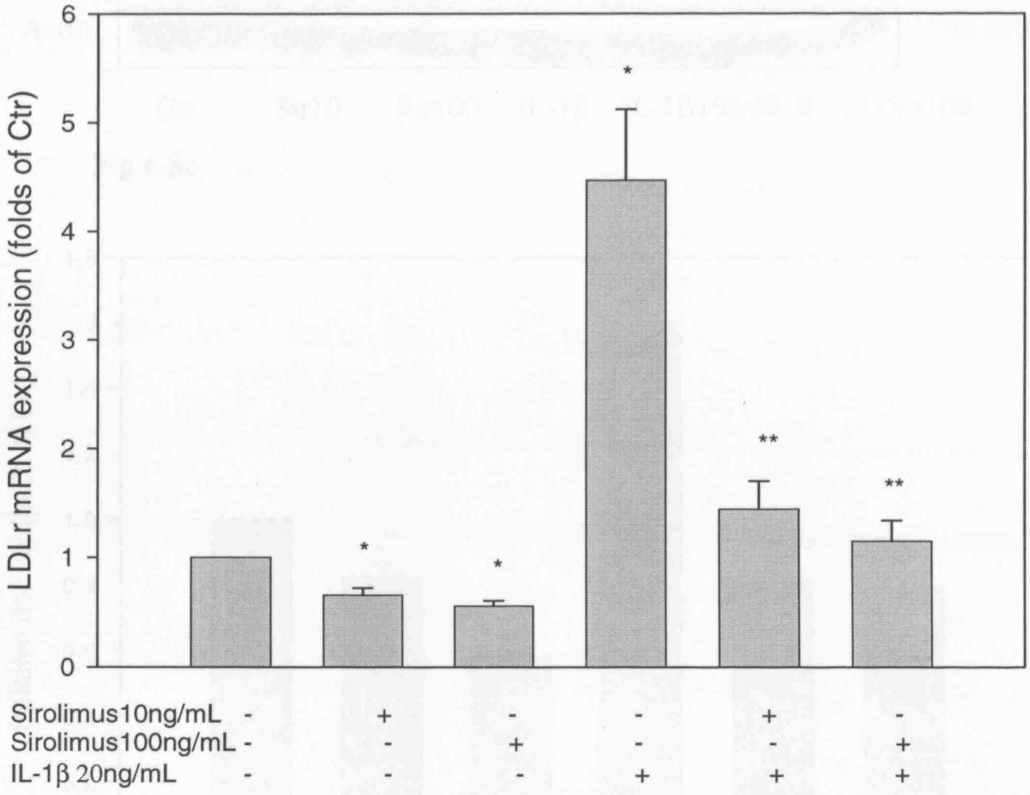

Fig 6.3a The effect of Sirolimus on the mRNA expression of LDLr in HepG2 cells. HepG2 cells were incubated in serum-free medium (control, Ctr) or serum-free medium with 10-100 ng/ml of Sirolimus (Sir10, Sir 100) or 20 ng/ml of IL-1β (IL-1β) or 20 ng/ml of IL-1β plus 10-100 ng/ml of Sirolimus (IL-1β+Sir10, IL-1β+Sir100) for 24 hours. The mRNA expression of LDLr was determined following the ΔΔCt protocol for real-time RT-PCR as described in the section of Methods. β-actin served as the housekeeping gene. Results represented Mean ± SD from four experiments. * p <0.001 *vs* control, ** p <0.001 *vs* IL-1β group.

Fig 6.3b

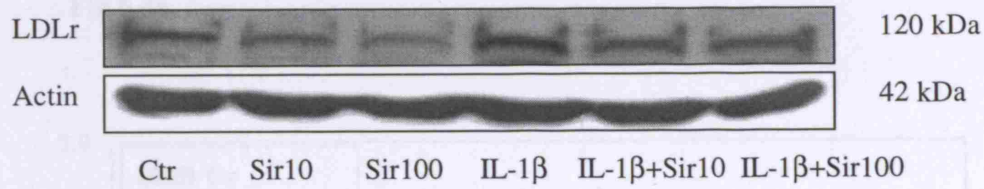

Fig 6.3c

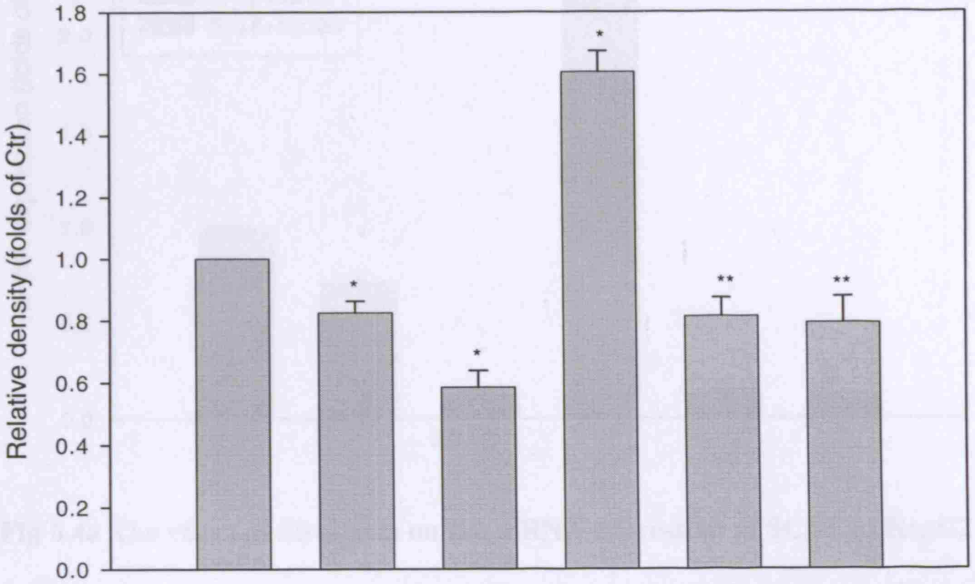

Fig 6.3b & 6.3c The effect of Sirolimus on the protein expression of LDLr in HepG2 cells. HepG2 cells were incubated in serum-free medium (control, Ctr) or serum-free medium with 10-100 ng/ml of Sirolimus (Sir10, Sir 100) or 20 ng/ml of IL-1β (IL-1β) or 20 ng/ml of IL-1β plus 10-100 ng/ml of Sirolimus (IL-1β+Sir10, IL-1β+Sir100) for 24 hours. The protein level of LDLr was examined by Western Blot. The histogram represented Mean ± SD of the densitometric scans of LDLr protein bands from four experiments, normalized by comparison with actin, and expressed as a percentage of the control. * p <0.001 *vs* control, ** p <0.001 *vs* IL-1β group.

Fig 6.4a

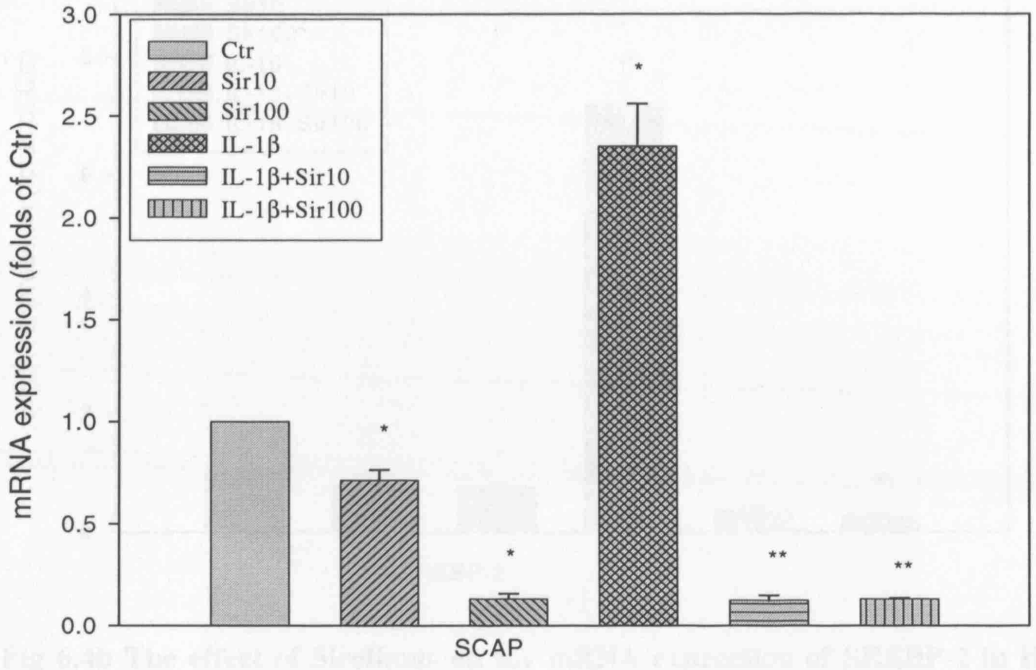

Fig 6.4a The effect of Sirolimus on the mRNA expression of SCAP in HepG2 cells. HepG2 cells were incubated in serum-free medium (control, Ctr) or serum-free medium with 10-100 ng/ml of Sirolimus (Sir10, Sir 100) or 20 ng/ml of IL-1β (IL-1β) or 20 ng/ml of IL-1β plus 10-100 ng/ml of Sirolimus (IL-1β+Sir10, IL-1β+Sir100) for 24 hours. The mRNA expression of SCAP was determined following the ΔΔCt protocol for real-time RT-PCR as described in the section of Methods. β-actin served as the housekeeping gene. Results represented Mean ± SD from four independent experiments. * p <0.001 *vs* control, ** p <0.001 *vs* IL-1β group.

Fig 6.4b

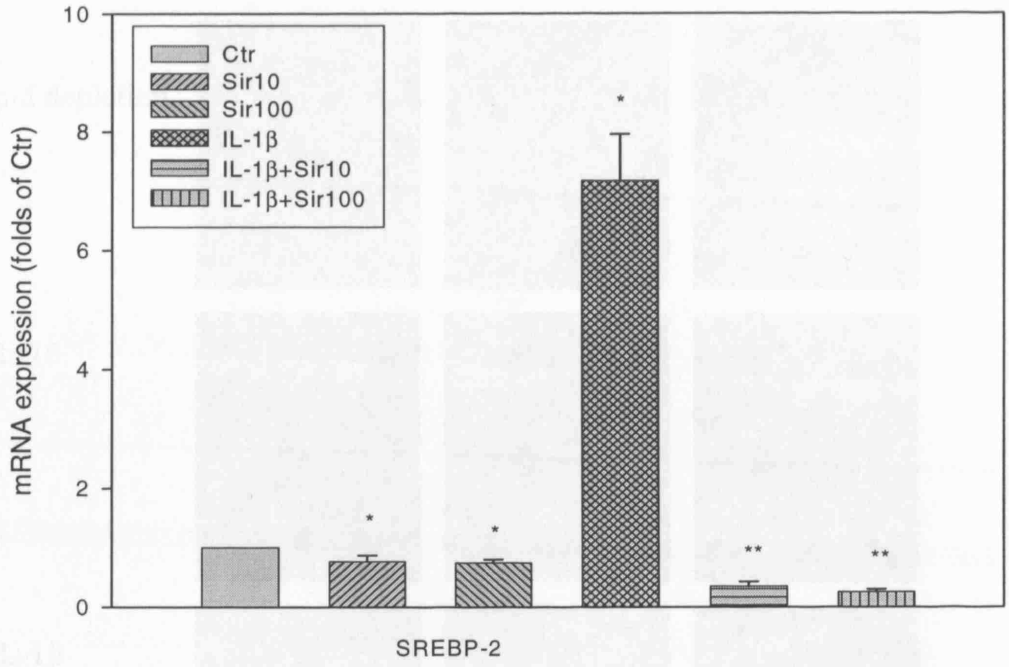

Fig 6.4b The effect of Sirolimus on the mRNA expression of SREBP-2 in HepG2 cells. HepG2 cells were incubated in serum-free medium (control, Ctr) or serum-free medium with 10-100 ng/ml of Sirolimus (Sir10, Sir 100) or 20 ng/ml of IL-1β (IL-1β) or 20 ng/ml of IL-1β plus 10-100 ng/ml of Sirolimus (IL-1β+Sir10, IL-1β+Sir100) for 24 hours. The mRNA expression of SREBP-2 was determined following the ΔΔCt protocol for real-time RT-PCR as described in the section of Methods. β-actin served as the housekeeping gene. Results represented Mean ± SD from four independent experiments. * p <0.001 *vs* control, ** p <0.001 *vs* IL-1β group.

Fig 6.4c

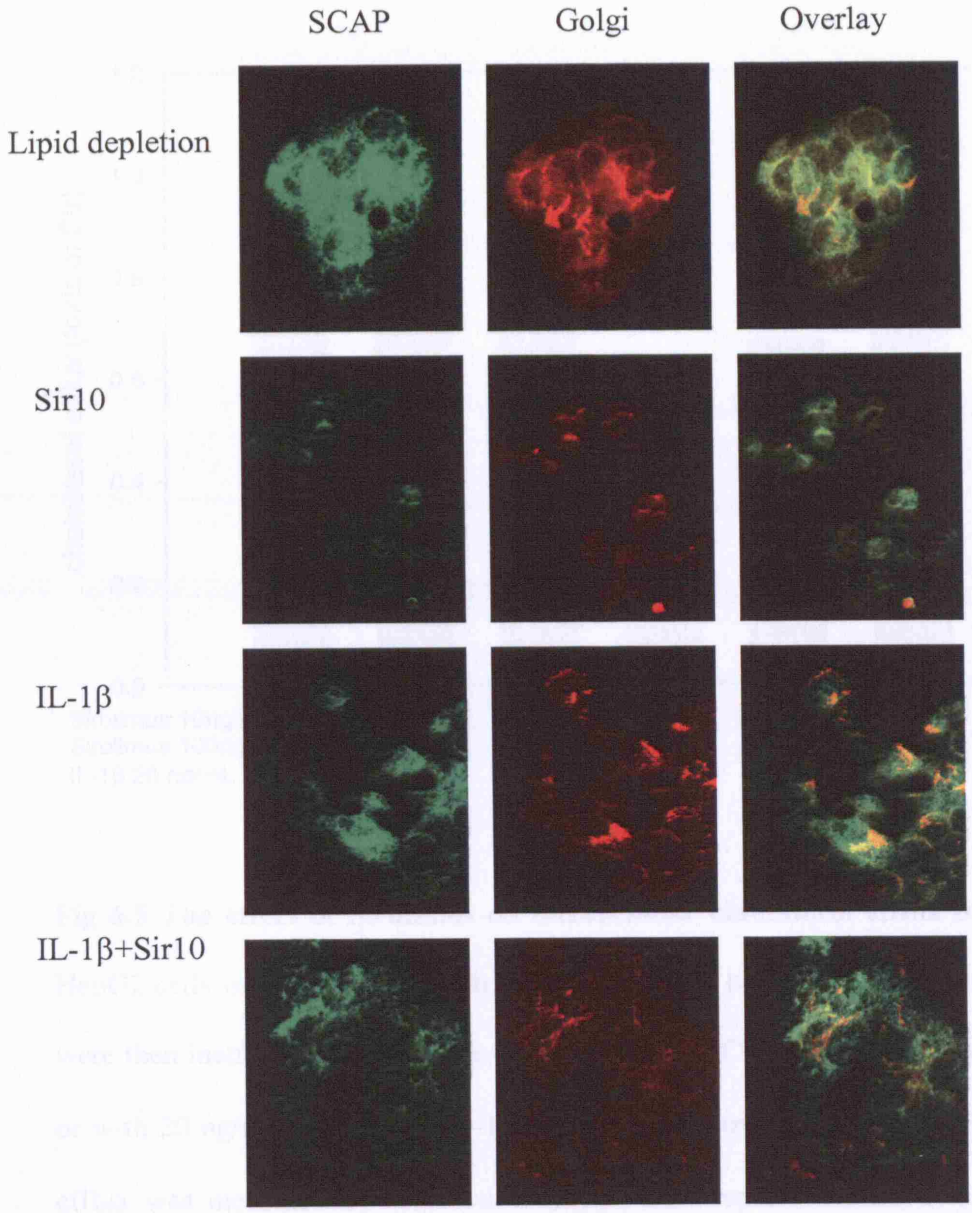

Fig 6.4c The effect of Sirolimus on the translocation of SCAP from the ER to the Golgi in HepG2 cells. HepG2 cells cultured in chamber slides were washed, fixed, and permeabilized. The cells were then incubated with rabbit anti-human SCAP antibody (1:200 dilution) and an anti-human Golgi antibody (mouse anti-human Golgi-97, 1:200 dilution), followed by a secondary fluorescent antibodies (goat anti-rabbit Fluor 488 for SCAP and goat anti-mouse Fluor 594 for Golgi). After washing, the cells were examined by confocal microscopy.

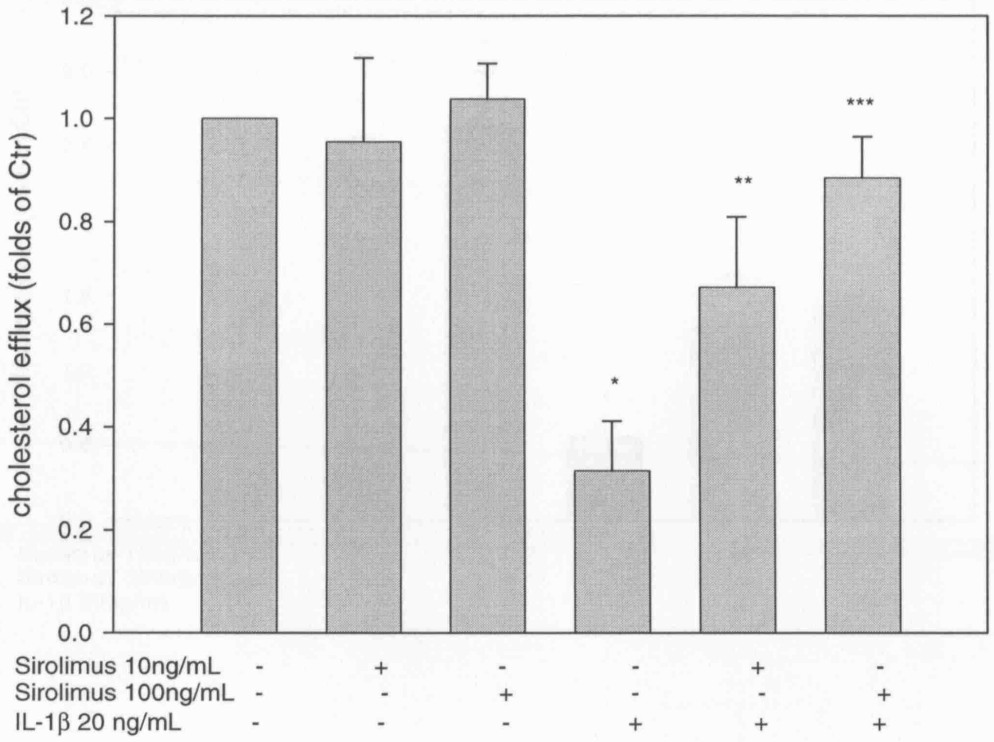

Fig 6.5 The effect of Sirolimus on intracellular cholesterol efflux in HepG2 cells. HepG2 cells were pre-loaded with cholesterol for 48 hours. The cholesterol loaded cells were then incubated in serum-free medium (control, Ctr) or serum-free medium without or with 20 ng/ml of IL-1β or 10-100 ng/ml of Sirolimus for 24 hours. The cholesterol efflux was measured by radioactive counts. Data represented Mean ± SD from four independent experiments. * p <0.001 *vs* control, ** p <0.01 *vs* IL-1β group, *** p <0.001 *vs* IL-1β group.

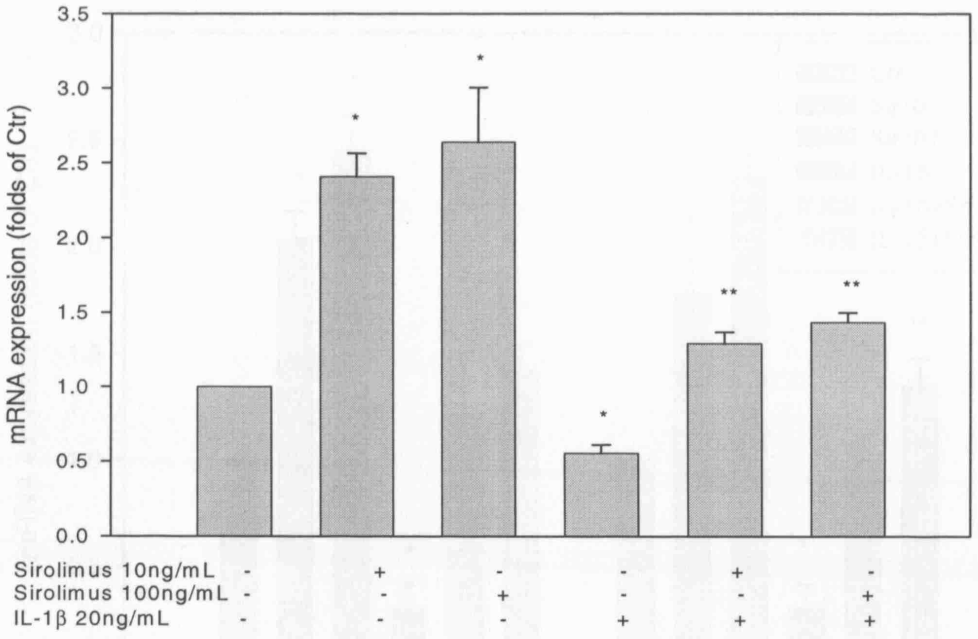

Fig 6.6 The effect of Sirolimus on mRNA expression of ABCA1 in cholesterol-loaded HepG2 cells. HepG2 cells were incubated in serum-free medium (control, Ctr) or serum-free medium with 20 ng/ml of IL-1β (IL-1β) or 10 ng/ml of Sirolimus (Sir10) or 100 ng/ml of Sirolimus (Sir100) or 20 ng/ml of IL-1β plus 10 ng/ml of Sirolimus (IL-1β+Sir10) or 20 ng/ml of IL-1β plus 100 ng/ml of Sirolimus (IL-1β+Sir100) for 24 hours. The mRNA expression of ABCA1 was determined following the ΔΔCt protocol for real-time RT-PCR as described in the section of Methods. β-actin served as the housekeeping gene. Results represented Mean ± SD from four experiments * p <0.001 *vs* control, ** p <0.001 *vs* IL-1β group.

Fig 6.7

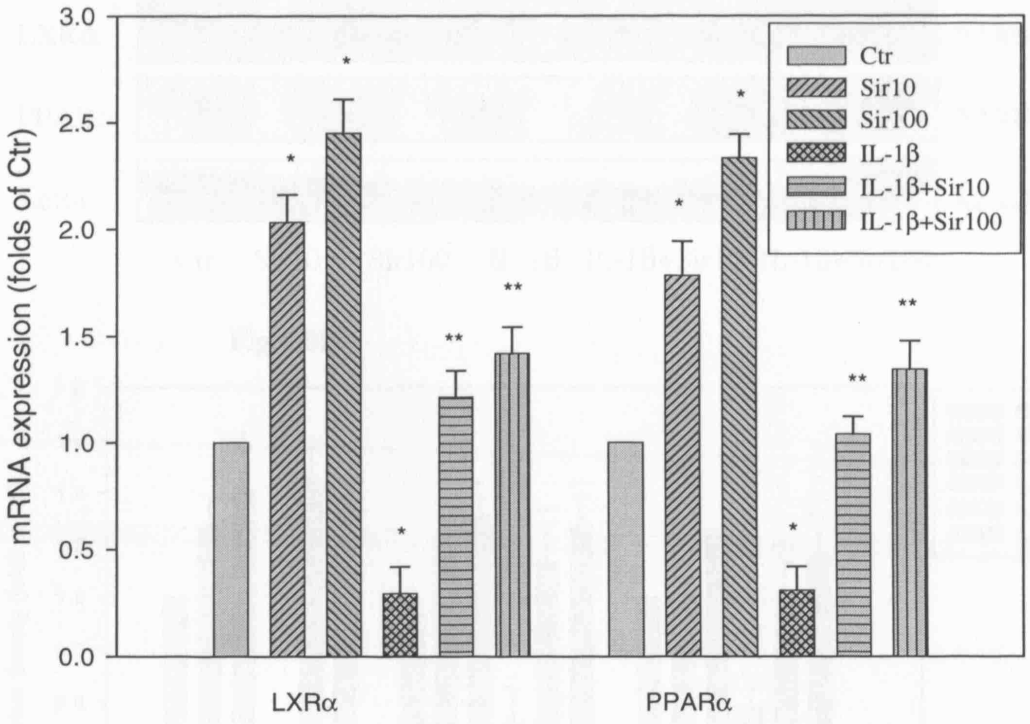

Fig 6.7 The effect of Sirolimus on the mRNA of LXRα and PPARα in cholesterol-loaded HepG2 cells. HepG2 cells were incubated in serum-free medium (control, Ctr) or serum-free medium with 10-100 ng/ml of Sirolimus (Sir10, Sir 100) or 20 ng/ml of IL-1β (IL-1β) or 20 ng/ml of IL-1β plus 10-100 ng/ml of Sirolimus (IL-1β+Sir10, IL-1β+Sir100) for 24 hours. The mRNA expression of LXRα and PPARα was determined following the ΔΔCt protocol for real-time RT-PCR as described in the section of Methods. β-actin served as the housekeeping gene. Results represented Mean ± SD from four experiments. * p <0.001 *vs* control, ** p <0.001 *vs* IL-1β group.

Fig 6.8a

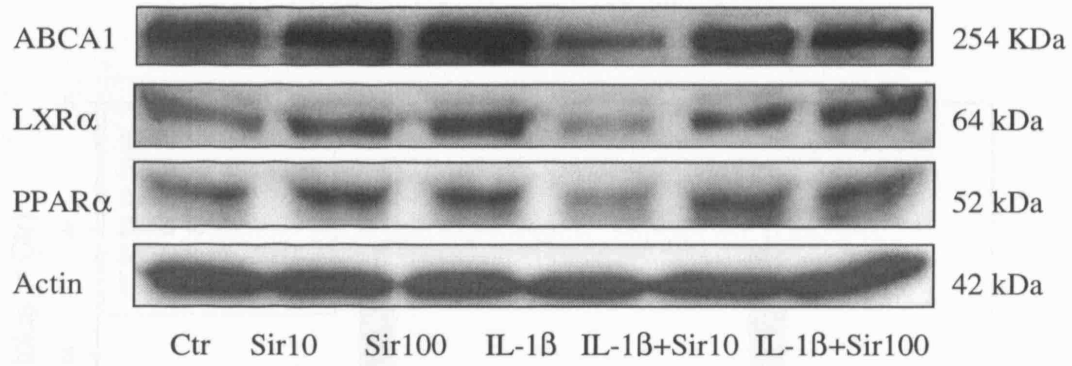

Fig 6.8b

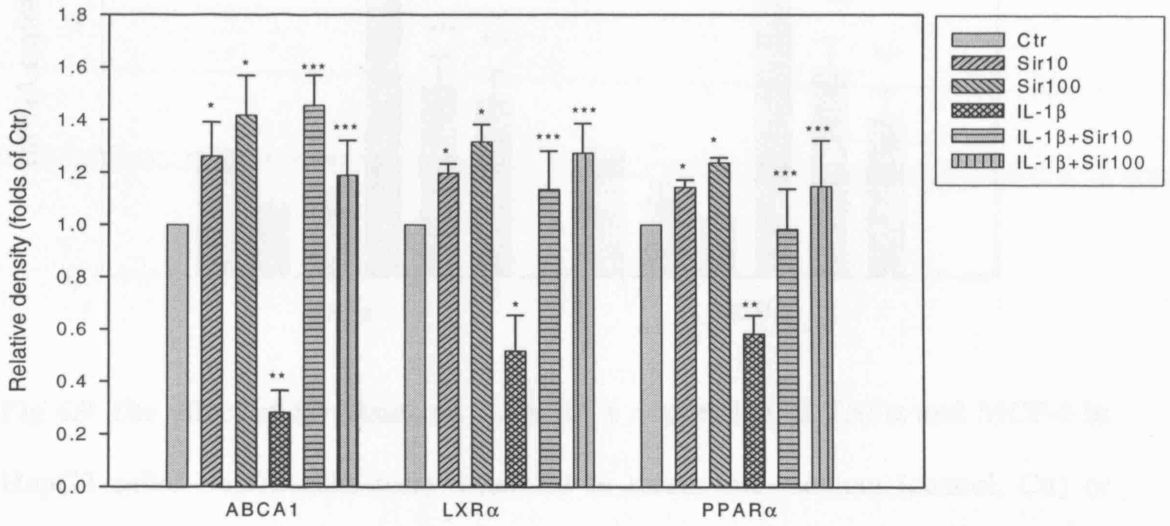

Fig 6.8a & 6.8b The effect of Sirolimus on the protein expression of ABCA1, LXRα and PPARα in cholesterol-loaded HepG2 cells. HepG2 cells were incubated in serum-free medium (control, Ctr) or serum-free medium with 10-100 ng/ml of Sirolimus (Sir10, Sir 100) or 20 ng/ml of IL-1β (IL-1β) or 20 ng/ml of IL-1β plus 10-100 ng/ml of Sirolimus (IL-1β+Sir10, IL-1β+Sir100) for 24 hours. The protein levels of ABCA1, LXRα and PPARα were examined by Western Blot. The histograms represented Mean ± SD of the densitometric scans of protein bands from four experiments, normalised by comparison with actin, and expressed as a percentage of the control. * p <0.001 *vs* control, ** p <0.001 *vs* control, *** p <0.001 *vs* IL-1β group.

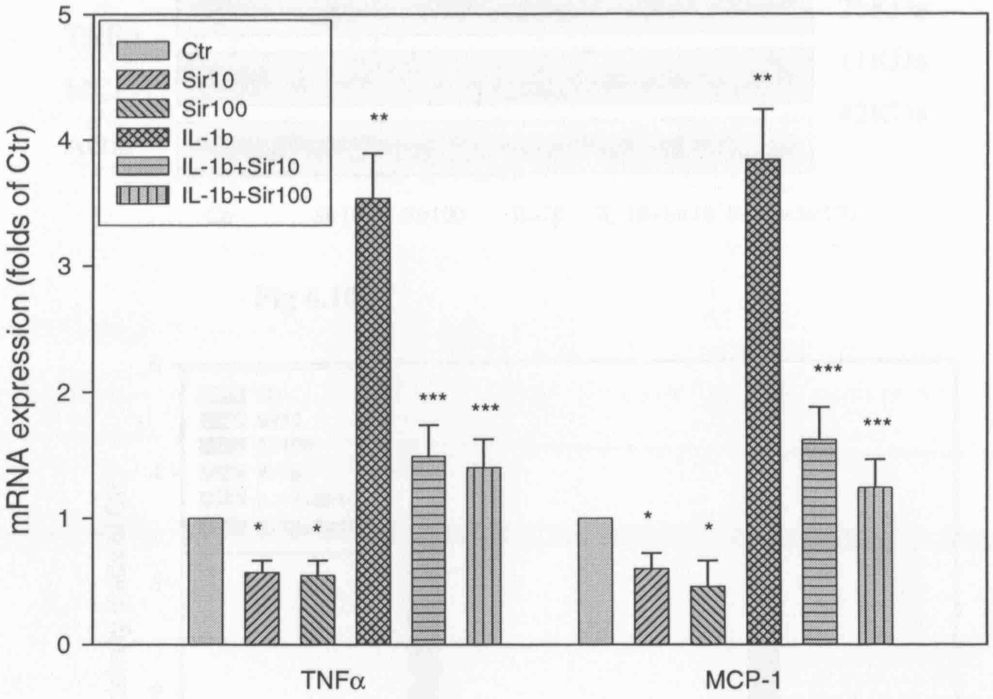

Fig 6.9 The effect of Sirolimus on the mRNA expression of TNFα and MCP-1 in HepG2 cells. HepG2 cells were incubated in serum-free medium (control, Ctr) or serum-free medium with 10-100 ng/ml of Sirolimus (Sir10, Sir 100) or 20 ng/ml of IL-1β (IL-1β) or 20 ng/ml of IL-1β plus 10-100 ng/ml of Sirolimus (IL-1β+Sir10, IL-1β+Sir100) for 24 hours. The mRNA expression of TNFα and MCP-1 was determined following the ΔΔCt protocol for real-time RT-PCR as described in the section of Methods. β-actin served as the housekeeping gene. Results represented Mean ± SD from four experiments. * p <0.001 *vs* control, ** p <0.001 *vs* control, *** p <0.001 *vs* IL-1β group.

Fig 6.10a

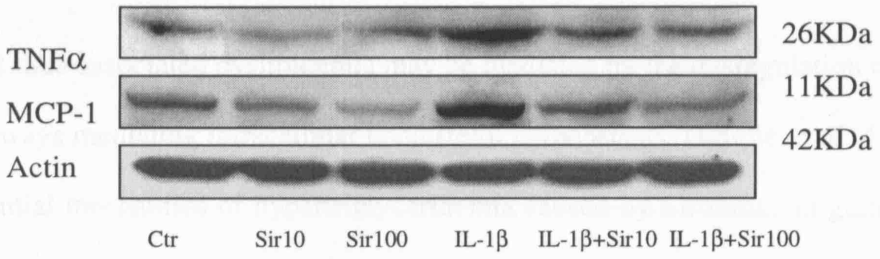

Fig 6.10b

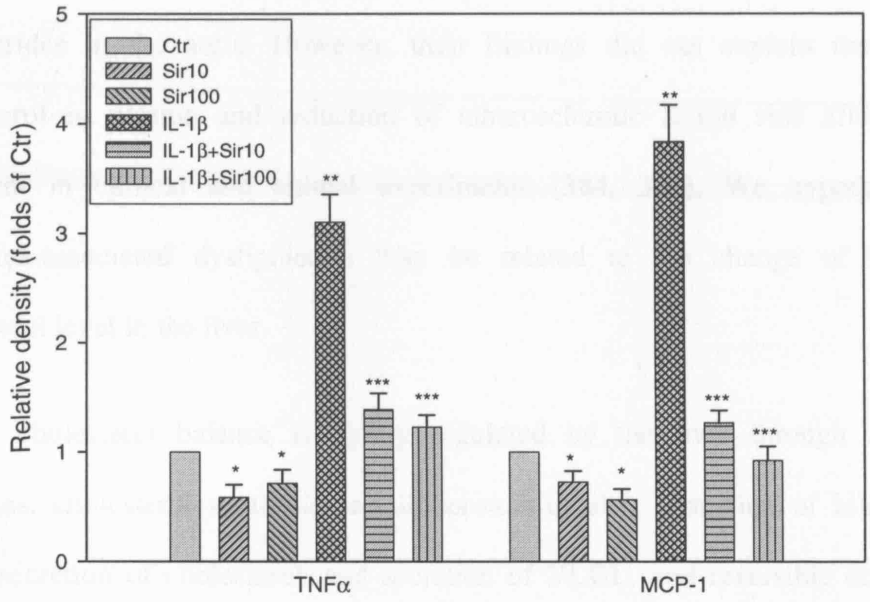

Fig 6.10a & 6.10b The effect of Sirolimus on the protein expression of TNFα and MCP-1 in HepG2 cells. HepG2 cells were incubated in serum-free medium (control, Ctr) or serum-free medium with 10-100 ng/ml of Sirolimus (Sir10, Sir 100) or 20 ng/ml of IL-1β (IL-1β) or 20 ng/ml of IL-1β plus 10-100 ng/ml of Sirolimus (IL-1β+Sir10, IL-1β+Sir100) for 24 hours. The protein levels of TNFα and MCP-1 were examined by Western Blot. The histograms represented Mean ± SD of the densitometric scans of protein bands from four experiments, normalised by comparison with actin, and expressed as a percentage of the control. * p <0.01 *vs* control, ** p <0.001 *vs* control, *** p <0.001 *vs* IL-1β group.

6.4 Discussion

Sirolimus-associated dyslipidemia may be mediated by the dysregulation of multi-signal pathways mediating intracellular cholesterol homeostasis. Dimple *et al* (454) reported a potential mechanism of hypertriglyceridemia caused by Sirolimus in guinea pigs. They demonstrated that Sirolimus disrupted triglycerides metabolism by altering the insulin signalling pathway, inducing increased secretion of VLDL and promoting deposition of triglycerides in the aorta. However, their findings did not explain the change of cholesterol in plasma and reduction of atherosclerotic lesion size after Sirolimus treatment in clinical and animal experiments (384, 386). We hypothesized that Sirolimus-associated dyslipidemia may be related to the change of intracellular cholesterol level in the liver.

Plasma cholesterol balance is tightly regulated by the liver through three major processes: cholesterol synthesis and lipoprotein uptake, formation of bile acids and biliary secretion of cholesterol, and secretion of VLDL, and reversible conversion of cholesterol to cholesteryl esters. The hepatic LDLr is the primary receptor for binding and internalisation of plasma-derived LDL-cholesterol and regulates plasma LDL concentrations by promoting the clearance of atherogenic LDL particles. We demonstrated that Sirolimus decreased intracellular lipid accumulation by reducing LDLr mediated cholesterol uptake in HepG2 cells induced by IL-1β. The down-regulation of LDLr induced by Sirolimus is probably due to an inhibitory effect on the SCAP/SREBP2 pathway. Confocal microscopy showed that Sirolimus attenuated translocation of SCAP escorting SREBP-2 from the ER to the Golgi, which prevented the formation of nuclear SREBP-2 to activate LDLr gene transcription in nucleus.

In this study, we demonstrated that Sirolimus dose-dependently increased ABCA1 gene expression in the absence or presence of IL-1β. Sirolimus also increased LXRα and

PPARα mRNA and protein expression in the absence or presence of IL-1β, which has been shown to contribute to the cholesterol efflux by synergistically up-regulating ABCA1 expression. We examined the function of ABCA1 by measuring cholesterol efflux using ApoA1 as an acceptor. As we demonstrated in other cell types, IL-1β decreased cholesterol efflux. However, Sirolimus reversed the reduction of cholesterol efflux induced by IL-1β, though the effect of Sirolimus alone on cholesterol efflux was not very obvious. Interestingly, Sirolimus inhibited TNFα and MCP-1 synthesis in HepG2 cells in the absence or presence of IL-1β, suggesting that amelioration of cholesterol homeostasis mediated by Sirolimus may partly be due to inhibition of inflammatory responses.

The current model for reverse cholesterol transport proposes that HDL transports excess cholesterol derived primarily from peripheral cells to the liver for removal. ABCA1 plays an important role in cholesterol efflux from peripheral cells. However, the role of ABCA1 mediated hepatic cholesterol efflux in HDL regulation remains unclear. Recent studies in ABCA1 transgenic mice suggest that ABCA1 may play a key role in hepatic cholesterol efflux which modulates cholesterol homeostasis in the liver. It establishes the liver as one of the major sources of plasma HDL-C (455) and hepatic ABCA1 is primarily responsible for regulating the level of plasma HDL (451, 455-457). This is against the conventional understanding. The finding that Sirolimus increased ABCA1 gene expression and cholesterol efflux in HepG2 cells in this study is also intriguing, and needs further studies to sort out the contribution of HDL cholesterol concentration from the liver and the classical reverse cholesterol transport from the peripheral tissues. It is possible that in physiological conditions, Sirolimus does not increase hepatic cholesterol efflux but restores the reduction of ABCA1 gene expression and cholesterol efflux inhibited by IL-1β to maintain cholesterol homeostasis in the liver. Hepatic

cholesterol efflux may regulate plasma HDL level and result in an expansion of apoB-lipoprotein cholesterol pool size via enhanced transfer of HDL-cholesterol to apoB-lipoproteins and delayed catabolism of cholesterol-enriched apoB-lipoproteins (458). The overall effect of Sirolimus on HDL and apoE lipoprotein needs to be further tested *in vivo* experiments.

We examined mRNA and protein expression of VLDLr in HepG2 cells, finding that its expression was too low to detectable. The Sirolimus-associated hypertriglyceridemia is not linked to dysregulation of hepatic VLDLr.

It has been reported that the therapeutic window for Sirolimus in human whole-blood is about 5-15 ng/ml (459) which is close to the concentrations used in this study. Taken together, these findings suggest that Sirolimus may result in an accumulation of LDL cholesterol in plasma by reducing hepatic LDLr expression. This may provide an explanation for hyperlipidemia caused by Sirolimus. The same effect also has been observed in peripheral cells in our previous studies (422), suggesting that Sirolimus reduces intracellular cholesterol level by increasing plasma cholesterol concentration. The amelioration of intracellular cholesterol homeostasis may protect cells from injuries caused by overloaded lipid and inflammatory cytokines or prevent the formation of foam cells, which is very important in reducing the risk of cardiovascular diseases in transplant patients. As experimental results from cell culture may not be reflected *in vivo*, we will further explore potential mechanism of Sirolimus in anti-atherosclerosis and its side effects in apoE KO mice under inflammatory stress.

CHAPTER 7. THE ANTI-ATHEROSCLEROTIC EFFECTS OF SIROLIMUS ON APOLIPOPROTEIN E KNOCKOUT MICE

7.1 Introduction

In previous several chapters, our *in vitro* studies demonstrated that inflammatory stress accelerated cholesterol accumulation and foam cell formation by disrupted cholesterol homeostasis. Sirolimus showed a significant anti-inflammatory effect. Hence, Sirolimus down-regulated LDLr-mediated cholesterol influx, down-regulated HMGR mediated cholesterol biosynthesis, and up-regulated ABCA1 mediated cholesterol efflux. These findings may explain the potential mechanisms of Sirolimus in anti-atherosclerosis. In addition, it may improve our understanding for Sirolimus-associated dyslipidemia happened in some clinical patients. To validate the results *in vitro* studies, we carried out *in vivo* studies by setting up an inflamed atherosclerotic animal model in apoE KO mice.

ApoE KO mice have been widely used as an atherosclerotic mouse model. At present, a few researchers have done some work in apoE KO mice to explore potential mechanisms of Sirolimus in anti-atherosclerosis (385-387, 389, 413, 460, 461). Their findings mainly concentrated on following several lines of evidence: i) Sirolimus inhibited monocyte chemotaxis (385, 387); ii) Sirolimus inhibited production of some inflammatory cytokines (386, 389); iii) Sirolimus was correlated with changes of endothelial nitric oxide synthase and matrix metalloproteinases (388, 389).

Sirolimus-associated dyslipidemia also has been investigated in apoE KO mouse model. Pakala *et al* (460) reported that Sirolimus had no effect on serum total cholesterol and triglyceride in ApoE KO mice; Naoum *et al* (389) showed that Sirolimus didn't affect serum total cholesterol, but its use resulted in a higher level of serum total triglyceride in ApoE KO mice; Elloso *et al* (386) reported that Sirolimus didn't affect serum total cholesterol and VLDL-cholesterol, but induced a higher levels of serum HDL-cholesterol and LDL-cholesterol in ApoE KO mice. Interestingly, Basso *et al* (413)

found that serum total cholesterol level was decreased in Sirolimus treated ApoE KO mice compared to controls. Although these studies showed some discrepancies, all of them confirmed anti-atherosclerotic effects of Sirolimus in ApoE KO mice.

The potential mechanism of Sirolimus in anti-atherosclerosis remains unclear. In this project, we hypothesized that Sirolimus prevented the progression of atherosclerotic lesion and foam cell formation by reducing intracellular cholesterol levels through normalisation of intracellular cholesterol homeostasis disrupted by inflammatory stress. Therefore, the *in vivo* study was to further investigate the effects of Sirolimus on cholesterol trafficking in ApoE KO mice under inflammatory stress induced by casein.

7.2 Materials and methods

7.2.1 The preparation of casein

7.2.1.1 Materials

1) Casein (Cat. NO. 904520, ICN Biochemicals, UK).

2) Sodium hydrogen carbonate ($NaHCO_3$, Cat. NO. S-8875, Sigma, Poole, Dorset, UK)

7.2.1.2 Procedures

1) Added 100 g casein into 1 liter of 50 mmol/l $NaHCO_3$ solution (4.2 g $NaHCO_3$ per liter of dH_2O).

2) Warmed up to assist the solubilization process after which a fairly viscous solution was obtained.

3) Aliquoted and stored at -20 ° C prior to use

7.2.2 The preparation of Sirolimus (387, 461)

7.2.2.1 Materials

1) Sirolimus (Cat. NO. AY-22989-39, Wyeth, Berkshire, UK)

2) Carboxymethylcellulose sodium (Cat. NO. C5013-500G, Sigma, Poole, Dorset, UK)

3) Polysorbat 80 (Cat. NO. 59924, Sigma, Poole, Dorset, UK)

7.2.2.2 Procedures

1) Preparation of Vehicle: Weighed 0.2 g of carboxymethylcellulose sodium, 0.25 g of polysorbate 80, then dissolved in 100 ml of dH_2O with stirring. Finally it was sterilized by autoclaving for use.

2) Preparation of Sirolimus suspension

Weighed 240 mg of Sirolimus in a sterile glass tissue grinder; added vehicle to 100 ml and homogenized with a stirrer-mounted plunger to make a uniform suspension containing 2.4 mg/ml of Sirolimus. The homogenization should be done until the suspension could be drawn easily through a 25-gauge syringe. Care should be taken to assure that the suspension remains uniformly distributed during dilutions and administration. The mice would be treated by Sirolimus with 8 mg/kg subcutaneous injection *q.o.d* (386) for 8 weeks.

7.2.3 The preparation of animal

7.2.3.1 Materials

1) Male apoE KO mice: The mice were in C57BL/6 genetic background.

2) Western Diet (Cat. NO. TD 88137, Harlan Teklad, UK): containing 0.15 % cholesterol, 21 % fat.

3) Sirolimus (Cat. NO. AY-22989-39, Wyeth, Berkshire, UK)

4) Casein (Cat. NO. 904520, ICN Biochemicals, UK).

5) Sirolimus suspension buffer

7.2.3.2 Procedures

The protocol was approved by Institutional Animal Care and Use Committee of the Research Institute, University College London. Male apoE KO mice obtained from Comparative Biological Unit of Royal Free Medical School were used in experiments. The mice were housed in a warm environment with 12-hour light and dark cycles. Eight-week-old male mice were fed with Western Diet for 8 weeks. The mice were divided into 4 groups (n=7, each group): control group, Sirolimus suspension buffer was subcutaneously injected at the back (0.1 ml sc. *q.o.d*); Sirolimus group, Sirolimus was subcutaneously injected at the back (8 mg/kg, sc. *q.o.d*,); casein group, 10 % casein was subcutaneously injected at the back (0.5 ml casein sc. *qd*, Monday to Friday of every week); Casein plus Sirolimus group, casein and Sirolimus were ssubcutaneously injected at the back respectively. Dietary intake of the animals was monitored weekly. Subsets of apoE KO mice from each group were weighed once every week, respectively.

7.2.4 Termination of animal experiments and preparation of tissues

The experiments were terminated at the end of the eighth week. I would like to thank my colleagues for their kind help in terminating *in vivo* experiments.

7.2.4.1 Materials

1) Pentobarbitone sodium Ph. Eur. Solution (Cat. NO. XVD132, Animalcare Ltd, York, UK)

2) Tissue-Tek® O.C.T. compound (Cat. NO. R1180, Agar, Essex, UK)

3) 2-methylbutane, anhydrous (Cat. NO. 277258, Sigma, Poole, Dorset, UK)

7.2.4.2 Procedures

1) Made a lethal anaesthesia by intraperitoneally injecting 0.5 ml of 10 % pentobarbitone sodium solution to ApoE KO mouse;

2) Weighed the body weight;

3) Sprayed mouse fur with ethanol to prevent loose fur in air.

4) Pinned mouse down with four limbs and cut the skin open.

5) Cut off the chest bone and exposed the heart;

6) Removed blood from right ventricle using a 1 ml of syringe and placed on ice.

7) Perfused with 40 ml of cold PBS solution for 5 minutes. Full perfusion was determined when lungs were clear and liver changed into pale colour.

8) Exposed the abdomen, and then excised the spleen, liver, kidney, fat and muscle. After cut off some tissues from them, immediately froze in liquid nitrogen for Tissue-Tek® O.C.T compound embedding.

9) O.C.T embedding: Placed tissues in the centre of the mould. Poured, not by squeezing, O.C.T into mould, to prevent bubbles until full of the mould. Ensured there were no gaps at the edge of mould. Placed cork circle onto O.C.T and pressed down firmly, but not as to displace O.C.T. Added 1-2 inches of 2-methylbutane into a plastic container and allowed to slowly harden (turn white) inside liquid nitrogen. Placed the mould in container for a few minutes to allow O.C.T to harden and placed it in -80 ^{o}C before sectioning.

10) Followed aorta down the back of spinal cord and cut thymus/near neck.

11) Removed excess tissue around aorta on dry tissue using blunt edge of scissors to remove background.

12) Whole clean aorta preparation: Placed aorta/heart in dish containing PBS and removed excess tissue under dissecting microscope with tweezers. Using scalpel, cut aorta nearest heart (keep heart in O.C.T at room temperature). Ensured full removal of excess fat around aorta, changing PBS regularly to reduce background as much as

possible. Cut open the whole aorta through intima using a mini scissor. Stained aorta with Oil Red O for a flat preparation. After that, moved aorta onto the slide and formed a Y shape at the root of aorta by using a dissecting scissor. Placed a cover slip over aorta after dropping a few mounting media. The lesions of aorta were stained as visibly red.

13) Aortic root preparation: Aortic root was located inside heart, where most lesions were located in atherosclerosis. Heart was stored in O.C.T at room temperature (It should be no tissue degradation as fixed already). Located aorta (dark colour and muscular walls) using dissecting microscope and placed heart on its side. With a scalpel, cut the heart below the tips of the atria in line with the aorta (approximately halfway). Placed aorta in the centre of mould with the aorta facing upwards. This allowed more control of sectioning starting from the ventricle to the aortic root. Poured, not by squeezing, O.C.T into mould, to prevent bubbles until level with mould. Ensured there were no gaps at the edge of mould. Placed cork circle onto O.C.T and pressed down firmly, but not as to displace O.C.T. Added 1-2 inches of 2-methylbutane into a plastic container and allowed to harden (turn white) inside liquid nitrogen. Placed mould in container for a few minutes to allow O.C.T to harden and placed it in -80 ^{o}C before sectioning.

14) Cross-sectioning: Before sectioning, took sections from -80^{o}C and placed in -20^{o}C for 2 hours-overnight, which allowed sections to equilibrate with the similar temperature in cryostat machine, preventing fractures of tissue when cutting.

15) Analysis: Using image pro-plus software drew around image, analysed colour and size of lesion.

7.2.5 Haematoxylin and Eosin staining

The oxidation product of haematoxylin is haematin, and is the active ingredient in the staining solution. Haematoxylin is not classified as a dye since the molecule does not possess chromophore. However, haematin exhibits indicator-like properties, being blue and less soluble in aqueous alkaline conditions, being red and more soluble in alcoholic acidic conditions. In acidic conditions, haematin binds to lysine residues of nuclear histones by linkage via a metallic ion mordant of aluminium. To ensure saturation of chemical binding sites, the stain is applied longer than necessary, resulting in the overstaining of the tissues with much non-specific background colouration. This undesirable colouration is selectively removed by controlled leaching in an alcoholic acidic solution (acid alcohol), the process being termed "differentiation". Differentiation is arrested by returning to an alkaline environment, whereupon the haematin takes on a blue hue, the process of "blueing-up". The haematin demonstrates cell nuclei.

Full cellular detail is obtained by counterstaining with the eosin mixture. There are three commonly used forms of eosin - eosin yellowish (tetrabromofluorescein, disodium salt), eosin bluish (the dinitro- dibromo-derivative), and eosin alcohol soluble (the ethyl derivative), the former is preferred. Colour enhancement is achieved by fortifying the stain with phloxine, a chemical member of the same family as eosin (halogenated fluorosceins). The mechanism of their staining is not fully understood, but is believed to be of an electrostatic nature. Visualisations most acceptable to the histologist are obtained by applying the dyes in acidic conditions, whereby more intense specific colourations are obtained, the more acidic tissue components taking up the dye to a greater intensity, hence the addition of acetic acid.

7.2.5.1 Materials:

1) Acetic acid (Cat. NO. A6283, Sigma, Poole, Dorset, UK):

2) 10 % Formalin (Cat. NO. F-1635, Sigma, Poole, Dorset, UK)

3) Haematoxylin solution (Cat. NO. GHS332, Sigma, Poole, Dorset, UK): added 2 ml of acetic acid per 100 ml of haematoxylin solution

4) Eosin (Cat. NO. 34197, BDH chemicals Ltd, Poole, U.K): dissolved 1.0 g of eosin yellowish in 100 ml of dH_2O. After that, added two drops acetic acid to eosin solution for use.

5) Hydrochloric acid (Cat. NO. 101252F, VWR International, Leicestershire, U.K)

6) Acidic alcohol: Added 1 ml of hydrochloric acid per 100 ml of 70 % ethanol

7) DPX mountant (Cat. NO. 360294H, VWR International, Leicestershire, U.K)

7.2.5.2 Procedures:

1) Thawed slides at room temperature for 5 minutes

2) Placed slides in 10 % formalin for 1 minute

3) Blotted excess liquid

4) Placed slides in haematoxylin solution for 4 minutes

5) Washed under running water until excess dye had gone

6) Placed slides in acidic alcohol for 2 minutes

7) Placed slides in eosin for 1 minute

8) Washed under running water until excess dye had gone

9) Allowed slides to dry and mounted with DPX and cover slides.

7.2.6 Evaluation of aortic lesions by Oil Red O staining

Five-μm-thick sections were made, beginning with the ascending aorta and proceeding through the entire aortic sinus until the ventricular chamber was reached. The sections were stained with Oil Red O and counter stained with Harris hematoxylin to quantify

the extent of atherosclerotic lesions using computerized morphometry. The procedures of Oil Red O staining have been previously described in Chapter 2.

7.2.7 Immunohistochemistry analysis

7.2.7.1 Materials

1) Primary antibody: rabbit anti-human SCAP polyclonal antibody (made by our laboratory); Mouse anti-human SREBP-2 monoclonal antibody (purified from Hybridoma, Cat.NO.CRL-2545^{TM}, LGC Promochem, Teddington, Middlesex, UK); Chicken anti-human LDLr polyclonal antibody (Cat.NO.ab14056, Abcam, Cambridge, UK)

2) Biotinylated secondary antibody: Anti-mouse IgG (Cat. No. PK-6102, Vector Laboratories, Bath, UK); Anti-rabbit IgG (Cat. No. BA-1000, Vector Laboratories, Bath, UK); Anti-chicken IgG (Cat. No. BA-9010, Vector Laboratories, Bath, UK)

3) Blocking serum: Normal horse serum (Cat. No. PK-6102, Vector Laboratories, Bath, UK); normal goat serum (Cat. No. S-1000, Vector Laboratories, Bath, UK)

4) Reagent A and B (Cat. No. PK-6102, Vector Laboratories, Bath, UK).

5) Endogenous Avidin + Biotin Blocking System: Avidin blocking and Biotin blocking (Cat. No. ab3387, Abcam, Cambridge, UK)

6) Peroxidase substrate kit DAB (Cat. No. SK-4100, Vector Laboratories, Bath, UK).

7.2.7.2 The preparation of working solution, DAB staining and Standard ABC procedures

These procedures were previously described in Chapter 5.

7.2.8 Lipid profile assay

The serum lipid profile in apoE KO mice (total cholesterol, total triglyceride, LDL and HDL) were measured at Lipid laboratory of Clinical Biochemistry Department in Royal Free Medical School.

7.2.9 ELISA for cytokines (SAA, TNFα, and MCP-1)

7.2.9.1 Mouse SAA assay

Nonspecific inflammatory responses are the most basic of the host defence mechanisms. If the initial inflammatory stimulus results in sufficient tissue damage, a systemic response ensues. It is characterised in part by a greatly increased synthesis of a group of serum proteins termed acute-phase reactants. The prototype acute-phase reactant in humans is CRP. Mouse CRP occurs in very low concentration in the serum and has not yet been documented as an acute-phase reactant (104, 105). The documented acute-phase reactants in mice include SAA and SAP (105-107). SAA is an acute-phase protein with 12-14 KDa of molecular weight, which is produced primarily by the liver in response to IL-1, IL-6, and TNF. During acute events, the rise in the level of SAA in blood exhibits the most intense and rapid increase among all acute-phase proteins. SAA reaches a concentration of up to 1 mg/ml in the sera of acutely ill patients. This concentration is 100 - 1000 times as the normal physiological level. Increased levels of SAA correlate with the presence of pathogens. A decrease of SAA level during antimicrobial therapy is reportedly a good indicator of efficacious antibiotic therapy in patients. The immunomodulatory effects of SAA in the regulation of immune response to T-dependent antigens, the reduction of prostaglandin E2 and the fever response, coupled with the remarkable increase of SAA level during an inflammatory incident, have created an interest in its utility for monitoring inflammation in a variety of disease conditions.

7.2.9.1.1 Principle of the method

A solid phase sandwich ELISA was used to check the SAA level in the mouse serum. A monoclonal antibody specific for SAA has been coated onto the wells of the microtiter strips provided. During the first incubation, standards of known mouse SAA content, controls and unknown samples were pipetted into the coated wells, followed by the addition of biotinylated second monoclonal antibody. After washing, Streptavidin-Peroxidase (enzyme) was added, which binded to the biotinylated antibody to complete the four-member sandwich. After a second incubation, a substrate solution was added, which was acted upon by the bound enzyme to produce colour. The intensity of this coloured product was directly proportional to the concentration of mouse SAA presented in the original specimen.

7.2.9.1.2 Materials

1) Mouse SAA ELISA kit (Cat. NO. A2275-60V, United States Biological Ltd)

2) Model 3550 microplate reader (Bio-Rad, U.S.A)

7.2.9.1.3 Preparation of solutions

1) Reconstitution and dilution of mouse SAA Standard: Reconstituted standard to 10 μg/ml with 1.2 ml of Standard Diluent Buffer. Swirled or mixed gently for 10 minutes to ensure complete reconstitution. Used the standard within 15 minutes of reconstitution or aliquot and stored at -80 °C; prepared 300 μl of standard by making serial dilutions as 0, 0.155, 0.31, 0.62, 1.25, 2.5, 5, 10 μg/ml.

2) The preparation of Streptavidin-HRP working solution: diluted 100x concentrated solution of Streptavidin-HRP by using Streptavidin-HRP Diluent Buffer within 1 hour of use.

3) The preparation of wash buffer: diluted 25x Wash Buffer with dH_2O for use.

4) Low control and High control: Reconstituted with 2.8 ml and 1.6 ml of diluent buffer respectively.

7.2.9.1.4 Procedures

1) Determined the number of 8-well strips needed for the assay. Inserted strips in the frames for current use.

2). Tissue culture samples should be analyzed neat.

3) Added 100 µl of the Standard Diluent Buffer to zero wells. Wells reserved for chromogen blank should be left empty.

4) Added 100 µl of the Standards to the appropriate microtiter wells.

5) Prepared duplicate wells for each serum sample with 50 times' dilution by incubation buffer.

6) Pipetted 50 µl of biotinylated anti-mouse SAA (Biotin) solution into each well except the chromogen blanks. Mixed by tapping on the side of the plate for 30 seconds. Covered plate with plate cover and incubated for 1 hour at 37 °C.

7) Washed wells 4 times, and then added 100 µl Streptavidin-HRP working solution to each well except the chromogen blanks. Covered plate with plate cover and incubated for 30 minutes at room temperature.

8) Washed wells 4 times, and then added 100 µl of stabilized chromogen to each well. The liquid in the wells would begin to turn blue. Incubated for 15 minutes at room temperature in the dark.

9) Added 100 µl of Stop solution to each well. Mixed by gently tapping side of plate. The solution in the wells should change from blue to yellow. Read the absorbance of each well at 450 nm within 30 minutes after adding Stop solution.

10) Calculated the mouse SAA concentrations for unknown samples and controls from the standard curve.

7.2.9.2 Mouse serum TNFα assay

The AssayMax Mouse TNFα ELISA kit is designed for detection of TNFα in mouse serum or cell culture supernatants. This assay employs a quantitative sandwich enzyme immunoassay technique that measures TNFα in 3.5 hours. A murine monoclonal antibody specific for mouse TNFα has been pre-coated onto a microplate. TNFα in standards and samples is sandwiched by the immobilized antibody and a biotinylated polyclonal antibody specific for mouse TNFα, which is recognized by a streptavidin-peroxidase conjugate. All unbound material is then washed away and a peroxidase enzyme substrate is added. The colour development is stopped and the intensity of the colour is measured.

7.2.9.2.1 Materials

1) Mouse TNFα ELISA Kit (Cat. NO. EMT-2010-1, Assaypro, Cambridge, UK)

2) Model 3550 microplate reader (Bio-Rad, U.S.A)

7.2.9.2.2 Reagent preparation

1) Freshly diluted all reagents and brought all reagents to room temperature before use. If crystals have formed in the concentrate, mix gently until the crystals have completely dissolved.

2) Standard curve: Reconstituted the 4 ng of mouse TNFα Standard with 1 ml of EIA Diluent to generate a 4 ng/ml of solution. Allowed the standard to sit for 10 minutes with gentle agitation prior to making dilutions. Prepared triplicate standard points by serially diluting the TNFα standard solution two-fold with equal volume of EIA Diluent

to produce 2, 1, 0.5, 0.25, 0.125, and 0.0625 ng/ml. EIA Diluent served as the zero standard (0 ng/ml).

3) EIA Diluent Concentrate (10x): Diluted the EIA Diluent Concentrate 1:10 with reagent grade water.

4) Biotinylated TNFα antibody (100x): Spun down the antibody briefly and diluted the desired amount of the antibody 1:100 with EIA Diluent.

5) Wash Buffer Concentrate (10x): Diluted the Wash Buffer Concentrate 1:10 with reagent grade water.

6) Streptavidin-Peroxidase Conjugate (100x): Spun down the SP Conjugate briefly and diluted the desired amount of the conjugate 1:100 with EIA Diluent.

7.2.9.2.3 Procedures

1) Prepared all reagents, working standards and samples as instructed. Brought all reagents to room temperature before use. The assay was performed at room temperature (20-30 ^{0}C).

2) Removed excess microplate strips from the plate frame and returned them immediately to the foil pouch with desiccant inside. Resealed the pouch securely to minimize exposure to water vapour and stored in a vacuum desiccator.

3) Added 50 µl of Standard or sample (10 times' dilution for mouse serum) per well. Covered wells and incubated for two hours.

4) Washed five times with 200 µl of Wash buffer. Inverted the plate and decanted the contents, and hit it 4-5 times on absorbent paper towel to complete remove liquid at each step.

5) Added 50 µl of Biotinylated TNFα antibody to each well and incubated for 1 hour.

6) Washed five times with 200 µl of Wash buffer as above.

7) Added 50 µl of Streptavidin-Peroxidase Conjugate per well and incubated for 30 minutes. Turned on the microplate reader and set up the program in advance.

8) Washed five times with 200 µl of Wash Buffer as above.

9) Added 50 µl of Chromogen Substrate per well and incubated for approximately 10 minutes or till the optimal blue colour density developed. Gently tapped the plate to ensure thorough mixing and broke the bubbles in the well with pipetted tip.

10) Added 50 µl of Stop solution to each well. The colour would change from blue to yellow.

11) Read the absorbance on a microplate reader at a wavelength of 450 nm immediately.

7.2.9.3 Mouse serum MCP-1 assay

7.2.9.3.1 Materials

1) Mouse MCP-1 Biotrak ELISA System (Cat. NO. RPN2703, GE Healthcare, Buckinghamshire, UK)

2) Model 3550 microplate reader (Bio-Rad, U.S.A)

7.2.9.3.2 Reagent preparation

1) Wash buffer: diluted 30x wash buffer with distilled or deionized water and Mixed thoroughly. Wash buffer would be at room temperature prior to use in the assay.

2) Standards: Reconstituted standard with distilled or deionised water using the reconstitution volume stated on the vial label. Mixed by gently inverting the vial until contents were dissolved. Used the sample diluent to prepare the standard curve dilutions. Prepared 1:2 serial dilutions for the standard curve as follows: Pipetted 150 µl of sample diluent into each tube. Pipetted 150 µl of the reconstituted standard into the first tube, 1000 pg/ml, and mixed. Pipetted 150 µl of this dilution into the next tube, 500

pg/ml and mixed. Repeated serial dilutions five more times. The standard curve comprised points at: 1000 pg/ml, 500 pg/ml, 250 pg/ml, 125 pg/ml, 62 pg/ml, 31 pg/ml, 16 pg/ml and 0 pg/ml.

3) Streptavidin-HRP solution: Prepared streptavidin-HRP solution no more than 15 minutes prior to use. To prepare streptavidin-HRP solution, added 30 µl of streptavidin-HRP concentrate to 12 ml streptavidin-HRP dilution buffer and mixed gently.

7.2.9.3.3 Procedures

1) Determined the number of strips required. Set these strips in the plate frame. Recorded the locations of the zero standard, mouse MCP-1 standards and test samples. Seven standards and one zero must be run in duplicate with each series of unknown samples.

2) Added 50 µl sample diluent into each well. Added 50 µl of standards or test samples (5 times' dilution for mouse serum) in duplicate to each well. Carefully covered the plate with an adhesive plate cover. Incubated for 1 hour at room temperature.

3) At the end of the incubation period, Washed the plate three times with wash buffer. Added 100 µl of biotinylated antibody reagent to each well. Incubated for 1 hour at room temperature.

4) At the end of the incubation period, washed the plate three times with wash buffer. Using a single or multichannel pipette, added 100 µl of prepared streptavidin-HRP solution to each well. Incubated the plate for 30 minutes at room temperature.

5) At the end of the incubation, washed the plate three times. Pipetted 100 µl of premixed TMB substrate solution into each well. Allowed enzymatic colour reaction to develop in the dark at room temperature for 30 minutes. The substrate reaction yielded a blue solution that turned yellow when stop solution was added.

6) After 30 minutes, Added 100 µl of Stop solution to each well.

7) Measured the absorbance on an ELISA reader by setting dual wavelengths at 450 nm for measuring wavelength and 550 nm for reference wavelength. The plate must be read within 30 minutes of stopping the reaction.

7.2.10 Real-time RT-PCR

7.2.10.1 The preparation of samples

7.2.10.1.1 Materials

1) Tissue homogenizer (Cat. NO. 985370-07, BioSpec Products Inc, USA)

2) RNAgents denaturing solution (Cat.NO.Z5651, Promega, Southampton, UK).

7.2.10.1.2 Procedures

1) Samples to be extracted should be as fresh as possible to obtain optimal performance from this system. Otherwise, froze the samples immediately in liquid nitrogen and then stored at -70°C for future use. The volumes of reagents might be adjusted proportionally for different amounts of starting material (Table 7.1).

2) Dispensed the recommended volume of denaturing solution into a sterile tube and chilled on ice for five minutes.

3) Placed the fresh or frozen tissue sample into the denaturing solution and disrupted the tissue with a homogenizer on high setting for 15~30 seconds. Ensured that no fragments of tissue or clumps of cells were visible. Processed the samples as quickly as possible. Samples homogenized in denaturing solution might be stored indefinitely at -70°C.

The following steps, the isolation and purification of total RNA, reverse transcription, and real-time PCR were already previously described in Chapter 2. All mouse Taqman primers designed by Primer Express Software V2.0 were shown in Table 2.6 in Chapter 2.

Table 7.1 Tube size and volumes of reagents to be used for varying tissue mass and cell number

Recommended Tube Size (minimum)	Tissue	Cultured Cells	Denaturing Solution	2M Sodium Acetate	Phenol: Chloroform: IAA	Denaturing Solution*
30ml	1,000mg	1.0×10^8	12ml	1,200µl	12ml	5ml
30ml	750mg	7.5×10^7	9ml	900µl	9ml	
15ml	500mg	5.0×10^7	6ml	600µl	6ml	
15ml	250mg	2.5×10^7	3ml	300µl	3ml	2.5ml
15ml	100mg	1.0×10^7	1.2ml	120µl	1.2ml	
2ml	75mg	7.5×10^6	900µl	90µl	900µl	
1.5ml	50mg	5.0×10^6	600µl	60µl	600µl	500µl
1.5ml	25mg	2.5×10^6	300µl	30µl	300µl	
0.5ml	10mg	1.0×10^6	120µl	12µl	120µl	100µl
0.5ml	5mg	5.0×10^5	60µl	6µl	60µl	

Abbreviation: IAA = Isoamyl Alcohol.

*Refers to the second resuspension with Denaturing Solution.

Note: Samples of 75mg or less, or 7.5×10^6 cells or fewer, can be processed in microcentrifuge tubes. For tissue mass or cell numbers not listed in Table 1, use the next highest listed volume or proportionally scale the solutions to the sample size.

Do not exceed 1g tissue or 1×10^8 cells per 12ml (or 1µg per 5µl) of Denaturing Solution.

7.2.11 Western Blot

1) Extracted proteins through disrupting and homogenizing tissues in 3 ml ice-cold lysis buffer per gram of tissue with a homogenizer.

2) The other procedures were already previously described in Chapter 2.

7.3 Results

7.3.1 ApoE KO mice used in experiments and isolated aorta, heart and kidney

Fig 7.1 showed apoE KO mice in experiments. Fig 7.2 showed isolated aorta, heart, and kidney from apoE KO mice after experimental extermination.

7.3.2 Induction of systemic inflammation and anti-inflammatory effect of Sirolimus in apoE KO mice

We induced an inflamed atherosclerotic model in apoE KO mice by injecting with 10% casein. There was a significant increase of SAA, TNFα, and MCP-1 in the serum of casein injected mice compared to the control (Fig 7.3, Fig 7.4, and Fig 7.5), suggesting that systemic inflammation is successfully induced. Interestingly, Sirolimus markedly inhibited the increase of SAA, TNFα and MCP-1 in the serum of apoE KO mice in the absence or presence of casein injection, which indicated an anti-inflammatory effect.

7.3.3 Comparison of body weight in apoE KO mice in the absence or presence of Sirolimus or casein injection

We observed the change of body weight in apoE KO mice treated by Sirolimus or casein. Each apoE KO mouse was allocated the same quantities of Western Diet per day. The body weight for each mouse was determined at the start and termination. As shown in Fig 7.6, the body weights in apoE KO mice were not significantly different among different groups at the start. However, at the termination of experiments the body weights were decreased in Sirolimus treated apoE KO mice and in casein treated apoE KO mice compared to controls. Furthermore, there was a more significant decreased body weight in the Sirolimus plus casein treated group compared to the casein only group.

7.3.4 Serum lipid profile analysis in apoE KO mice in the absence or presence of Sirolimus or casein injection

Fig 7.7 showed that there were significantly decreased serum levels of total cholesterol, total triglyceride, LDL, and HDL in casein injected apoE KO mice compared to controls. There was no difference in the serum levels of total cholesterol, total triglyceride, LDL, and HDL among different groups after Sirolimus treatment. These

results suggest that systemic inflammation causes hypolipidemia in apoE KO mice. However, Sirolimus treatment did not result in changes in the serum lipid profile (total cholesterol, total triglyceride, LDL, and HDL) in apoE KO mice.

7.3.5 The effect of Sirolimus on formation of atherosclerotic plaque in apoE KO mice

Next, we checked the formation of atherosclerotic plaque in aortas of apoE KO mice by Oil Red O staining with computer-assisted image analysis. As shown in Fig 7.8 and Fig 7.9a & b, Sirolimus significantly reduced atherosclerotic lesion size compared to the control. Inflammatory stress induced by casein injection exacerbated formation of atherosclerotic plaque, however, it was inhibited by Sirolimus. This suggests Sirolimus protects against atherogenesis.

7.3.6 The effect of Sirolimus on LDLr mediated pathway in aortas of apoE KO mice.

Furthermore, we checked the effect of Sirolimus on the LDLr mediated pathway in aortas of apoE KO mice by immunohistochemical staining. Results showed that inflammatory stress increased the protein expression of LDLr, SCAP and SREBP-2 in aortas of casein injected apoE KO mice. However, Sirolimus inhibited the protein expression of LDLr, SCAP and SREBP-2 in aortas of apoE KO mice in the absence or presence of casein injection (Fig 7.10, Fig 7.11, and Fig 7.12). This suggests that Sirolimus ameliorates dysregulation of LDLr mediated pathway induced by inflammatory stress and prevents the progression of atherosclerosis.

7.3.7 The effect of Sirolimus on lipid accumulation in the livers of apoE KO mice

The liver is the central organ for lipid metabolism. Therefore we also investigated the effect of Sirolimus on lipid accumulation in the livers of apoE KO mice. Results showed inflammatory stress significantly increased lipid accumulation with the

appearance of multiple fat vacuoles in the liver of casein injected mice (Fig 7.13a C and Fig 7.13b C). However, Sirolimus inhibited the lipid accumulation and formation of fat vacuoles induced by inflammatory stress (Fig 7.13a D and Fig 7.13b D), which was further confirmed by quantification of cholesterol ester in the liver (Fig 7.14).

7.3.8 The effects of Sirolimus on cholesterol homeostasis in the livers of apoE KO mice in the presence or absence of inflammatory stress

To explore potential mechanisms, we further investigated the effect of Sirolimus on cholesterol homeostasis in the livers of inflamed apoE KO mice. First, we checked LDLr mediated cholesterol uptake in the liver. Inflammatory stress up-regulated the expression of SCAP, SREBP-2, and LDLr in the liver. However, Sirolimus inhibited the expression of SCAP, SREBP-2, and LDLr induced by inflammatory stress (Fig 7.15, Fig 7.16a and Fig 7.16b).

Efflux of cholesterol and phospholipids mainly mediated by ABCA1 plays an important role in the maintenance of cholesterol homeostasis. Therefore, we also examined the ABCA1 mediated cholesterol efflux pathway in the liver of apoE KO mice. Sirolimus significantly increased the gene and protein expression of ABCA1, LXRα and PPARα in the liver that was inhibited by inflammatory stress (Fig 7.17, Fig 7.19a and Fig 7.19b). We also checked liver ABCG1 mRNA expression, a regulatory protein of cholesterol efflux system coordinated with ABCA1 to modulate intracellular cholesterol efflux. Sirolimus increased ABCG1 mRNA expression in the liver in the absence or presence of inflammatory stress (Fig 7.18).

7.3.9 The effects of Sirolimus on the production of inflammatory cytokines in the livers of apoE KO mice in the presence or absence of casein injection

Our *in vitro* studies have shown that Sirolimus inhibited the production of inflammatory cytokines. Accordingly, we checked the effect of Sirolimus on the production of

inflammatory cytokines in the livers of apoE KO mice. As predicted, Sirolimus significantly inhibited synthesis of inflammatory cytokines in the livers in the absence or presence of casein injection (Fig 7.20, Fig 7.21a and Fig 7.21b).

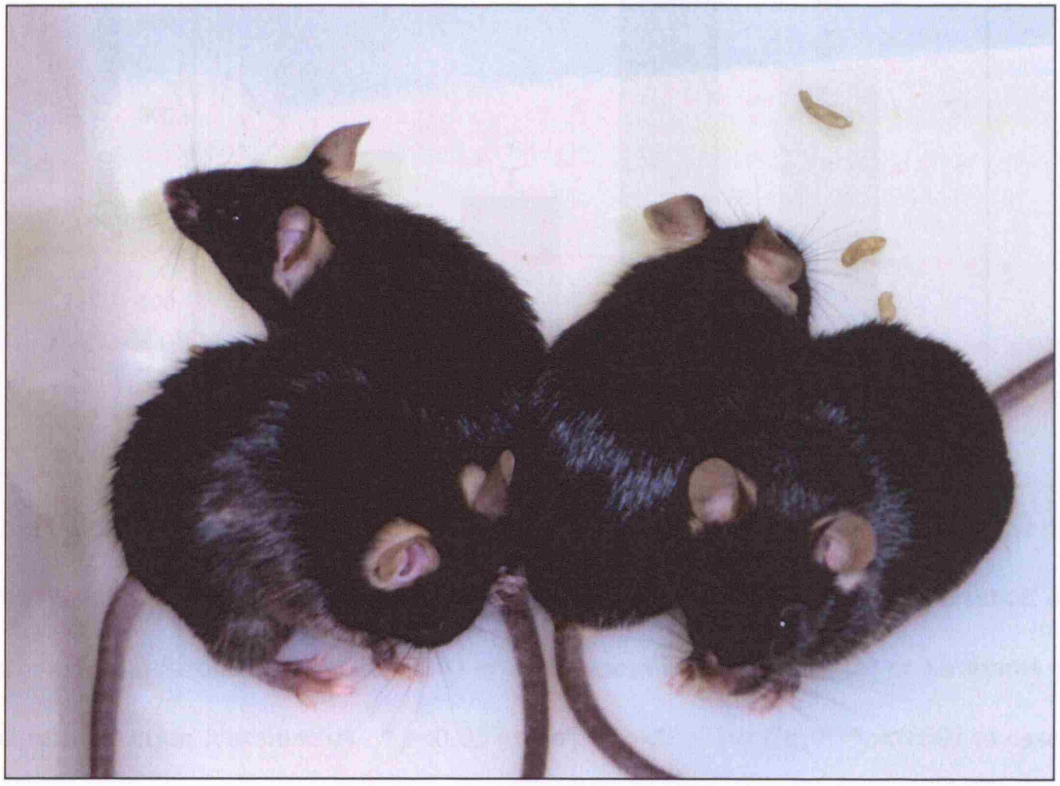

Fig 7.1 ApoE KO mice in experiments

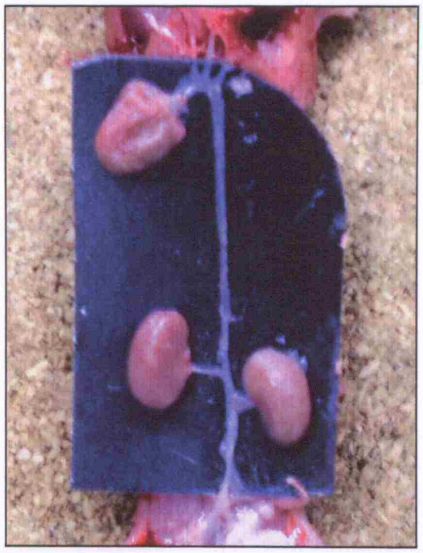

Fig 7.2 Isolated aorta, heart and kidney from apoE KO mice

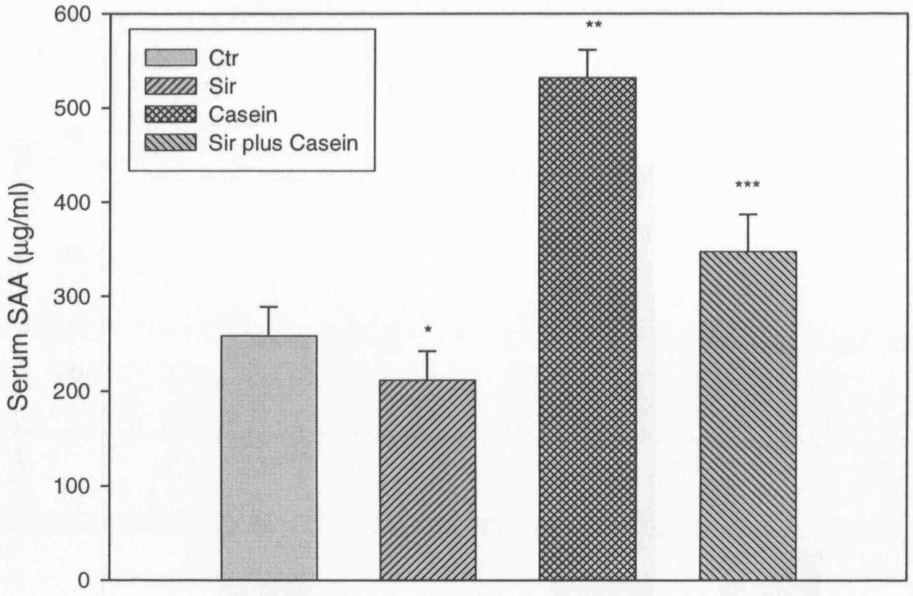

Fig 7.3 Serum level of SAA at the termination of experiments (n=7). ApoE KO mice were fed with Western Diet for eight weeks in the absence (Ctr) or presence of 8 mg/kg/q.o.d Sirolimus injection (Sir) or 10% casein injection (casein) or Sirolimus plus casein injection (casein+Sir). * $p<0.05$ *vs* Ctr, ** $p<0.001$*vs* Ctr, ***$p<0.001$ *vs* casein.

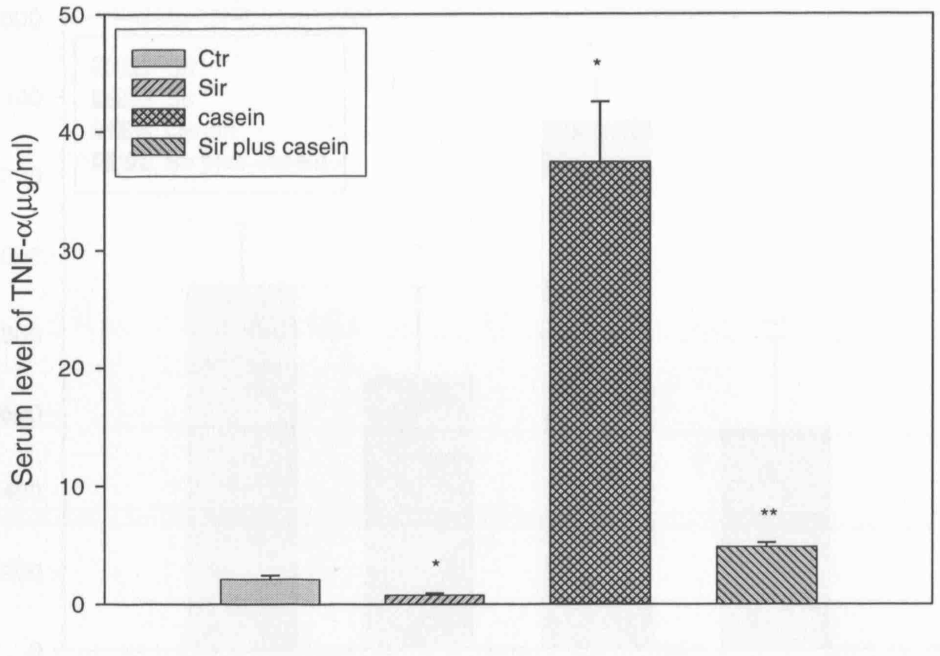

Fig 7.4 Serum level of TNFα at the termination of experiments (n=7). ApoE KO mice were fed with Western Diet for eight weeks in the absence (Ctr) or presence of 8 mg/kg/q.o.d Sirolimus injection (Sir) or 10% casein injection (casein) or Sirolimus plus casein injection (casein+Sir). * $p<0.001$ *vs* Ctr, ** $p<0.001$ *vs* casein.

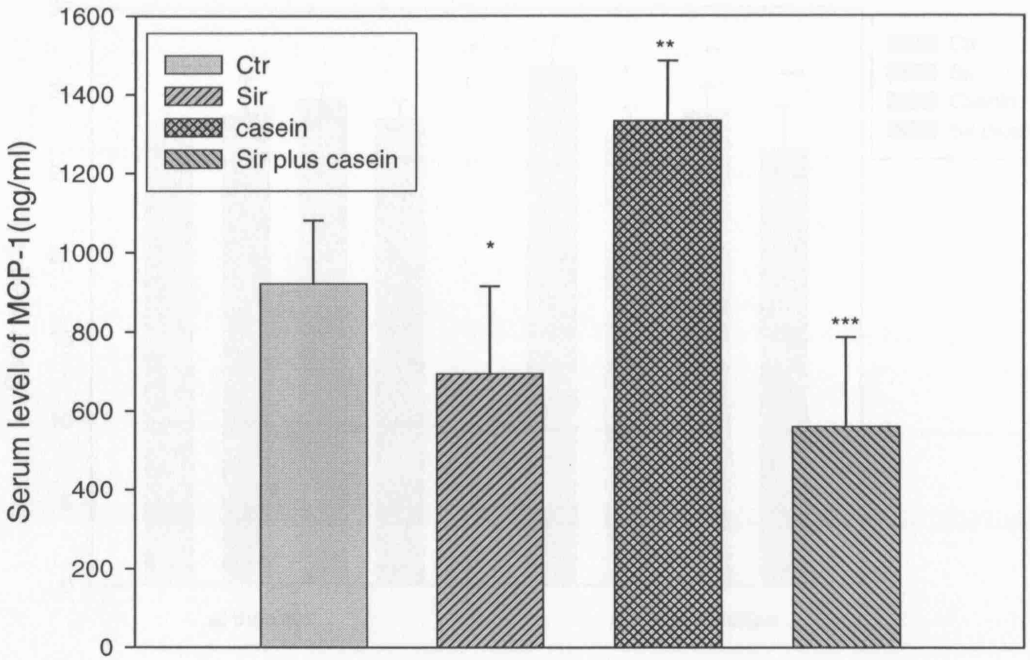

Fig 7.5 Serum level of MCP-1 at the termination of experiments (n=7). ApoE KO mice were fed with Western Diet for eight weeks in the absence (Ctr) or presence of 8 mg/kg/q.o.d Sirolimus injection (Sir) or 10 % casein injection (casein) or Sirolimus plus casein injection (casein+Sir). * $p<0.05$ *vs* Ctr, ** $p<0.001$ *vs* Ctr, ***$p<0.005$ *vs* casein.

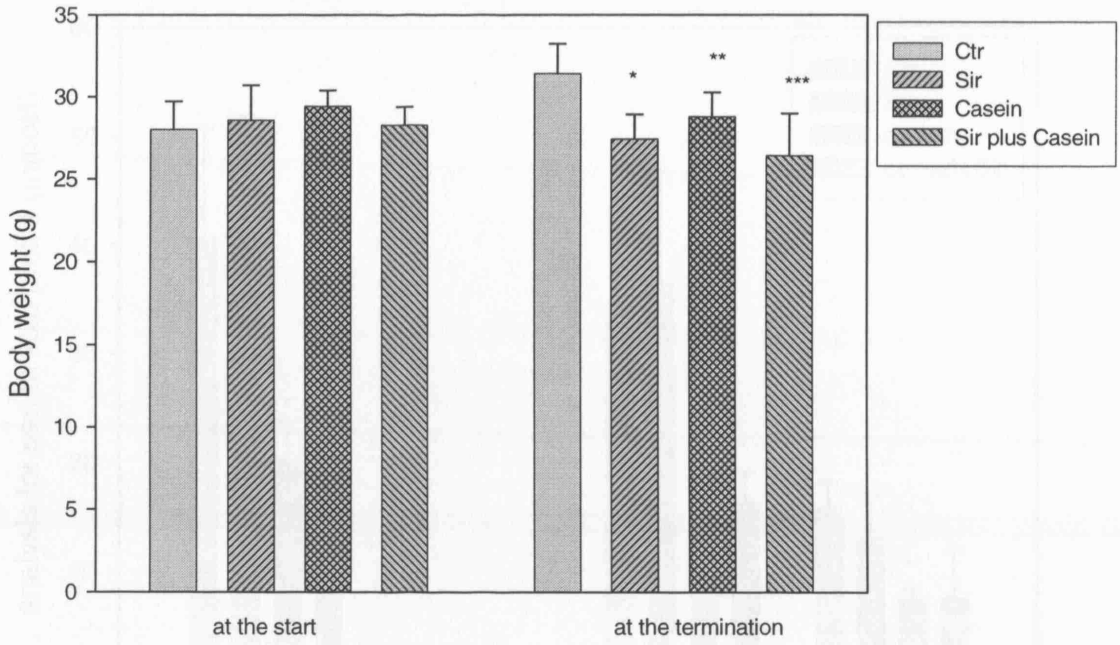

Fig 7.6 Comparison of body weight in different groups at the start and termination of experiments (n=7). ApoE KO mice were fed with Western Diet for eight weeks in the absence (Ctr) or presence of 8 mg/kg/q.o.d Sirolimus injection (Sir) or 10% casein injection (casein) or Sirolimus plus casein injection (casein+Sir). * $p<0.001$ *vs* Ctr, ** $p<0.01$ *vs* Ctr, ***$p<0.05$ *vs* casein. For the body weight at the start, there was no significance among different groups.

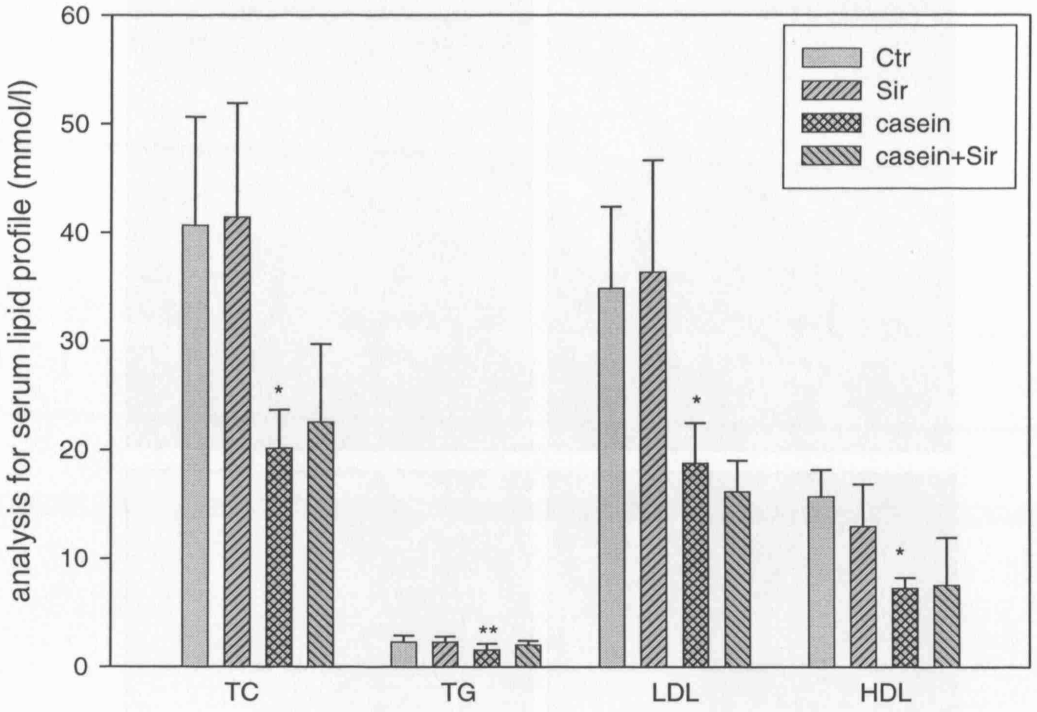

Fig 7.7 Serum lipid profile analysis in different groups at the termination of experiments (n=7). ApoE KO mice were fed with Western Diet for eight weeks in the absence (Ctr) or presence of 8 mg/kg/q.o.d Sirolimus injection (Sir) or 10% casein injection (casein) or Sirolimus plus casein injection (casein+Sir). Abbreviations: TC, total cholesterol; TG, triglyceride; LDL, low density lipoprotein; HDL, high density lipoprotein; * $p<0.001$ *vs* Ctr, ** $p<0.05$ *vs* Ctr.

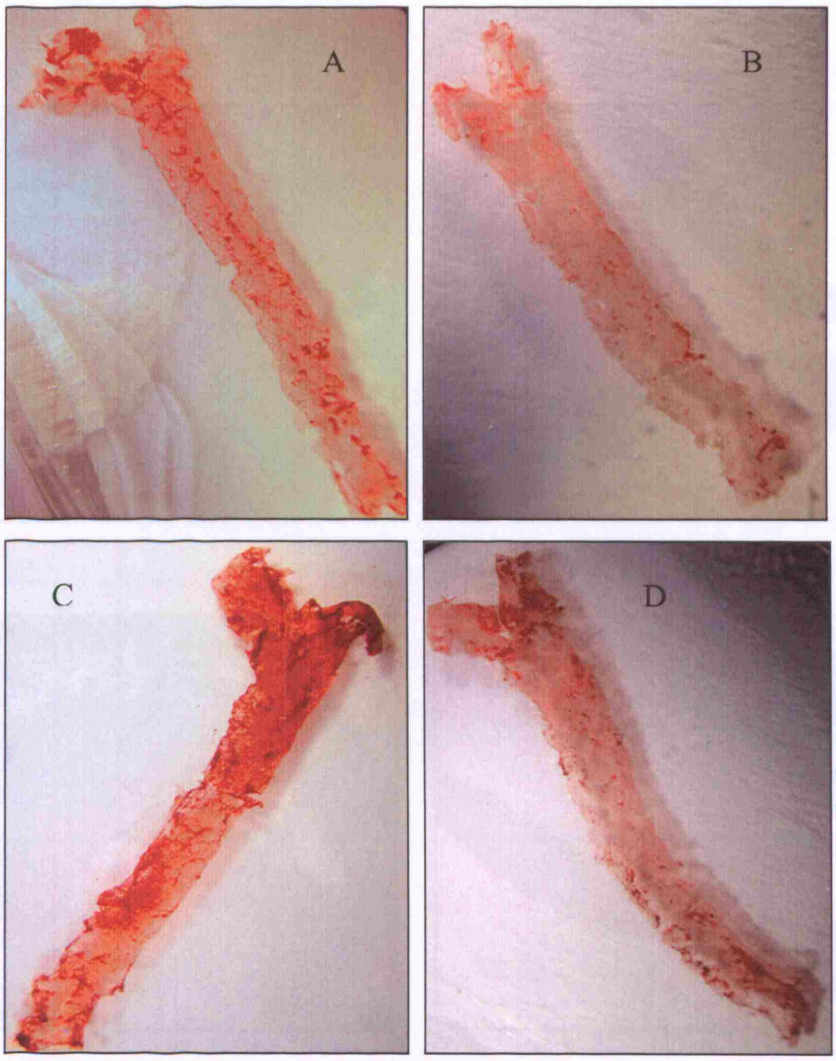

Fig 7.8 The flat preparation of aorta stained by Oil Red O. ApoE KO mice were fed with Western Diet for eight weeks in the absence (Ctr, A) or presence of 8 mg/kg/q.o.d Sirolimus injection (Sir, B) or 10% casein injection (casein, C) or Sirolimus plus casein injection (casein+Sir, D). Sirolimus inhibited lipid accumulation, especially inhibited lipid accumulation in aortas of casein injected apoE KO mice.

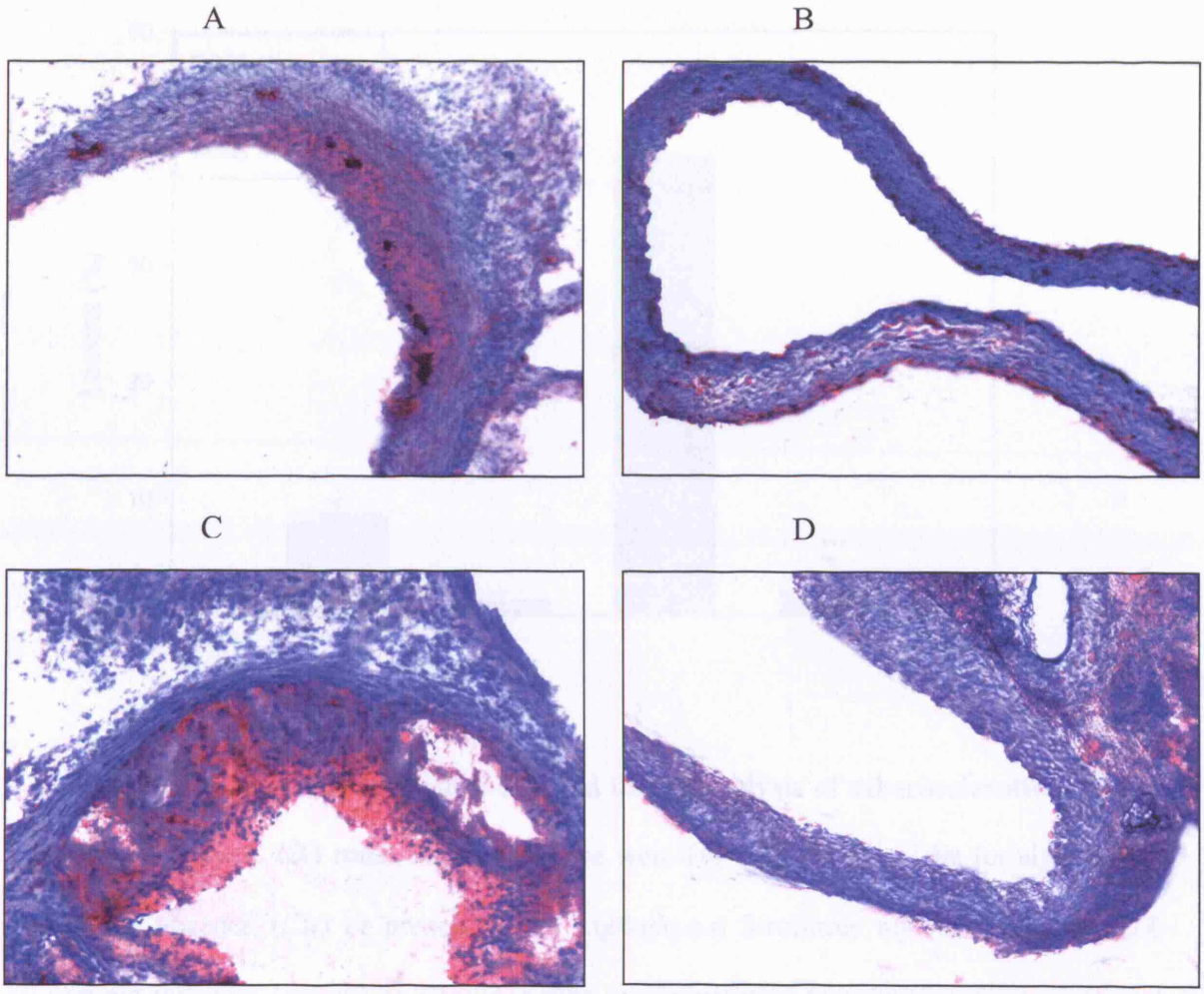

Fig 7.9a The effect of Sirolimus on the formation of atherosclerotic plaque in apoE KO mice. ApoE KO mice were fed with Western Diet for eight weeks in the absence (Ctr, A) or presence of 8 mg/kg/q.o.d Sirolimus injection (Sir, B) or 10% casein injection (casein, C) or Sirolimus plus casein injection (casein+Sir, D). Cross-sectional aortas from apoE KO mice were used to check formation of atherosclerotic plaque by Oil Red O staining. Sirolimus inhibited formation of atherosclerotic plaque, especially in aortas of casein injected apoE KO mice.

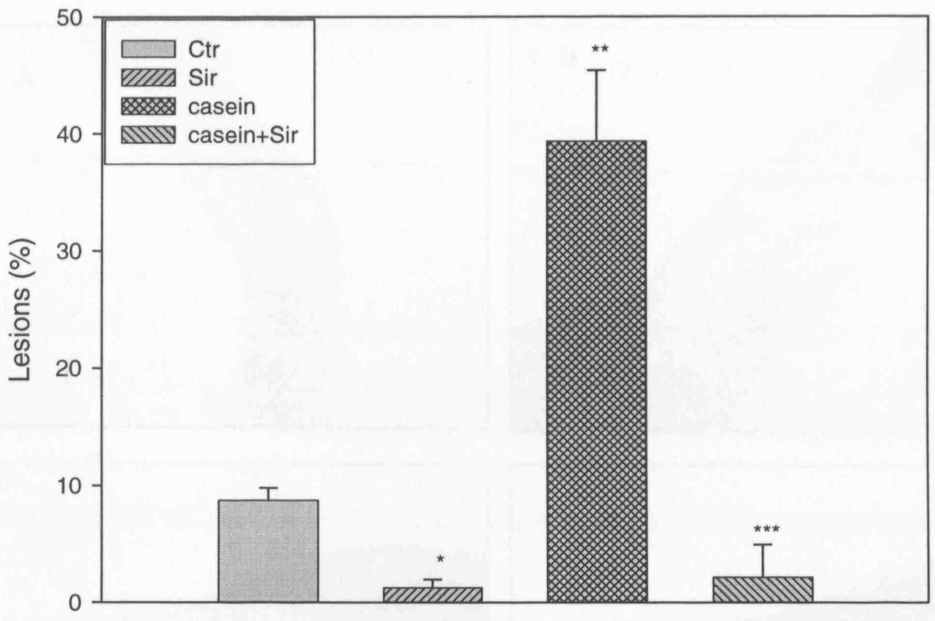

Fig 7.9b Quantitative computer-assisted image analysis of atherosclerotic lesion in aortas of apoE KO mice. ApoE KO mice were fed with Western Diet for eight weeks in the absence (Ctr) or presence of 8 mg/kg/q.o.d Sirolimus injection (Sir) or 10% casein injection (casein) or Sirolimus plus casein injection (casein+Sir). Cross-sectional aortas stained by Oil Red O were quantified using computer-assisted image analysis. Data represent the percentage surface area of the aorta occupied by lesions in apoE KO mice in 4 typical sections from different mouse of each group. * $P<0.01$ *vs* control, ** $P<0.01$ *vs* control, *** $P<0.01$ *vs* casein group.

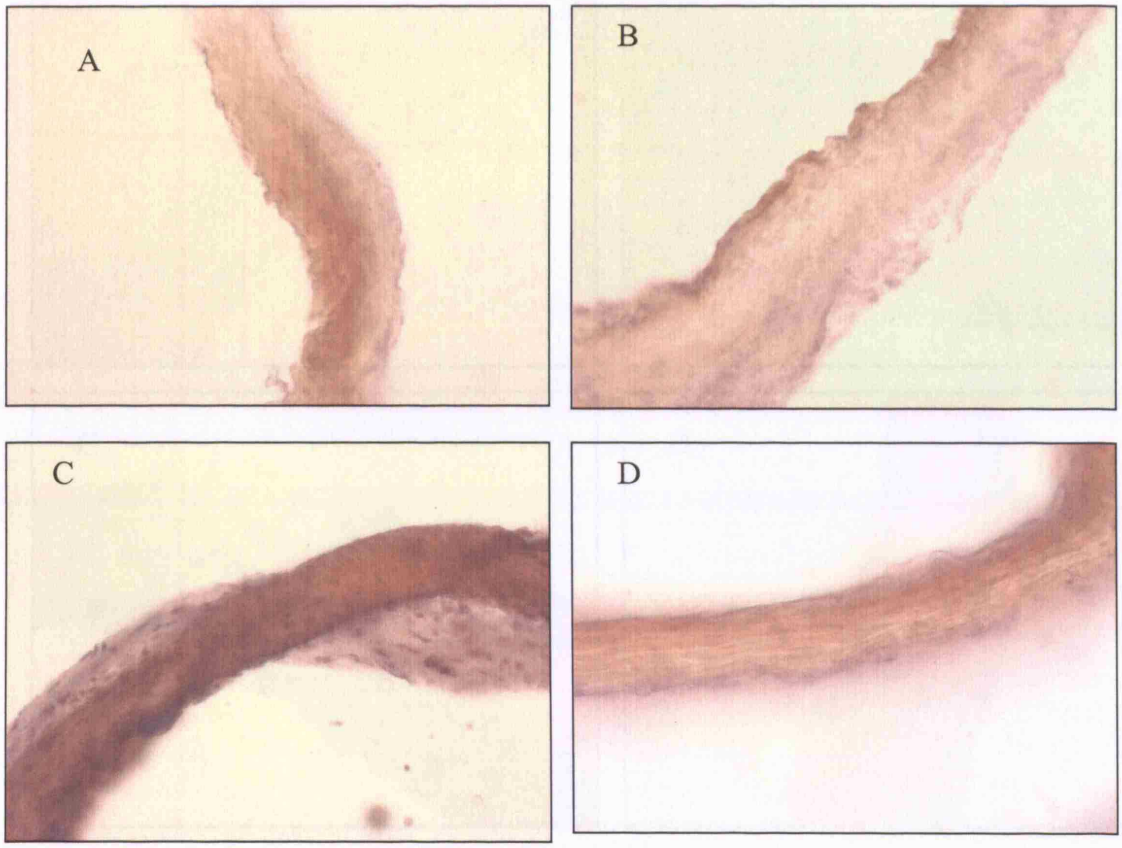

Fig 7.10 The effect of Sirolimus on LDLr expression in aortas of apoE KO mice. ApoE KO mice were fed with Western Diet for eight weeks in the absence (Ctr, A) or presence of 8 mg/kg/q.o.d Sirolimus injection (Sir, B) or 10% casein injection (casein, C) or Sirolimus plus casein injection (casein+Sir, D). Sirolimus inhibited LDLr expression, especially inhibited the increase of LDLr expression induced by casein injection.

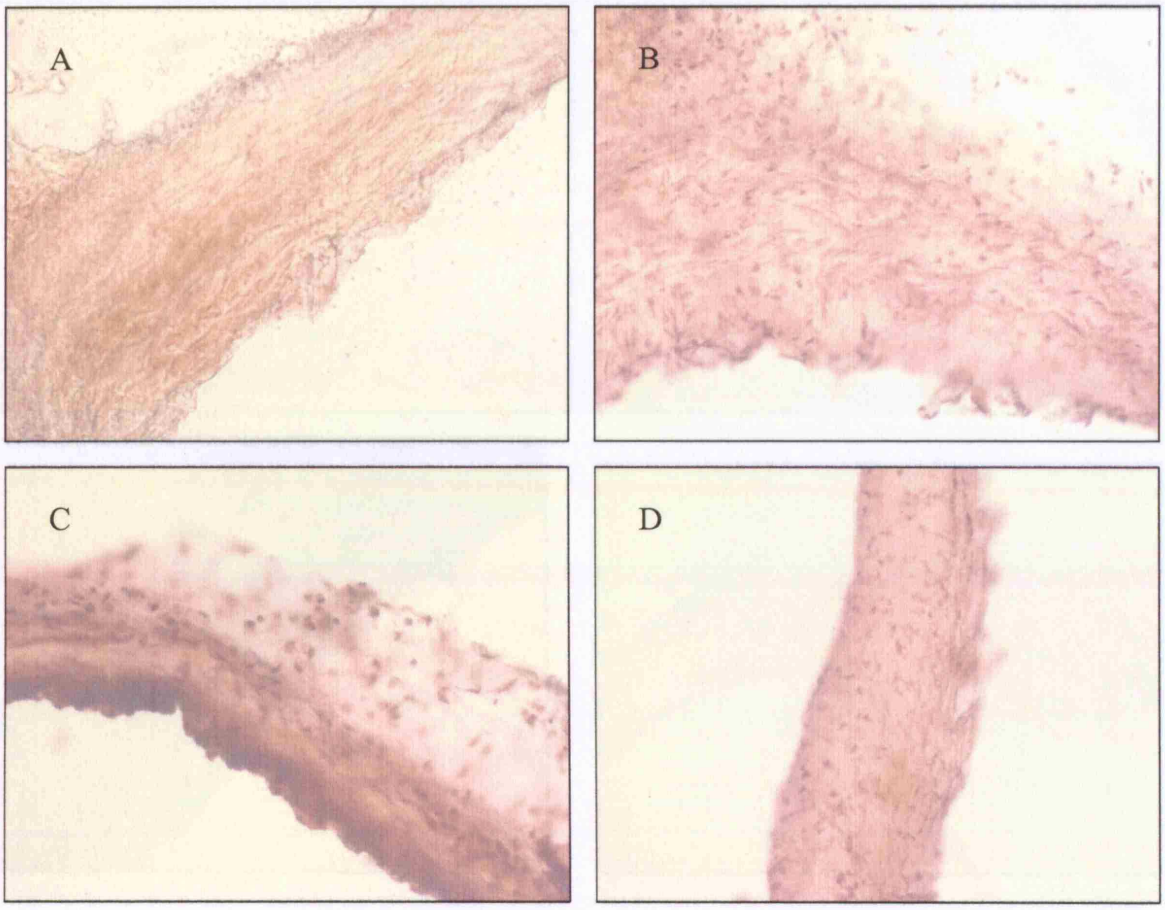

Fig 7.11 The effect of Sirolimus on SCAP expression in aortas of apoE KO mice. ApoE KO mice were fed with Western Diet for eight weeks in the absence (Ctr, A) or presence of 8 mg/kg/q.o.d Sirolimus injection (Sir, B) or 10% casein injection (casein, C) or Sirolimus plus casein injection (casein+Sir, D). Sirolimus inhibited SCAP expression, especially inhibited the increase of SCAP expression in casein injected apoE KO mice.

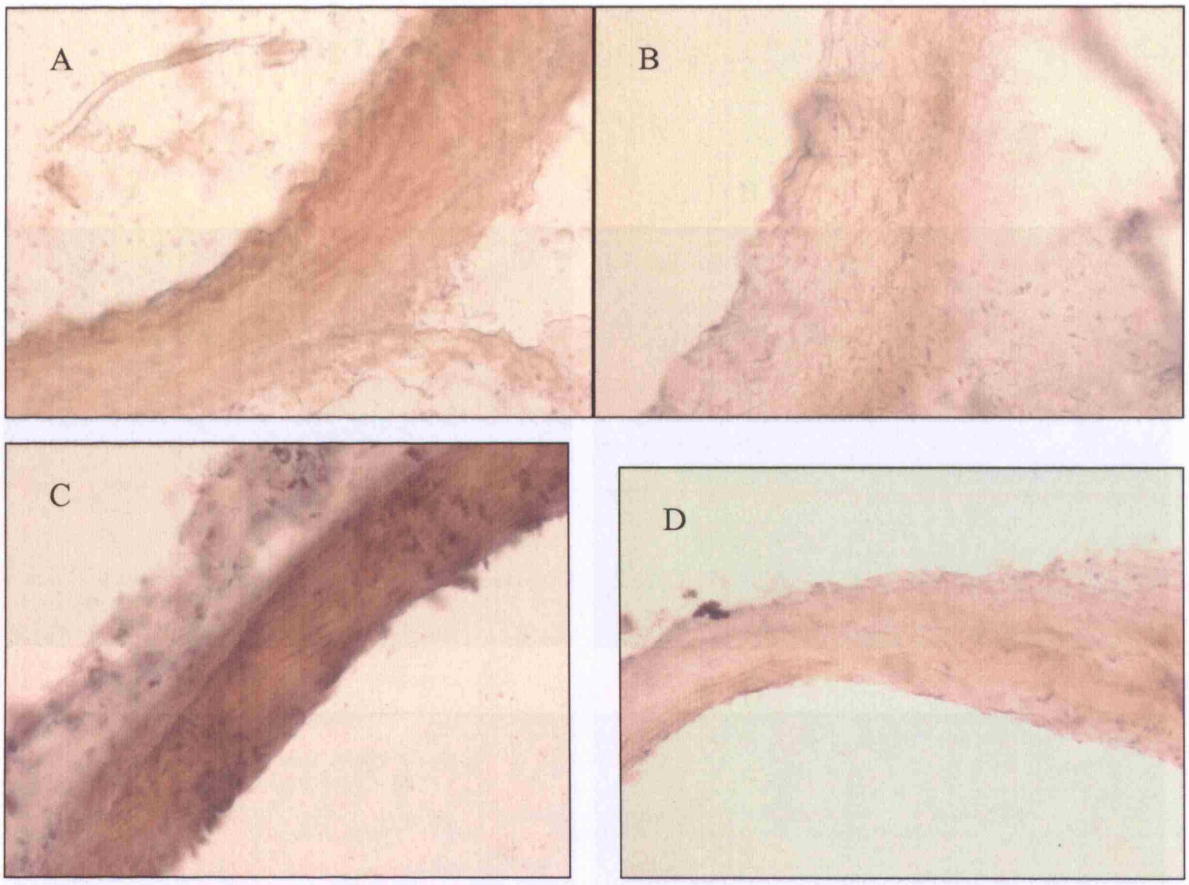

Fig 7.12 The effect of Sirolimus on SREBP-2 expression in aortas of apoE KO mice. ApoE KO mice were fed with Western Diet for eight weeks in the absence (Ctr, A) or presence of 8 mg/kg/q.o.d Sirolimus injection (Sir, B) or 10% casein injection (casein, C) or Sirolimus plus casein injection (casein+Sir, D). Sirolimus inhibited SREBP-2 expression, especially inhibited the increase of SREBP-2 expression in casein injected apoE KO mice.

Fig 7.13a

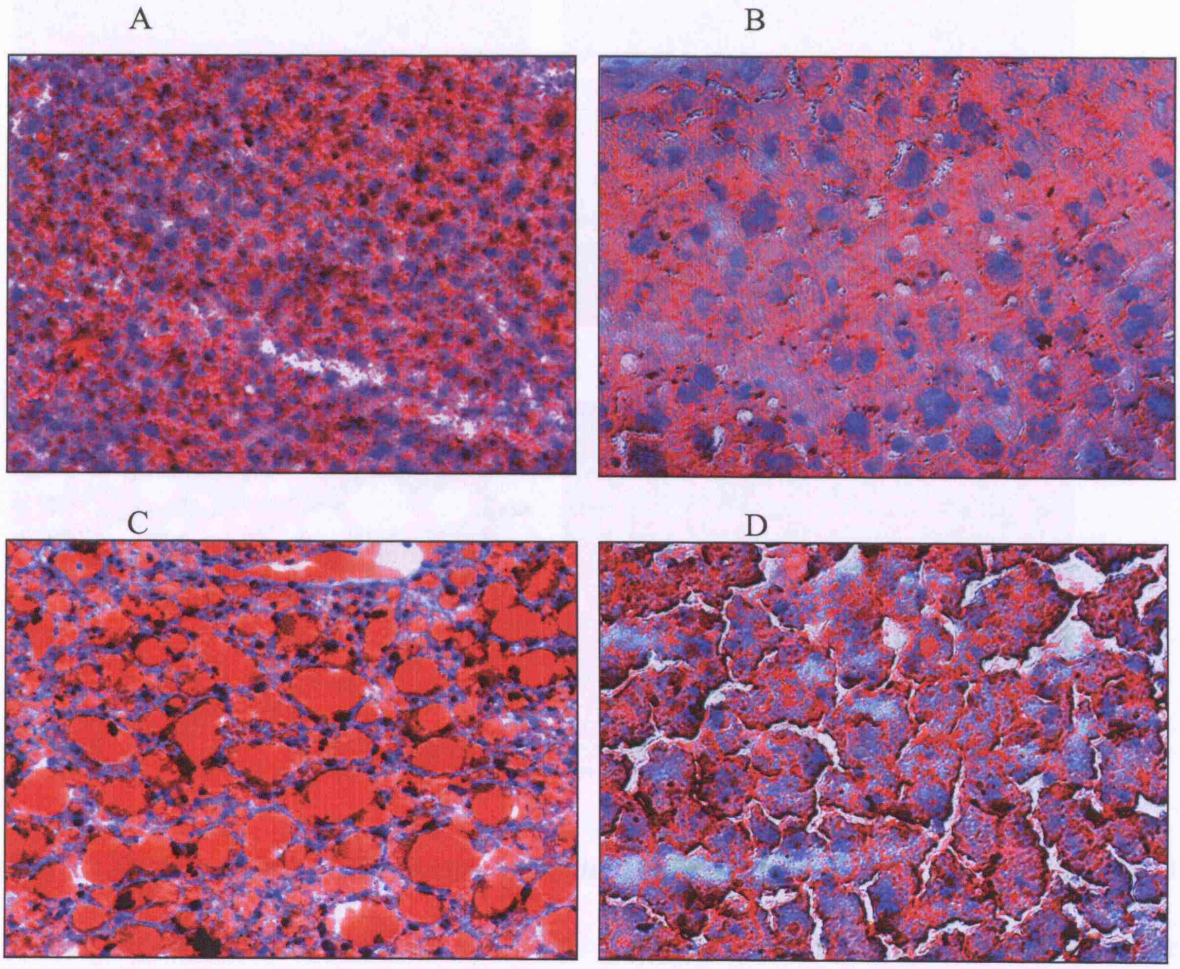

Fig 7.13a The effect of Sirolimus on lipid accumulation in the livers of apoE KO mice checked by Oil Red O staining. ApoE KO mice were fed with Western Diet for eight weeks in the absence (Ctr, A) or presence of 8 mg/kg/q.o.d Sirolimus injection (Sir, B) or 10% casein injection (casein, C) or Sirolimus plus casein injection (casein+Sir, D). Cross-sectional liver tissues from apoE KO mice were used to check lipid accumulation by Oil Red O staining (400x). Sirolimus inhibited lipid accumulation in the liver, especially in the livers of casein injected apoE KO mice.

Fig 7.13b

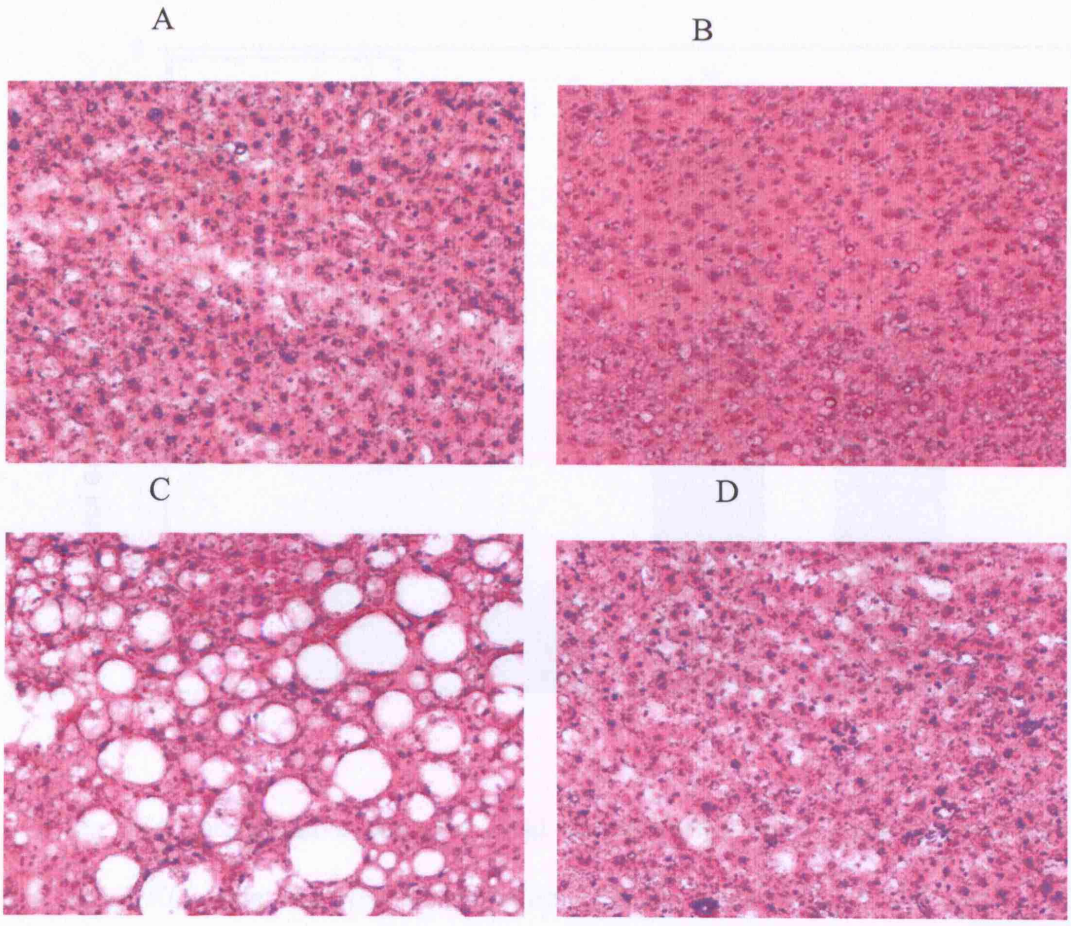

Fig 7.13b The effect of Sirolimus on lipid accumulation in the livers of apoE KO mice checked by HE staining. ApoE KO mice were fed with Western Diet for eight weeks in the absence (Ctr, A) or presence of 8 mg/kg/q.o.d Sirolimus injection (Sir, B) or 10% casein injection (casein, C) or Sirolimus plus casein injection (casein+Sir, D). Cross-sectional liver tissues from apoE KO mice were used to check lipid accumulation and formation of fat vacuoles by haematoxylin & eosin staining (200x). Sirolimus inhibited lipid accumulation with the appearance of fat vacuoles in the liver of apoE KO mice induced by casein injection.

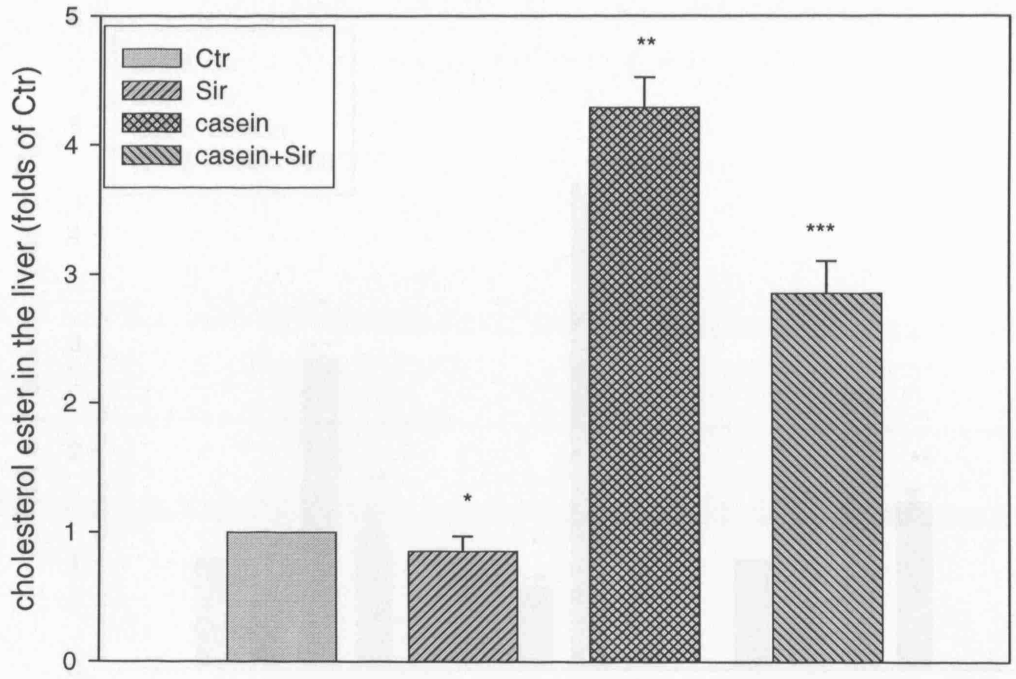

Fig 7.14 Quantitative assay for lipid accumulation in the liver of apoE KO mice. ApoE KO mice were fed with Western Diet for eight weeks in the absence (Ctr) or presence of 8 mg/kg/q.o.d Sirolimus injection (Sir) or 10% casein injection (casein) or Sirolimus plus casein injection (casein+Sir). The cholesterol ester in the liver was quantified and normalised by total protein of liver tissue. Results were expressed as Mean ± SD of 6 wells. $*P < 0.05$ *vs* control. $**P < 0.001$ *vs* control. $***P < 0.01$ *vs* casein group.

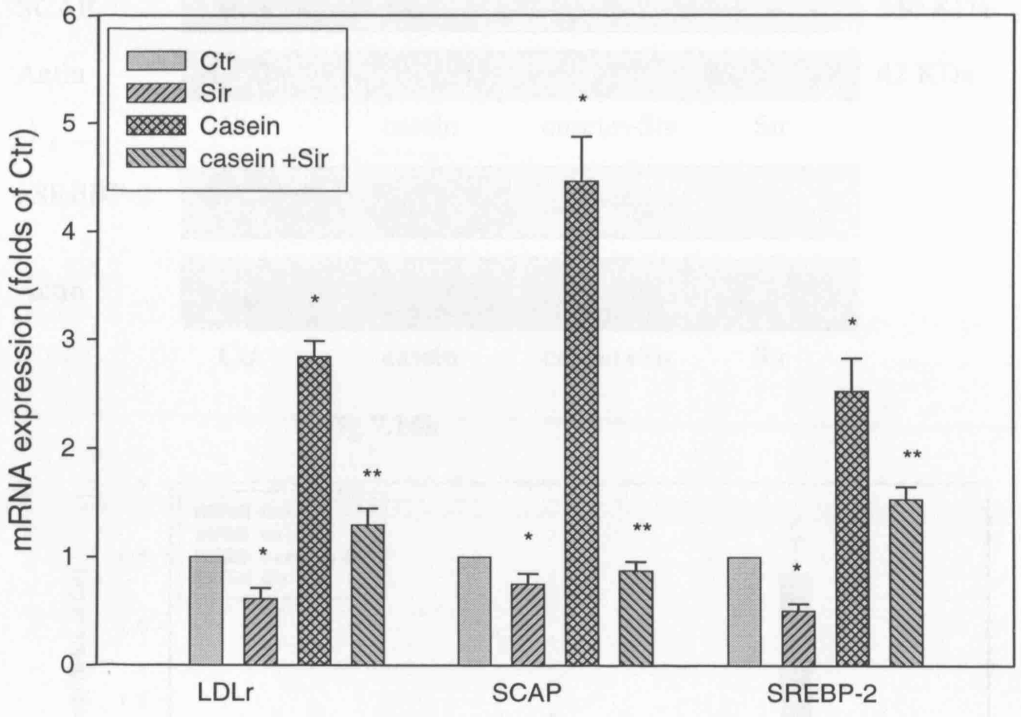

Fig 7.15 The effect of Sirolimus on the mRNA expression of LDLr, SCAP and SREBP-2 in the livers of apoE KO mice. ApoE KO mice were fed with Western Diet for eight weeks in the absence (Ctr) or presence of Sirolimus injection (Sir, 8 mg/kg/q.o.d) or 10% casein injection (casein) or Sirolimus plus casein injection (casein+Sir). After termination of experiments, total RNAs were extracted from the livers of apoE KO mice for gene expression analysis. The mRNA expression of SCAP, SREBP-2, and LDLr was determined by real-time PCR. β-actin served as the housekeeping gene Results represented the Mean ± SD (n=4). * p <0.001 *vs* control, ** p<0.001 *vs* casein injection group.

Fig 7.16a

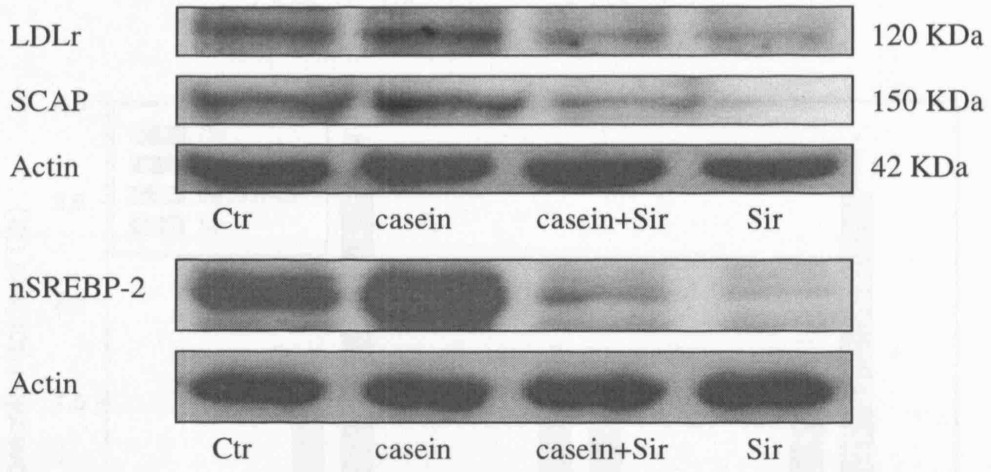

Fig 7.16b

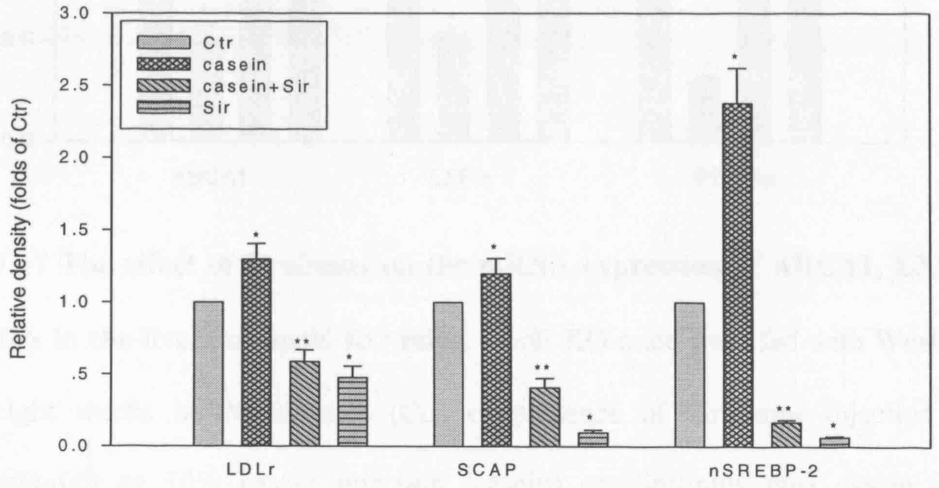

Fig 7.16a and Fig 7.16b The effect of Sirolimus on protein expression of LDLr, SCAP and nSEREBP-2 in the livers of apoE KO mice. ApoE KO mice were fed with Western Diet for eight weeks in the absence (Ctr) or presence of Sirolimus injection (Sir, 8 mg/kg/q.o.d) or 10% casein injection (casein) or Sirolimus plus casein injection (casein+Sir). After termination of experiments, the protein expression of SCAP, nSREBP-2, and LDLr in the livers was examined by Western Blot. The histogram represented Mean ± SD of the densitometric scans of protein bands from four experiments, normalised by comparison with actin, and expressed as a percentage of the control. * p <0.001 *vs* control, ** p <0.001 *vs* casein.

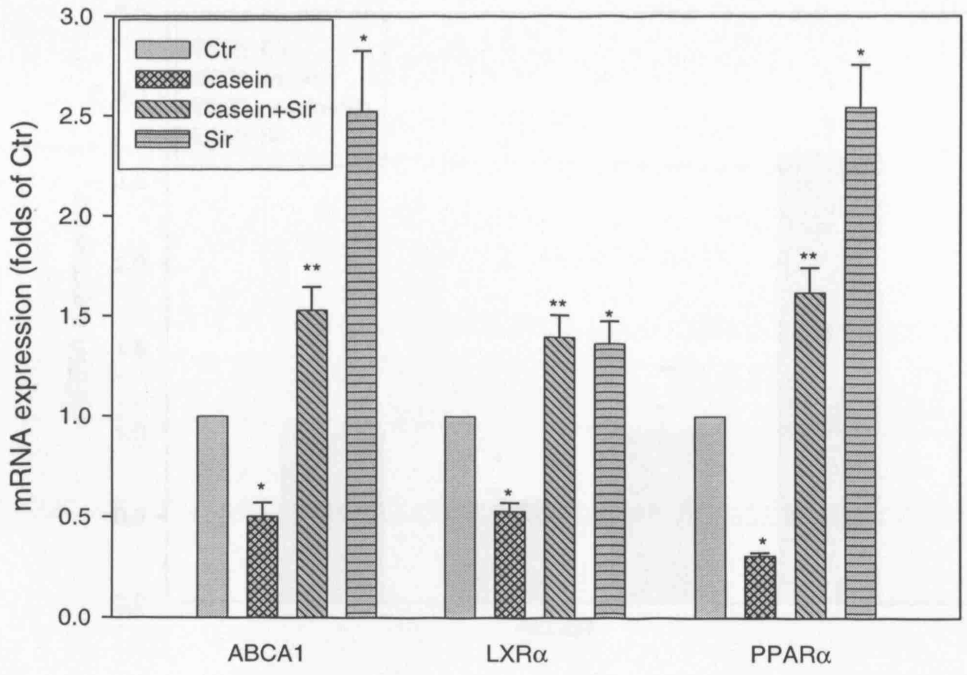

Fig 7.17 The effect of Sirolimus on the mRNA expression of ABCA1, LXRα and PPARα in the livers of apoE KO mice. ApoE KO mice were fed with Western Diet for eight weeks in the absence (Ctr) or presence of Sirolimus injection (Sir, 8 mg/kg/q.o.d) or 10% casein injection (casein) or Sirolimus plus casein injection (casein+Sir). After termination of experiments, total RNAs were extracted from the livers of apoE KO mice for gene expression analysis. The mRNA expression of ABCA1, LXRα and PPARα in the livers was determined by real-time PCR. β-actin served as the housekeeping gene Results represented the Mean ± SD (n=4). * p <0.001 *vs* control, ** p<0.001 *vs* casein injection group.

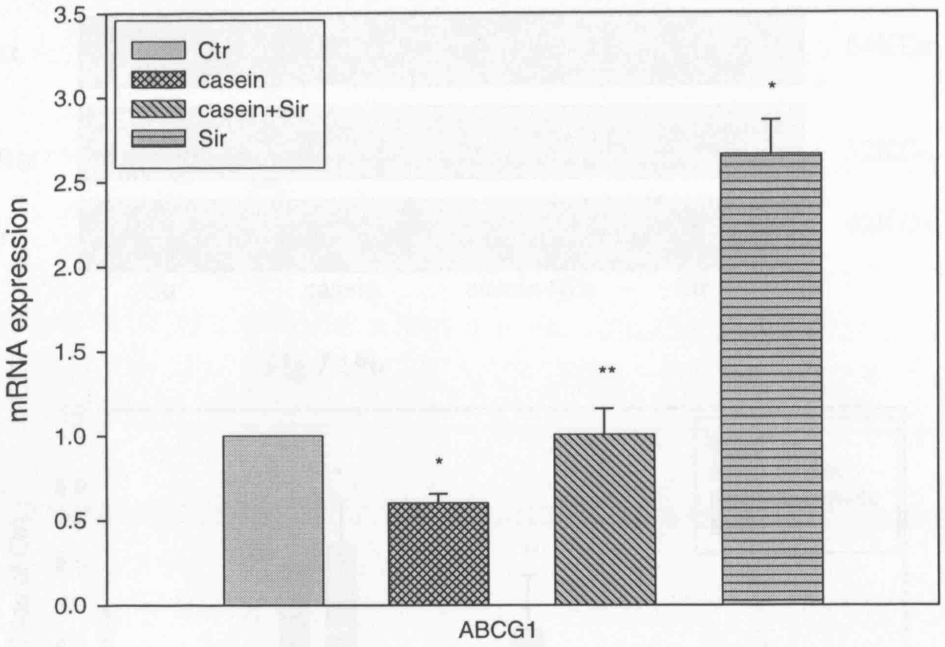

Fig 7.18 The effect of Sirolimus on the mRNA expression of ABCG1 in the livers of apoE KO mice. ApoE KO mice were fed with Western Diet for eight weeks in the absence (Ctr) or presence of Sirolimus injection (Sir, 8 mg/kg/q.o.d) or 10% casein injection (casein) or Sirolimus plus casein injection (casein+Sir). After termination of experiments, total RNAs were extracted from the livers of apoE KO mice for gene expression analysis. The mRNA expression of ABCG1 was determined by real-time PCR. β-actin served as the housekeeping gene Results represented the Mean ± SD (n=4). * p <0.001 *vs* control, ** p<0.001 *vs* casein injection group.

Fig 7.19a

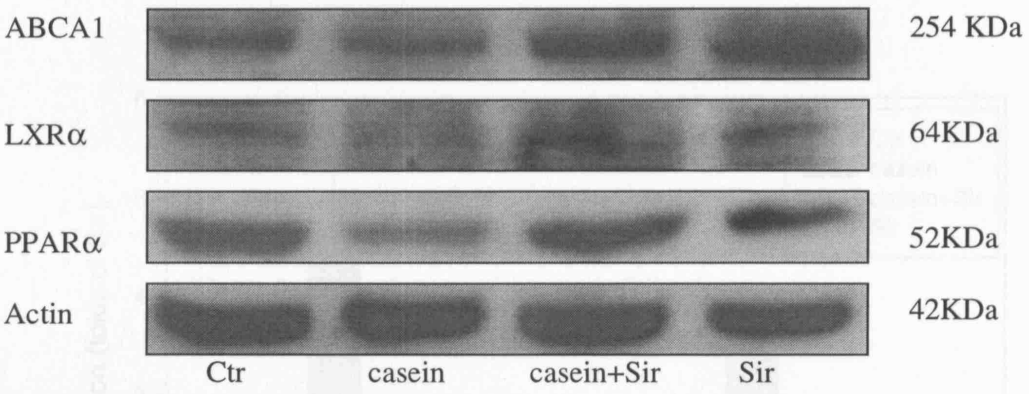

Fig 7.19b

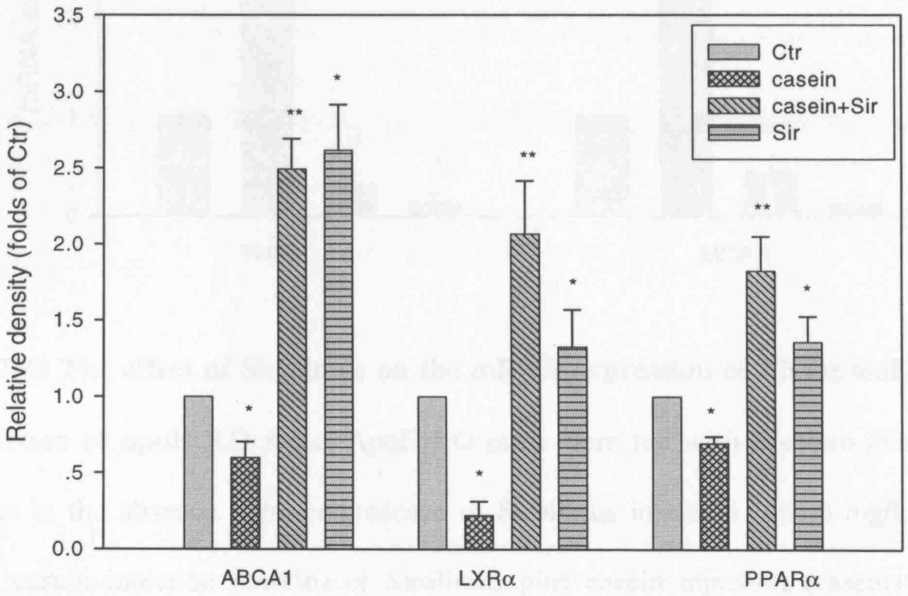

Fig 7.19a and Fig 7.19b The effect of Sirolimus on protein expression of ABCA1, LXRα, and PPARα in the livers of apoE KO mice. ApoE KO mice were divided into 4 groups: control (dH_2O injection), casein injection, casein plus Sirolimus, Sirolimus. The protein expression of ABCA1, LXRα, and PPARα was examined by Western Blot. The histogram represented Mean ± SD of the densitometric scans of protein bands from four experiments, normalised by comparison with actin, and expressed as a percentage of the control. * p <0.001 *vs* control, ** p <0.001 *vs* casein.

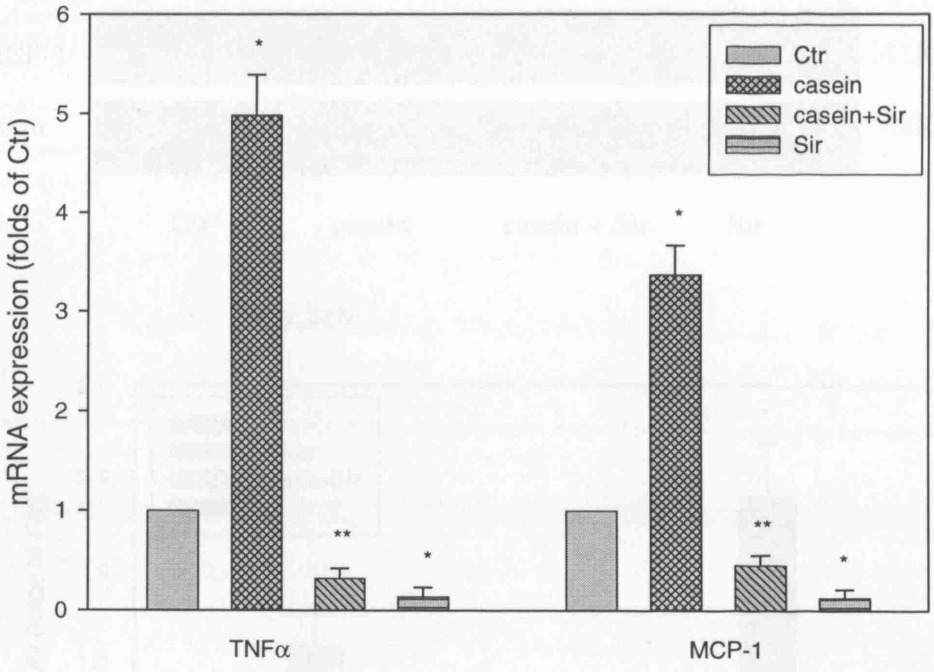

Fig 7.20 The effect of Sirolimus on the mRNA expression of TNFα and MCP-1 in the livers of apoE KO mice. ApoE KO mice were fed with Western Diet for eight weeks in the absence (Ctr) or presence of Sirolimus injection (Sir, 8 mg/kg/q.o.d) or 10% casein injection (casein) or Sirolimus plus casein injection (casein+Sir). After termination of experiments, total RNAs were extracted from the livers of apoE KO mice for gene expression analysis. The mRNA expression of TNFα and MCP-1 was determined by real-time PCR. β-actin served as the housekeeping gene Results represented the Mean ± SD (n=4). * p <0.001 *vs* control, ** p<0.001 *vs* casein injection group.

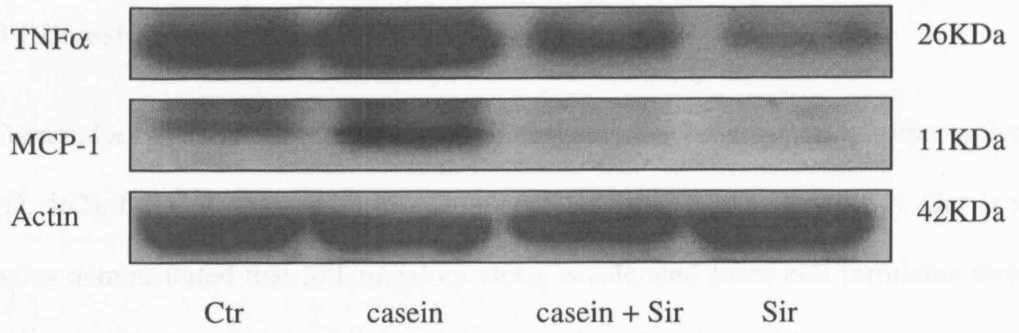

Fig 7.21b

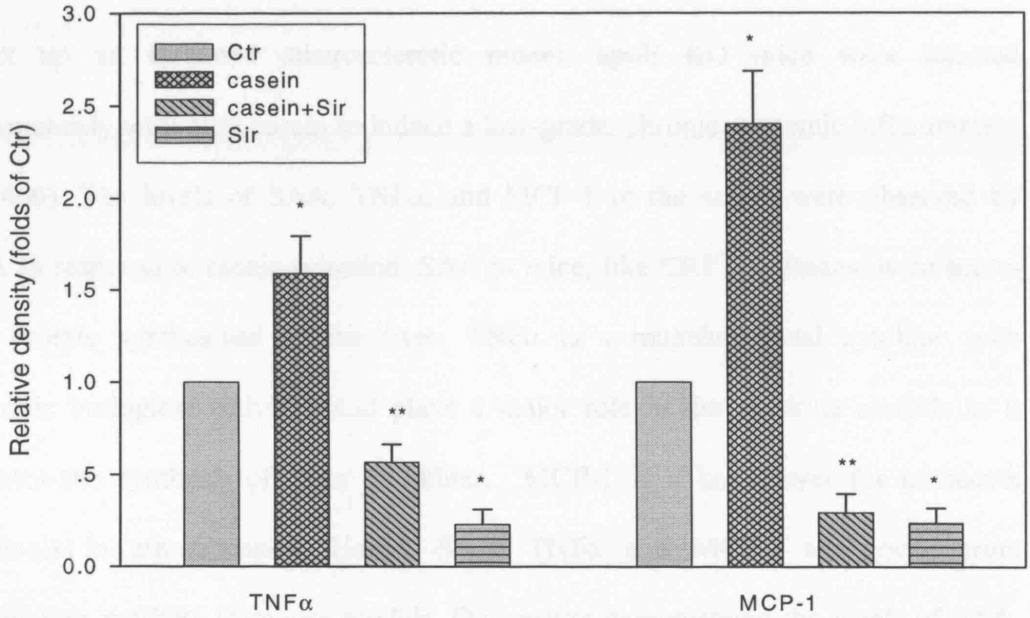

Fig 7.21a and Fig 7.21b The effect of Sirolimus on protein expression of TNFα and MCP-1 in the livers of apoE KO mice. ApoE KO mice were fed with Western Diet for eight weeks in the absence (Ctr) or presence of Sirolimus injection (Sir, 8 mg/kg/q.o.d) or 10% casein injection (casein) or Sirolimus plus casein injection (casein+Sir). After termination of experiments, the protein expression of TNFα and MCP-1 was examined by Western Blot. The histogram represented Mean ± SD of the densitometric scans of protein bands from four experiments, normalised by comparison with actin, and expressed as a percentage of the control. * p <0.001 *vs* control, ** p <0.001 *vs* casein.

7.4 Discussion

Inflammatory stress exacerbates dyslipidemia and the progression of atherosclerosis (462, 463). Inflammation and dyslipidemia act as 'partners in crime' (464). Our *in vitro* studies demonstrated that inflammatory stress accelerated foam cell formation through disruption of cholesterol homeostasis, suggesting that it could be a key factor in atherogenesis.

To set up an inflamed atherosclerotic model, apoE KO mice were injected subcutaneously with 10% casein to induce a low-grade, chronic, systemic inflammation (465, 466). The levels of SAA, TNFα, and MCP-1 in the serum were observed by ELISA in response to casein injection. SAA in mice, like CRP in humans, is an acute-phase protein synthesized by the liver. TNFα is a multifunctional cytokine with pleiotropic biological activities and plays a major role in the cytokine cascade as it stimulates the synthesis of other cytokines. MCP-1 is a key player for monocyte chemotaxis in atherogenesis. Hence, SAA, TNFα and MCP-1 are good serum inflammatory markers in mouse models. Our results demonstrated the levels of SAA, TNFα, and MCP-1 in the serum of casein injected mice was increased compared to the control, confirming the successful induction of inflammatory stress in the mice.

Furthermore, the atherosclerotic lesion size was increased in the aortas of casein injected apoE KO mice compared to the control as indicated by Oil Red O staining in cross sections and aorta flat preparations. Interestingly, serum levels of total cholesterol, total triglyceride, LDL and HDL in casein injected apoE KO mice significantly decreased compared to the control although inflammatory stress deteriorated atherosclerotic plaque formation. This observation is similar to the phenomenon that high cardiovascular mortality in haemodialysis patients is associated with low plasma cholesterol level ("reverse epidemiology") (467-470). These data suggest that

inflammation exacerbates atherosclerotic plaque formation and lowers serum cholesterol level.

We demonstrated that Sirolimus significantly inhibited inflammatory cytokine production of SAA, TNFα and MCP-1 in inflamed ApoE KO mice induced by casein injection. We found no difference in serum lipid profile (total cholesterol, total triglyceride, LDL, HDL) in apoE KO mice compared Sirolimus treated group to the control, which is in accordance with the previous results in some studies (386, 387).

We also compared changes in body weights in different groups of apoE KO mice. There was no difference in body weights among groups at the start of the experiment. The body weights at termination were decreased in the apoE KO mice of Sirolimus treated and casein injection groups compared to controls. The decrease of the body weights could be caused by nutritional effects or correlated with the inhibition of mTOR pathway which is involved in appetite regulation. The inhibitory effect of Sirolimus on body weight also has been reported by Pakala *et al* (387).

Next, we checked LDLr mediated cholesterol uptake in the aortas of apoE KO mice. By immunochemistry staining, we demonstrated that inflammatory stress significantly up-regulated the expression of SCAP, SREBP-2, and LDLr in the aortas of casein injected apoE KO mice compared to controls. However, Sirolimus inhibited the expression of SCAP, SREBP-2, and LDLr in the aortas of apoE KO mice induced by casein. This suggests that Sirolimus decreases cholesterol uptake in the aortas of apoE KO mice by down-regulating the LDLr mediated pathway, which is very important in the prevention of progression of atherosclerosis.

Much attention has been paid to the liver, the central organ of lipid metabolism, as a therapeutic target for atherosclerosis (348). Impaired cholesterol trafficking in the liver

may cause dyslipidemia and accelerate progression of atherosclerosis. Liver LDLr is of primary importance in binding and internalisation of plasma-derived LDL-cholesterol and in regulating plasma LDL concentration. Our results demonstrated that inflammatory stress increased lipid accumulation with the appearance of fat vacuoles in the livers of casein injected mice compared to controls and was a possible cause of fatty liver. However, this appearance was inhibited by Sirolimus. Further analysis showed that Sirolimus down-regulated the gene and protein expression of SCAP, SREBP-2, and LDLr induced by inflammatory stress in the livers of apoE KO mice.

ABCA1 is an important mediator for the cellular efflux of phospholipids and cholesterol from cell to lipid-free apoA-I and the formation of HDL particles. It has been demonstrated that inactivation of ABCA1 in the livers of mice causes profound low HDL in the plasma (451), suggesting that ABCA1 is an important source of circulating HDL. LXRs and PPARs are important nuclear receptors for activating ABCA1 (313). Our results showed that inflammatory stress inhibited gene and protein expression of PPARα, LXRα, and ABCA1. However, Sirolimus overrode the inhibition of PPARα, LXRα, and ABCA1 expression induced by inflammatory stress, which may restore cholesterol efflux from cells.

Taken together, our *in vivo* studies confirmed and validated our results *in vitro*. Inflammatory stress exacerbated cholesterol accumulation and foam cell formation in the aorta and also in the liver through the disruption of cholesterol trafficking. Sirolimus inhibited the production of inflammatory cytokines and ameliorated cholesterol homeostasis by down-regulating LDLr mediated cholesterol uptake and up-regulating ABCA1 mediated cholesterol efflux, thereby preventing the progression of atherosclerosis and fatty liver.

CHAPTER 8. GENERAL DISCUSSION AND CONCLUSION

During the last decade atherosclerosis as a chronic inflammatory process has led to extensive investigation of risk factors or pathways that are responsible for the initiation and perpetuation of vascular inflammation. It is clear that inflammatory processes, such as expression of adhesion molecules and the production of chemokines and cytokines, are critical for the development and progression of atherosclerotic lesions. Both experimental and clinical studies have demonstrated that a marked activation of local and systemic inflammatory response following stent implantation, which further triggers neointimal proliferation, matrix deposition, and restenosis. Local release of the drug coated with stents is thought to prevent restenosis and Sirolimus-coated stents are a promising approach to the inhibition of stent restenosis. The present study was carried out under this background.

8.1 Underlying mechanisms of the anti-atherosclerotic effect of Sirolimus

One of the major initial concerns of Sirolimus as an immunosuppressive drug in organ transplantation is its widely reported dyslipidemia. However it is quickly emerged that hyperlipidemia is dose-related and can be managed with statins. Notwithstanding this adverse effect earlier animal studies provided evidence for an antiatherosclerotic effect, thought to be mainly due to its antiproliferative property in Sirolimus-coated stents after angioplasty (1-7).

Although this drug caused dyslipidemia, it provided certain degree of protection against atherosclerosis. Therefore, the primary aim of the study was to use Sirolimus as a tool in dissecting out various aspects of inflammation-mediated disruption of cholesterol homeostasis in cells (human VSMCs, macrophages, and HepG2 cells) intimately involved in atherogenesis. We further validated our cell culture studies in inflamed apoE KO mice.

8.1.1 Anti-proliferative effect of Sirolimus to VSMCs

Increasing stent restenosis remains a significant clinical problem in patients of coronary intervention. It is caused by the accumulation of VSMCs and their associated extracellular matrix, resulting in neointimal formation. Treatment by Sirolimus-eluting stents in cardiovascular patients have shown encouraging reductions in stent restenosis (471) by inhibition of VSMC proliferation and migration as demonstrated by our results and previous studies (472). This effect is associated with inactivation of mTOR.

mTOR is a serine-threonine kinase, which is known to control cell growth, mRNA translation initiation, cell cycle progression from G1 to S phase, protein synthesis and DNA synthesis (390). mTOR is an integrator of multiple signals and adjust cell growth, proliferation, and metabolic homeostasis (391, 392). mTOR signalling is negatively regulated by tumour suppressor gene products Tuberous Sclerosis Complex (TSC-1 and TSC-2), phosphatase and tensin homolog (PTEN), and LKB, and positively by proto-oncogene Ras homolog enriched in brain (Rheb), thus adding to their regulation (393). Furthermore, mTOR phosphorylates two well-characterised downstream targets, namely, ribosomal protein S6 kinase 1 and 2 (S6K-1 and S6K-2) and the eukaryotic initiation factor 4E (eIF-4E) binding protein (4E-BP1).

Therefore, the property of anti-proliferation and anti-migration to VSMCs by Sirolimus (394) may be through blocking the mTOR pathway, which leads to translational arrest by regulating S6K-1, 4E-BP1, and cell cycle arrest from G1 to S phase. Since a putative direct anti-atherosclerotic effect of Sirolimus via the mTOR pathway is not our main target in this project, we restricted the work to the examination of Sirolimus on VSMC proliferation. The results showed that Sirolimus inhibited proliferation of VSMCs with dose-dependent manner which is in accordance with the results in previous studies (394).

8.1.2 Sirolimus ameliorates cholesterol homeostasis disrupted by inflammatory stress

Our pilot studies showed that Sirolimus decreased intracellular lipid accumulation in VSMCs, macrophages, and HepG2 cells as indicated by Oil Red O staining and intracellular cholesterol quantitative assay.

In order to explore potential mechanisms, we first checked lipoprotein receptor mediated lipid uptake *in vivo* and *in vitro* studies. Our results in VSMCs and HepG2 cells showed that Sirolimus inhibited LDLr expression to reduce LDLr mediated lipid uptake in the presence of inflammatory stress. The down-regulation of LDLr induced by Sirolimus may be due to an inhibitory effect on SCAP and SREBP2 expression. Confocal microscopy observation in VSMCs and HepG2 cells further demonstrated that Sirolimus attenuated translocation of SCAP escorting SREBP-2 from the ER to the Golgi, which prevented the formation of nuclear SREBP-2 and activation of LDLr gene transcription in the nucleus. These findings were further confirmed by *in vivo* study.

Sirolimus also inhibited VLDLr expression in VSMCs in the presence or absence of inflammatory stress. As VLDLr expression is not down-regulated by sterols (473), we did not check potential mechanism of this inhibitory effect on VLDLr in VSMCs. In HepG2 cells VLDLr expression is too low to be detected, which is in accordance with the conclusions of previous studies (195). Sirolimus did not affect the expression of VLDLr and LDLr in macrophages. We also found no obvious effect of Sirolimus on the expression of scavenger receptors (SR-A, CD36, e.t.c.) in VSMCs, macrophages, and HepG2 cells.

Secondly, we investigated the effects of Sirolimus on cholesterol biosynthesis mediated by HMGR, which is a rate-limiting enzyme of cholesterol biosynthesis (137). Our results in VSMCs showed that Sirolimus reduced cholesterol biosynthesis induced by

inflammatory stress. Further analysis showed Sirolimus inhibited the mRNA and protein expression of HMGR. The inhibitory effect of Sirolimus on HMGR mRNA expression was partly due to the decrease of SCAP/SREBP-2 complex translocation from the ER to the Golgi, which was caused by the decreased ratio of HMGR/Insig-1 mRNA expression and by the potentiated binding of Insig-1 protein to SCAP, resulting in inactivation of HMGR gene transcription. Insig-1 is a key cytoplasmic membrane protein for modulating HMGR degradation (286). Our results showed that Sirolimus accelerated HMGR degradation in VSMCs by increasing Insig-1 expression and potentiating the binding of Insig-1 protein to HMGR.

Thirdly, we demonstrated that Sirolimus increased ABCA1 gene expression in the absence or presence of inflammatory stress as demonstrated in cholesterol loaded VSMCs, macrophages, and HepG2 cells. We further examined the function of ABCA1 by measuring cholesterol efflux using ApoA1 as an acceptor. As we demonstrated in VSMCs, macrophages and HepG2 cells, inflammatory stress decreased cholesterol efflux. However, Sirolimus reversed the reduction of cholesterol efflux induced by inflammatory cytokines, though the Sirolimus alone weakly affected cholesterol efflux. Sirolimus also increased the mRNA and protein expression of LXRα and PPARα in the absence or presence of inflammatory stress, which synergistically amplified the ABCA1 pathway (313). These suggest that Sirolimus up-regulates ABCA1 mediated cholesterol efflux in the presence of inflammatory stress, which is also demonstrated by our *in vivo* study in the aortas and livers of apoE KO mice.

In summary, Sirolimus down-regulated LDLr mediated cholesterol uptake, down-regulated HMGR mediated cholesterol biosynthesis, and up-regulated ABCA1 mediated cholesterol efflux. The amelioration of dysregulation of cholesterol homeostasis induced by inflammatory stress prevented VSMCs and macrophages from transforming

into foam cells, thereby retarding the progression of atherosclerosis. For hepatic cells, the amelioration of intracellular cholesterol homeostasis may protect cells from injuries caused by lipid overload and inflammatory cytokines. In addition, cell culture studies also helped us to confirm three specific effects of inflammation on cholesterol homeostasis: i) increased receptor-mediated cholesterol influx; ii) inhibited cholesterol efflux; iii) increased cholesterol biosynthesis.

8.1.3 Anti-inflammatory effect of Sirolimus

Atherosclerosis is an inflammatory disease (6). The combination of inflammation and dyslipidemia aggravates the problems (464). Systemic inflammation exacerbated dyslipidemia and the progression of atherosclerosis (462, 463). Our results in VSMCs and macrophages and previous studies in mesangial cells (376) demonstrated that inflammation disrupted LDLr mediated negative feedback regulation and reduced ABCA1 mediated cholesterol efflux. Therefore, in this project we investigated a possible beneficial effect of Sirolimus on anti-inflammation, which may play an important role in preventing progression of atherosclerosis. Our results *in vitro* showed that Sirolimus inhibited inflammatory cytokine production (IL-6, TNFα, IL-8, and MCP-1) in cells, which may indirectly result in the amelioration of cholesterol homeostasis disrupted by inflammatory stress. The *in vivo* studies further confirmed the results of *in vitro* studies. Sirolimus significantly decreased serum levels of TNFα and SAA, and inhibited the expression of TNFα and MCP-1 in the tissues (aorta, liver) of inflamed apoE KO mice. Accordingly, Sirolimus significantly reduced the lesion size of atherosclerotic plaque in the aortas of inflamed apoE KO mice compared to controls. Potential mechanisms for the anti-inflammatory function of Sirolimus need to be elucidated in the future work.

8.2 Further work

In this project, we demonstrated *in vitro* and *in vivo* studies that anti-atherosclerotic effects of Sirolimus were through: 1) down-regulation of LDLr mediated cholesterol uptake; 2) down-regulation of HMGR mediated cholesterol biosynthesis; 3) up-regulation of PPARs-LXRs-ABCA1 mediated cholesterol efflux; 4) down-regulation of inflammatory cytokine production. Since Sirolimus is an inhibitor of mTOR kinase (391, 474), we assumed that Sirolimus mediated these effects may be achieved through the mTOR pathway. Future work needs to be done in this research area to obtain more evidence to elucidate potential mechanisms.

8.2.1 Inflammatory stress may disrupt LDLr-SCAP-SREBP-2 pathway and PPARs-LXRs-ABCA1 pathway via the mTOR

Recently some studies have reported that stimulation of inflammatory cytokines may result in the activation of the mTOR pathway. Lee *et al* (475) demonstrated inflammatory cytokines, such as TNFα and IL-1β induced phosphorylation of the mTOR substrate p70 S6 kinase in breast cancer cells and untransformed mammary epithelial cells. Lim *et al* (476) also found that phosphatidic acid activated mTOR substrate p70 S6 kinase in RAW264.7 cells, which was mainly mediated by excreted inflammatory cytokines (IL-1β, IL-6, TNFα, and inducible nitric oxide) stimulated by phosphatidic acid. Glantschnig *et al* (477) demonstrated that the cytokine signalling (M-CSF, TNFα, and RANK) intermediated for mTOR/ribosomal protein S6 kinase activation including phosphatidy linositol-3 kinase, Akt, Erks and geranylgeranylated proteins to promote osteoclast survival. Furthermore, mTOR kinase can phosphorylate retinoblastoma protein to drive cell cycle progression for cell growth and proliferation (478, 479). Nathe *et al* (480) reported that IL-1β increased the phosphorylation of

retinoblastoma protein to drive the transition of cells from G1 to S phase in the cell cycle.

Taken together, these studies suggested that inflammatory cytokines may be an important mediator for activation of the mTOR pathway. Our current work with previous studies (376, 422, 428, 481) have shown that inflammatory stress disrupted LDLr mediated cholesterol uptake, cholesterol biosynthesis, and ABCA1 mediated cholesterol efflux. Therefore, we hypothesized that activated mTOR signal pathway by inflammatory cytokines may be involved in dysregulation of cholesterol homeostasis, which can be ameliorated by Sirolimus.

8.2.2 Anti-inflammatory effects of Sirolimus may be mediated by mTOR pathway

In this project, we demonstrated that Sirolimus had a significant anti-inflammatory effect. However, potential mechanism was not fully explored. This issue will be a target of our future work.

It is well-known that inflammatory cytokine production induced by inflammatory stress (LPS, TNFα, IL-1β, etc.) are modulated by nuclear factor-kappa B (NF-κB) (482, 483). NF-κB is a ubiquitously expressed family of transcription factors controlling the expression of numerous genes involved in immunity and inflammation (484, 485). NF-κB, typically a heterodimer of 50 kDa (p50) and 65 kDa (RelA) subunits, is sequestered in the cytoplasm as an inactive form by its association with IκBα, the prototype of a family of inhibitory proteins termed IκB proteins (484, 485). Activation of NF-κB is initiated through phosphorylation of IκBα on two specific serine residues (Ser32 and Ser36) by a macromolecular cytoplasmic IκB kinase (IKK) (486) complex composed of the catalytic subunits IKKα and IKKβ, and the regulatory subunit NEMO/IKKγ (484, 485). Phosphorylation marks IκBα for polyubiquitination by the E3-SCFβ-TrCP

ubiquitin ligase and, subsequently, its degradation by the 26S proteasome (485, 487). Degradation of IκBα unmasks the nuclear localization signal of NF-κB, thus allowing its translocation to the nucleus where it activates transcription of target genes including inflammatory cytokines.

Recently some studies (488-491) demonstrated phosphoinositide 3-kinase (PI3K)/Akt signal pathway activation increased NF-κB-dependent gene transcription. In addition, Ghosh *et al* (492) reported tumour suppressor genes *TSC1* (Hamartin) and *TSC2* (Tuberin)-deficient murine embryo fibroblast showed reduced induction of NF-κB dependent transcripts. Since PI3K/Akt signal pathway, *TSC1* and *TSC2* are upstream regulators of mTOR pathway, it suggest there is a crosstalk between the NF-κB mediated gene transcription and the mTOR pathway.

Therefore, we assumed that anti-inflammatory effect of Sirolimus is through the inactivation of NF-κB, thereby resulting in a decreased inflammatory cytokine production. This inhibitory effect may result from the crosstalk between mTOR and NF-κB pathways and it will be explored in the future work.

8.3 Conclusion

In summary, in this project we explored potential mechanisms of Sirolimus in anti-atherosclerosis. Our results *in vitro* and *in vivo* demonstrated that anti-atherosclerotic effects of Sirolimus were through: 1) Amelioration of disrupted cholesterol homeostasis induced by inflammation via decreasing LDLr mediated cholesterol uptake, decreasing HMGR mediated cholesterol biosynthesis, and increasing ABCA1mediated cholesterol efflux; 2) Inhibition of inflammatory cytokine production and VSMC proliferation. These findings may improve current understanding for the anti-atherosclerotic effect of Sirolimus. Our studies also suggest that Sirolimus is a useful tool in dissecting out

various pathogenic pathways of atherosclerosis, which has a major influence on normalising disrupted cholesterol homeostasis, anti-proliferation, and anti-inflammation.

Inflammatory stress is an aggregating factor in progression of atherosclerosis (464). Therefore, the combination of lipid lowing agents with anti-inflammatory agents could be necessary in anti-atherosclerotic therapies. Our results suggest Sirolimus may be useful for preventing atherosclerosis in some patients, especially in conditions characterised by inflammatory stress. Future work will concentrate on this research area to explore further potential mechanisms mediated by Sirolimus.

REFERENCES

1. Braunwald E. Cardiovascular Medicine at the Turn of the Millennium: Triumphs, Concerns, and Opportunities. New Eng J Med 1997; 337(19):1360-1369.

2. Yamashita S, Hirano K, Sakai N, Matsuzawa Y. Molecular biology and pathophysiological aspects of plasma cholesteryl ester transfer protein. Biochim Biophys Acta 2000; 1529(1-3):257-275.

3. Ross R, Harker L. Hyperlipidemia and Atherosclerosis. Science 1976; 193(4258):1094-1100.

4. Libby P. Inflammation in atherosclerosis. Nature 2002; 420(6917):868-874.

5. Libby P, Ridker PM, Maseri A. Inflammation and atherosclerosis. Circulation 2002; 105(9):1135-1143.

6. Ross R. Atherosclerosis--an inflammatory disease. N Engl J Med 1999; 340(2):115-126.

7. Gautier EL, Huby T, Ouzilleau B, Doucet C, Saint-Charles F, Gremy G, et al. Enhanced Immune System Activation and Arterial Inflammation Accelerates Atherosclerosis in Lupus-Prone Mice. Arterioscler Thromb Vasc Biol 2007; 27(7):1625-1631.

8. Sato H, Miida T, Wada Y, Maruyama M, Murakami S, Hasegawa H, et al. Atherosclerosis is accelerated in patients with long-term well-controlled Systemic Lupus Erythematosus (SLE). Clinica Chimica Acta 2007; 385(1-2):35-42.

9. WallbergJonsson S, Ohman ML, Dahlqvist SR. Cardiovascular morbidity and mortality in patients with seropositive rheumatoid arthritis in northern Sweden. J Rheumatol 1997; 24(3):445-451.

10. Hansson GK, Berne GP. Atherosclerosis and the immune system. Acta Paediatrica 2004; 93:63-69.

11. Getz GS. Thematic review series: The Immune System and Atherogenesis. Immune function in atherogenesis. J Lipid Res 2005; 46(1):1-10.

12. Hansson GK. Inflammation, atherosclerosis, and coronary artery disease - Reply. N Engl J Med 2005; 353(4):429-430.

13. Robertson AK, Hansson GK. T Cells in Atherogenesis: For Better or For Worse? Arterioscler Thromb Vasc Biol 2006; 26(11):2421-2432.

14. Wick G, Knoflach M, Xu QB. Autoimmune and inflammatory mechanisms in atherosclerosis. Annu Rev Immunol 2004; 22:361-403.

15. Methe H, Edelman ER. Cell-matrix contact prevents recognition and damage of endothelial cells in states of heightened immunity. Circulation 2006; 114:I233-I238.

16. Weis M, von Scheidt W. Coronary artery disease in the transplanted heart. Annu Rev Med 2000; 51:81-100.

17. Quehenberger O. Thematic Review Series: The Immune System and Atherogenesis. Molecular mechanisms regulating monocyte recruitment in atherosclerosis. J Lipid Res 2005; 46(8):1582-1590.

18. Weis M, Schlichting CL, Engleman EG, Cooke JP. Endothelial Determinants of Dendritic Cell Adhesion and Migration: New Implications for Vascular Diseases. Arterioscler Thromb Vasc Biol 2002; 22(11):1817-1823.

19. Llodra J, Angeli V, Liu J, Trogan E, Fisher EA, Randolph GJ. From the Cover: Emigration of monocyte-derived cells from atherosclerotic lesions characterizes

regressive, but not progressive, plaques. Proc Natl Acad Sci USA 2004; 101(32):11779-11784.

20. Ludewig B, Laman JD. The in and out of monocytes in atherosclerotic plaques: Balancing inflammation through migration. Proc Natl Acad Sci USA 2004; 101(32):11529-11530.

21. Kofler S, Nickel T, Weis M. Role of cytokines in cardiovascular diseases: a focus on endothelial responses to inflammation. Clin Sci 2005; 108(3):205-213.

22. Methe H, Brunner S, Wiegand D, Nabauer M, Koglin J, Edelman ER. Enhanced T-helper-1 lymphocyte activation patterns in acute coronary syndromes. J Am Coll Cardiol 2005; 45(12):1939-1945.

23. Methe H, Kim JO, Kofler S, Weis M, Nabauer M, Koglin J. Expansion of Circulating Toll-Like Receptor 4-Positive Monocytes in Patients With Acute Coronary Syndrome. Circulation 2005; 111(20):2654-2661.

24. Binder CJ, Chang MK, Shaw PX, Miller YI, Hartvigsen K, Dewan A, et al. Innate and acquired immunity in atherogenesis. Nat Med 2002; 8(11):1218-1226.

25. Shah PK, Chyu KY, Fredrikson GN, Nilsson J. Immunomodulation of atherosclerosis with a vaccine. Nat Clin Pract Cardiovasc Med 2005; 2(12):639-646.

26. Sherer Y, Shoenfeld Y. Mechanisms of disease: atherosclerosis in autoimmune diseases. Nat Clin Pract Rheumatol 2006; 2(2):99-106.

27. Giles T, Post W, Blumenthal RS, Bathon JM. Therapy insight: managing cardiovascular risk in patients with rheumatoid arthritis. Nat Clin Pract Rheumatol 2006; 2(6):320-329.

28. Roman MJ. Prevalence and correlates of accelerated atherosclerosis in systemic lupus erythematosus. N Engl J Med 2006; 355(16):1746.

29. Karin M, Lawrence T, Nizet V. Innate immunity gone awry: Linking microbial infections to chronic inflammation and cancer. Cell 2006; 124(4):823-835.

30. Kawai T, Akira S. Pathogen recognition with Toll-like receptors. Curr Opin Immunol 2005; 17(4):338-344.

31. Michelsen KS, Arditi M. Toll-like receptor signaling and atherosclerosis. Curr Opin Hematol 2006; 13(3):163-168.

32. Bjorkbacka H. Multiple roles of Toll-like receptor signaling in atherosclerosis. Curr Opin Lipidol 2006; 17(5):527-533.

33. Bjorkbacka H, Kunjathoor VV, Moore KJ, Koehn S, Ordija CM, Lee MA, et al. Reduced atherosclerosis in MyD88-null mice links elevated serum cholesterol levels to activation of innate immunity signaling pathways. Nat Med 2004; 10(4):416-421.

34. Michelsen KS, Wong MH, Shah PK, Zhang W, Yano J, Doherty TM, et al. Lack of Toll-like receptor 4 or myeloid differentiation factor 88 reduces atherosclerosis and alters plaque phenotype in mice deficient in apolipoprotein E. Proc Natl Acad Sci USA 2004; 101(29):10679-10684.

35. Mullick AE, Tobias PS, Curtiss LK. Modulation of atherosclerosis in mice by Toll-like receptor 2. J Clin Invest 2005; 115(11):3149-3156.

36. Nestle FO, Banchereau J, Hart D. Dendritic cells: On the move from bench to bedside. Nat Med 2001; 7(7):761-765.

37. Bobryshev YV. Dendritic cells in atherosclerosis: current status of the problem and clinical relevance. Eur Heart J 2005; 26(17):1700-1704.

38. Millonig G, Niederegger H, Rabl W, Hochleitner BW, Hoefer D, Romani N, et al. Network of Vascular-Associated Dendritic Cells in Intima of Healthy Young Individuals. Arterioscler Thromb Vasc Biol 2001; 21(4):503-508.

39. Yilmaz A, Weber J, Cicha I, Stumpf C, Klein M, Raithel D, et al. Decrease in Circulating Myeloid Dendritic Cell Precursors in Coronary Artery Disease. J Am Coll Cardiol 2006; 48(1):70-80.

40. Niessner A, Sato K, Chaikof EL, Colmegna I, Goronzy JJ, Weyand CM. Pathogen-Sensing Plasmacytoid Dendritic Cells Stimulate Cytotoxic T-Cell Function in the Atherosclerotic Plaque Through Interferon-{alpha}. Circulation 2006; 114(23):2482-2489.

41. Munro JM, Vanderwalt JD, Munro CS, Chalmers JAC, Cox EL. An Immunohistochemical Analysis of Human Aortic Fatty Streaks. Hum Pathol 1987; 18(4):375-380.

42. Stary HC, Chandler AB, Glagov S, Guyton JR, Insull W, Rosenfeld ME, et al. A Definition of Initial, Fatty Streak, and Intermediate Lesions of Atherosclerosis - A Report from the Committee on Vascular-Lesions of the Council on Arteriosclerosis, American-Heart-Association. Circulation 1994; 89(5):2462-2478.

43. Nilsson J. Cytokines and Smooth-Muscle Cells in Atherosclerosis. Cardiovasc Res 1993; 27(7):1184-1190.

44. Rajavashisth TB, Andalibi A, Territo MC, Berliner JA, Navab M, Fogelman AM, et al. Induction of endothelial cell expression of granulocyte and macrophage colony-stimulating factors by modified low-density lipoproteins. Nature 1990; 344:254-257.

45. Chappell DC, Varner SE, Nerem RM, Medford RM, Alexander RW. Oscillatory Shear Stress Stimulates Adhesion Molecule Expression in Cultured Human Endothelium. Circ Res 1998; 82(5):532-539.

46. Iiyama K, Hajra L, Iiyama M, Li H, DiChiara M, Medoff BD, et al. Patterns of Vascular Cell Adhesion Molecule-1 and Intercellular Adhesion Molecule-1 Expression in Rabbit and Mouse Atherosclerotic Lesions and at Sites Predisposed to Lesion Formation. Circ Res 1999; 85(2):199-207.

47. Lin MC, mus-Jacobs F, Chen HH, Parry GCN, Mackman N, Shyy JYJ, et al. Shear Stress Induction of the Tissue Factor Gene. J Clin Invest 1997; 99(4):737-744.

48. Nagel T, Resnick N, Atkinson WJ, Dewey CF, Gimbrone MA. Sheer Stress Selectively Up-Regulates Intercellular-Adhesion Molecule-1 Expression in Cultured Human Vascular Endothelial-Cells. J Clin Invest 1994; 94(2):885-891.

49. Kim CJ, Khoo JC, Gillotte-Taylor K, Li A, Palinski W, Glass CK, et al. Polymerase Chain Reaction-Based Method for Quantifying Recruitment of Monocytes to Mouse Atherosclerotic Lesions In Vivo : Enhancement by Tumor Necrosis Factor-{alpha} and Interleukin-1{beta}. Arterioscler Thromb Vasc Biol 2000; 20(8):1976-1982.

50. Lee RT, Libby P. The Unstable Atheroma. Arterioscler Thromb Vasc Biol 1997; 17(10):1859-1867.

51. Schonbeck U, Mach F, Sukhova GK, Murphy C, Bonnefoy JY, Fabunmi RP, et al. Regulation of Matrix Metalloproteinase Expression in Human Vascular Smooth Muscle Cells by T Lymphocytes : A Role for CD40 Signaling in Plaque Rupture? Circ Res 1997; 81(3):448-454.

52. Frostegard J, Ulfgren AK, Nyberg P, Hedin U, Swedenborg J, Andersson U, et al. Cytokine expression in advanced human atherosclerotic plaques: dominance of pro-inflammatory (Th1) and macrophage-stimulating cytokines. Atherosclerosis 1999; 145(1):33-43.

53. Tenaglia MD, Buda MD, Wilkins MD, Barron MD, Jeffords BS, Vo BS, et al. Levels of Expression of P-Selectin, E-Selectin, and Intercellular Adhesion Molecule-1 in Coronary Atherectomy Specimens from Patients With Stable and Unstable Angina Pectoris. Am J Cardiol 1997; 79(6):742-747.

54. Simon AD, Yazdani S, Wang WZ, Schwartz A, Rabbani LE. Circulating levels of IL-1 beta, a prothrombotic cytokine, are elevated in unstable angina versus stable angina. J Thromb Thrombolysis 2000; 9(3):217-222.

55. Jander S, Sitzer M, Schumann R, Schroeter M, Siebler M, Steinmetz H, et al. Inflammation in High-Grade Carotid Stenosis : A Possible Role for Macrophages and T Cells in Plaque Destabilization. Stroke 1998; 29(8):1625-1630.

56. DeGraba TJ. Expression of inflammatory mediators and adhesion molecules in human atherosclerotic plaque. Neurology 1997; 49(5):S15-S19.

57. DeGraba TJ, Siren AL, Penix L, McCarron RM, Hargraves R, Sood S, et al. Increased Endothelial Expression of Intercellular Adhesion Molecule-1 in Symptomatic Versus Asymptomatic Human Carotid Atherosclerotic Plaque. Stroke 1998; 29(7):1405-1410.

58. Gimbrone MA, Resnick N, Nagel T, Khachigian LM, Collins T, Topper JN. Hemodynamics, endothelial gene expression, and atherogenesis. Ann N Y Acad Sci 1997; 811:1-11.

59. Luscher TF, Barton M. Biology of the endothelium. Clin Cardiol 1997; 20(11):3-10.

60. Libby P. Changing concepts of atherogenesis. J Int Med 2000; 247(3):349-358.

61. Li HG, Forstermann U. Nitric oxide in the pathogenesis of vascular disease. J Pathol 2000; 190(3):244-254.

62. Tedgui A, Mallat Z. Anti-inflammatory mechanisms in the vascular wall. Circ Res 2001; 88(9):877-887.

63. Cooke JP, Dzau VJ. Nitric oxide synthase: Role in the genesis of vascular disease. Annu Rev Med 1997; 48:489-509.

64. Gown AM, Tsukada T, Ross R. Human Atherosclerosis .2. Immunocytochemical Analysis of the Cellular Composition of Human Atherosclerotic Lesions. Am J Pathol 1986; 125(1):191-207.

65. Jonasson L, Holm J, Skalli O, Bondjers G, Hansson GK. Regional accumulations of T cells, macrophages, and smooth muscle cells in the human atherosclerotic plaque. Arteriosclerosis 1986; 6(2):131-138.

66. Ross R. The pathogenesis of atherosclerosis: a perspective for the 1990s. Nature 1993; 362:801-809.

67. Goldstein JL, Ho YK, Basu SK, Brown MS. Binding site on macrophages that mediates uptake and degradation of acetylated low density lipoprotein, producing massive cholesterol deposition. Proc Natl Acad Sci USA 1979; 76: 333-337.

68. Rosenfeld ME, Khoo JC, Miller E, Parthasarathy S, Palinski W, Witztum JL. Macrophage-derived foam cells freshly isolated from rabbit atherosclerotic lesions degrade modified lipoproteins, promote oxidation of low-density

lipoproteins, and contain oxidation-specific lipid-protein adducts. J Clin Invest 1991; 87(1):90-99.

69. Libby P, Ordovas JM, Auger KR, Robbins AH, Birinyi LK, Dinarello CA. Endotoxin and Tumor-Necrosis-Factor Induce Interleukin-1 Gene-Expression in Adult Human Vascular Endothelial-Cells. Am J Pathol 1986; 124(2):179-185.

70. Libby P, Friedman GB, Salomon RN. Cytokines As Modulators of Cell-Proliferation in Fibrotic Diseases. Am Rev Respir Dis 1989; 140(4):1114-1117.

71. Ross R, Masuda J, Raines EW, Gown AM, Katsuda S, Sasahara M, et al. Localization of Pdgf-B Protein in Macrophages in All Phases of Atherogenesis. Science 1990; 248(4958):1009-1012.

72. Gordon D, Reidy MA, Benditt EP, Schwartz SM. Cell-Proliferation in Human Coronary-Arteries. Proc Natl Acad Sci USA 1990; 87(12):4600-4604.

73. Rosenfeld ME, Ross R. Macrophage and smooth muscle cell proliferation in atherosclerotic lesions of WHHL and comparably hypercholesterolemic fat-fed rabbits. Arteriosclerosis 1990; 10(5):680-687.

74. Clowes AW, Schwartz SM. Significance of quiescent smooth muscle migration in the injured rat carotid artery. Circ Res 1985; 56(1):139-145.

75. Libby P, Warner SJC, Salomon RN, Birinyi LK. Production of Platelet-Derived Growth-Factor Like Mitogen by Smooth-Muscle Cells from Human Atheroma. N Engl J Med 1988; 318(23):1493-1498.

76. Sjolund M, Hedin U, Sejersen T, Heldin CH, Thyberg J. Arterial smooth muscle cells express platelet-derived growth factor (PDGF) A chain mRNA, secrete a PDGF-like mitogen, and bind exogenous PDGF in a phenotype- and growth state-dependent manner. J Cell Biol 1988; 106(2):403-413.

77. Thyberg J, Hedin U, Sjolund M, Palmberg L, Bottger BA. Regulation of Differentiated Properties and Proliferation of Arterial Smooth-Muscle Cells. Arteriosclerosis 1990; 10(6):966-990.

78. Wolfbauer G, Glick JM, Minor LK, Rothblat GH. Development of the smooth muscle foam cell: uptake of macrophage lipid inclusions. Proc Natl Acad Sci USA 1986; 83(20):7760-7764.

79. Rong JX, Shapiro M, Trogan E, Fisher EA. Transdifferentiation of mouse aortic smooth muscle cells to a macrophage-like state after cholesterol loading. Proc Natl Acad Sci USA 2003; 100(23):13531-13536.

80. Boring L, Gosling J, Cleary M, Charo IF. Decreased lesion formation in CCR2-/- mice reveals a role for chemokines in the initiation of atherosclerosis. Nature 1998; 394(6696):894-897.

81. Dong ZM, Chapman SM, Brown AA, Frenette PS, Hynes RO, Wagner DD. The combined role of P- and E-selectins in atherosclerosis. J Clin Invest 1998; 102(1):145-152.

82. Smith JD, Trogan E, Ginsberg M, Grigaux C, Tian J, Miyata M. Decreased atherosclerosis in mice deficient in both macrophage colony-stimulating factor (op) and apolipoprotein E. Proc Natl Acad Sci USA 1995; 92(18):8264-8268.

83. Mazer SP, Rabbani LE. Evidence for C-reactive protein's role in (CRP) vascular disease: atherothrombosis, immuno-regulation and CRP. J Thromb Thrombolysis 2004; 17(2):95-105.

84. Hak AE, Stehouwer CDA, Bots ML, Polderman KH, Schalkwijk CG, Westendorp ICD, et al. Associations of C-Reactive Protein With Measures of Obesity, Insulin Resistance, and Subclinical Atherosclerosis in Healthy, Middle-Aged Women. Arterioscler Thromb Vasc Biol 1999; 19(8):1986-1991.

85. Hernandez C, Francisco G, Chacon P, Mesa J, Simo R. Biological variation of lipoprotein(a) in a diabetic population. Analysis of the causes and clinical implications. Clin Chem Lab Med 2003; 41(8):1075-1080.

86. Lemieux I, Pascot A, Prud'homme D, Almeras N, Bogaty P, Nadeau A, et al. Elevated C-Reactive Protein : Another Component of the Atherothrombotic Profile of Abdominal Obesity. Arterioscler Thromb Vasc Biol 2001; 21(6):961-967.

87. Packard CJ, O'Reilly DSJ, Caslake MJ, McMahon AD, Ford I, Cooney J, et al. Lipoprotein-Associated Phospholipase A2 as an Independent Predictor of Coronary Heart Disease. New Eng J Med 2000; 343(16):1148-1155.

88. Yasojima K, Schwab C, Mcgeer EG, Mcgeer PL. Generation of C-reactive protein and complement components in atherosclerotic plaques. Am J Pathol 2001; 158(3):1039-1051.

89. Verma S, Wang CH, Li SH, Dumont AS, Fedak PWM, Badiwala MV, et al. A Self-Fulfilling Prophecy: C-Reactive Protein Attenuates Nitric Oxide Production and Inhibits Angiogenesis. Circulation 2002; 106(8):913-919.

90. Pasceri V, Willerson JT, Yeh ET. Direct proinflammatory effect of C-reactive protein on human endothelial cells. Circulation 2000; 102(18):2165-2168.

91. Pasceri V, Chang J, Willerson JT, Yeh ETH. Modulation of C-Reactive Protein-Mediated Monocyte Chemoattractant Protein-1 Induction in Human Endothelial Cells by Anti-Atherosclerosis Drugs. Circulation 2001; 103(21):2531-2534.

92. Zwaka TP, Hombach V, Torzewski J. C-reactive protein-mediated low density lipoprotein uptake by macrophages: implications for atherosclerosis. Circulation 2001; 103(9):1194-7.

93. Szmitko PE, Wang CH, Weisel RD, de Almeida JR, Anderson TJ, Verma S. New Markers of Inflammation and Endothelial Cell Activation: Part I. Circulation 2003; 108(16):1917-1923.

94. Wang CH, Li SH, Weisel RD, Fedak PWM, Dumont AS, Szmitko P, et al. C-Reactive Protein Upregulates Angiotensin Type 1 Receptors in Vascular Smooth Muscle. Circulation 2003; 107(13):1783-1790.

95. Torzewski J, Torzewski M, Bowyer DE, Frohlich M, Koenig W, Waltenberger J, et al. C-reactive protein frequently colocalizes with the terminal complement complex in the intima of early atherosclerotic lesions of human coronary arteries. Arterioscler Thromb Vasc Biol 1998; 18(9):1386-92.

96. Steel DM, Whitehead AS. The Major Acute-Phase Reactants - C- reactive protein, Serum Amyloid-P Component and Serum Amyloid-A Protein. Immunol Today 1994; 15(2):81-88.

97. de Beer MC, Yuan T, Kindy MS, Asztalos BF, Roheim PS, de Beer FC. Characterization of constitutive human serum amyloid A protein (SAA4) as an apolipoprotein. J Lipid Res 1995; 36(3):526-534.

98. Malle E, deBeer FC. Human serum amyloid A (SAA) protein: A prominent acute-phase reactant for clinical practice. Eur J Clin Invest 1996; 26(6):427-435.

99. Johnson BD, Kip KE, Marroquin OC, Ridker PM, Kelsey SF, Shaw LJ, et al. Serum Amyloid A as a Predictor of Coronary Artery Disease and Cardiovascular Outcome in Women: The National Heart, Lung, and Blood Institute-Sponsored Women's Ischemia Syndrome Evaluation (WISE). Circulation 2004; 109(6):726-732.

100. Jousilahti P, Salomaa V, Rasi V, Vahtera E, Palosuo T. The association of c-reactive protein, serum amyloid a and fibrinogen with prevalent coronary heart

disease -- baseline findings of the PAIS project. Atherosclerosis 2001; 156(2):451-456.

101. Ridker PM, Hennekens CH, Buring JE, Rifai N. C-reactive protein and other markers of inflammation in the prediction of cardiovascular disease in women. N Engl J Med 2000; 342(12):836-843.

102. Ridker PM, Rifai N, Pfeffer MA, Sacks FM, Moye LA, Goldman S, et al. Inflammation, Pravastatin, and the Risk of Coronary Events After Myocardial Infarction in Patients With Average Cholesterol Levels. Circulation 1998; 98(9):839-844.

103. Danesh J, Wheeler JG, Hirschfield GM, Eda S, Eiriksdottir G, Rumley A, et al. C-reactive protein and other circulating markers of inflammation in the prediction of coronary heart disease. N Engl J Med 2004; 350(14):1387-1397.

104. Le PT, Muller MT, Mortensen RF. Acute phase reactants of mice. I. Isolation of serum amyloid P- component (SAP) and its induction by a monokine. J Immunol 1982; 129(2):665-672.

105. Pepys MB, Baltz M, Gomer K, Davies AJS, Doenhoff M. Serum Amyloid P-Component Is An Acute-Phase Reactant in the Mouse. Nature 1979; 278(5701):259-261.

106. Gabay C, Kushner I. Acute-Phase Proteins and Other Systemic Responses to Inflammation. New Eng J Med 1999; 340(6):448-454.

107. Uhlar CM, Whitehead AS. Serum amyloid A, the major vertebrate acute-phase reactant. Eur J Biochem 1999; 265(2):501-523.

108. Ferroni P, Basili S, Vieri M, Martini F, Labbadia G, Bellomo A, et al. Soluble P-selectin and proinflammatory cytokines in patients with polygenic type IIa hypercholesterolemia. Haemostasis 1999; 29(5):277-285.

109. Pasqui AL, Di Renzo M, Bova G, Maffei S, Pompella G, Auteri A, et al. Pro-inflammatory/anti-inflammatory cytokine imbalance in acute coronary syndromes. Clin Exp Med 2006; 6(1):38-44.

110. Signorelli SS, Mazzarino MC, Pino LD, Malaponte G, Porto C, Pennisi G, et al. High circulating levels of cytokines (IL-6 and TNFa), adhesion molecules (VCAM-1 and ICAM-1) and selectins in patients with peripheral arterial disease at rest and after a treadmill test. Vasc Med 2003; 8(1):15-19.

111. Teplyakov AI, Pryschepova EV, Kruchinsky NG, Chegerova TI. Cytokines and soluble cell adhesion molecules - Possible markers of inflammatory response in atherosclerosis. Ann N Y Acad Sci 2000; 902:320-322.

112. Harris TB, Ferrucci L, Tracy RP, Corti MC, Wacholder S, Ettinger WH, et al. Associations of elevated interleukin-6 and C-reactive protein levels with mortality in the elderly. Am J Med 1999; 106(5):506-512.

113. Seino Y, Ikeda U, Ikeda M, Yamamoto K, Misawa Y, Hasegawa T, et al. Interleukin 6 gene transcripts are expressed in human atherosclerotic lesions. Cytokine 1994; 6(1):87-91.

114. Ikeda U, Ikeda M, Seino Y, Takahashi M, Kano S, Shimada K. Interleukin-6 Gene Transcripts Are Expressed in Atherosclerotic Lesions of Genetically Hyperlipidemic Rabbits. Atherosclerosis 1992; 92(2-3):213-218.

115. Grimble RF. Inflammatory status and insulin resistance. Curr Opin Clin Nutr Metab Care 2002; 5(5):551-559.

116. Ikeda U, Ito T, Shimada K. Interleukin-6 and acute coronary syndrome. Clin Cardiol 2001; 24(11):701-704.

117. Ridker PM, Rifai N, Stampfer MJ, Hennekens CH. Plasma concentration of interleukin-6 and the risk of future myocardial infarction among apparently healthy men. Circulation 2000; 101(15):1767-1772.

118. Yamashita H, Shimada K, Seki E, Mokuno H, Daida H. Concentrations of interleukins, interferon, and C-reactive protein in stable and unstable angina pectoris. Am J Cardiol 2003; 91(2):133-136.

119. Wang X, Feuerstein GZ, Gu JL, Lysko PG, Yue TL. Interleukin-1[beta] induces expression of adhesion molecules in human vascular smooth muscle cells and enhances adhesion of leukocytes to smooth muscle cells. Atherosclerosis 1995; 115(1):89-98.

120. Filonzi EL, Zoellner H, Stanton H, Hamilton JA. Cytokine Regulation of Granulocyte-Macrophage Colony-Stimulating Factor and Macrophage-Colony-Stimulating Factor Production in Human Arterial Smooth-Muscle Cells. Atherosclerosis 1993; 99(2):241-252.

121. Ng SB, Tan YH, Guy GR. Differential Induction of the Interleukin-6 Gene by Tumor-Necrosis-Factor and Interleukin-1. J Biol Chem 1994; 269(29):19021-19027.

122. Hasdai D, Scheinowitz M, Leibovitz E, Sclarovsky S, Eldar M, Barak V. Increased serum concentrations of interleukin-1 beta in patients with coronary artery disease. Heart 1996; 76(1):24-28.

123. Hotamisligil GS, Shargill NS, Spiegelman BM. Adipose Expression of Tumor-Necrosis-Factor-Alpha - Direct Role in Obesity-Linked Insulin Resistance. Science 1993; 259(5091):87-91.

124. Clausell N, Delima VC, Molossi S, Liu P, Turley E, Gotlieb AI, et al. Expression of Tumor-Necrosis-Factor-Alpha and Accumulation of Fibronectin

in Coronary-Artery Restenotic Lesions Retrieved by Atherectomy. Br Heart J 1995; 73(6):534-539.

125. Ridker PM, Rifai N, Pfeffer M, Sacks F, Lepage S, Braunwald E. Elevation of tumor necrosis factor-alpha and increased risk of recurrent coronary events after myocardial infarction. Circulation 2000; 101(18):2149-2153.

126. Rosenson RS, Tangney CC, Levine DM, Parker TS, Gordon BR. Elevated soluble tumor necrosis factor receptor levels in non-obese adults with the atherogenic dyslipoproteinemia. Atherosclerosis 2004; 177(1):77-81.

127. Ono SJ, Nakamura T, Miyazaki D, Ohbayashi M, Dawson M, Toda M. Chemokines: Roles in leukocyte development, trafficking, and effector function. J Allergy Clin Immunol 2003; 111(6):1185-1199.

128. Nelken NA, Coughlin SR, Gordon D, Wilcox JN. Monocyte Chemoattractant Protein-1 in Human Atheromatous Plaques. Clin Res 1991; 39(2):A335.

129. Takeya M, Yoshimura T, Leonard EJ, Takahashi K. Detection of Monocyte Chemoattractant Protein-1 in Human Atherosclerotic Lesions by An Anti-Monocyte Chemoattractant Protein-1 Monoclonal-Antibody. Hum Pathol 1993; 24(5):534-539.

130. Ylaherttuala S, Lipton BA, Rosenfeld ME, Sarkioja T, Yoshimura T, Leonard EJ, et al. Expression of Monocyte Chemoattractant Protein-1 in Macrophage-Rich Areas of Human and Rabbit Atherosclerotic Lesions. Proc Natl Acad Sci USA 1991; 88(12):5252-5256.

131. Navab M, Berliner JA, Watson AD, Hama SY, Territo MC, Lusis AJ, et al. The Yin and Yang of Oxidation in the Development of the Fatty Streak: A Review Based on the 1994 George Lyman Duff Memorial Lecture. Arterioscler Thromb Vasc Biol 1996; 16(7):831-842.

132. Han KH, Han KO, Green SR, Quehenberger O. Expression of the monocyte chemoattractant protein-1 receptor CCR2 is increased in hypercholesterolemia: differential effects of plasma lipoproteins on monocyte function. J Lipid Res 1999; 40(6):1053-1063.

133. Gosling J, Slaymaker S, Gu L, Tseng S, Zlot CH, Young SG, et al. MCP-1 deficiency reduces susceptibility to atherosclerosis in mice that overexpress human apolipoprotein B. J Clin Invest 1999; 103(6):773-778.

134. Gu L, Okada Y, Clinton SK, Gerard C, Sukhova GK, Libby P, et al. Absence of monocyte chemoattractant protein-1 reduces atherosclerosis in low density lipoprotein receptor-deficient mice. Mol Cell 1998; 2(2):275-281.

135. Hayes IM, Jordan NJ, Towers S, Smith G, Paterson JR, Earnshaw JJ, et al. Human Vascular Smooth Muscle Cells Express Receptors for CC Chemokines. Arterioscler Thromb Vasc Biol 1998; 18(3):397-403.

136. Reape TJ, Groot PH. Chemokines and atherosclerosis. Atherosclerosis 1999; 147(2):213-225.

137. Goldstein JL, Brown MS. Regulation of the mevalonate pathway. Nature 1990; 343(6257):425-430.

138. Goldstein JL, Basu SK, Brown MS. Receptor-mediated endocytosis of low-density lipoprotein in cultured cells. Methods Enzymol 1983; 98:241-260.

139. Yamamoto T, Davis CG, Goldstein JL, Russell DW. The human LDL receptor: a cysteine-rich protein with multiple Alu sequences in its mRNA. Cell 1995; 39:27-38.

140. Herz J, Hamann U, Rogne S, Myklebost O, Gausepohl H, Stanley KK. Surface location and high affinity for calcium of a 500-kd liver membrane protein

closely related to the LDL-receptor suggest a physiological role as lipoprotein receptor. EMBO J 1988; 7(13):4119-4127.

141. Saito A, Pietromonaco S, Loo AK, Farquhar MG. Complete Cloning and Sequencing of rat gp330/"megalin," a Distinctive Member of the Low Density Lipoprotein Receptor Gene Family. Proc Natl Acad Sci USA 1994; 91(21):9725-9729.

142. Takahashi S, Kawarabayasi Y, Nakai T, Sakai J, Yamamoto T. Rabbit very low density lipoprotein receptor: a low density lipoprotein receptor-like protein with distinct ligand specificity. Proc Natl Acad Sci USA 1992; 89(19):9252-9256.

143. Kim DH, Iijima H, Goto K, Sakai J, Ishii H, Kim HJ, et al. Human Apolipoprotein E Receptor 2. J Biol Chem 1996; 271(14):8373-8380.

144. Yamazaki H, Bujo H, Kusunoki J, Seimiya K, Kanaki T, Morisaki N, et al. Elements of Neural Adhesion Molecules and a Yeast Vacuolar Protein Sorting Receptor Are Present in a Novel Mammalian Low Density Lipoprotein Receptor Family Member. J Biol Chem 1996; 271(40):24761-24768.

145. Ishii H, Kim DH, Fujita T, Endo Y, Saeki S, Yamamoto TT. cDNA Cloning of a New Low-Density Lipoprotein Receptor-Related Protein and Mapping of Its Gene (LRP3) to Chromosome Bands 19q12-q13.2. Genomics 1998; 51(1):132-135.

146. Tomita Y, Kim DH, Magoori K, Fujino T, Yamamoto TT. A Novel Low-Density Lipoprotein Receptor-Related Protein with Type II Membrane Protein-Like Structure Is Abundant in Heart. J Biochem (Tokyo) 1998; 124(4):784-789.

147. Kim DH, Inagaki Y, Suzuki T, Ioka RX, Yoshioka SZ, Magoori K, et al. A New Low Density Lipoprotein Receptor Related Protein, LRP5, Is Expressed in

Hepatocytes and Adrenal Cortex, and Recognizes Apolipoprotein E. J Biochem (Tokyo) 1998; 124(6):1072-1076.

148. Brown SD, Twells RCJ, Hey PJ, Cox RD, Levy ER, Soderman AR, et al. Isolation and Characterization ofLRP6,a Novel Member of the Low Density Lipoprotein Receptor Gene Family. Biochem Bioph Res Comm 1998; 248(3):879-888.

149. Liu CX, Musco S, Lisitsina NM, Forgacs E, Minna JD, Lisitsyn NA. LRP-DIT, a Putative Endocytic Receptor Gene, Is Frequently Inactivated in Non-Small Cell Lung Cancer Cell Lines. Cancer Res 2000; 60(7):1961-1967.

150. Sugiyama T, Kumagai H, Morikawa Y, Wada Y, Sugiyama A, Yasuda K, et al. A novel low-density lipoprotein receptor-related protein mediating cellular uptake of apolipoprotein E-enriched beta-VLDL in vitro. Biochemistry 2000; 39(51):15817-15825.

151. Lindgren V, Luskey KL, Russell DW, Francke U. Human Genes Involved in Cholesterol Metabolism: Chromosomal Mapping of the Loci for the Low Density Lipoprotein Receptor and 3-hydroxy-3-methylglutaryl-coenzyme A Reductase with cDNA Probes. Proc Natl Acad Sci USA 1985; 82(24):8567-8571.

152. Sudhof TC, van der Westhuyzen DR, Goldstein JL, Brown MS, Russell DW. Three direct repeats and a TATA-like sequence are required for regulated expression of the human low density lipoprotein receptor gene. J Biol Chem 1987; 262(22):10773-10779.

153. Chang R, Yang E, Chamblis D, Kumar A, Wise J, Mehta KD. In vivo role of the Sp1 site neighboring sterol-responsive element-1 in controlling low-density

lipoprotein receptor gene expression. Biochem Biophys Res Commun 1996; 218(3):733-739.

154. Smith JR, Osborne TF, Goldstein JL, Brown MS. Identification of nucleotides responsible for enhancer activity of sterol regulatory element in low density lipoprotein receptor gene. J Biol Chem 1990; 265(4):2306-2310.

155. Wilson GM, Vasa MZ, Deeley RG. Stabilization and cytoskeletal-association of LDL receptor mRNA are mediated by distinct domains in its 3' untranslated region. J Lipid Res 1998; 39(5):1025-1032.

156. Catapano AL. The low density lipoprotein receptor: Structure, function and pharmacological modulation. Pharmacol Ther 1989; 43(2):187-219.

157. Soutar AK, Knight BL. Structure and regulation of the LDL-receptor and its gene. Br Med Bull 1990; 46(4):891-916.

158. Rawson RB. The SREBP pathway--insights from Insigs and insects. Nat Rev Mol Cell Biol 2003; 4(8):631-640.

159. Yokoyama C, Wang X, Briggs MR, Admon A, Wu J, Hua X, et al. SREBP-1, a basic-helix-loop-helix-leucine zipper protein that controls transcription of the low density lipoprotein receptor gene. Cell 1993; 75(1):187-197.

160. Briggs MR, Yokoyama C, Wang X, Brown MS, Goldstein JL. Nuclear protein that binds sterol regulatory element of low density lipoprotein receptor promoter. I. Identification of the protein and delineation of its target nucleotide sequence. J Biol Chem 1993; 268(19):14490-14496.

161. Wang X, Briggs MR, Hua X, Yokoyama C, Goldstein JL, Brown MS. Nuclear protein that binds sterol regulatory element of low density lipoprotein receptor promoter. II. Purification and characterization. J Biol Chem 1993; 268(19):14497-14504.

162. Horton JD, Goldstein JL, Brown MS. SREBPs: activators of the complete program of cholesterol and fatty acid synthesis in the liver. J Clin Invest 2002; 109(9):1125-1131.

163. Hua X, Sakai J, Ho YK, Goldstein JL, Brown MS. Hairpin orientation of sterol regulatory element-binding protein- 2 in cell membranes as determined by protease protection. J Biol Chem 1995; 270(49):29422-29427.

164. Wang X, Sato R, Brown MS, Hua X, Goldstein JL. SREBP-1, a membrane-bound transcription factor released by sterol-regulated proteolysis. Cell 1994; 77(1):53-62.

165. Nohturfft A, Brown MS, Goldstein JL. Topology of SREBP cleavage-activating protein, a polytopic membrane protein with a sterol-sensing domain. J Biol Chem 1998; 273(27):17243-17250.

166. Hua X, Nohturfft A, Goldstein JL, Brown MS. Sterol resistance in CHO cells traced to point mutation in SREBP cleavage-activating protein. Cell 1996; 87(3):415-426.

167. Adams CM, Goldstein JL, Brown MS. Cholesterol-induced conformational change in SCAP enhanced by Insig proteins and mimicked by cationic amphiphiles. Proc Natl Acad Sci USA 2003; 100(19):10647-10652.

168. Brown AJ, Sun L, Feramisco JD, Brown MS, Goldstein JL. Cholesterol addition to ER membranes alters conformation of SCAP, the SREBP escort protein that regulates cholesterol metabolism. Mol Cell 2002; 10(2):237-245.

169. Radhakrishnan A, Sun LP, Kwon HJ, Brown MS, Goldstein JL. Direct binding of cholesterol to the purified membrane region of SCAP: mechanism for a sterol-sensing domain. Mol Cell 2004; 15(2):259-268.

170. Yabe D, Brown MS, Goldstein JL. Insig-2, a second endoplasmic reticulum protein that binds SCAP and blocks export of sterol regulatory element-binding proteins. Proc Natl Acad Sci USA 2002; 99(20):12753-12758.

171. Yang T, Espenshade PJ, Wright ME, Yabe D, Gong Y, Aebersold R, et al. Crucial step in cholesterol homeostasis: sterols promote binding of SCAP to INSIG-1, a membrane protein that facilitates retention of SREBPs in ER. Cell 2002; 110(4):489-500.

172. Espenshade PJ, Li WP, Yabe D. Sterols block binding of COPII proteins to SCAP, thereby controlling SCAP sorting in ER. Proc Natl Acad Sci USA 2002; 99(18):11694-11699.

173. Brown MS, Goldstein JL. A proteolytic pathway that controls the cholesterol content of membranes, cells, and blood. Proc Natl Acad Sci USA 1999; 96(20):11041-8.

174. Nohturfft A, DeBose-Boyd RA, Scheek S, Goldstein JL, Brown MS. Sterols regulate cycling of SREBP cleavage-activating protein (SCAP) between endoplasmic reticulum and Golgi. Proc Natl Acad Sci USA 1999; 96(20):11235-40.

175. Duncan EA, Brown MS, Goldstein JL, Sakai J. Cleavage site for sterol-regulated protease localized to a leu- Ser bond in the lumenal loop of sterol regulatory element-binding protein-2. J Biol Chem 1997; 272(19):12778-12785.

176. Duncan EA, Dave UP, Sakai J, Goldstein JL, Brown MS. Second-site cleavage in sterol regulatory element-binding protein occurs at transmembrane junction as determined by cysteine panning. J Biol Chem 1998; 273(28):17801-17809.

177. Hirano Y, Yoshida M, Shimizu M, Sato R. Direct Demonstration of Rapid Degradation of Nuclear Sterol Regulatory Element-binding Proteins by the Ubiquitin-Proteasome Pathway. J Biol Chem 2001; 276(39):36431-36437.

178. Auwerx JH, Chait A, Wolfbauer G, Deeb SS. Involvement of second messengers in regulation of the low- density lipoprotein receptor gene. Mol Cell Biol 1989; 9(6):2298-2302.

179. Seidah NG, Benjannet S, Wickham L, Marcinkiewicz J, Jasmin SB, Stifani S, et al. The secretory proprotein convertase neural apoptosis-regulated convertase 1 (NARC-1): Liver regeneration and neuronal differentiation. Proc Natl Acad Sci USA 2003; 100(3):928-933.

180. Abifadel M, Varret M, Rabes JP, Allard D, Ouguerram K, Devillers M, et al. Mutations in PCSK9 cause autosomal dominant hypercholesterolemia. Nat Genet 2003; 34(2):154-156.

181. Leren TP. Mutations in the PCSK9 gene in Norwegian subjects with autosomal dominant hypercholesterolemia. Clin Genet 2004; 65(5):419-422.

182. Shioji K, Mannami T, Kokubo Y, Inamoto N, Takagi S, Goto Y, et al. Genetic variants in PCSK9 affect the cholesterol level in Japanese. J Hum Genet 2004; 49(2):109-114.

183. Timms KM, Wagner S, Samuels ME, Forbey K, Goldfine H, Jammulapati S, et al. A mutation in PCSK9 causing autosomal-dominant hypercholesterolemia in a Utah pedigree. Hum Genet 2004; 114(4):349-353.

184. Maxwell KN, Breslow JL. Adenoviral-mediated expression of Pcsk9 in mice results in a low-density lipoprotein receptor knockout phenotype. Proc Natl Acad Sci USA 2004; 101(18):7100-7105.

185. Rashid S, Curtis DE, Garuti R, Anderson NN, Bashmakov Y, Ho YK, et al. Decreased plasma cholesterol and hypersensitivity to statins in mice lacking Pcsk9. Proc Natl Acad Sci USA 2005; 102(15):5374-5379.

186. Lagace TA, Curtis DE, Garuti R, Mcnutt MC, Park SW, Prather HB, et al. Secreted PCSK9 decreases the number of LDL receptors in hepatocytes and in livers of parabiotic mice. J Clin Invest 2006; 116(11):2995-3005.

187. Wilson GM, Roberts EA, Deeley RG. Modulation of LDL receptor mRNA stability by phorbol esters in human liver cell culture models. J Lipid Res 1997; 38(3):437-446.

188. Zubiaga AM, Belasco JG, Greenberg ME. The nonamer UUAUUUAUU is the key AU-rich sequence motif that mediates mRNA degradation. Mol Cell Biol 1995; 15(4):2219-2230.

189. Knouff C, Malloy S, Wilder J, Altenburg MK, Maeda N. Doubling Expression of the Low Density Lipoprotein Receptor by Truncation of the 3'-Untranslated Region Sequence Ameliorates Type III Hyperlipoproteinemia in Mice Expressing the Human ApoE2 Isoform. J Biol Chem 2001; 276(6):3856-3862.

190. Goto D, Okimoto T, Ono M, Shimotsu H, Abe K, Tsujita Y, et al. Upregulation of Low Density Lipoprotein Receptor by Gemfibrozil, a Hypolipidemic Agent, in Human Hepatoma Cells Through Stabilization of mRNA Transcripts. Arterioscler Thromb Vasc Biol 1997; 17(11):2707-2712.

191. Kong WJ, Wei J, Abidi P, Lin MH, Inaba S, Li C, et al. Berberine is a novel cholesterol-lowering drug working through a unique mechanism distinct from statins. Nat Med 2004; 10(12):1344-1351.

192. Nakahara M, Fujii H, Maloney PR, Shimizu M, Sato R. Bile Acids Enhance Low Density Lipoprotein Receptor Gene Expression via a MAPK Cascade-mediated Stabilization of mRNA. J Biol Chem 2002; 277(40):37229-37234.

193. Hiltunen TP, Yla-Herttuala S. Expression of lipoprotein receptors in atherosclerotic lesions. Atherosclerosis 1998; 137 Suppl: S81-8.

194. Soutar AK, Naoumova RP. Mechanisms of Disease: genetic causes of familial hypercholesterolemia. Nat Clin Pract Cardiovasc Med 2007; 4(4):214-225.

195. Takahashi S, Sakai J, Fujino T, Miyamori I, Yamamoto TT. The very low density lipoprotein (VLDL) receptor - a peripheral lipoprotein receptor for remnant lipoproteins into fatty acid active tissues. Mol Cell Biochem 2003; 248(1-2):121-127.

196. Wyne KL, Pathak K, Seabra MC, Hobbs HH. Expression of the VLDL receptor in endothelial cells. Arterioscler Thromb Vasc Biol 1996; 16(3):407-415.

197. Sakai J, Hoshino A, Takahashi S, Miura Y, Ishii H, Suzuki H, et al. Structure, chromosome location, and expression of the human very low density lipoprotein receptor gene. J Biol Chem 1994; 269(3):2173-2182.

198. Suzuki J, Takahashi S, Oida K, Shimada A, Kohno M, Tamai T, et al. Lipid accumulation and foam cell formation in Chinese hamster ovary cells overexpressing very low density lipoprotein receptor. Biochem Biophys Res Commun 1995; 206(3):835-842.

199. Wittmaack FM, Gafvels ME, Bronner M, Matsuo H, McCrae KR, Tomaszewski JE, et al. Localization and regulation of the human very low density lipoprotein/apolipoprotein-E receptor: trophoblast expression predicts a role for the receptor in placental lipid transport. Endocrinology 1995; 136(1):340-348.

200. Jokinen EV, Landschulz KT, Wyne KL, Ho YK, Frykman PK, Hobbs HH. Regulation of the very low density lipoprotein receptor by thyroid hormone in rat skeletal muscle. J Biol Chem 1994; 269(42):26411-26418.

201. Kwok S, Singh-Bist A, Natu V, Kraemer FB. Dietary regulation of the very low density lipoprotein receptor in mouse heart and fat. Horm Metab Res 1997; 29(10):524-529.

202. Ishibashi T, Yokoyama K, Shindo J, Hamazaki Y, Endo Y, Sato T, et al. Potent cholesterol-lowering effect by human granulocyte-macrophage colony-stimulating factor in rabbits. Possible implications of enhancement of macrophage functions and an increase in mRNA for VLDL receptor. Arterioscler Thromb 1994; 14(10):1534-1541.

203. Masuzaki H, Jingami H, Yamamoto T, Nakao K. Effects of estradiol on very low density lipoprotein receptor mRNA levels in rabbit heart. FEBS Lett 1994; 347(2-3):211-214.

204. Kosaka S, Takahashi S, Masamura K, Kanehara H, Sakai J, Tohda G, et al. Evidence of Macrophage Foam Cell Formation by Very Low-Density Lipoprotein Receptor : Interferon-{{gamma}} Inhibition of Very Low-Density Lipoprotein Receptor Expression and Foam Cell Formation in Macrophages. Circulation 2001; 103(8):1142-1147.

205. Tiebel O, Oka K, Robinson K, Sullivan M, Martinez J, Nakamuta M, et al. Mouse very low-density lipoprotein receptor (VLDLR): gene structure, tissue-specific expression and dietary and developmental regulation. Atherosclerosis 1999; 145(2):239-251.

206. Gafvels ME, Paavola LG, Boyd CO, Nolan PM, Wittmaack F, Chawla A, et al. Cloning of a complementary deoxyribonucleic acid encoding the murine

homolog of the very low density lipoprotein/apolipoprotein-E receptor: expression pattern and assignment of the gene to mouse chromosome 19. Endocrinology 1994; 135(1):387-394.

207. Oka K, Ishimura-Oka K, Chu MJ, Sullivan M, Krushkal J, Li WH, et al. Mouse very-low-density-lipoprotein receptor (VLDLR) cDNA cloning, tissue-specific expression and evolutionary relationship with the low-density-lipoprotein receptor. Eur J Biochem 1994; 224(3):975-982.

208. Webb JC, Patel DD, Jones MD, Knight BL, Soutar AK. Characterization and tissue-specific expression of the human 'very low density lipoprotein (VLDL) receptor' mRNA. Hum Mol Genet 1994; 3(4):531-537.

209. Takahashi S, Oida K, Ookubo M, Suzuki J, Kohno M, Murase T, et al. Very low density lipoprotein receptor binds apolipoprotein E2/2 as well as apolipoprotein E3/3. FEBS Lett 1996; 386(2-3):197-200.

210. Boren J, Lookene A, Makoveichuk E, Xiang S, Gustafsson M, Liu H, et al. Binding of Low Density Lipoproteins to Lipoprotein Lipase Is Dependent on Lipids but Not on Apolipoprotein B. J Biol Chem 2001; 276(29):26916-26922.

211. Takahashi S, Suzuki J, Kohno M, Oida K, Tamai T, Miyabo S, et al. Enhancement of the Binding of Triglyceride-rich Lipoproteins to the Very Low Density Lipoprotein Receptor by Apolipoprotein E and Lipoprotein Lipase. J Biol Chem 1995; 270(26):15747-15754.

212. Argraves KM, Battey FD, MacCalman CD, McCrae KR, Gσfvels M, Kozarsky KF, et al. The Very Low Density Lipoprotein Receptor Mediates the Cellular Catabolism of Lipoprotein Lipase and Urokinase-Plasminogen Activator Inhibitor Type I Complexes. J Biol Chem 1995; 270(44):26550-26557.

213. Goudriaan JR, Tacken PJ, Dahlmans VEH, Gijbels MJJ, van Dijk KW, Havekes LM, et al. Protection From Obesity in Mice Lacking the VLDL Receptor. Arterioscler Thromb Vasc Biol 2001; 21(9):1488-1493.

214. Tacken PJ, Teusink B, Jong MC, Harats D, Havekes LM, van Dijk KW, et al. LDL receptor deficiency unmasks altered VLDL triglyceride metabolism in VLDL receptor transgenic and knockout mice. J Lipid Res 2000; 41(12):2055-2062.

215. Kohno M, Takahashi S, Oida K, Suzuki J, Tamai T, Yamamoto T, et al. 1 alpha,25-dihydroxyvitamin D3 induces very low density lipoprotein receptor mRNA expression in HL-60 cells in association with monocytic differentiation. Atherosclerosis 1997; 133(1):45-49.

216. Argraves KM, Kozarsky KF, Fallon JT, Harpel PC, Strickland DK. The atherogenic lipoprotein Lp(a) is internalized and degraded in a process mediated by the VLDL receptor. J Clin Invest 1997; 100(9):2170-2181.

217. Hiltunen TP, Luoma JS, Nikkari T, Yla-Herttuala S. Expression of LDL receptor, VLDL receptor, LDL receptor-related protein, and scavenger receptor in rabbit atherosclerotic lesions: marked induction of scavenger receptor and VLDL receptor expression during lesion development. Circulation 1998; 97(11):1079-1086.

218. Multhaupt HA, Gafvels ME, Kariko K, Jin H, Arenas-Elliot C, Goldman BI, et al. Expression of very low density lipoprotein receptor in the vascular wall. Analysis of human tissues by in situ hybridization and immunohistochemistry. Am J Pathol 1996; 148(6):1985-1997.

219. Nakazato K, Ishibashi T, Shindo J, Shiomi M, Maruyama Y. Expression of very low density lipoprotein receptor mRNA in rabbit atherosclerotic lesions. Am J Pathol 1996; 149(6):1831-1838.

220. Yagyu H, Lutz EP, Kako Y, Marks S, Hu Y, Choi SY, et al. Very low density lipoprotein (VLDL) receptor-deficient mice have reduced lipoprotein lipase activity. Possible causes of hypertriglyceridemia and reduced body mass with VLDL receptor deficiency. J Biol Chem 2002; 277(12):10037-10043.

221. Elomaa O, Kangas M, Sahlberg C, Tuukkanen J, Sormunen R, Liakka A, et al. Cloning of a novel bacteria-binding receptor structurally related to scavenger receptors and expressed in a subset of macrophages. Cell 1995; 80(4):603-609.

222. Emi M, Asaoka H, Matsumoto A, Itakura H, Kurihara Y, Wada Y, et al. Structure, organization, and chromosomal mapping of the human macrophage scavenger receptor gene. J Biol Chem 1993; 268(3):2120-2125.

223. Freeman M, Ashkenas J, Rees DJG, Kingsley DM, Copeland NG, Jenkins NA, et al. An Ancient, Highly Conserved Family of Cysteine-Rich Protein Domains Revealed by Cloning Type I and Type II Murine Macrophage Scavenger Receptors. Proc Natl Acad Sci USA 1990; 87(22):8810-8814.

224. Gough PJ, Greaves DR, Gordon S. A naturally occurring isoform of the human macrophage scavenger receptor (SR-A) gene generated by alternative splicing blocks modified LDL uptake. J Lipid Res 1998; 39(3):531-543.

225. Kangas M, Brannstrom A, Elomaa O, Matsuda Y, Eddy R, Shows TB, et al. Structure and Chromosomal Localization of the Human and Murine Genes for the Macrophage MARCO Receptor. Genomics 1999; 58(1):82-89.

226. Nakamura K, Funakoshi H, Miyamoto K, Tokunaga F, Nakamura T. Molecular Cloning and Functional Characterization of a Human Scavenger Receptor with

C-Type Lectin (SRCL), a Novel Member of a Scavenger Receptor Family. Biochem Bioph Res Comm 2001; 280(4):1028-1035.

227. Armesilla AL, Vega MA. Structural organization of the gene for human CD36 glycoprotein. J Biol Chem 1994; 269(29):18985-18991.

228. Cao G, Garcia CK, Wyne KL, Schultz RA, Parker KL, Hobbs HH. Structure and localization of the human gene encoding SR-BI/CLA-1. Evidence for transcriptional control by steroidogenic factor 1. J Biol Chem 1997; 272(52):33068-33076.

229. Webb NR, de Villiers WJ, Connell PM, de Beer FC, van der Westhuyzen DR. Alternative forms of the scavenger receptor BI (SR-BI). J Lipid Res 1997; 38(7):1490-1495.

230. Adachi H, Tsujimoto M. FEEL-1, a Novel Scavenger Receptor with in Vitro Bacteria-binding and Angiogenesis-modulating Activities. J Biol Chem 2002; 277(37):34264-34270.

231. Luoma J, Hiltunen T, Sarkioja T, Moestrup SK, Gliemann J, Kodama T, et al. Expression of a2-macroglobulin receptor/low density li8poprotein receptor related protein and scavenger rceptor in human atherosclerotic lesions. J Clin Invest 1994; 93:2014-2021.

232. Ylaherttuala S. Expression of lipoprotein receptors and related molecules in atherosclerotic lesions. Curr Opin Lipidol 1996; 7(5):292-297.

233. Moore KJ, Freeman MW. Scavenger Receptors in Atherosclerosis: Beyond Lipid Uptake. Arterioscler Thromb Vasc Biol 2006; 26(8):1702-1711.

234. Stulnig TM, Klocker H, Harwood HJ, Jr., Jurgens G, Schonitzer D, Jarosch E, et al. In Vivo LDL Receptor and HMG-CoA Reductase Regulation in Human

Lymphocytes and Its Alterations During Aging. Arterioscler Thromb Vasc Biol 1995; 15(7):872-878.

235. Kodama T, Doi T, Suzuki H, Takahashi K, Wada Y, Gordon S. Collagenous macrophage scavenger receptors. Curr Opin Lipidol 1996; 7(5):287-291.

236. Krieger M, Acton S, Ashkenas J, Pearson A, Penman M, Resnick D. Molecular flypaper, host defense, and atherosclerosis. Structure, binding properties, and functions of macrophage scavenger receptors. J Biol Chem 1993; 268(7):4569-4572.

237. Krieger M, Herz J. Structures and functions of multiligand lipoprotein receptors: macrophage scavenger receptors and LDL receptor-related protein (LRP). Annu Rev Biochem 1994; 63:601-637.

238. Kodama T, Freeman M, Rohrer L, Zabrecky J, Matsudaira P, Krieger M. Type I macrophage scavenger receptor contains a-helical and X collagen-like coiled coils. Nature 1990; 343:531-535.

239. Rohrer L, Freeman M, Kodama T, Penman M, Krieger M. Coiled-coil fibrous domains mediate ligand binding by macrophage scavenger receptor type II. Nature 1990; 343(6258):570-572.

240. Steinberg D. Low density lipoprotein oxidation and its pathobiological significance. J Biol Chem 1997; 272(34):20963-20966.

241. Freeman M, Ekkel Y, Rohrer L, Penman M, Freedman NJ, Chisolm GM, et al. Expression of type I and type II bovine scavenger receptors in Chinese hamster ovary cells: lipid droplet accumulation and nonreciprocal cross competition by acetylated and oxidized low density lipoprotein. Proc Natl Acad Sci USA 1991; 88(11):4931-4935.

242. Gough PJ, Greaves DR, Suzuki H, Hakkinen T, Hiltunen MO, Turunen M, et al. Analysis of macrophage scavenger receptor (SR-A) expression in human aortic atherosclerotic lesions. Arterioscler Thromb Vasc Biol 1999; 19(3):461-471.

243. Suzuki H, Kurihara Y, Takeya M, Kamada N, Kataoka M, Jishage K, et al. A role for macrophage scavenger receptors in atherosclerosis and susceptibility to infection. Nature 1997; 386(6622):292-296.

244. Sakaguchi H, Takeya M, Suzuki H, Hakamata H, Kodama T, Horiuchi S, et al. Role of macrophage scavenger receptors in diet-induced atherosclerosis in mice. Lab Invest 1998; 78(4):423-434.

245. de Winther MPJ, Gijbels MJJ, Van Dijk KW, Havekes LM, Hofker MH. Transgenic mouse models to study the role of the macrophage scavenger receptor class A in atherosclerosis. Int J Tissue React 2000; 22(2-3):85-91.

246. Swerlick RA, Lee KH, Wick TM, Lawley TJ. Human dermal microvascular endothelial but not human umbilical vein endothelial cells express CD36 in vivo and in vitro. J Immunol 1992; 148(1):78-83.

247. Matsumoto K, Hirano Ki, Nozaki S, Takamoto A, Nishida M, Nakagawa-Toyama Y, et al. Expression of Macrophage (M{phi}) Scavenger Receptor, CD36, in Cultured Human Aortic Smooth Muscle Cells in Association With Expression of Peroxisome Proliferator Activated Receptor-{gamma}, Which Regulates Gain of M{phi}-Like Phenotype In Vitro, and Its Implication in Atherogenesis. Arterioscler Thromb Vasc Biol 2000; 20(4):1027-1032.

248. Kunjathoor VV, Febbraio M, Podrez EA, Moore KJ, Andersson L, Koehn S, et al. Scavenger Receptors Class A-I/II and CD36 Are the Principal Receptors Responsible for the Uptake of Modified Low Density Lipoprotein Leading to Lipid Loading in Macrophages. J Biol Chem 2002; 277(51):49982-49988.

249. Endemann G, Stanton LW, Madden KS, Bryant CM, White RT, Protter AA. CD36 is a receptor for oxidized low density lipoprotein. J Biol Chem 1993; 268(16):11811-11816.

250. Nozaki S, Kashiwagi H, Yamashita S, Nakagawa T, Kostner B, Tomiyama Y, et al. Reduced Uptake of Oxidized Low-Density Lipoproteins in Monocyte-Derived Macrophages from Cd36-Deficient Subjects. J Clin Invest 1995; 96(4):1859-1865.

251. Febbraio M, Podrez EA, Smith JD, Hajjar DP, Hazen SL, Hoff HF, et al. Targeted disruption of the class B scavenger receptor CD36 protects against atherosclerotic lesion development in mice. J Clin Invest 2000; 105(8):1049-1056.

252. Febbraio M, Guy E, Silverstein RL. Stem cell transplantation reveals that absence of macrophage CD36 is protective against atherosclerosis. Arterioscler Thromb Vasc Biol 2004; 24(12):2333-2338.

253. Guy E, Kuchibhotla S, Silverstein R, Febbraio M. Continued inhibition of atherosclerotic lesion development in long term Western diet fed CD36 degrees/apoE degrees mice. Atherosclerosis 2007; 192(1):123-130.

254. Marleau S, Harb D, Bujold K, Avallone R, Iken K, Wang YF, et al. EP 80317, a ligand of the CD36 scavenger receptor, protects apolipoprotein E-deficient mice from developing atherosclerotic lesions. FASEB J 2005; 19(10):1869-71.

255. Acton S, Rigotti A, Landschulz KT, Xu S, Hobbs HH, Krieger M. Identification of scavenger receptor SR-BI as a high density lipoprotein receptor. Science 1996; 271(5248):518-520.

256. Rigotti A, Miettinen HE, Krieger M. The role of the high-density lipoprotein receptor SR-BI in the lipid metabolism of endocrine and other tissues. Endocr Rev 2003; 24(3):357-387.

257. Yancey PG, Bortnick AE, Kellner-Weibel G, de la Llera-Moya M, Phillips MC, Rothblat GH. Importance of different pathways of cellular cholesterol efflux. Arterioscler Thromb Vasc Biol 2003; 23(5):712-719.

258. Arai T, Wang N, Bezouevski M, Welch C, Tall AR. Decreased atherosclerosis in heterozygous low density lipoprotein receptor-deficient mice expressing the scavenger receptor BI transgene. J Biol Chem 1999; 274(4):2366-2371.

259. Kozarsky KF, Donahee MH, Glick JM, Krieger M, Rader DJ. Gene transfer and hepatic overexpression of the HDL receptor SR-BI reduces atherosclerosis in the cholesterol-fed LDL receptor-deficient mouse. Arterioscler Thromb Vasc Biol 2000; 20(3):721-727.

260. Ueda Y, Gong E, Royer L, Cooper PN, Francone OL, Rubin EM. Relationship between expression levels and atherogenesis in scavenger receptor class B, type I transgenics. J Biol Chem 2000; 275(27):20368-20373.

261. Braun A, Zhang SW, Miettinen HE, Ebrahim S, Holm TM, Vasile E, et al. Probucol prevents early coronary heart disease and death in the high-density lipoprotein receptor SR-BI/apolipoprotein E double knockout mouse. Proc Natl Acad Sci USA 2003; 100(12):7283-7288.

262. Holm TM, Braun A, Trigatti BL, Brugnara C, Sakamoto M, Krieger M, et al. Failure of red blood cell maturation in mice with defects in the high-density lipoprotein receptor SR-BI. Blood 2002; 99(5):1817-1824.

263. Mardones P, Quinones V, Amigo L, Moreno M, Miquel JF, Schwarz M, et al. Hepatic cholesterol and bile acid metabolism and intestinal cholesterol

absorption in scavenger receptor class B type I-deficient mice. J Lipid Res 2001; 42(2):170-180.

264. Miettinen HE, Rayburn H, Krieger M. Abnormal lipoprotein metabolism and reversible female infertility in HDL receptor (SR-BI)-deficient mice. J Clin Invest 2001; 108(11):1717-1722.

265. Rigotti A, Trigatti BL, Penman M, Rayburn H, Herz J, Krieger M. A targeted mutation in the murine gene encoding the high density lipoprotein (HDL) receptor scavenger receptor class B type I reveals its key role in HDL metabolism. Proc Natl Acad Sci USA 1997; 94(23):12610-12615.

266. Huszar D, Varban ML, Rinninger F, Feeley R, Arai T, Fairchild-Huntress V, et al. Increased LDL cholesterol and atherosclerosis in LDL receptor-deficient mice with attenuated expression of scavenger receptor B1. Arterioscler Thromb Vasc Biol 2000; 20(4):1068-1073.

267. Out R, Hoekstra M, Spijkers JAA, Kruijt JK, Van Eck M, Bos IST, et al. Scavenger receptor class B type I is solely responsible for the selective uptake of cholesteryl esters from HDL by the liver and the adrenals in mice. J Lipid Res 2004; 45(11):2088-2095.

268. Covey SD, Krieger M, Wang W, Penman M, Trigatti BL. Scavenger receptor class B type I-mediated protection against atherosclerosis in LDL receptor-negative mice involves its expression in bone marrow-derived cells. Arterioscler Thromb Vasc Biol 2003; 23(9):1589-1594.

269. Braun A, Trigatti BL, Post MJ, Sato K, Simons M, Edelberg JM, et al. Loss of SR-BI expression leads to the early onset of occlusive atherosclerotic coronary artery disease, spontaneous myocardial infarctions, severe cardiac dysfunction,

and premature death in apolipoprotein E-deficient mice. Circ Res 2002; 90(3):270-276.

270. Trigatti B, Rayburn H, Vinals M, Braun A, Miettinen H, Penman M, et al. Influence of the high density lipoprotein receptor SR-BI on reproductive and cardiovascular pathophysiology. Proc Natl Acad Sci USA 1999; 96(16):9322-9327.

271. Chinetti G, Gbaguidi FG, Griglio S, Mallat Z, Antonucci M, Poulain P, et al. CLA-1/SR-BI is expressed in atherosclerotic lesion macrophages and regulated by activators of peroxisome proliferator-activated receptors. Circulation 2000; 101(20):2411-7.

272. Hirano K, Yamashita S, Nakagawa Y, Ohya T, Matsuura F, Tsukamoto K, et al. Expression of human scavenger receptor class B type I in cultured human monocyte-derived macrophages and atherosclerotic lesions. Circ Res 1999; 85(1):108-116.

273. Ji Y, Jian B, Wang N, Sun Y, Moya ML, Phillips MC, et al. Scavenger receptor BI promotes high density lipoprotein-mediated cellular cholesterol efflux. J Biol Chem 1997; 272(34):20982-20985.

274. Van Eck M, Bos IST, Hildebrand RB, Van Rij BT, Van Berkel TJC. Dual role for scavenger receptor class B, type I on bone marrow-derived cells in atherosclerotic lesion development. Am J Pathol 2004; 165(3):785-794.

275. Zhang WW, Yancey PG, Su YR, Babaev VR, Zhang YM, Fazio S, et al. Inactivation of macrophage scavenger receptor class B type I promotes atherosclerotic lesion development in apolipoprotein E-deficient mice. Circulation 2003; 108(18):2258-2263.

276. Singer II, Kawka DW, Kazazis DM, Alberts AW, Chen JS, Huff JW, et al. Hydroxymethylglutaryl-coenzyme A Reductase-Containing Hepatocytes are Distributed Periportally in Normal and Mevinolin-Treated Rat Livers. Proc Natl Acad Sci USA 1984; 81(17):5556-5560.

277. Bloch K. Summing-Up. Annu Rev Biochem 1987; 56:1-19.

278. Brown MS, Goldstein JL. Receptor-Mediated Control of Cholesterol Metabolism. Science 1976; 191:150-154.

279. Porter JA. Cholesterol modification of hedgehog signaling proteins in animal development. Science 1996; 274(5293):1597.

280. Tint GS, Irons M, Elias ER, Batta AK, Frieden R, Chen TS, et al. Defective Cholesterol-Biosynthesis Associated with the Smith-Lemli-Opitz Syndrome. N Engl J Med 1994; 330(2):107-113.

281. Irons M, Elias ER, Tint GS, Salen G, Frieden R, Buie TM, et al. Abnormal Cholesterol-Metabolism in the Smith-Lemli-Opitz Syndrome - Report of Clinical and Biochemical Findings in 4 Patients and Treatment in One Patient. Am J Med Genet 1994; 50(4):347-352.

282. Grundy SM. Cholesterol and Coronary Heart-Disease - A New Era. JAMA 1986; 256(20):2849-2858.

283. Olender EH, Simon RD. The intracellular targeting and membrane topology of 3-hydroxy-3- methylglutaryl-CoA reductase. J Biol Chem 1992; 267(6):4223-4235.

284. Jingami H, Brown MS, Goldstein JL, Anderson RG, Luskey KL. Partial deletion of membrane-bound domain of 3-hydroxy-3-methylglutaryl coenzyme A reductase eliminates sterol-enhanced degradation and prevents formation of crystalloid endoplasmic reticulum. J Cell Biol 1987; 104(6):1693-1704.

285. Xu L, Simoni RD. The inhibition of degradation of 3-hydroxy-3-methylglutaryl coenzyme A (HMG-CoA) reductase by sterol regulatory element binding protein cleavage-activating protein requires four phenylalanine residues in span 6 of HMG-CoA reductase transmembrane domain. Arch Biochem Biophys 2003; 414(2):232-243.

286. Sever N, Yang T, Brown MS, Goldstein JL, DeBose-Boyd RA. Accelerated degradation of HMG CoA reductase mediated by binding of insig-1 to its sterol-sensing domain. Mol Cell 2003; 11(1):25-33.

287. Sever N, Song BL, Yabe D, Goldstein JL, Brown MS, Bose-Boyd RA. Insig-dependent Ubiquitination and Degradation of Mammalian 3-Hydroxy-3-methylglutaryl-CoA Reductase Stimulated by Sterols and Geranylgeraniol. J Biol Chem 2003; 278(52):52479-52490.

288. Sato R, Goldstein JL, Brown MS. Replacement of Serine-871 of Hamster 3-Hydroxy-3-Methylglutaryl-CoA Reductase Prevents Phosphorylation by AMP-Activated Kinase and Blocks Inhibition of Sterol Synthesis Induced by ATP Depletion. Proc Natl Acad Sci USA 1993; 90(20):9261-9265.

289. Tabernero L, Bochar DA, Rodwell VW, Stauffacher CV. Substrate-induced closure of the flap domain in the ternary complex structures provides insights into the mechanism of catalysis by 3-hydroxy-3-methylglutaryl-CoA reductase. Proc Natl Acad Sci USA 1999; 96(13):7167-7171.

290. Hardie DG. Minireview: The AMP-Activated Protein Kinase Cascade: The Key Sensor of Cellular Energy Status. Endocrinology 2003; 144(12):5179-5183.

291. Dale S, Arro M, Becerra B, Morrice NG, Boronat A, Hardie DG, et al. Bacterial Expression of the Catalytic Domain of 3-Hydroxy-3-Methylglutaryl-Coa Reductase (Isoform Hmgr1) from Arabidopsis-Thaliana, and Its Inactivation by

Phosphorylation at Ser577 by Brassica-Oleracea 3-Hydroxy-3-Methylglutaryl-Coa Reductase Kinase. Eur J Biochem 1995; 233(2):506-513.

292. Maron DJ, Fazio S, Linton MF. Current perspectives on statins. Circulation 2000; 101(2):207-213.

293. Vaughan CJ, Gotto AM, Basson CT. The evolving role of statins in the management of atherosclerosis. J Am Coll Cardiol 2000; 35(1):1-10.

294. Rothblat GH, de la Llera-Moya M, Atger V, Kellner-Weibel G, Williams DL, Phillips MC. Cell cholesterol efflux: integration of old and new observations provides new insights. J Lipid Res 1999; 40(5):781-796.

295. Gu X, Kozarsky K, Krieger M. Scavenger Receptor Class B, Type I-mediated [3H] Cholesterol Efflux to High and Low Density Lipoproteins Is Dependent on Lipoprotein Binding to the Receptor. J Biol Chem 2000; 275(39):29993-30001.

296. Wang N, Silver DL, Costet P, Tall AR. Specific Binding of ApoA-I, Enhanced Cholesterol Efflux, and Altered Plasma Membrane Morphology in Cells Expressing ABC1. J Biol Chem 2000; 275(42):33053-33058.

297. Phillips MC, Johnson WJ, Rothblat GH. Mechanisms and consequences of cellular cholesterol exchange and transfer. Biochim Biophys Acta 1987; 906(2):223-276.

298. Liadaki KN, Liu T, Xu S, Ishida BY, Duchateaux PN, Krieger JP, et al. Binding of high density lipoprotein (HDL) and discoidal reconstituted HDL to the HDL receptor scavenger receptor class B type I. Effect of lipid association and APOA-I mutations on receptor binding. J Biol Chem 2000; 275(28):21262-21271.

299. Wang N, Silver DL, Thiele C, Tall AR. ATP-binding Cassette Transporter A1 (ABCA1) Functions as a Cholesterol Efflux Regulatory Protein. J Biol Chem 2001; 276(26):23742-23747.

300. Fielding CJ, Fielding PE. Cellular cholesterol efflux. Biochim Biophys Acta 2001; 1533(3):175-189.

301. Santamarina-Fojo S, Peterson K, Knapper C, Qiu Y, Freeman L, Cheng JF, et al. Complete genomic sequence of the human ABCA1 gene: Analysis of the human and mouse ATP-binding cassette A promoter. Proc Natl Acad Sci USA 2000; 97(14):7987-7992.

302. Rust S, Rosier M, Funke H, Real J, Amoura Z, Piette JC, et al. Tangier disease is caused by mutations in the gene encoding ATP- binding cassette transporter 1. Nat Genet 1999; 22(4):352-5.

303. Langmann T, Klucken J, Reil M, Liebisch G, Luciani MF, Chimini G, et al. Molecular cloning of the human ATP-binding cassette transporter 1 (hABC1): evidence for sterol-dependent regulation in macrophages. Biochem Biophys Res Commun 1999; 257(1):29-33.

304. Liao H, Langmann T, Schmitz G, Zhu Y. Native LDL Upregulation of ATP-Binding Cassette Transporter-1 in Human Vascular Endothelial Cells. Arterioscler Thromb Vasc Biol 2002; 22(1):127-132.

305. Chawla A, Repa JJ, Evans RM, Mangelsdorf DJ. Nuclear Receptors and Lipid Physiology: Opening the X-Files. Science 2001; 294(5548):1866-1870.

306. Lu TT, Repa JJ, Mangelsdorf DJ. Orphan nuclear receptors as eLiXiRs and FiXeRs of sterol metabolism. J Biol Chem 2001; 276(41):37735-37738.

307. Wagner BL, Valledor AF, Shao G, Daige CL, Bischoff ED, Petrowski M, et al. Promoter-specific roles for liver X receptor/corepressor complexes in the

regulation of ABCA1 and SREBP1 gene expression. Mol Cell Biol 2003; 23(16):5780-5789.

308. Fu X, Menke JG, Chen Y, Zhou G, MacNaul KL, Wright SD, et al. 27-Hydroxycholesterol Is an Endogenous Ligand for Liver X Receptor in Cholesterol-loaded Cells. J Biol Chem 2001; 276(42):38378-38387.

309. Repa JJ, Turley SD, Lobaccaro JA, Medina J, Li L, Lustig K, et al. Regulation of absorption and ABC1-mediated efflux of cholesterol by RXR heterodimers. Science 2000; 289(5484):1524-1529.

310. Venkateswaran A, Laffitte BA, Joseph SB, Mak PA, Wilpitz DC, Edwards PA, et al. Control of cellular cholesterol efflux by the nuclear oxysterol receptor LXR alpha. Proc Natl Acad Sci USA 2000; 97(22):12097-102 2001;97(22):12097-102.

311. Chawla A, Boisvert WA, Lee CH, Laffitte BA, Barak Y, Joseph SB, et al. A PPAR gamma-LXR-ABCA1 pathway in macrophages is involved in cholesterol efflux and atherogenesis. Mol Cell 2001; 7(1):161-71.

312. Chinetti G, Lestavel S, Bocher V, Remaley AT, Neve B, Torra IP, et al. PPAR-alpha and PPAR-gamma activators induce cholesterol removal from human macrophage foam cells through stimulation of the ABCA1 pathway. Nat Med 2001; 7(1):53-8.

313. Schmitz G, Langmann T. Transcriptional regulatory networks in lipid metabolism control ABCA1 expression. Biochim Biophys Acta 2005; 1735(1):1-19.

314. Wellington CL, Walker EKY, Suarez A, Kwok A, Bissada N, Singaraja R, et al. ABCA1 mRNA and protein distribution patterns predict multiple different roles and levels of regulation. Lab Invest 2002; 82(3):273-283.

315. Uehara Y, Engel T, Li Z, Goepfert C, Rust S, Zhou X, et al. Polyunsaturated Fatty Acids and Acetoacetate Downregulate the Expression of the ATP-Binding Cassette Transporter A1. Diabetes 2002; 51(10):2922-2928.

316. Wang Y, Oram JF. Unsaturated Fatty Acids Inhibit Cholesterol Efflux from Macrophages by Increasing Degradation of ATP-binding Cassette Transporter A1. J Biol Chem 2002; 277(7):5692-5697.

317. Ou J, Tu H, Shan B, Luk A, Bose-Boyd RA, Bashmakov Y, et al. Unsaturated fatty acids inhibit transcription of the sterol regulatory element-binding protein-1c (SREBP-1c) gene by antagonizing ligand-dependent activation of the LXR. Proc Natl Acad Sci USA 2001; 98(11):6027-6032.

318. Wang Y, Kurdi-Haidar B, Oram JF. LXR-mediated activation of macrophage stearoyl-CoA desaturase generates unsaturated fatty acids that destabilize ABCA1. J Lipid Res 2004; 45(5):972-980.

319. Martinez LO, gerholm-Larsen B, Wang N, Chen W, Tall AR. Phosphorylation of a Pest Sequence in ABCA1 Promotes Calpain Degradation and Is Reversed by ApoA-I. J Biol Chem 2003; 278(39):37368-37374.

320. Yamauchi Y, Hayashi M, be-Dohmae S, Yokoyama S. Apolipoprotein A-I Activates Protein Kinase C{alpha} Signaling to Phosphorylate and Stabilize ATP Binding Cassette Transporter A1 for the High Density Lipoprotein Assembly. J Biol Chem 2003; 278(48):47890-47897.

321. Wang N, Chen W, Linsel-Nitschke P, Martinez LO, gerholm-Larsen B, Silver DL, et al. A PEST sequence in ABCA1 regulates degradation by calpain protease and stabilization of ABCA1 by apoA-I. J CLin Invest 2003; 111(1):99-107.

322. Arakawa R, Yokoyama S. Helical Apolipoproteins Stabilize ATP-binding Cassette Transporter A1 by Protecting It from Thiol Protease-mediated Degradation. J Biol Chem 2002; 277(25):22426-22429.

323. Oram JF, Wolfbauer G, Vaughan AM, Tang C, Albers JJ. Phospholipid Transfer Protein Interacts with and Stabilizes ATP-binding Cassette Transporter A1 and Enhances Cholesterol Efflux from Cells. J Biol Chem 2003; 278(52):52379-52385.

324. Albrecht C, Soumian S, Amey JS, Sardini A, Higgins CF, Davies AH, et al. ABCA1 Expression in Carotid Atherosclerotic Plaques. Stroke 2004; 35(12):2801-2806.

325. Kennedy MA, Venkateswaran A, Tarr PT, Xenarios I, Kudoh J, Shimizu N, et al. Characterization of the human ABCG1 gene: liver X receptor activates an internal promoter that produces a novel transcript encoding an alternative form of the protein. J Biol Chem 2001; 276(42):39438-39447.

326. Nakamura K, Kennedy MA, Baldan A, Bojanic DD, Lyons K, Edwards PA. Expression and Regulation of Multiple Murine ATP-binding Cassette Transporter G1 mRNAs/Isoforms That Stimulate Cellular Cholesterol Efflux to High Density Lipoprotein. J Biol Chem 2004; 279(44):45980-45989.

327. Vaughan AM, Oram JF. ABCG1 Redistributes Cell Cholesterol to Domains Removable by High Density Lipoprotein but Not by Lipid-depleted Apolipoproteins. J Biol Chem 2005; 280(34):30150-30157.

328. Wang N, Lan DB, Chen WG, Matsuura F, Tall AR. ATP-binding cassette transporters G1 and G4 mediate cellular cholesterol efflux to high-density lipoproteins. Proc Natl Acad Sci USA 2004; 101(26):9774-9779.

329. Kennedy MA, Barrera GC, Nakamura K, Baldan A, Tarr P, Fishbein MC, et al. ABCG1 has a critical role in mediating cholesterol efflux to HDL and preventing cellular lipid accumulation. Cell Metab 2005; 1(2):121-131.

330. Li AC, Binder CJ, Gutierrez A, Brown KK, Plotkin CR, Pattison JW, et al. Differential inhibition of macrophage foam-cell formation and atherosclerosis in mice by PPAR{alpha}, {beta}/{delta}, and {gamma}. J Clin Invest 2004; 114(11):1564-1576.

331. Suzuki S, Nishimaki-Mogami T, Tamehiro N, Inoue K, Arakawa R, be-Dohmae S, et al. Verapamil Increases the Apolipoprotein-Mediated Release of Cellular Cholesterol by Induction of ABCA1 Expression Via Liver X Receptor-Independent Mechanism. Arterioscler Thromb Vasc Biol 2004; 24(3):519-525.

332. Brown MS, Kovanen PT, Goldstein JL. Regulation of plasma cholesterol by lipoprotein receptors. Science 1981; 212:128-135.

333. Sherrill BC, Dietschy JM. Characterization of the sinusoidal transport process responsible for uptake of chylomicrons by the liver. J Biol Chem 1978; 253(6):1859-1867.

334. Windler E, Chao Y, Havel RJ. Determinants of hepatic uptake of triglyceride-rich lipoproteins and their remnants in the rat. J Biol Chem 1980; 255(11):5475-5480.

335. Carew TE, Pittman RC, Steinberg D. Tissue sites of degradation of native and reductively methylated [14C] sucrose-labeled low density lipoprotein in rats. Contribution of receptor-dependent and receptor-independent pathways. J Biol Chem 1982; 257(14):8001-8008.

336. Spady DK, Bilheimer DW, Dietschy JM. Rates of Receptor-Dependent and - Independent Low Density Lipoprotein Uptake in the Hamster. Proc Natl Acad Sci USA 1983; 80(11):3499-3503.

337. Hui DY, Innerarity TL, Mahley RW. Lipoprotein binding to canine hepatic membranes. Metabolically distinct apo-E and apo-B, E receptors. J Biol Chem 1981; 256(11):5646-5655.

338. Glomset JA. Plasma Lecithin - Cholesterol Acyltransferase Reaction. J Lipid Res 1968; 9(2):155-&.

339. Ross R, Glomset JA. Atherosclerosis and the arterial smooth muscle cell: Proliferation of smooth muscle is a key event in the genesis of the lesions of atherosclerosis. Science 1973; 180(93):1332-1339.

340. Miller GJ, Miller NE. Plasma-High-Density-Lipoprotein Concentration and Development of Ischemic Heart-Disease. Lancet 1975; 1(7897):16-19.

341. de la Llera-Moya M, Rothblat GH, Connelly MA, Kellner-Weibel G, Sakr SW, Phillips MC, et al. Scavenger receptor BI (SR-BI) mediates free cholesterol flux independently of HDL tethering to the cell surface. J Lipid Res 1999; 40(3):575-580.

342. Williams DL, Connelly MA, Temel RE, Swarnakar S, Phillips MC, de la Llera-Moya M, et al. Scavenger receptor BI and cholesterol trafficking. Curr Opin Lipidol 1999; 10(4):329-339.

343. Krajewska WM, Maslowska I. Caveolins: Structure and function in signal transduction. Cell Mol Biol Lett 2004; 9(2):195-220.

344. Murata M, Peranen J, Schreiner R, Wieland F, Kurzchalia TV, Simons K. Vip21/Caveolin Is A Cholesterol-Binding Protein. Proc Natl Acad Sci USA 1995; 92(22):10339-10343.

345. Smart EJ, Ying YS, Donzell WC, Anderson RGW. A role for caveolin in transport of cholesterol from endoplasmic reticulum to plasma membrane. J Biol Chem 1996; 271(46):29427-29435.

346. Escher G, Krozowski Z, Croft KD, Sviridov D. Expression of sterol 27-hydroxylase (CYP27A1) enhances cholesterol efflux. J Biol Chem 2003; 278(13):11015-11019.

347. Kawano M, Miida T, Fielding CJ, Fielding PE. Quantitation of Pre-Beta-Hdl-Dependent and Nonspecific Components of the Total Efflux of Cellular Cholesterol and Phospholipid. Biochemistry 1993; 32(19):5025-5028.

348. Fuchs M. Bile Acid Regulation of Hepatic Physiology: III. Regulation of bile acid synthesis: past progress and future challenges. Am J Physiol Gastrointest Liver Physiol 2003; 284(4):G551-G557.

349. Horton JD, Shimano H, Hamilton RL, Brown MS, Goldstein JL. Disruption of LDL receptor gene in transgenic SREBP-1a mice unmasks hyperlipidemia resulting from production of lipid-rich VLDL. J Clin Invest 1999; 103(7):1067-1076.

350. Targher G, Arcaro G. Non-alcoholic fatty liver disease and increased risk of cardiovascular disease. Atherosclerosis 2007; 191(2):235-240.

351. Targher G. Non-alcoholic fatty liver disease, the metabolic syndrome and the risk of cardiovascular disease: the plot thickens. Diabet Med 2007; 24(1):1-6.

352. Bhat BG, Rapp SR, Beaudry JA, Napawan N, Butteiger DN, Hall KA, et al. Inhibition of ileal bile acid transport and reduced atherosclerosis in apoE-/- mice by SC-435. J Lipid Res 2003; 44(9):1614-1621.

353. Gerbod-Giannone MC, del Castillo-Olivares A, Janciauskiene S, Gil G, Hylemon PB. Suppression of Cholesterol 7alpha -Hydroxylase Transcription

and Bile Acid Synthesis by an alpha 1-Antitrypsin Peptide via Interaction with alpha 1-Fetoprotein Transcription Factor. J Biol Chem 2002; 277(45):42973-42980.

354. Ohashi R, Mu H, Wang X, Yao Q, Chen C. Reverse cholesterol transport and cholesterol efflux in atherosclerosis. QJM 2005; 98(12):845-856.

355. Ishibashi S, Goldstein JL, Brown MS, Herz J, Burns DK. Massive Xanthomatosis and Atherosclerosis in Cholesterol-Fed Low-Density-Lipoprotein Receptor-Negative Mice. J Clin Invest 1994; 93(5):1885-1893.

356. Zhang SH, Reddick RL, Piedrahita JA, Maeda N. Spontaneous hypercholesterolemia and arterial lesions in mice lacking apolipoprotein E. Science 1992; 258(5081):468-71.

357. Terkeltaub R, Boisvert VA, Curtiss LK. Chemokines and atherosclerosis. Curr Opin Lipidol 1998; 9(5):397-405.

358. Shattil SJ, Ginsberg MH. Integrin signaling in vascular biology. J Clin Invest 1997; 100(11):S91-S95.

359. Steinberg D, Parthasarathy S, Carew TE, Khoo JC, Witztum JL. Beyond Cholesterol - Modifications of Low-Density Lipoprotein That Increase Its Atherogenicity. N Engl J Med 1989; 320(14):915-924.

360. Stemme S, Faber B, Holm J, Wiklund O, Witztum JL, Hansson GK. T-Lymphocytes from Human Atherosclerotic Plaques Recognize Oxidized Low-Density-Lipoprotein. Proc Natl Acad Sci USA 1995; 92(9):3893-3897.

361. Ruan XZ, Kang ZQ, Li XW, Zheng FL. Minimally modified low densitylipoprotein stimulates tumour necrosis factor alpha secretion from rat mesangial cells. Kindney Int 1995; Suppl 595.

362. Cushing SD, Berliner JA, Valente AJ, Territo MC, Navab M, Parhami F, et al. Minimally modified low density lipoprotein induces monocyte chemotactic protein 1 in human endothelial cells and smooth muscle cells. Proc Natl Acad Sci USA 1990; 87(13):5134-5138.

363. Ku G, Thomas CE, Akeson AL, Jackson RL. Induction of interleukin 1 beta expression from human peripheral blood monocyte-derived macrophages by 9-hydroxyoctadecadienoic acid. J Biol Chem 1992; 267(20):14183-14188.

364. Cominacini L, Garbin U, Pasini AF, Davoli A, Campagnola M, Contessi, et al. Antioxidants inhibit the expression of intercellular cell adhesion molecule-1 and vascular cell adhesion molecule-1 induced by oxidized LDL on human umbilical vein endothelial cells. Free Radic Biol Med 1997; 22(1-2):117-127.

365. Frostegard J, Wu R, Haegerstrand A, Patarroyo M, Lefvert AK, Nilsson, et al. Mononuclear leukocytes exposed to oxidized low density lipoprotein secrete a factor that stimulates endothelial cells to express adhesion molecules. Atherosclerosis 1993; 103(2):213-219.

366. Quinn MT, Parthasarathy S, Fong LG, Steinberg D. Oxidatively modified low density lipoproteins: A potential role in recruitment and retention of monocyte/macrophages during atherogenesis. Proc Natl Acad Sci USA 1987; 2995:2998.

367. Ding G, van Goor H, Frye J, Diamond JR. Transforming growth factor-beta expression in macrophages during hypercholesterolemic states. Am J Physiol 1994; 267(6 Pt 2):F937-43.

368. Simon BC, Cunningham LD, Cohen RA. Oxidized Low-Density Lipoproteins Cause Contraction and Inhibit Endothelium-Dependent Relaxation in the Pig Coronary-Artery. J Clin Invest 1990; 86(1):75-79.

369. Rahman MM, Varghese Z, Fuller BJ, Moorhead JF. Renal vasoconstriction induced by oxidized LDL is inhibited by scavengers of reactive oxygen species and L-arginine. Clin Nephrol 1999; 51(2):98-107.

370. Rahman MM, Varghese Z, Moorhead JF. Paradoxical increase in nitric oxide synthase activity in hypercholesterolaemic rats with impaired renal function and decreased activity of nitric oxide. Nephrol Dial Transplant 2001; 16(2):262-268.

371. Feingold KR, Hardardottir I, Grunfeld C. Beneficial effects of cytokine induced hyperlipidemia. Z Ernahrungswiss 1998; 37 Suppl 1:66-74.:66-74.

372. Fernando RL, Varghese Z, Moorhead JF. Oxidation of low-density lipoproteins by rat mesangial cells and the interaction of oxidized low-density lipoproteins with rat mesangial cells in vitro. Nephrol Dial Transplant 1993; 8(6):512-518.

373. Fernando RL, Varghese Z, Moorhead JF. Differential ability of cells to promote oxidation of low density lipoproteins in vitro. Clin Chim Acta 1998; 269(2):159-173.

374. Ruan XZ, Varghese Z, Powis SH, Moorhead JF. Human mesangial cells express inducible macrophage scavenger receptor. Kidney Int 1999; 56(2):440-451.

375. Ruan XZ, Varghese Z, Fernando R, Moorhead JF. Cytokine regulation of low-density lipoprotein receptor gene transcription in human mesangial cells. Nephrol Dial Transplant 1998; 13(6):1391-1397.

376. Ruan XZ, Varghese Z, Powis SH, Moorhead JF. Dysregulation of LDL receptor under the influence of inflammatory cytokines: a new pathway for foam cell formation. Kidney Int 2001; 60(5):1716-1725.

377. Ruan XZ, Moorhead JF, Fernando R, Wheeler DC, Powis SH, Varghese Z. PPAR Agonists Protect Mesangial Cells from Interleukin 1beta-Induced

Intracellular Lipid Accumulation by Activating the ABCA1 Cholesterol Efflux Pathway. J Am Soc Nephrol 2003; 14(3):593-600.

378. Kahan BD, Podbielski J, Napoli KL, Katz SM, Meier-Kriesche HU, Van Buren CT. Immunosuppressive effects and safety of a sirolimus/cyclosporine combination regimen for renal transplantation. Transplantation 1998; 66(8):1040-1046.

379. Keogh A, Richardson M, Ruygrok P, Spratt P, Galbraith A, O'Driscoll G, et al. Sirolimus in de novo heart transplant recipients reduces acute rejection and prevents coronary artery disease at 2 years - A randomized clinical trial. Circulation 2004; 110(17):2694-2700.

380. Trotter JF, Wachs M, Bak T, Trouillot T, Stolpman N, Everson GT, et al. Liver transplantation using sirolimus and minimal corticosteroids (3-day taper). Liver Transpl 2001; 7(4):343-351.

381. Shitrit D, Rahamimov R, Gidon S, Bakal I, Bargil-Shitrit A, Milton S, et al. Use of sirolimus and low-dose calcineurin inhibitor in lung transplant recipients with renal impairment: Results of a controlled pilot study. Kidney Int 2005; 67(4):1471-1475.

382. Marx SO, Marks AR. Bench to bedside - The development of rapamycin and its application to stent restenosis. Circulation 2001; 104(8):852-855.

383. Viklicky O, Zou HQ, Muller V, Lacha J, Szabo A, Heemann U. SDZ-RAD prevents manifestation of chronic rejection in rat renal allografts. Transplantation 2000; 69(4):497-502.

384. Morice M, Serruys PW, Sousa JE, Fajadet J, Hayashi EB, Perin M, et al. A randomized comparison of a sirolimus-eluting stent with a standard stent for coronary revascularization. N Engl J Med 2002; 346(23):1773-1780.

385. Castro C, Campistol JM, Sancho D, Sanchez-Madrid F, Casals E, Andres V. Rapamycin attenuates atherosclerosis induced by dietary cholesterol in apolipoprotein-deficient mice through a p27 Kip1 -independent pathway. Atherosclerosis 2004; 172(1):31-38.

386. Elloso MM, Azrolan N, Sehgal SN, Hsu PL, Phiel KL, Kopec CA, et al. Protective effect of the immunosuppressant sirolimus against aortic atherosclerosis in apo e-deficient mice. Am J Transplant 2003; 3(5):562-569.

387. Pakala R, Stabile E, Dang GJ, Clavijo L, Waksman R. Rapamycin attenuates atherosclerotic plaque progression in apolipoprotein E knockout mice - Inhibitory effect on monocyte chemotaxis. J Cardiovasc Pharmacol 2005; 46(4):481-486.

388. Naoum JJ, Zhang S, Woodside KJ, Song W, Guo Q, Belalcazar LM, et al. Aortic eNOS expression and phosphorylation in Apo-E knockout mice: Differing effects of rapamycin and simvastatin. Surgery 2004; 136(2):323-328.

389. Naoum JJ, Woodside KJ, Zhang S, Rychahou PG, Hunter GC. Effects of rapamycin on the arterial inflammatory response in atherosclerotic plaques in Apo-E knockout mice. Transplant Proc 2005; 37(4):1880-1884.

390. Brown EJ, Albers MW, Shin TB, Ichikawa K, Keith CT, Lane WS, et al. A Mammalian Protein Targeted by G1-Arresting Rapamycin-Receptor Complex. Nature 1994; 369(6483):756-758.

391. Hay N, Sonenberg N. Upstream and downstream of mTOR. Genes Dev 2004; 18(16):1926-1945.

392. Jaeschke A, Dennis PB, Thomas G. mTOR: A mediator of intracellular Homeostasis. Curr Top Microbiol Immunol 2004; 279:283-298.

393. Tee AR, Blenis J, Proud CG. Analysis of mTOR signaling by the small G-proteins, Rheb and RhebL1. FEBS Lett 2005; 579(21):4763-4768.

394. Poon M, Marx SO, Gallo R, Badimon JJ, Taubman MB, Marks AR. Rapamycin inhibits vascular smooth muscle cell migration. J Clin Invest 1996; 98(10):2277-2283.

395. Stoscheck CM. Quantitation of Protein. Methods Enzymol 1990; 182:50-68.

396. LOWRY OH, ROSEBROUGH NJ, FARR AL, RANDALL RJ. Protein measurement with the Folin phenol reagent. J Biol Chem 1951; 193(1):265-275.

397. Smith PK, Krohn RI, Hermanson GT, Mallia AK, Gartner FH, Provenzano MD, et al. Measurement of Protein Using Bicinchoninic Acid. Anal Biochem 1985; 150(1):76-85.

398. Bradford MM. Rapid and Sensitive Method for Quantitation of Microgram Quantities of Protein Utilizing Principle of Protein-Dye Binding. Anal Biochem 1976; 72(1-2):248-254.

399. Reisner AH, Nemes P, Bucholtz C. Use of Coomassie Brilliant Blue G250 Perchloric-Acid Solution for Staining in Electrophoresis and Isoelectric Focusing on Polyacrylamide Gels. Anal Biochem 1975; 64(2):509-516.

400. Spector T. Refinement of Coomassie Blue Method of Protein Quantitation - Simple and Linear Spectrophotometric Assay for Less-Than-Or-Equal-to 0.5 to 50 Mu-G of Protein. Anal Biochem 1978; 86(1):142-146.

401. Decker T, Lohmannmatthes ML. A Quick and Simple Method for the Quantitation of Lactate-Dehydrogenase Release in Measurements of Cellular Cyto-Toxicity and Tumor Necrosis Factor (TNF) Activity. J Immunol Methods 1988; 115(1):61-69.

402. Legrand C, Bour JM, Jacob C, Capiaumont J, Martial A, Marc A, et al. Lactate-Dehydrogenase (Ldh) Activity of the Number of Dead Cells in the Medium of Cultured Eukaryotic Cells As Marker. J Biotechnol 1993; 31(2):234.

403. Chirgwin JM, Przybyla AE, MacDonald RJ, Rutter WJ. Isolation of biologically active ribonucleic acid from sources enriched in ribonuclease. Biochemistry 1979; 18(24):5294-5299.

404. Perry RP, La Torre J, Kelley DE, Greenberg JR. On the lability of poly(A) sequences during extraction of messenger RNA from polyribosomes. Biochim Biophys Acta 1972; 262(2):220-226.

405. Dignam JD, Lebovitz RM, Roeder RG. Accurate Transcription Initiation by Rna Polymerase-Ii in A Soluble Extract from Isolated Mammalian Nuclei. Nucleic Acids Res 1983; 11(5):1475-1489.

406. Wang XD, Sato R, Brown MS, Hua XX, Goldstein JL. Srebp-1, A Membrane-Bound Transcription Factor Released by Sterol-Regulated Proteolysis. Cell 1994; 77(1):53-62.

407. Xu QB, Oberhuber G, Gruschwitz M, Wick G. Immunology of Atherosclerosis - Cellular Composition and Major Histocompatibility Complex Class-Ii Antigen Expression in Aortic Intima, Fatty Streaks, and Atherosclerotic Plaques in Young and Aged Human Specimens. Clin Immunol Immunopathol 1990; 56(3):344-359.

408. Kaul D. Molecular link between cholesterol, cytokines and atherosclerosis. Mol Cell Biochem 2001; 219(1-2):65-71.

409. Greaves DR, Channon KM. Inflammation and immune responses in atherosclerosis. Trends Immunol 2002; 23(11):535-541.

410. Degertekin M, Regar E, Tanabe K, Lee CH, Serruys PW. Sirolimus eluting stent in the treatment of atherosclerosis coronary artery disease. Minerva Cardioangiol 2002; 50(5):405-418.

411. Lemos PA, Regar E, Serruys PW. Drug-eluting stents in the treatment of atherosclerotic coronary heart disease. Indian Heart J 2002; 54(2):212-216.

412. Schofer J, Schluter M, Gershlick AH, Wijns W, Garcia E, Schampaert E, et al. Sirolimus-eluting stents for treatment of patients with long atherosclerotic lesions in small coronary arteries: double-blind, randomised controlled trial (E-SIRIUS). Lancet 2003; 362(9390):1093-1099.

413. Basso MD, Nambi P, Adelman SJ. Effect of sirolimus on the cholesterol content of aortic arch in ApoE knockout mice. Transplant Proc 2003; 35(8):3136-3138.

414. Hoogeveen RC, Ballantyne CM, Pownall HJ, Opekun AR, Hachey DL, Jaffe JS, et al. Effect of sirolimus on the metabolism of ApoB100-containing lipoproteins in renal transplant patients. Transplantation 2001; 72(7):1244-1250.

415. Morales JM. Cardiovascular risk profile in patients treated with sirolimus after renal transplantation. Kidney Int 2005; 67:S69-S73.

416. Morrisett JD, Abdel-Fattah G, Hoogeveen R, Mitchell E, Ballantyne CM, Pownall HJ, et al. Effects of sirolimus on plasma lipids, lipoprotein levels, and fatty acid metabolism in renal transplant patients. J Lipid Res 2002; 43(8):1170-1180.

417. Galea J, Armstrong J, Gadsdon P, Holden H, Francis SE, Holt CM. Interleukin-1 beta in coronary arteries of patients with ischemic heart disease. Arterioscler Thromb Vasc Biol 1996; 16(8):1000-1006.

418. Lu LF, Fiscus RR. Interleukin-1[beta] causes different levels of nitric oxide-mediated depression of contractility in different positions of rat thoracic aorta. Life Sci 1999; 64(16):1373-1381.

419. Moyer CF, Sajuthi D, Tulli H, Williams JK. Synthesis of Il-1 Alpha and Il-1 Beta by Arterial Cells in Atherosclerosis. Am J Pathol 1991; 138(4):951-960.

420. Merhi-Soussi F, Kwak BR, Magne D, Chadjichristos C, Berti M, Pelli G, et al. Interleukin-1 plays a major role in vascular inflammation and atherosclerosis in male apolipoprotein E-knockout mice. Cardiovasc Res 2005; 66(3):583-593.

421. Tousoulis D, Antoniades C, Koumallos N, Stefanadis C. Pro-inflammatory cytokines in acute coronary syndromes: From bench to bedside. Cytokine Growth Factor Rev 2006; 17(4):225-233.

422. Ruan XZ, Moorhead JF, Tao JL, Ma KL, Wheeler DC, Powis SH, et al. Mechanisms of Dysregulation of Low-Density Lipoprotein Receptor Expression in Vascular Smooth Muscle Cells by Inflammatory Cytokines. Arterioscler Thromb Vasc Biol 2006; 26(5):1150-5.

423. Morrisett JD, Abdel-Fattah G, Kahan BD. Sirolimus changes lipid concentrations and lipoprotein metabolism in kidney transplant recipients. Transplant Proc 2003; 35(3 Suppl):143S-150S.

424. Varghese Z, Fernando R, Moorhead JF, Powis SH, Ruan XZ. Effects of sirolimus on mesangial cell cholesterol homeostasis: a novel mechanism for its action against lipid-mediated injury in renal allografts. Am J Physiol Renal Physiol 2005; 289(1):F43-F48.

425. Oliveira JGG, Xavier P, Sampaio SM, Henriques C, Tavares I, Mendes AA, et al. Compared to mycophenolate mofetil, rapamycin induces significant changes

on growth factors and growth factor receptors in the early days postkidney transplantation. Transplantation 2002; 73(6):915-920.

426. Wasowska BA, Zheng XX, Strom TB, Kupiec-Weglinski JW. Adjunctive rapamycin and CsA treatment inhibits monocyte/macrophage associated cytokines/chemokines in sensitized cardiac graft recipients. Transplantation 2001; 71(8):1179-1183.

427. Doran AC, Meller N, McNamara CA. Role of Smooth Muscle Cells in the Initiation and Early Progression of Atherosclerosis. Arterioscler Thromb Vasc Biol 2008; 28(5):812-819.

428. Ma KL, Ruan XZ, Powis SH, Moorhead JF, Varghese Z. Anti-atherosclerotic effects of sirolimus on human vascular smooth muscle cells. Am J Physiol Heart Circ Physiol 2007; 292(6):H2721-H2728.

429. Song BL, Sever N, Bose-Boyd RA. Gp78, a membrane-anchored ubiquitin ligase, associates with Insig-1 and couples sterol-regulated ubiquitination to degradation of HMG CoA reductase. Mol Cell 2005; 19(6):829-840.

430. Owen JS, Goodall H, Mistry P, Harry DS, Day RC, McIntyre N. Abnormal high density lipoproteins from patients with liver disease regulate cholesterol metabolism in cultured human skin fibroblasts. J Lipid Res 1984; 25(9):919-931.

431. Roitelman J, Simoni RD. Distinct sterol and nonsterol signals for the regulated degradation of 3-hydroxy-3-methylglutaryl-CoA reductase. J Biol Chem 1992; 267(35):25264-25273.

432. Goldstein JL, Brown MS. Progress in understanding the LDL receptor and HMG-CoA reductase, two membrane proteins that regulate the plasma cholesterol. J Lipid Res 1984; 25(13):1450-1461.

433. Soccio RE, Breslow JL. Intracellular Cholesterol Transport. Arterioscler Thromb Vasc Biol 2004; 24(7):1150-1160.

434. goechea-Alonso MT, Ericsson J. SREBP in signal transduction: cholesterol metabolism and beyond. Curr Opin Cell Biol 2007; 19(2):215-222.

435. Kruth HS, Huang W, Ishii I, Zhang WY. Macrophage foam cell formation with native low density lipoprotein. J Biol Chem 2002; 277(37):34573-34580.

436. Van Eck M, Pennings M, Hoekstra M, Out R, Van Berkel TJC. Scavenger receptor BI and ATP-binding cassette transporter A1 in reverse cholesterol transport and atherosclerosis. Curr Opin Lipidol 2005; 16(3):307-315.

437. Dean M, Hamon Y, Chimini G. The human ATP-binding cassette (ABC) transporter superfamily. J Lipid Res 2001; 42(7):1007-1017.

438. Rye KA, Barter PJ. Formation and metabolism of prebeta-migrating, lipid-poor apolipoprotein A-I. Arterioscler Thromb Vasc Biol 2004; 24(3):421-428.

439. Soumian S, Albrecht C, Davies AH, Gibbs RGJ. ABCA1 and atherosclerosis. Vasc Med 2005; 10(2):109-119.

440. Hoekstra M, Kruijt J, Van Eck M, Van Berkel TJC. Specific gene expression of ATP-binding cassette transporters and nuclear hormone receptors in rat liver parenchymal, endothelial, and Kupffer cells. J Biol Chem 2003; 278(28):25448-25453.

441. Klucken J, Buchler C, Orso E, Kaminski WE, Porsch-Ozcurumez M, Liebisch G, et al. ABCG1 (ABC8), the human homolog of the Drosophila white gene, is a regulator of macrophage cholesterol and phospholipid transport. Proc Natl Acad Sci USA 2000; 97(2):817-22.

442. Venkateswaran A, Repa JJ, Lobaccaro JMA, Bronson A, Mangelsdorf DJ, Edwards PA. Human white/murine ABC8 mRNA levels are highly induced in lipid-loaded macrophages - A transcriptional role for specific oxysterols. J Biol Chem 2000; 275(19):14700-14707.

443. Jessup W, Gelissen IC, Gaus K, Kritharides L. Roles of ATP binding cassette transporters A1 and G1, scavenger receptor BI and membrane lipid domains in cholesterol export from macrophages. Curr Opin Lipidol 2006; 17(3):247-257.

444. Jessup W, Kritharides L. Metabolism of oxidized LDL by macrophages. Curr Opin Lipidol 2000; 11(5):473-481.

445. Mathe D, Adam R, Malmendier C, Gigou M, Lontie JF, Dubois D, et al. Prevalence of Dyslipidemia in Liver-Transplant Recipients. Transplantation 1992; 54(1):167-168.

446. Kahan BD, Yakupoglu YK, Schoenberg L, Knight RJ, Katz SM, Lai D, et al. Low incidence of malignancy among sirolimus/cyclosporine-treated renal transplant recipients. Transplantation 2005; 80(6):749-758.

447. Galanis E, Buckner JC, Maurer MJ, Kreisberg JL, Ballman K, Boni J, et al. Phase II trial of temsirolimus (CCI-779) in recurrent glioblastoma multiforme: A north central cancer treatment group study. J Clin Oncol 2005; 23(23):5294-5304.

448. Massy ZA, De Bandt JP, Morelon E, Thevenin M, Lacour B, Kreis H. Hyperlipidaemia and post-heparin lipase activities in renal transplant recipients treated with sirolimus or cyclosporin A. Nephrol Dial Transplant 2000; 15(6):928.

449. Chueh SCJ, Kahan BD. Dyslipidemia in renal transplant recipients treated with a sirolimus and cyclosporine-based immunosuppressive regimen: Incidence, risk factors, progression, and prognosis. Transplantation 2003; 76(2):375-382.

450. Blum CB. Effects of sirolimus on lipids in renal allograft recipients: An analysis using the Framingham risk model. Am J Transplant 2002; 2(6):551-559.

451. Timmins JM, Lee JY, Boudyguina E, Kluckman KD, Brunham LR, Mulya A, et al. Targeted inactivation of hepatic Abca1 causes profound hypoalphalipoproteinemia and kidney hypercatabolism of apoA-I. J Clin Invest 2005; 115(5):1333-1342.

452. Aden DP, Fogel A, Plotkin S, Damjanov I, Knowles BB. Controlled Synthesis of Hbsag in A Differentiated Human-Liver Carcinoma-Derived Cell-Line. Nature 1979; 282(5739):615-616.

453. Javitt NB. Hep G2 cells as a resource for metabolic studies: lipoprotein, cholesterol, and bile acids. FASEB J 1990; 4(2):161-168.

454. Aggarwal D, Fernandez ML, Soliman GA. Rapamycin, an mTOR inhibitor, disrupts triglyceride metabolism in guinea pigs. Metabolism 2006; 55(6):794-802.

455. Basso F, Freeman L, Knapper CL, Remaley A, Stonik J, Neufeld EB, et al. Role of the hepatic ABCA1 transporter in modulating intrahepatic cholesterol and plasma HDL cholesterol concentrations. J Lipid Res 2003; 44(2):296-302.

456. Singaraja RR, Stahmer B, Brundert M, Merkel M, Heeren J, Bissada N, et al. Hepatic ATP-binding cassette transporter A1 is a key molecule in high-density lipoprotein cholesteryl ester metabolism in mice. Arterioscler Thromb Vasc Biol 2006; 26(8):1821-1827.

457. Wellington CL, Brunham LR, Zhou S, Singaraja RR, Visscher H, Gelfer A, et al. Alterations of plasma lipids in mice via adenoviral-mediated hepatic overexpression of human ABCA1. J Lipid Res 2003; 44(8):1470-1480.

458. Joyce CW, Wagner EM, Basso F, Amar MJ, Freeman LA, Shamburek RD, et al. ABCA1 overexpression in the liver of LDLr-KO mice leads to accumulation of pro-atherogenic lipoproteins and enhanced atherosclerosis. J Biol Chem 2006; 281(44):33053-33065.

459. Moloney ED, O'Mahony U, Kirwan M, McCarthy J, Hurley J, Wood AE, et al. Pharmacokinetics of sirolimus in heart transplant recipients with chronic renal impairment. Transplant Proc 2004; 36(5):1547-1550.

460. Pakala R, Stabile E, Finegold AA, Hellinga D, Seabron R, Baffour R, et al. Oral rapamycin attenuates atherosclerotic plaque progression in ApoE knockout mice. Circulation 2004; 110(17):53.

461. Waksman R, Pakala R, Burnett MS, Gulick CP, Leborgne L, Fournadjiev J, et al. Oral rapamycin inhibits growth of atherosclerotic plaque in apoE knock-out mice. Cardiovasc Radiat Med 2003; 4(1):34-38.

462. Frostegard J. Atherosclerosis in Patients With Autoimmune Disorders. Arterioscler Thromb Vasc Biol 2005; 25(9):1776-1785.

463. Hahn BH, Grossman J, Chen W, McMahon M. The pathogenesis of atherosclerosis in autoimmune rheumatic diseases: Roles of inflammation and dyslipidemia. J Autoimmun 2007; 28(2-3):69-75.

464. Steinberg D. Atherogenesis in perspective: hypercholesterolemia and inflammation as partners in crime. Nat Med 2002; 8(11):1211-1217.

465. Hirschfield GM, Gallimore JR, Kahan MC, Hutchinson WL, Sabin CA, Benson GM, et al. Transgenic human C-reactive protein is not proatherogenic in

apolipoprotein E-deficient mice. Proc Natl Acad Sci USA 2005; 102(23):8309-8314.

466. Ling PR, Smith RJ, Kie S, Boyce P, Bistrian BR. Effects of protein malnutrition on IL-6-mediated signaling in the liver and the systemic acute-phase response in rats. Am J Physiol Regul Integr Comp Physiol 2004; 287(4):R801-R808.

467. Avram MM, Bonomini LV, Sreedhara R, Mittman N. Predictive value of nutritional markers (albumin, creatinine, cholesterol, and hematocrit) for patients on dialysis for up to 30 years. Am J Kidney Dis 1996; 28(6):910-917.

468. Bologa RM, Levine DM, Parker TS, Cheigh JS, Serur D, Stenzel KH, et al. Interleukin-6 predicts hypoalbuminemia, hypocholesterolemia, and mortality in hemodialysis patients. Am J Kidney Dis 1998; 32(1):107-114.

469. Iseki K, Yamazato M, Tozawa M, Takishita S. Hypocholesterolemia is a significant predictor of death in a cohort of chronic hemodialysis patients. Kidney Int 2002; 61(5):1887-1893.

470. Lowrie EG, Lew NL. Death risk in hemodialysis patients: the predictive value of commonly measured variables and an evaluation of death rate differences between facilities. Am J Kidney Dis 1990; 15(5):458-482.

471. Sousa JE, Costa MA, Abizaid A, Abizaid AS, Feres F, Pinto IM, et al. Lack of neointimal proliferation after implantation of sirolimus-coated stents in human coronary arteries: a quantitative coronary angiography and three-dimensional intravascular ultrasound study. Circulation 2001; 103(2):192-195.

472. Marx SO, Jayaraman T, Go LO, Marks AR. Rapamycin-FKBP inhibits cell cycle regulators of proliferation in vascular smooth muscle cells. Circ Res 1995; 76(3):412-417.

473. Takahashi S, Sakai J, Fujino T, Hattori H, Zenimaru Y, Suzuki J, et al. The very low-density lipoprotein (VLDL) receptor: characterization and functions as a peripheral lipoprotein receptor. J Atheroscler Thromb 2004; 11(4):200-208.

474. Wang X, Proud CG. The mTOR Pathway in the Control of Protein Synthesis. Physiology 2006; 21(5):362-369.

475. Lee DF, Kuo HP, Chen CT, Hsu JM, Chou CK, Wei Y, et al. IKK[beta] Suppression of TSC1 Links Inflammation and Tumor Angiogenesis via the mTOR Pathway. Cell 2007; 130(3):440-455.

476. Lim HK, Choi YA, Park W, Lee T, Ryu SH, Kim SY, et al. Phosphatidic Acid Regulates Systemic Inflammatory Responses by Modulating the Akt-Mammalian Target of Rapamycin-p70 S6 Kinase 1 Pathway. J Biol Chem 2003; 278(46):45117-45127.

477. Glantschnig H, Fisher JE, Wesolowski G, Rodan GA, Reszka AA. M-CSF, TNF [alpha] and RANK ligand promote osteoclast survival by signaling through mTOR/S6 kinase. Cell Death Differ 2003; 10(10):1165-1177.

478. Giles FJ, Albitar M. Mammalian target of rapamycin as a therapeutic target in leukemia. Curr Mol Med 2005; 5(7):653-661.

479. Zohlnhofer D, Nuhrenberg TG, Neumann FJ, Richter T, May AE, Schmidt R, et al. Rapamycin Effects Transcriptional Programs in Smooth Muscle Cells Controlling Proliferative and Inflammatory Properties. Mol Pharmacol 2004; 65(4):880-889.

480. Nathe TJ, Deou J, Walsh B, Bourns B, Clowes AW, Daum G. Interleukin-1{beta} Inhibits Expression of p21(WAF1/CIP1) and p27(KIP1) and Enhances Proliferation in Response to Platelet-Derived Growth Factor-BB in Smooth Muscle Cells. Arterioscler Thromb Vasc Biol 2002; 22(8):1293-1298.

481. Ma KL, Ruan XZ, Powis SH, Chen Y, Moorhead JF, Varghese Z. Sirolimus modifies cholesterol homeostasis in hepatic cells: a potential molecular mechanism for sirolimus-associated dyslipidemia. Transplantation 2007; 84(8):1029-1036.

482. Karin M. How NF-kappa B is activated: the role of the I kappa B kinase (IKK) complex. Oncogene 1999; 18(49):6867-6874.

483. Sweet MJ, Hume DA. Endotoxin signal transduction in macrophages. J Leukoc Biol 1996; 60(1):8-26.

484. Ghosh S, Karin M. Missing Pieces in the NF-[kappa] B Puzzle. Cell 2002; 109(2, Supplement 1):S81-S96.

485. Karin M, Ben-Neriah Y. Phosphorylation meets ubiquitination: The control of NF-kappa B activity. Annu Rev Immunol 2000; 18:621-23.

486. Smith CW, Marlin SD, Rothlein R, Toman C, Anderson DC. Cooperative Interactions of Lfa-1 and Mac-1 with Intercellular-Adhesion Molecule-1 in Facilitating Adherence and Transendothelial Migration of Human-Neutrophils Invitro. J Clin Invest 1989; 83(6):2008-2017.

487. Ben-Neriah Y. Regulatory functions of ubiquitination in the immune system. Nat Immunol 2002; 3(1):20-26.

488. Kim NH, Jeon S, Lee HJ, Lee AY. Impaired PI3K//Akt Activation-Mediated NF-[kappa]B Inactivation Under Elevated TNF-[alpha] Is More Vulnerable to Apoptosis in Vitiliginous Keratinocytes. J Invest Dermatol 2007; 127(11):2612-2617.

489. Lee SO, Lou W, Nadiminty N, Lin X, Gao AC. Requirement for NF-kappa B in interleukin-4-induced androgen receptor activation in prostate cancer cells. Prostate 2005; 64(2):160-167.

490. Sugimori K, Matsui K, Motomura H, Tokoro T, Wang JY, Higa S, et al. BMP-2 prevents apoptosis of the N1511 chondrocytic cell line through PI3K/Akt-mediated NF-kappa B activation. J Bone Miner Metab 2005; 23(6):411-419.

491. Xie P, Browning DD, Hay N, Mackman N, Ye RD. Activation of NF-kappa B by Bradykinin through a Galpha q- and Gbeta gamma -dependent Pathway That Involves Phosphoinositide 3-Kinase and Akt. J Biol Chem 2000; 275(32):24907-24914.

492. Ghosh S, Tergaonkar V, Rothlin CV, Correa RG, Bottero V, Bist P, et al. Essential role of tuberous sclerosis genes TSC1 and TSC2 in NF-[kappa] B activation and cell survival. Cancer Cell 2006; 10(3):215-226.

APPENDIXES

Inflammatory Stress Exacerbates Lipid Accumulation in Hepatic Cells and Fatty Livers of Apolipoprotein E Knockout Mice

Kun L. Ma,[1] Xiong Z. Ruan,[1,2] Stephen H. Powis,[1] Yaxi Chen,[2] John F. Moorhead,[1] and Zac Varghese[1]

The prevailing theory in non-alcoholic fatty liver disease (NAFLD) is the "two-hit" hypothesis. The first hit mainly consists of lipid accumulation, and the second is subsequent systemic inflammation. The current study was undertaken to investigate whether inflammatory stress exacerbates lipid accumulation in liver and its underlying mechanisms. We used interleukin-1β (IL-1β) and tumor necrosis factor alpha (TNF-α) stimulation in human hepatoblastoma cell line (HepG2) cells and primary hepatocytes *in vitro,* and casein injection in apolipoprotein E knockout mice *in vivo* to induce inflammatory stress. The effects of inflammatory stress on cholesterol accumulation were examined by histochemical staining and a quantitative intracellular cholesterol assay. The gene and protein expressions of molecules involved in cholesterol trafficking were examined by real-time polymerase chain reaction (PCR) and western blot. Cytokine production in the plasma of apolipoprotein E knockout mice was measured by enzyme-linked immunosorbent assay. Our results showed that inflammatory stress increased cholesterol accumulation in hepatic cells and in the livers of apolipoprotein E knockout mice. Further analysis showed that inflammatory stress increased the expression of low-density lipoprotein (LDL) receptor (LDLr), sterol regulatory element–binding protein (SREBP) cleavage activating protein (SCAP), and SREBP-2. Confocal microscopy showed that IL-1β increased the translocation of SCAP/SREBP-2 complex from endoplasmic reticulum (ER) to Golgi in HepG2 cells, thereby activating LDLr gene transcription. IL-1β, TNF-α, and systemic inflammation induced by casein injection also inhibited expression of adenosine triphosphate–binding cassette transporter A1 (ABCA1), peroxisome proliferator-activated receptor-α (PPAR-α), and liver X receptor-α (LXRα). This inhibitory effect may cause cholesterol efflux reduction. *Conclusion*: Inflammatory stress up-regulates LDLr-mediated cholesterol influx and down-regulates ABCA1-mediated cholesterol efflux *in vivo and in vitro*. This may exacerbate the progression of NAFLD by disrupting cholesterol trafficking control, especially during the second hit phase of liver damage. (HEPATOLOGY 2008;48:770-781.)

Abbreviations: ABCA1, adenosine triphosphate–binding cassette transporter A1; ApoE KO, apolipoprotein E knockout; ER, endoplasmic reticulum; HDL, high-density lipoprotein; HepG2, human hepatoblastoma cell line; IL-1β, interleukin-1β; LDL, low-density lipoprotein; LDLr, low-density lipoprotein receptor; LXRα, liver X receptor alpha; MCP-1, monocyte chemoattractant protein-1; mRNA, messenger RNA; NAFLD, non-alcoholic fatty liver disease; PCR, polymerase chain reaction; PPARα, peroxisome proliferator-activated receptor-α; SAA, serum amyloid A; SCAP, sterol regulatory element-binding protein cleavage-activating protein; SD, standard deviation; SREBP, sterol regulatory element-binding protein; TNF-α, tumor necrosis factor alpha.

From the [1]Centre for Nephrology, Royal Free and University College Medical School, Royal Free Campus, University College London, UK; and the [2]Centre for Lipid Research, Key Laboratory of Molecular Biology on Infectious Diseases, Second Affiliated Hospital, Chongqing Medical University, People's Republic of China.

Received November 9, 2007; accepted May 8, 2008.

Supported by the Royal Free Hospital Special Trustees Grant-115 through Dr. Zac Varghese, the Moorhead Trust, the National Natural Science Foundation of China (Key Program, No. 30530360, 30772295) and the National Basic Research Program of China (2006CB503907).

Address reprint requests to: Dr. Xiong Z. Ruan, Centre for Nephrology, Royal Free & University College Medical School, University College London, Royal Free campus, Rowland Hill Street, London NW3 2PF, UK; or Centre for Lipid Research, Key Laboratory of Molecular Biology on Infectious Diseases, Second Affiliated Hospital, Chongqing Medical University, People's Republic of China. E-mail: x.ruan@medsch.ucl.ac.uk; fax: (44)-2078302125.

Published online in Wiley InterScience (www.interscience.wiley.com).

DOI 10.1002/hep.22423

Potential conflict of interest: Nothing to report.

Non-alcoholic fatty liver disease (NAFLD) is increasingly recognized as a leading cause of liver damage and cirrhosis in developed countries. Although the exact mechanisms leading to NAFLD are incompletely understood, the "two-hit hypothesis" has become an important theoretical framework for understanding its pathogenesis.[1] The first hit mainly consists of lipid accumulation in the liver in the form of triglycerides and free fatty acids accompanied by small amounts of cholesterol, cholesterol ester, and phospholipid, a process that is closely linked with insulin resistance.[2] The second hit involves an inflammatory insult to the liver. The cytokines or chemokines released by hepatocytes or activated neutrophils further exacerbate hepatic tissue injuries induced by the first hit.[3] The dysregulation of both triglycerides and free fatty acids in NAFLD have been elucidated in many studies, but the contribution of cholesterol under inflammatory stress in the progression of NAFLD seems to have been neglected.

It is well known that cholesterol is the primary lipid synthesized in the liver, and cholesterol synthesis is tightly regulated by a feedback system that maintains intracellular cholesterol homeostasis.[4] The low-density lipoprotein receptor (LDLr) plays a pivotal role in maintaining cholesterol homeostasis in hepatic cells. LDLr gene expression in mammalian cells is predominantly regulated by a negative-feedback mechanism that depends on the mediation of intracellular cholesterol concentration by sterol regulatory element-binding proteins (SREBPs) and SREBP cleavage activating protein (SCAP).[5] When cells have sufficient cholesterol, SCAP and SREBP-2 form a complex retained in the endoplasmic reticulum (ER), where they are inactive as transcription factors; intracellular cholesterol is limited by down-regulation of LDLr. When cells demand cholesterol, SCAP escorts the SREBP-2 from the ER to the Golgi for activation by proteolytic cleavage. The cleaved N-terminal fragments of SREBP-2 then translocate to the nucleus, where they activate LDLr gene transcription.

Table 1. HumanTaqMan Primers for Real-Time PCR

Genes	Human TaqMan Primers
LDLr	5′-GTGTCACAGCGGCGAATG-3′sense
	5′-CGCACTCTTTGATGGGTTCA-3′antisense
SCAP	5′-GGGAACTTCTGGCAGAATGACT-3′sense
	5′-CTGGTGGATGGTCCCAATG-3′antisense
SREBP-2	5′-CCGCCTGTTCCGATGTACAC-3′sense
	5′-TGCACATTCAGCCAGGTTCA-3′antisense
$ABCA_1$	5′-GCAGCAGAGCGAGTACTTCGTT-3′sense
	5′-CAAGACTATGCAGCAATGTTTTTGT-3′antisense
LXRα	5′-AGAAGAACAGATCCGCCTGAAG-3′sense
	5′-GGCAAGGATGTGGCATGAG-3′antisense
PPARα	5′-CGTGCTTCCTGCTTCATAGATAAG-3′sense
	5′-GTGGTAGCGCTGGTCTAC-3′antisense
β-actin	5′-CCTGGCACCCAGCACAAT-3′sense
	5′-GCCGATCCACACGGAGTACT-3′antisense

Table 2. Mouse TaqMan Primers for Real-Time PCR

Genes	Mouse Taqman Primers
LDLr	5′-CTGTGGGCTCCATAGGCTATCT-3′ sense
	5′-GCGGTCCAGGGTCATCTTC-3′ antisense
SCAP	5′-ACTGGACTGAAGGCAGGTCAA-3′ sense
	5′-GCCTCTAGTCTAGGTCCAAAGAGTTG-3′ antisense
SREBP-2	5′-GCGCCAGGAGAACATGGT-3′ sense
	5′-CGATGCCCTTCAGGAGCTT-3′ antisense
ABCA1	5′-ACTTAGGGCACAATTCCACAAGA-3′ sense
	5′-CTCCTGTGGTGTTTCTGGATGA-3′ antisense
PPARα	5′-TCAGGGTACCACTACGGAGTTCA-3′ sense
	5′-CCGAATAGTTCGCCGAAAGA-3′ antisense
LXRα	5′-GGAGTGTCGACTTCGCAAATG-3′ sense
	5′-TCAAGCGGATCTGTTCTTCTGA-3′ antisense
β-actin	5′-ACGGCCAGGTCATCACTATTG-3′ sense
	5′-CACAGGATTCCATACCCAAGAAG-3′ antisense

Efflux of cholesterol is mainly mediated by adenosine triphosphate–binding cassette transporter A1 (ABCA1). Liver ABCA1-mediated cholesterol efflux is an important source of circulating high-density lipoprotein (HDL), as demonstrated by the fact that inactivation of ABCA1 in the liver of mice results in a profoundly low plasma HDL.[6]). Liver X receptors (LXRs) and peroxisome-proliferator activated receptors (PPARs) are important nuclear receptors that control the transcription of a number of specific genes. Some studies have demonstrated that LXRs and PPARs up-regulate ABCA1 expression, thereby providing an amplification loop for ABCA1 expression.[7] All of these studies conclude that liver cholesterol homeostasis is tightly regulated to maintain free cholesterol concentration at low physiological levels.

The current study was undertaken to provide an explanation for the accumulation of cholesterol, cholesterol ester, and phospholipids in the fatty liver of NAFLD, especially during the second hit, by studying the effects of inflammatory stress on LDLr-mediated cholesterol uptake and ABCA1- mediated cholesterol efflux in human hepatoblastoma cell line (HepG2), primary hepatocytes from C57BL/6 mice, and the liver of inflamed apolipoprotein knockout (ApoE KO) mice.

Materials and Methods

Cell Culture. HepG2 cells (European Collection of Cell Cultures, UK) were cultured with Dulbecco's Modified Eagle's Medium/Ham's Nutrient mixture F-12 containing 10% fetal bovine serum. Primary

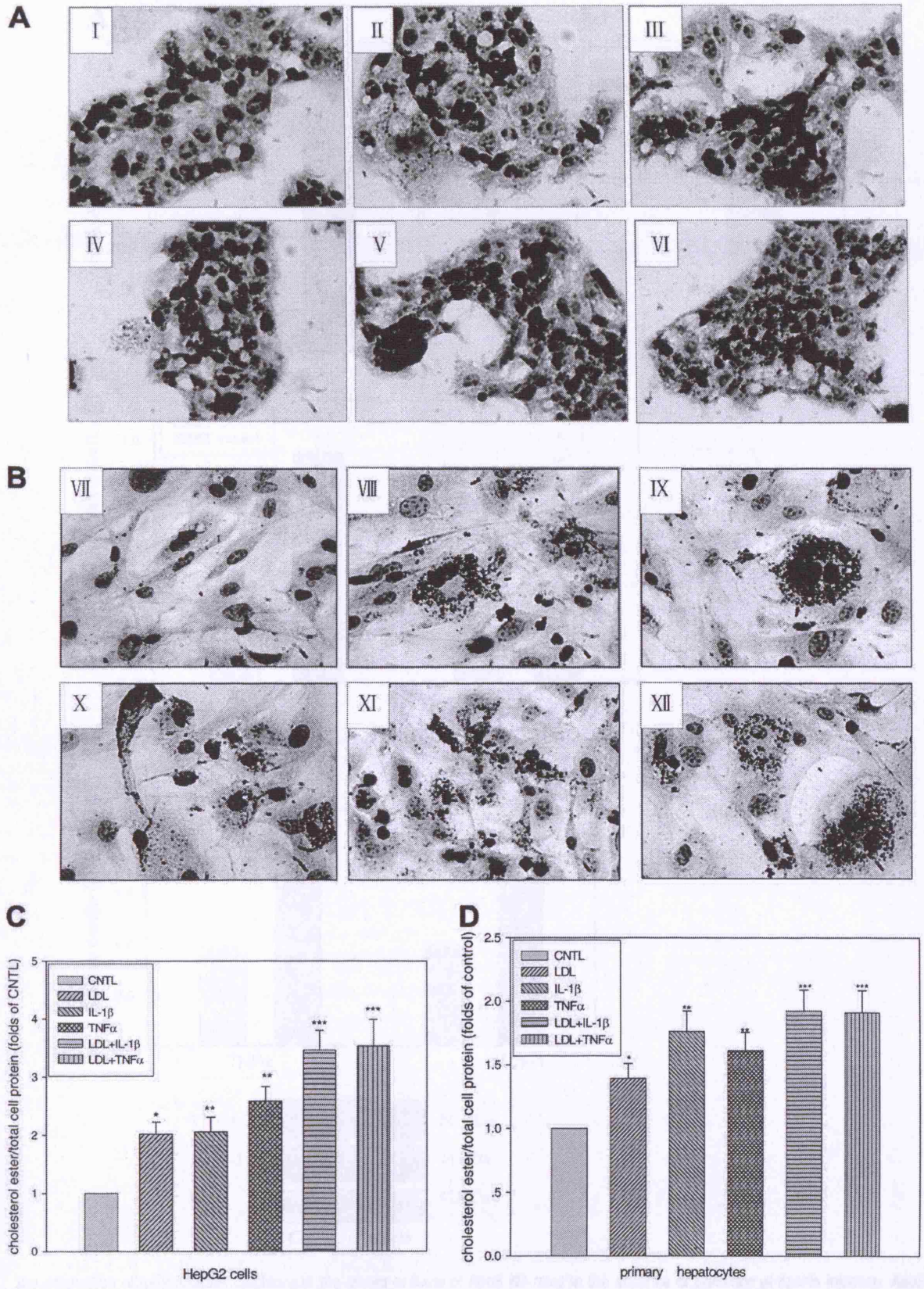

Fig. 1. Observation of lipid accumulation in hepatic cells after treatments of LDL or inflammatory cytokines. HepG2 cells (A) and primary hepatocytes (B) were incubated for 24 hours in serum-free medium (I,VII), or medium containing 200 g/mL native LDL (II,VIII) or 20 ng/mL IL-1β (III,IX), or 50 ng/mL TNF-α (IV, X), or 20 ng/mL IL-1β plus 200 g/mL native LDL (V,XI), or 50 ng/mL TNF-α plus 200 g/mL native LDL (VI,XII). The cells were examined for lipid inclusion by Oil Red O staining. The results are typical of those observed in four separate experiments ($\times$400). The concentration of cholesterol ester in HepG2 cells (C) and primary hepatocytes (D) was measured as described in Materials and Methods. Values are mean $\pm$ standard deviation (SD) of duplicate wells from four experiments. *$P < 0.01$ versus control, **$P < 0.01$ versus control, ***$P < 0.05$ versus LDL group.

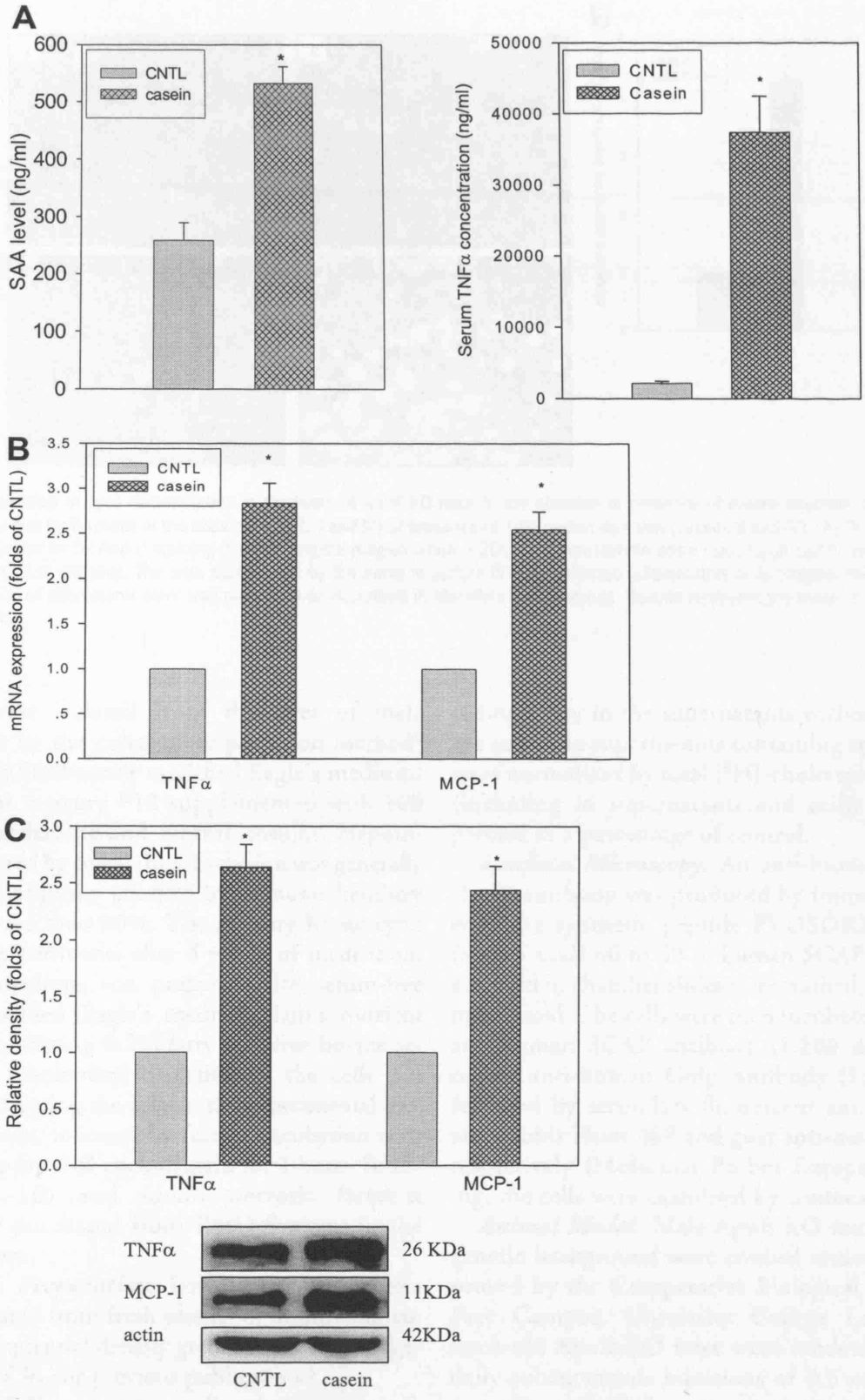

Fig. 2. The production of inflammatory cytokines in the serum or livers of ApoE KO mice in the absence or presence of casein injection. ApoE KO mice were fed with the western diet for 8 weeks in the absence (CNTL) or presence of 10% casein injection (casein). (A) The level of SAA and TNF-α in the serum of ApoE KO mice was checked by enzyme-linked immunosorbent assay. Results represent the mean $\pm$ SD (n = 7). *$P < 0.01$ versus control. (B) The mRNA expression of TNF-α and MCP-1 in the livers of ApoE KO was determined by real-time PCR. Beta-actin served as the housekeeping gene Results represent the mean $\pm$ SD (n = 4). *$P < 0.001$ versus control. (C) The protein levels of TNF-α and MCP-1 in the livers of ApoE KO mice were examined by western blot. The histogram represents mean $\pm$ SD of the densitometric scans for TNF-α and MCP-1 protein bands from four experiments, normalized by comparison with β-actin, and expressed as a percentage of control and protein. *$P < 0.01$ versus control.

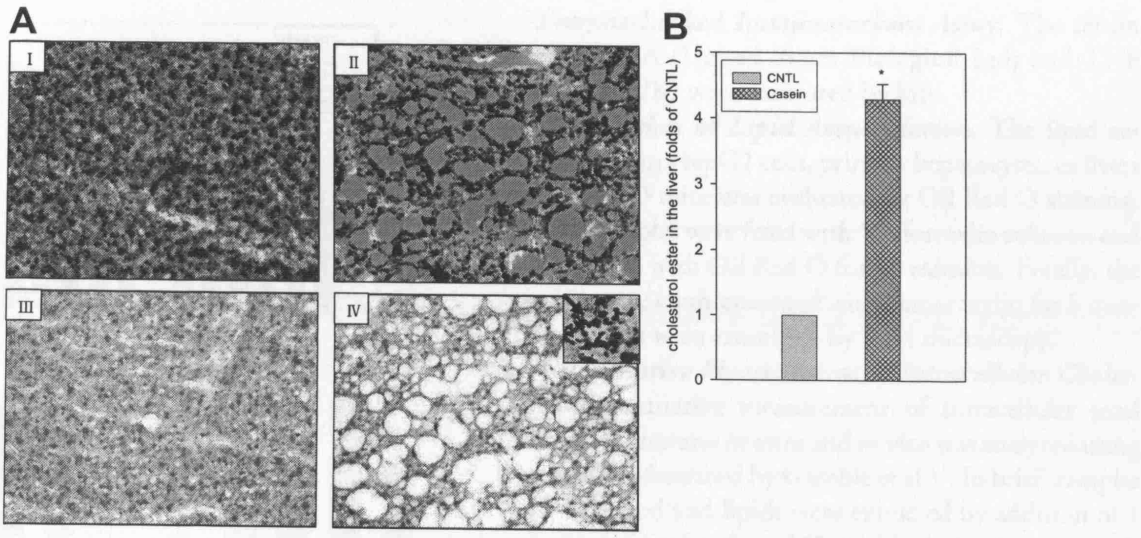

Fig. 3. The observation of lipid accumulation in the livers of ApoE KO mice in the absence or presence of casein injection. ApoE KO mice were fed with the western diet for 8 weeks in the absence (CNTL, I and III) or presence of 10% casein injection (casein, II and IV). (A) The lipid accumulation in the livers was checked by Oil Red O staining (I and II, original magnification ×200) and hematoxylin-eosin staining (III and IV, original magnification ×200) using 5-μm-thick sections. The area pointed out by the arrow in picture IV was infiltrated inflammatory cells (original magnification ×400). (B) The concentration of cholesterol ester was measured as described in Materials and Methods. Results represent the mean ± SD (n = 7). *$P <$ 0.01 versus control.

hepatocytes were isolated from the liver of male C57BL/6 mice by the collagenase perfusion method[8] and cultured in Dulbecco's modified Eagle's medium/Ham's nutrient mixture F12 supplemented with 100 nmol/L dexamethasone and 1 g/mL insulin. Hepatocyte viability tested by trypan blue exclusion was generally 92%, and cellular purity checked by immunochemistry staining was more than 90%. The primary hepatocytes were used for experiments after 4 weeks of incubation. Experimental medium was prepared with serum-free Dulbecco's modified Eagle's medium/Ham's nutrient mixture F12 containing 0.2% fatty acid-free bovine serum albumin. Cholesterol depletion in the cells was achieved by incubating the cells in the experimental medium for 23 hours, followed by further incubation with 1% 2-hydroxypropyl-β-cyclodextrin for 1 hour. Interleukin-1β (IL-1β) and tumor necrotic factor-α (TNF-α) were purchased from R&D Systems in the United Kingdom.

Lipoprotein Preparation. Low-density lipoprotein (LDL) was isolated from fresh plasma of healthy human volunteers by sequential density gradient ultracentrifugation as described in our previous publication.[9]

Cholesterol Efflux. $ApoA_1$-mediated cholesterol efflux studies were performed as described in our previous study.[10] In brief, after treatment, the radioactivity in both the supernatants and cellular lipids was measured by scintillation counting. $ApoA_1$-induced [^{3}H]-cholesterol efflux was calculated by subtracting the radioactivity in the supernatants without apoA1 from the counts in supernatants containing apoA1. The data were normalized by total [^{3}H]-cholesterol radioactivity (including in supernatants and cells) and were expressed as a percentage of control.

Confocal Microscopy. An anti-human SCAP polyclonal antibody was produced by immunizing rabbits with the synthetic peptide PVDSDRKQGEPTEQC (amino acids 66 to 69 of human SCAP). HepG2 cells cultured in chamber slides were washed, fixed, and permeabilized. The cells were then incubated with a rabbit anti-human SCAP antibody (1:200 dilution) and a mouse anti-human Golgi antibody (1:200 dilution), followed by secondary fluorescent antibodies of goat anti-rabbit Fluor 488 and goat anti-mouse Fluor 594, respectively (Molecular Probes Europe). After washing, the cells were examined by confocal microscopy.

Animal Model. Male ApoE KO mice in C57BL/6 genetic background were studied under protocols approved by the Comparative Biological Unit of Royal Free Campus, University College London. Eight-week-old ApoE KO mice were randomly assigned to daily subcutaneous injections of 0.5 mL 10% casein (n = 7) or distilled water as a control. The mice were fed a Western diet (Harlan, TD88137) containing 21% fat and 0.15% of cholesterol for 8 weeks. At termination, blood samples were taken for serum amyloid A (SAA) and TNF assays, and liver samples were used for histological assessments.

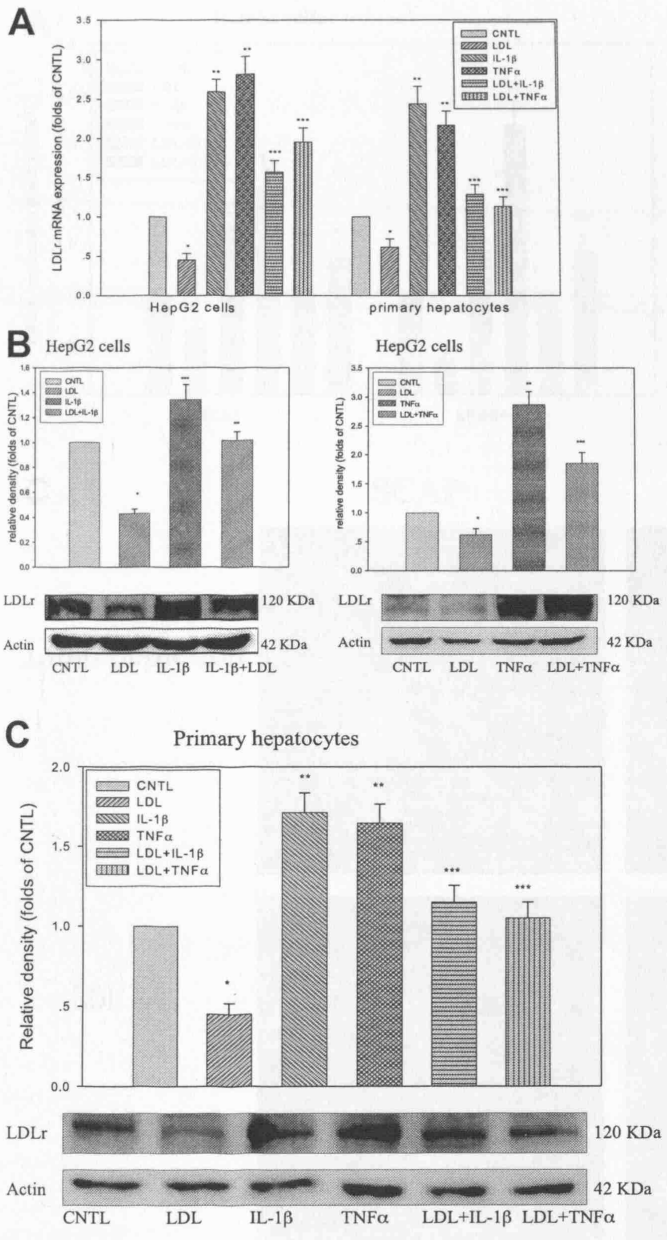

Fig. 4. Effects of inflammatory cytokines on mRNA and protein expression of LDLr in HepG2 cells and primary hepatocytes. Cells were incubated in serum-free medium (CNTL) or serum-free medium with 200 μg/mL native LDL (LDL) or 20 ng/mL IL-1β (IL-1β) or 50 ng/mL TNF-α (TNF-α) or 20 ng/mL IL-1 plus 200 μg/mL native LDL (LDL+IL-1) or 50 ng/mL TNF-α plus 200 μ/mL native LDL (LDL+TNF-α) for 24 hours. (A) The mRNA expression of LDLr was determined by real-time PCR, and β-actin served as the housekeeping gene. Results represent the mean $\pm$ SD (n = 4). *$P < 0.01$ versus control, **$P < 0.01$ versus control, ***$P < 0.01$ versus LDL group. (B, C) The protein level of LDLr was examined by western blot. The histogram represents mean $\pm$ SD of the densitometric scans for LDLr protein bands from four experiments, normalized by comparison with β-actin, and expressed as a percentage of control. *$P < 0.05$ versus control, **$P < 0.01$ versus control, ***$P < 0.01$ versus LDL group.

Enzyme-Linked Immunosorbent Assay. The serum levels of SAA (United States Biological Ltd) and TNF (Assaypro, UK) were measured by kits.

Observation of Lipid Accumulation. The lipid accumulation in HepG2 cells, primary hepatocytes, or livers of ApoE KO mice was evaluated by Oil Red O staining. Briefly, samples were fixed with 5% formalin solution and then stained with Oil Red O for 30 minutes. Finally, the samples were counterstained with hematoxylin for 5 minutes. Results were examined by light microscopy.

Quantitative Measurement of Intracellular Cholesterol. Quantitative measurement of intracellular total and free cholesterol *in vitro* and *in vivo* was analyzed using the method described by Gamble et al.[11]. In brief, samples were collected and lipids were extracted by addition of 1 mL chloroform/methanol (2:1). The lipid phase was collected, dried in vacuum, and then dissolved in 2-propanol containing 10% Triton X-100. The concentration of total and free cholesterol was analyzed using a standard curve and normalized by total protein from cells or liver tissues. The concentration of cholesterol ester was calculated using total cholesterol minus free cholesterol.

Real-Time Reverse Transcription Polymerase Chain Reaction. Total RNAs were isolated from cells or liver homogenates from ApoE KO mice using the guanidinium-phenol-chloroform method. Real-time reverse transcription polymerase chain reaction (PCR) was performed in an ABI 7000 Sequence Detection System using SYBR Green dye according to the manufacturer's protocol. All the Taqman primers (Sigma-Genosys, UK) were designed by Primer Express Software V2.0 (Applied Biosystems, UK) (Tables 1 and 2).

Western Blot. The total proteins from cell extracts or liver homogenates of ApoE KO mice were separated by sodium dodecyl sulfate polyacrylamide gel electrophoresis. The membranes were blocked with blocking buffer for 1 hour at room temperature after gel transferring. The membranes were then incubated with anti-human or anti-mouse polyclonal antibodies of LDLr, SCAP, PPARα, LXRα, TNF-α (Abcam, UK), SREBP-2 monoclonal antibody (LGC Promochem, UK), and monoclonal antibodies of monocyte chemoattractant protein-1 (MCP-1) and ABCA1 (Abcam, UK) for 1 hour, followed by horseradish peroxidase–labeled second antibodies for another hour. Finally, the signals were detected using enhanced chemiluminescence advanced system (Amersham Biosciences, UK).

Data Analysis. In all experiments, data were evaluated for statistical significance using one-way analysis of variance followed by Q-test. A difference was considered significant if the P value was less than 0.05.

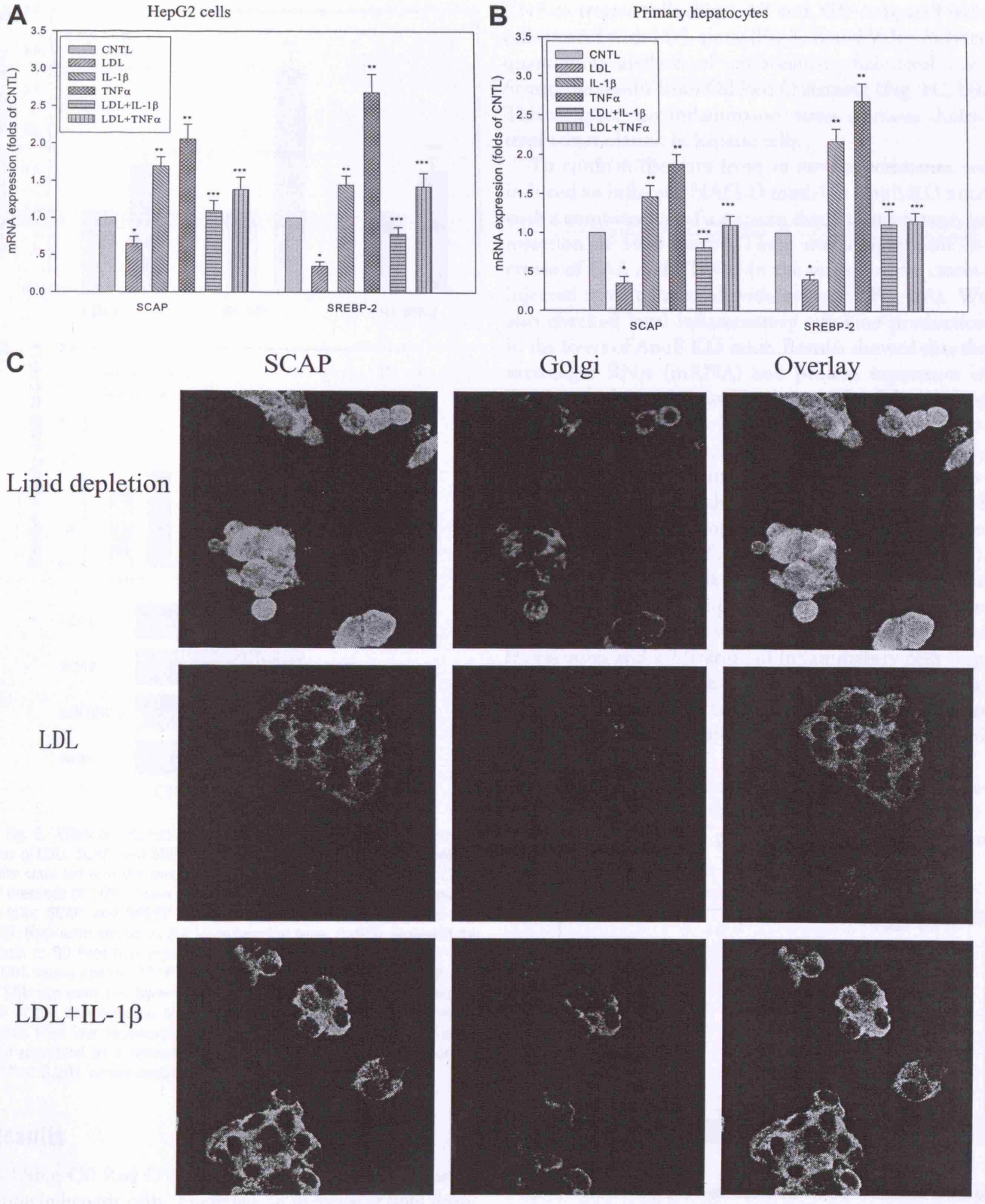

Fig. 5. Effect of inflammatory cytokines on the mRNA expression of SCAP and SREBP-2 in HepG2 cells and primary hepatocytes. Cells were incubated in serum-free medium (CNTL) or serum-free medium with 200 μg/mL native LDL (LDL) or 20 ng/mL IL-1β (IL-1β) or 50 ng/mL of TNF-α (TNF-α) or 20 ng/mL IL-1β plus 200 g/mL of native LDL (LDL+IL-1β) or 50 ng/mL of TNF-α plus 200 g/mL native LDL (LDL+TNFα) for 24 hours. (A, B) The mRNA expression of SCAP and SREBP-2 was determined by real-time PCR. Beta-actin served as the housekeeping gene. Results represent the mean $\pm$ SD from four experiments. *$P < 0.01$ versus control, **$P < 0.01$ versus control, ***$P < 0.01$ versus LDL group. (C) HepG2 cells were treated with lipid depletion condition, cholesterol loading (200 μg/mL native LDL), or inflammatory stress (20 ng/mL IL-1β plus 200 μg/mL native LDL) for 24 hours. The translocation of SCAP from the ER to the Golgi in HepG2 cells was detected by confocal microscopy.

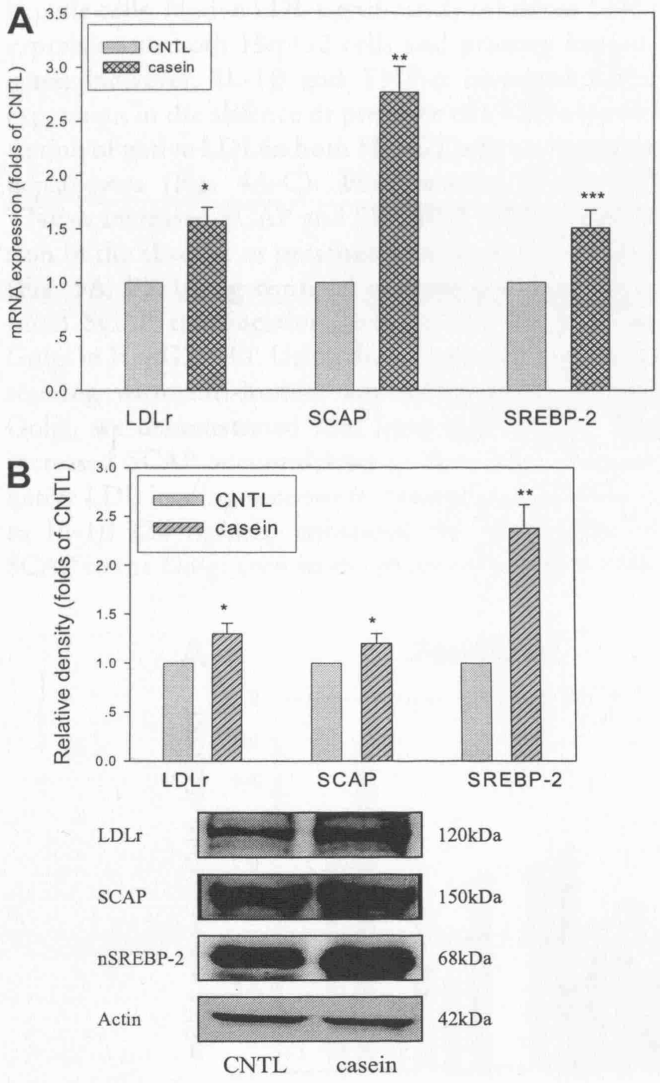

Fig. 6. Effect of inflammatory stress on the mRNA and protein expression of LDLr, SCAP, and SREBP-2 in the livers of ApoE KO mice. ApoE KO mice were fed with the western diet for 8 weeks in the absence (CNTL) or presence of 10% casein injection (casein). (A) The mRNA expression of LDLr, SCAP, and SREBP-2 in the livers was determined by real-time PCR. Beta-actin served as the housekeeping gene. Results represent the mean ± SD from four experiments. $*P < 0.05$ versus control, $**P < 0.001$ versus control, $***P < 0.05$ versus control. (B) The protein level of LDLr was examined by western blot. The histogram represents mean ± SD of the densitometric scans for LDLr, SCAP, and SREBP-2 protein bands from four experiments, normalized by comparison with β-actin, and expressed as a percentage of control. $*P < 0.05$ versus control, $**P < 0.001$ versus control.

Results

Using Oil Red O staining, we checked lipid accumulation in hepatic cells. There was an increase of lipid droplets in HepG2 cells and primary hepatocytes in the presence of native LDL (Fig. 1, II and VIII) or IL-1β (Fig.1, III and IX) or TNF-α (Fig.1, IV and X). There was more significant lipid droplet accumulation in LDL plus IL-1β–treated cells (Fig.1, V and XI) and in LDL plus TNF-α–treated cells (Fig.1, VI and XII) compared with cells treated with LDL alone (Fig.1, II and VIII). Further quantitative analysis of intracellular cholesterol confirmed the results from Oil Red O staining (Fig. 1C, D). This suggests that inflammatory stress increases cholesterol accumulation in hepatic cells.

To confirm the data from *in vitro* experiments, we induced an inflamed NAFLD model in ApoE KO mice with a combination of a western diet and subcutaneous injection of 10% casein. There was a significant increase of SAA and TNF-α in the serum in the casein-injected mice compared with controls (Fig. 2A). We also checked local inflammatory cytokine production in the livers of ApoE KO mice. Results showed that the messenger RNA (mRNA) and protein expression of TNF-α and MCP-1 in the livers of casein-injected mice were significantly increased compared with control mice (Fig. 2B, C), suggesting that inflammatory stress was successfully induced. Oil Red O and hematoxylin-eosin staining showed that a western diet for 8 weeks induced lipid droplet accumulation in the livers of the control group of ApoE KO (Fig. 3A, I and III). Interestingly, inflammatory stress induced by casein injection exacerbated lipid accumulation in the livers of the ApoE KO mice, with the appearance of massive fat vacuoles and infiltration of inflammatory cells (Fig. 3A, II and IV). Quantitative assay further demonstrated a significant accumulation of cholesterol ester in the liver of casein-injected mice compared with the control (Fig. 3B).

To investigate potential mechanisms of the phenomena, we evaluated the effect of inflammatory cytokines on the gene and protein expression of LDLr in

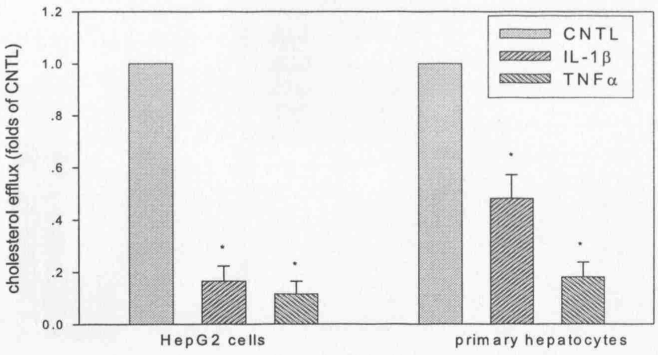

Fig. 7. Inflammatory cytokines reduce intracellular cholesterol efflux of HepG2 cells and primary hepatocytes loaded with cholesterol and 25-hydroxycholesterol. Cells were pre-loaded with cholesterol for 48 hours. The cholesterol-loaded cells were incubated in serum-free medium (CNTL) or serum-free medium with 20 ng/mL IL-1β (IL-1β) or serum-free medium with 50 ng/mL TNF-α (TNF-α) for 24 hours. Cholesterol efflux was measured as described in Materials and Methods. Data represent the mean ± SD from four independent experiments. $*P < 0.001$ versus control.

hepatic cells. Native LDL significantly inhibited LDLr expression in both HepG2 cells and primary hepatocytes. However, IL-1β and TNF-α increased LDLr expression in the absence or presence of a high concentration of native LDL in both HepG2 cells and primary hepatocytes (Fig. 4A-C). Furthermore, IL-1β and TNF-α increased SCAP and SREBP-2 mRNA expression in the absence or presence of native LDL loading (Fig. 5A, B). Using confocal microscopy, we investigated SCAP translocation between the ER and the Golgi in HepG2 cells. Using dual immunofluorescence staining with anti-human antibodies of SCAP and Golgi, we demonstrated that lipid depletion of cells increased SCAP accumulation in the Golgi, whereas native LDL loading reduced it. Interestingly, exposure to IL-1β (20 ng/mL) enhanced the localization of SCAP to the Golgi even in the presence of native LDL loading (Fig. 5C). These *in vitro* results were confirmed by the studies *in vivo* by showing that casein injection increased mRNA and protein expression of LDLr, SCAP, and SREBP-2 (Fig. 6A, B), which suggests that inflammation enhances the role of SCAP in escorting SREBPs from the ER to the Golgi to activate the expression of LDLr.

Because intracellular cholesterol homeostasis is controlled by influx and efflux, we further investigated the effect of inflammatory stress on intracellular cholesterol efflux. Our results showed that IL-1β and TNF-α significantly decreased cholesterol efflux from both HepG2 cells and primary hepatocytes in the presence of cholesterol loading (Fig. 7). We demonstrated that cholesterol loading increased gene and protein expressions of the ABCA1 pathway in hepatic cells. However, IL-1β and TNF-α inhibited gene and protein expres-

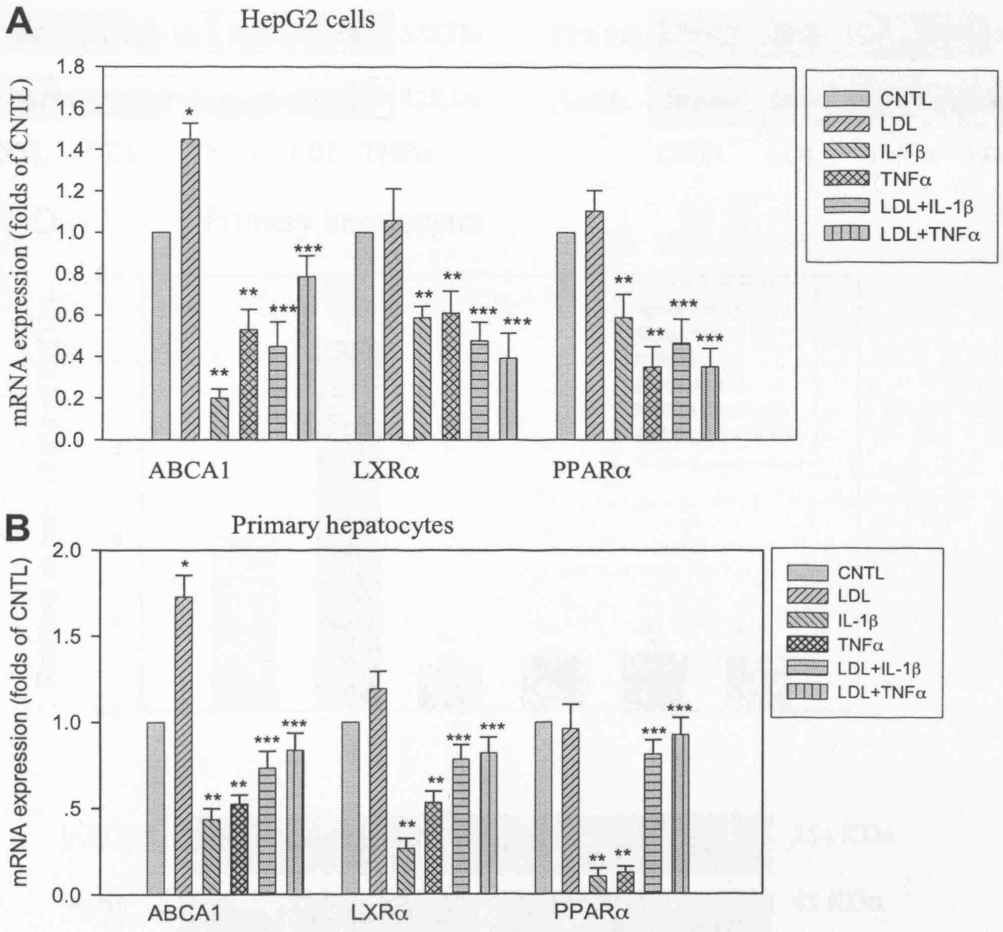

Fig. 8. Effect of inflammatory cytokines on the mRNA and protein expression of ABCA1, LXRα, and PPARα in HepG2 cells and primary hepatocytes. Cells were incubated in serum-free medium (CNTL) or serum-free medium with 200 μg/mL native LDL (LDL) or 20 ng/mL IL-1β (IL-1β) or 50 ng/mL TNF-α (TNF-α) or 20 ng/mL IL-1β plus 200 μ/mL native LDL (LDL+IL-1β) or 50 ng/mL TNF-α plus 200 g/mL native LDL (LDL+TNF-α) for 24 hours. The mRNA expression of ABCA1, LXRα, and PPARα in HepG2 cells (A) and primary hepatocytes (B) was determined by real-time PCR. Beta-actin served as the housekeeping gene. Results represent the mean $\pm$ SD from four experiments. *$P < 0.001$ versus control, **$P < 0.001$ versus control, ***$P < 0.001$ versus LDL group. The protein levels of ABCA1, LXRα, and PPARα in HepG2 cells (C) and primary hepatocytes (D) were examined by western blot. The histogram represents mean $\pm$ SD of the densitometric scans for LDLr protein bands from four experiments, normalized by comparison with β-actin, and expressed as a percentage of control. *$P < 0.01$ versus control, **$P < 0.001$ versus control, ***$P < 0.001$ versus LDL group.

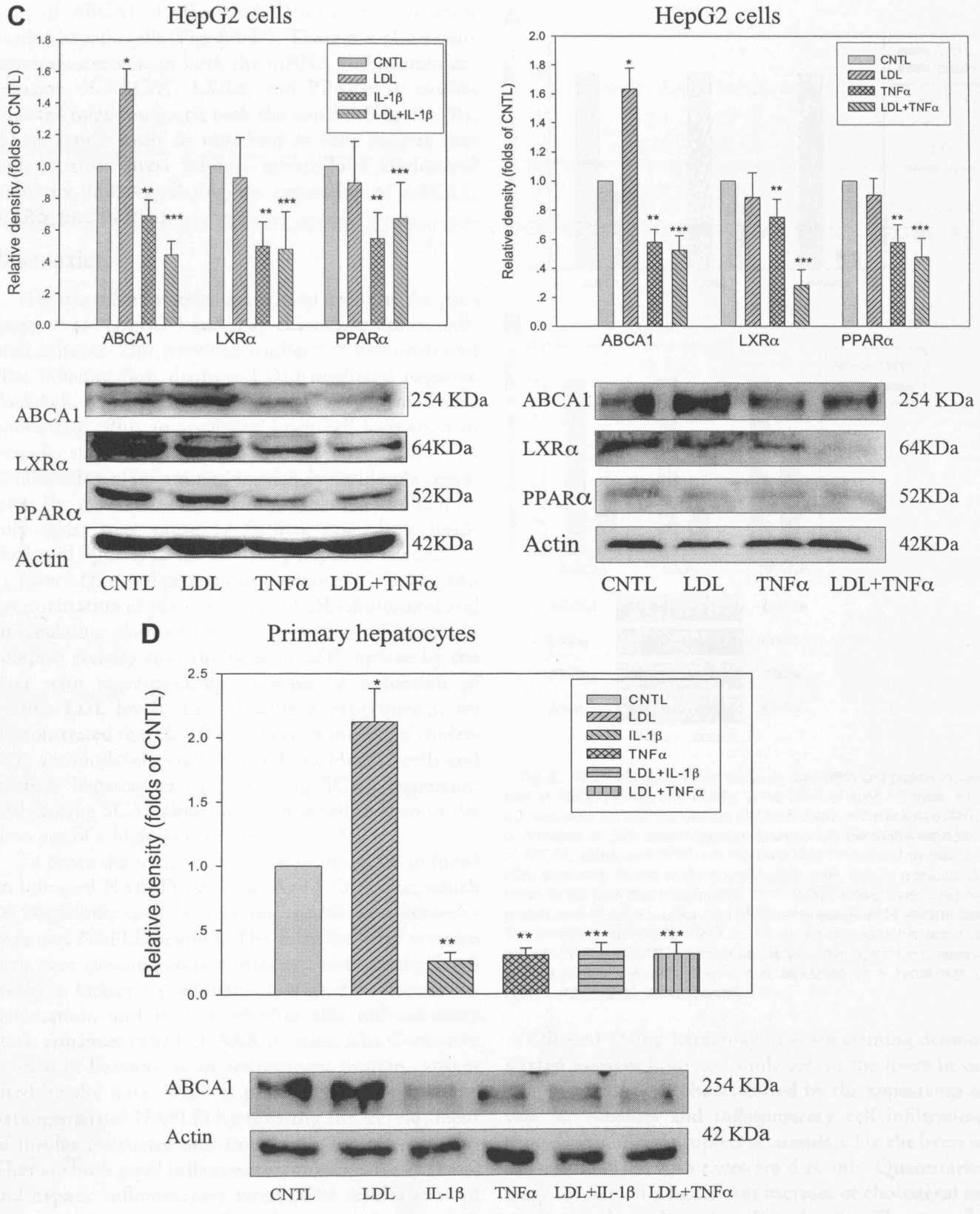

Fig. 8 (*Continued*)

sion of ABCA1, LXRα, and PPARα in cholesterol loaded hepatic cells (Fig. 8A-D). There was also a concomitant decrease in both the mRNA and protein expression of ABCA1, LXRα, and PPARα in casein-injected mice compared with the control (Fig. 9A, B). These results both *in vitro* and *in vivo* suggest that inflammatory stress inhibits intracellular cholesterol efflux by down-regulating the expression of ABCA1, LXRα, and PPARα.

Discussion

Hepatic inflammation is a critical event in the progression of NAFLD[3]) and may exacerbate lipid-mediated injuries. Our previous studies[12,13] demonstrated that inflammation disrupts LDLr-mediated negative feedback regulation and reduces ABCA1-mediated cholesterol efflux to accelerate foam cell formation in vascular smooth muscle cells and mesangial cells. The combination of inflammation with dyslipidemia aggravates the problem. These data suggest that inflammatory stress may cause or further exacerbate lipid-mediated injuries in the liver or peripheral tissues.

Liver LDLr is of primary importance in binding and internalization of plasma-derived LDL-cholesterol and in regulating plasma LDL concentrations. Changes in receptor activity alter the rates of LDL uptake by the liver with corresponding increase or reduction of plasma LDL levels. In cell culture experiments, we demonstrated that IL-1β and TNF-α increased cholesterol accumulation via LDLr in both HepG2 cells and primary hepatocytes by increasing SCAP expression and causing SCAP abnormal translocation even in the presence of a high concentration of LDL.

To prove the results from *in vitro* study, we induced an inflamed NAFLD model in ApoE KO mice, which are commonly used for creating models in atherosclerosis and NAFLD studies. The mice fed with western diet were subcutaneously injected with casein for 8 weeks to induce a predictable low-grade, systemic inflammation, and to test whether this inflammatory stress enhances NAFLD. SAA in mice, like C-reactive protein in humans, is an acute-phase protein synthesized by the liver. TNF-α plays a major role in the pathogenesis of NAFLD by favoring the development of insulin resistance and impaired glucose tolerance. They are both good inflammatory markers for systemic and hepatic inflammatory stress. Our results showed that casein injection significantly increased serum levels of SAA and TNF-α and up-regulated expression of TNF-α and MCP-1 in the liver, suggesting that systemic and local hepatic inflammatory stress was successfully induced in the mice.

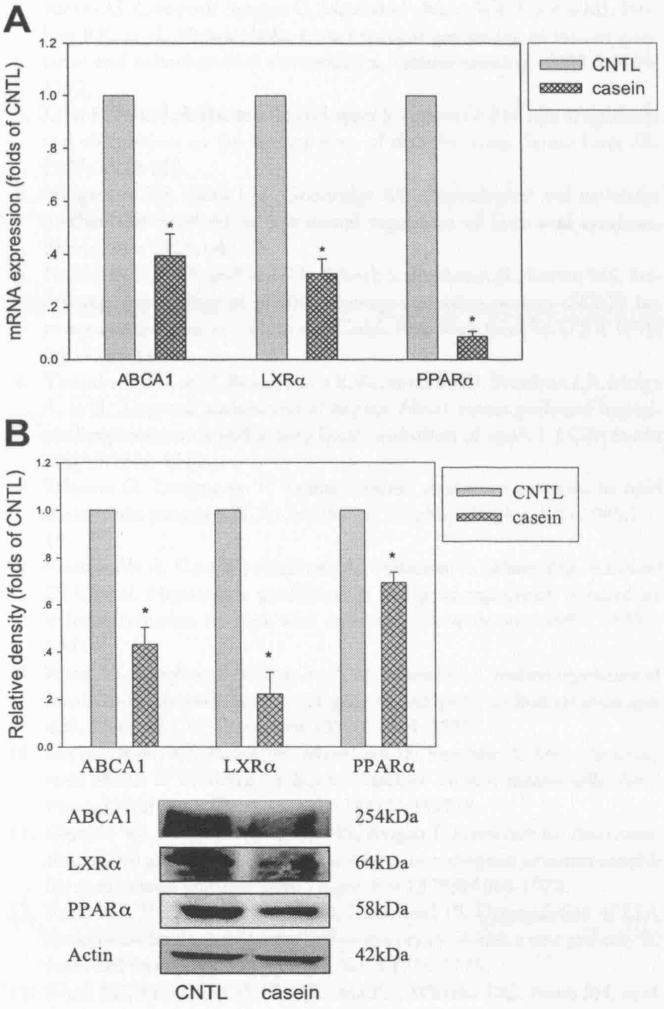

Fig. 9. Effect of inflammatory stress on the mRNA and protein expression of ABCA1, LXRα, and PPARα in the livers of ApoE KO mice. ApoE KO mice were fed with the western diet for 8 weeks in the absence (CNTL) or presence of 10% casein injection (casein). (A) The mRNA expression of ABCA1, LXRα, and PPARα in the livers was determined by real-time PCR. Beta-actin served as the housekeeping gene. Results represent the mean ± SD from four experiments. $*P < 0.001$ versus control. (B) The protein level of ABCA1, LXRα, and PPARα was examined by western blot. The histogram represents mean ± SD of the densitometric scans for ABCA1, PPARα, and LXRα protein bands from four experiments, normalized by comparison with β-actin, and expressed as a percentage of control. $*P < 0.01$ versus control.

Oil Red O and hematoxylin-eosin staining demonstrated massive lipid accumulation in the livers in casein-injected mice, characterized by the appearance of vast fat vacuoles and inflammatory cell infiltration, though some lipid droplets accumulated in the livers of control mice fed with a western diet only. Quantitative assay confirmed a significant increase of cholesterol ester in the liver of casein-injected mice. These results suggest a strong association between enhanced lipid accumulation in the liver and inflammatory stress.

Next, we studied the LDLr pathway to explore potential mechanisms of accelerated lipid accumulation

induced by inflammatory stress. Results showed that inflammatory stress up-regulated mRNA and protein expression of LDLr, SCAP, and SREBP-2 in the livers of casein-injected ApoE mice compared with control, which further supported our previous *in vitro* findings.

The ABCA1 pathway is also an important mediator for cellular efflux of phospholipids and cholesterol to apoA-I–containing lipoproteins in HDL. We showed that inflammatory stress reduced intracellular cholesterol efflux by inhibiting PPARα, LXRα, and ABCA1 gene and protein expression *in vitro* and *in vivo*, suggesting that inflammatory stress also accelerates the progression of fatty liver in an NAFLD model by reducing intracellular cholesterol efflux. This may explain why HDL-cholesterol is reduced and the triglyceride/HDL-cholesterol ratio is increased fivefold to sevenfold in NAFLD patients.[14]

We also evaluated liver function and liver fibrosis by measuring serum alanine aminotransferase and aspartate aminotransferase levels, and Masson's trichrome staining, respectively. Neither alanine aminotransferase nor aspartate aminotransferase were elevated, and there was no obvious fibrosis in control or casein injection group, suggesting that the model established in this study could be at an early stage of NAFLD.

Taken together, these findings *in vivo and in vitro* demonstrated that inflammatory stress disrupted cholesterol trafficking in the liver by reducing cholesterol efflux and increasing cholesterol influx. As NAFLD progresses, a subsequent or persistent inflammatory stimulus, the second hit, will worsen cholesterol trafficking. This, together with dysregulation of triglycerides and free fatty acids, will result in unlimited lipid accumulation and progression of NAFLD. In addition, the inflamed NAFLD model established in the experiments may be useful for studying the effect of low-grade inflammatory stress, especially rising from chronic inflammatory diseases characterized by an increased C-reactive protein level, as in Crohn's disease,[15] autoimmune diseases,[16,17] type 2 diabetes mellitus, or progressive NAFLD.[15,18]

References

1. Day CP, James OF. Steatohepatitis: a tale of two "hits"? Gastroenterology 1998;4:842-845.
2. Sanyal AJ, Campbell-Sargent C, Mirshahi F, Rizzo WB, Contos MJ, Sterling RK, et al. Nonalcoholic steatohepatitis: association of insulin resistance and mitochondrial abnormalities. Gastroenterology 2001;5:1183-1192.
3. Lalor P, Faint J, Aarbodem Y, Hubscher S, Adams D. The role of cytokines and chemokines in the development of steatohepatitis. Semin Liver Dis 2007;2:173-193.
4. Hillgartner FB, Salati LM, Goodridge AG. Physiological and molecular mechanisms involved in nutritional regulation of fatty acid synthesis. Physiol Rev 1995;1:47-76.
5. Nohturfft A, DeBose-Boyd RA, Scheek S, Goldstein JL, Brown MS. Sterols regulate cycling of SREBP cleavage-activating protein (SCAP) between endoplasmic reticulum and Golgi. Proc Natl Acad Sci U S A 1999; 20:11235-11240.
6. Timmins JM, Lee JY, Boudyguina E, Kluckman KD, Brunham LR, Mulya A, et al. Targeted inactivation of hepatic Abca1 causes profound hypoalphalipoproteinemia and kidney hypercatabolism of apoA-I. J Clin Invest 2005;5:1333-1342.
7. Schmitz G, Langmann T. Transcriptional regulatory networks in lipid metabolism control ABCA1 expression. Biochim Biophys Acta 2005;1:1-19.
8. Francavilla A, Carr BI, Azzarone A, Polimeno L, Wang ZQ, Vanthiel DH, et al. Hepatocyte proliferation and gene-expression induced by triiodothyronine in-vivo and in-vitro. HEPATOLOGY 1994;5:1237-1241.
9. Ruan XZ, Varghese Z, Fernando R, Moorhead JF. Cytokine regulation of low-density lipoprotein receptor gene transcription in human mesangial cells. Nephrol Dial Transplant 1998;6:1391-1397.
10. Ma KL, Ruan XZ, Powis SH, Moorhead JF, Varghese Z. Anti-atherosclerotic effects of sirolimus on human vascular smooth muscle cells. Am J Physiol Heart Circ Physiol 2007;6:H2721-H2728.
11. Gamble W, Vaughan M, Kruth HS, Avigan J. Procedure for determination of free and total cholesterol in micro- or nanogram amounts suitable for studies with cultured cells. J Lipid Res 1978;8:1068-1070.
12. Ruan XZ, Varghese Z, Powis SH, Moorhead JF. Dysregulation of LDL receptor under the influence of inflammatory cytokines: a new pathway for foam cell formation. Kidney Int 2001;5:1716-1725.
13. Ruan XZ, Moorhead JF, Tao JL, Ma KL, Wheeler DC, Powis SH, et al. Mechanisms of dysregulation of low-density lipoprotein receptor expression in vascular smooth muscle cells by inflammatory cytokines. Arterioscler Thromb Vasc Biol 2006;5:1150-1155.
14. Sung KC, Ryan MC, Kim BS, Cho YK, Kim BI, Reaven GM. Relationships between estimates of adiposity, insulin resistance and nonalcoholic fatty liver disease in a large group of nondiabetic korean adults. Diabetes Care 2007;8:2113-2118.
15. Canbay A, Bechmann LP, Best J, Jochum C, Treichel U, Gerken G. Crohn's disease-induced non-alcoholic fatty liver disease (NAFLD) sensitizes for severe acute hepatitis B infection and liver failure. Z Gastroenterol 2006;3:245-248.
16. Bleibel W, Thukral C, Robson SC. Overlap between systemic lupus erthematosus and nonalcoholic steatohepatisis: response. J Clin Gastroenterol 2006;6:561-562.
17. Tiegs G. Cellular and cytokine-mediated mechanisms of inflammation and its modulation in immune-mediated liver injury. Z Gastroenterol 2007;1:63-70.
18. Clark JM, Diehl AM. Hepatic steatosis and type 2 diabetes mellitus. Curr Diabetes Rep 2002;3:210-215.